

TRACE ELEMENT GEOCHEMISTRY OF THE MILK RIVER AQUIFER
GROUNDWATER, ALBERTA, CANADA

A Thesis Submitted to the
College of Graduate Studies and Research
in Partial Fulfillment of the Requirements
for the Degree of Master of Science
in the Department of Geological Sciences,
University of Saskatchewan,
Saskatoon, Saskatchewan.

By
M. Ashley Starzynski
Spring, 1998

© Copyright M. Ashley Starzynski, 1998. All rights reserved.

802001120076

Permission to Use

In presenting this thesis in partial fulfillment of the requirements for a Masters of Science degree from the University of Saskatchewan, I agree that the libraries of this university may make it freely available for inspection. I further agree that permission for copying of this thesis in any manner, in whole or in part, for scholarly purposes may be granted by my supervisors Drs. R. Kerrich and M. J. Hendry, or in their absence, by the head of the Department of Geological Sciences or Dean of Arts and Science. It is understood that any copying of this thesis, or parts thereof, shall not be allowed without my written permission. It is also understood that due recognition shall be given to me and the University of Saskatchewan in any scholarly use which may be made of any material in this thesis.

Requests for permission to copy or make other use of material in this thesis, in whole or in part, should be addressed to:

Head of the Department of Geological Sciences
114 Science Place, University of Saskatchewan
Saskatoon, Saskatchewan, S7N 5E2.

Abstract

Groundwater samples from 27 wells located along a 50 km flow path in the Milk River aquifer, Alberta, Canada, were analyzed for trace elements including rare earth elements (REEs). The objectives were to: 1) complete the suite of chemical elements determined for this extensively studied aquifer; 2) evaluate changes in concentrations of the trace elements and REEs along a hydraulically and chemically constrained section of the aquifer, and 3) observe the fate of these trace elements through a redox boundary.

The groundwater chemistry illustrates some similar trends to those reported by previous workers (Meyboom, 1960; Schwartz and Muelenbachs, 1979; Phillips et al., 1986; Hendry and Schwartz, 1988, 1990; and Hendry et al., 1991). There are small well defined increases in Na, Cl, Fe, Mg, Ca, Al, but a decrease in SO_4 , as the groundwater migrates from recharge. Calcite dissolution accounts for the increase in alkalinity as the groundwater migrates downgradient from the recharge area.

Some trace elements (B, Rb, Ba) display slight increases as the groundwater evolves from the recharge area, consistent with progressive water-rock reaction. In groundwater studies uranium has been found to be an excellent element for tracing the evolution of waters, because of its low natural concentrations and multi-valent characteristics. Higher concentrations encountered along the flow path at 20 km and 32-33 km, may reflect the redox front boundary and post-redox front boundaries, respectively. Groundwater with intermediate uranium concentrations are probably the result of minor mixing between the oxic and anoxic water masses. Similar, trends are seen with other multi-valent elements including manganese.

Groundwater studies using trace elements as hydrogeochemical tracers show that the groundwaters inherit their trace element budgets, including REE signatures, via interaction with the aquifer rocks. Solution complexation can also significantly affect

the dissolved REE signatures. Shale-normalized plots show that systematic patterns exist in REEs and transition metals in the Milk River aquifer groundwater. There are clear chemical trends as the groundwater migrates downflow from the recharge area. REE plots for the groundwater samples are generally either flat [Type 1 groundwater] to slightly enriched in the heavy REEs (HREEs) [Type 2 groundwater].

Speciation modeling of REEs in the alkaline Milk River aquifer groundwater has been evaluated primarily to assess the importance of carbonate complexes. Carbonate complexation is the most important complex for REEs in the groundwater system. Dicarbonato complexes ($\text{Ln}(\text{CO}_3)_2^-$) are predicted as the dominant species in comparison to the carbonato complexes (LnCO_3^+). Heavy REE enriched shale-normalized REE patterns are due to the formation of more stable HREE CO_3 complexes than the light REE CO_3 complexes in the groundwater.

In addition to using REEs as potential hydrogeochemical tracers in groundwaters, their chemical similarities to the trivalent actinides provides a proxy for the chemical behavior of these radionuclides in natural waters, and therefore an analogue for modeling the behavior of nuclear waste in groundwater systems.

Acknowledgments

I would like to thank my advisor Dr. Rob Kerrich, for financial and technical support, and the opportunity to undertake this project. Financial support through Dr. Kerrich was made possible by NSERC operating grants. I also graciously acknowledge my co-supervisor Dr. Jim Hendry for his support both financially and intellectually.

I would also like to thank my advisory committee, Drs. Malcolm Reeves, Jim Basinger, and Ben Rostron for their critical review and comments. I'm grateful to Steve Taylor and Xuiping Yan for their help in the field, and in the lab. Assistance with ICP-MS analysis was provided by Brian Morgan, who also answered my many questions on the equipment and sample preparation techniques. Acknowledgment must be given to Dr. Kevin Johannesson (Harry Reid Center for Environmental Studies, University of Nevada, Las Vegas) for generating the REE speciation modeling results. Special thanks are due to the lab personnel in the department of Geological Sciences, Dave Pezderic, Tom Bonli, Ray Kirkland and Blaine Novakovski for providing the essential knowledge, lab materials, space, and most importantly their time.

Other scientists who have contributed to my studies, through discussions and reviewing my work and parts of my thesis, include: E. Eberhardt, S. Balzer, C. Therens, A. Abeleira, R. Donahue, Y. Haiming, J. Dobrohoczki, P. Hollings, A. Polat, B. Reiter, and D. Schmid.

Finally, I acknowledge my wife Cori for making the ultimate sacrifice and putting up with my student lifestyle while inspiring me to finish my studies.

Table of Contents

Permission to Use	i
Abstract	ii
Acknowledgments	iv
Table of Contents	v
List of Tables	ix
List of Figures	x
Definition of Terms, Units, and List of Acronyms	xiii
1 Introduction and Scope	
1.1 Background	1
1.2 Rationale of Study	1
1.3 Trace Elements in Groundwater Studies	3
1.4 Structure of the Thesis	4
2 Geological and Hydrogeology Background	
2.1 Geology	9
2.2 Hydrogeology	11
2.3 Geochemistry	13
2.4 Proposed Geochemical Models	17
2.5 Halogens in the Milk River aquifer	21
2.6 Dissolved Gases	22
2.7 Age Dating Groundwaters	23
2.7.1 Radiocarbon and Stable Isotopes	23
2.7.2 Chloride and ³⁶ Cl Concentrations and Interpretations	25
2.7.3 Uranium-series Radionuclides	27
2.8 Summary	28

3 Methodology	
3.1 Groundwater Sampling Protocol	29
3.2 Field Sampling and Analysis	31
3.3 Analytical Methodologies	33
3.3.1 Instrumentation	33
3.3.2 ICP-MS	33
3.3.3 ICP-AES	34
3.3.4 Advantages and Disadvantages of ICP-AES and ICP-MS	35
3.4 ICP-AES - ICP-MS Intercomparison	35
3.4.1 Limits of Detection	37
3.4.2 Elements Analyzed by ICP-MS and ICP-AES	37
3.5 Intercomparison of Field Filtered and Unfiltered Samples	38
3.6 Geochemical Modeling	42
3.6.1 An Introduction to PHREEQC	42
3.6.2 PHREEQC as a Speciation Code	45
3.6.3 REE Speciation Modeling	46
4 Results and Discussion	
4.1 Structure of Chapter 4	48
4.2 The Hydrogeochemistry of the Milk River aquifer Groundwater	49
4.2.1 pH, Alkalinity, and Major Ion Chemistry of the Groundwater	49
4.2.2 Initial Condition - Solution Modeling of the Groundwater	52
4.3 Oxidation - Reduction Sequences in Confined Groundwater Systems	56
4.3.1 Redox Chemistry of the Milk River Groundwater	59
4.4 Select Trace Elements	65
4.4.1 Trace Element Concentrations Along the Flow Path	65
4.5 Rare Earth Elements	75
4.5.1 REE Concentrations Along the Flow Path	77
4.5.2 Shale-Normalized REE Patterns	79

4.5.3 REE Speciation Modeling of the Milk River Groundwater	88
4.5.4 Behavior of REEs in the Milk River Groundwater	93
4.5.5 Mineral Sources of REEs	93
4.6 Additional Trace Elements	96
4.6.1 Trace Element Concentrations Along the Flow Path	96
4.6.2 Transition Metals	107
4.6.3 Alkali Metals and Alkali Earth Metals	107
5 Conclusions	
5.1 Introduction	111
5.2 Field Filtering	111
5.3 The Principal Findings From This Study	112
5.3.1 Summary of the Major Elements and Ions	112
5.3.2 Summary of the Trace Elements	113
5.3.3 Summary of the Rare Earth Elements	114
5.3.4 Summary of the Transition Metals	115
5.3.5 Summary of the Alkali Metals and Alkali Earth Metals	116
5.4 Speciation Modeling of the Milk River Aquifer Groundwater	116
5.4.1 PHREEQC Initial Conditions	116
5.4.2 REE Speciation Modeling	117
5.5 Implications of Study	117
5.6 Recommendations and Future Work	118
References	120
Appendices	
Appendix A 1995-1997 Sample Locations	136
Appendix B ICP-AES and ICP-MS Analyses	138
Appendix C Major Cations and Anions Analyses	158
Appendix D Water Standards and Quality of Analysis	160

Appendix E Detection of Selected Elements for ICP-AES and ICP-MS	162
Appendix F The Effects of Field filtering on Select Elements	166
Appendix G Concentrations of Select Trace Elements <i>versus</i> Distance From Recharge	171
Appendix H PHREEQC Initial Solution Calculations	174
Appendix I Results of REE Speciation Modeling	186

List of Tables

1.1	Select studies and papers based on trace and rare earth elements in aqueous geochemistry, with sources.	5
3.1	Advantages and disadvantages of ICP-MS and ICP-AES.	36
4.1	Major anions and cations analyzed in the Milk River aquifer groundwater.	50
4.2	Major elements analyzed in the Milk River aquifer groundwater.	50
4.3	Saturation index values from speciation modeling using PHREEQC in the Milk River aquifer groundwater.	55
4.4	Oxidation states of select elements that occur in the Milk River aquifer groundwater.	58
4.5	Trace elements analyzed in the Milk River aquifer groundwater.	67
4.6	REE ratios for comparing Light REE and Heavy REE shale-normalized values.	86

List of Figures

2.1	Location of the Milk River aquifer in southern Alberta, Canada, illustrating the flow path studied.	10
2.1	The Geology of the Milk River aquifer.	12
2.2	Geological evolution of the Milk River aquifer.	14
2.3	Piezometric surface in the Milk River aquifer.	15
2.4	Spatial variations in dissolved ions.	16
2.5	Spatial variations in field pH, and calculated pCO ₂ .	18
2.6	Conceptual models to explain the origin of the distribution of chemical and isotopic species in the Milk River aquifer.	20
3.1	Sample locations in the Milk River aquifer and proposed flow paths.	30
3.2	Analysis of select filtered and unfiltered elements in the Milk River aquifer groundwaters (Fe, Al).	39
3.3	Analysis of select filtered and unfiltered elements in the Milk River aquifer groundwaters (Na, K, Mg, Ca).	40
3.4	Analysis of select filtered and unfiltered elements in the Milk River aquifer groundwaters (U, Th).	41
3.5	REE plots displaying the effects of field filtering on groundwater samples.	43
4.1	Field pH and alkalinity versus distance from recharge.	51
4.2	Cl ⁻ , Mg, and Al concentrations in the Milk River aquifer groundwater versus distance along the flow path.	53
4.3	Ca, Na, and K concentrations in the Milk River aquifer groundwater versus distance along the flow path.	54
4.4	PHREEQC initial condition - solution modeling of select phases in the Milk River aquifer groundwater.	57
4.5	Concentrations of Fe, SO ₄ , and CH ₄ in the Milk River aquifer groundwater versus distance along the flow path.	61
4.6	U and Mn concentrations in the Milk River aquifer groundwater	

	versus distance from recharge.	63
4.7	PHREEQC initial condition - solution modeling of uraninite in the Milk River aquifer groundwater.	64
4.8	Theoretical Eh values used in the speciation modeling, as determined by redox reactions in the Milk River aquifer groundwater.	66
4.9	B and Mo concentrations in the Milk River aquifer groundwater versus distance from recharge.	72
4.10	Rb and Ba concentrations in the Milk River aquifer groundwater versus distance from recharge.	73
4.11	PHREEQC initial condition - solution modeling of barite in the Milk River aquifer groundwater.	74
4.12	Li, Co, and Zn concentrations in the Milk River aquifer groundwater versus distance from recharge.	76
4.13	Sum of REE concentrations in the Milk River aquifer groundwater versus distance from recharge.	78
4.14	Light rare earth elements (LREEs) in the Milk River aquifer groundwater versus distance from recharge.	80
4.15	Heavy rare earth elements (HREEs) in the Milk River aquifer groundwater versus distance from recharge.	81
4.16	Shale-normalized REE patterns for groundwater samples from the Milk River aquifer (MR139, MR122, and MR123).	83
4.17	Shale-normalized REE patterns for groundwater samples from the Milk River aquifer (MR52, MR80, MR130, MR135, MR136 and MR129).	84
4.18	Shale-normalized REE patterns for groundwater samples from the Milk River aquifer (MR131, MR134, MR133, MR137, MR127, MR138, and MR123).	85
4.19	Lu/La, Er/Nd, and Eu/Eu* shale-normalized ratios versus distance for the Milk River aquifer groundwater samples.	87
4.20	Results of speciation modeling plotted as percent dissolved REEs	

	(% lanthanides) versus atomic number for groundwater samples (MR139, MR122, and MR123)	90
4.21	Results of speciation modeling plotted as percent dissolved REEs (% lanthanides) versus atomic number for groundwater samples (MR52, MR80, and MR130).	91
4.22	Results of speciation modeling plotted as percent dissolved REEs (% lanthanides) versus atomic number for groundwater samples (MR129, MR132, and MR119).	92
4.23	Plot of Nd, Sm, and Dy versus pH for the Milk River aquifer groundwater samples.	94
4.24	Plot of Nd, Sm, and Dy versus alkalinity for the Milk River aquifer groundwater samples.	95
4.25	Sr, P, and As concentrations in the Milk River aquifer groundwater versus distance from recharge.	98
4.26	Sr/Ca ratio in the Milk River aquifer groundwater along the flow path.	99
4.27	PHREEQC initial condition - solution modeling of strontianite in the Milk River aquifer groundwater.	100
4.28	Ti, Pb, and W concentrations in the Milk River aquifer groundwater versus distance from recharge.	101
4.29	Se, Ni, and Cu concentrations in the Milk River aquifer groundwater versus distance from recharge.	103
4.30	Cd and Zr concentrations in the Milk River aquifer groundwater versus distance from recharge.	104
4.31	Hf, Sc, and Ag concentrations in the Milk River aquifer groundwater versus distance from recharge.	105
4.32	Sn and Ta concentrations in the Milk River aquifer groundwater versus distance from recharge.	106
4.23	Specified transition metals normalized to PAAS for select groundwater from the 1995, 1996, and 1997 field sampling seasons.	108
4.34	Specified alkali and alkali earth metals normalized to PAAS	

for select groundwater from the 1995, 1996, and 1997 field
sampling seasons.

Definition of Terms, Units, and List of Acronyms

Piezometer A basic device for measurement of hydraulic head is a tube or pipe in which the elevation of a water level can be determined.

Hydraulic Head (h) The sum of the elevation of the point of measurement or elevation head (z), and the pressure head (ψ).

$$h = z + \psi$$

Hydraulic Conductivity(K) It is a function of the porous medium and fluid.
K (LT⁻¹)

$$K = \frac{Cd^2\rho g}{\mu}$$

Where: d = characteristic grain diameter
C = sorting or packing coefficient
 ρ = density
g = acceleration due to gravity
 μ = dynamic viscosity

Intrinsic Permeability (k) $k = Cd^2$ (same as above) k (L²)

Piezometric Surface (*Potentiometric Surface*) - If the water-level elevations in wells in a confined aquifer are plotted on a map and contoured, the resulting surface, which is actually a map of the hydraulic head in the aquifer is called the potentiometric surface.

Aquifer A saturated permeable geologic unit that can transmit and store significant quantities of water under ordinary hydraulic gradients.

Aquiclude A saturated permeable geologic unit that is incapable of transmitting water under ordinary hydraulic gradients.

Aquitard A less permeable geological unit which is capable of transmitting water but is not sufficient to allow the completion of production wells.

Transmissivity	For a confined aquifer of thickness b , is defined as $T = Kb$ Where: K = Hydraulic Conductivity (see above) b = Thickness of aquifer
Storativity (Storage Coefficient)	For a confined aquifer of thickness b , is defined as $S = S_s b$ Where: S_s = Specific Storage (see below) b = Thickness of aquifer
Specific Storage	In a saturated aquifer the volume of water that a unit volume of aquifer releases from storage under a unit decline in hydraulic head.
Evapotranspiration	A combination of evaporation and transpiration from the soil by plants.
Alkalinity	Is the measure of the capacity of a water to neutralize acid. In most natural water, the alkalinity is largely due to the presence of dissolved carbonate (CO_3^{2-}) and bicarbonate (HCO_3^-) ions (expressed as mg/l).
Colloids	Particles having diameters in the range $\sim 10^{-5} - 10^{-8}$ m.
mg/l	Milligrams of solute per liter of water, also equal to parts per million (ppm).
$\mu\text{g/l}$	Micrograms of solute per liter of water, also equal to parts per billion (ppb).
REE	Rare earth elements - in the periodic table elements 57 through 71.
ICP-MS	Inductively coupled plasma - mass spectrometry
ICP-AES	Inductively coupled plasma - atomic emission spectrometry
DIC	Dissolved inorganic carbon
DOC	Dissolved organic carbon

Chapter 1

Introduction and Scope

1.1 Background

The Milk River aquifer, Alberta, Canada was chosen for an International Atomic Energy Agency, Vienna (IAEA) sponsored study in 1985, given its relatively straightforward boundary conditions. This aquifer fits the definition of a confined groundwater system, dipping gently from the recharge area, and confined both above and below (Hendry et al., 1991; Schwartz and Muehlenbachs, 1979). A feature of this aquifer is that the groundwater becomes old (recent recharge to ~1 Ma) in a relatively short distance of 80 to 100 km downflow from the recharge area, making it appropriate for evaluating various groundwater dating techniques. As a result, the hydrogeology and geochemistry of the Milk River aquifer have been thoroughly studied. Notwithstanding the relatively well constrained boundary conditions, previous studies have revealed that the Milk River system is complex in terms of groundwater origin, and the evolution of its chemical and isotopic characteristics (Schwartz and Muehlenbachs, 1979; Schwartz et al., 1981; Domenico and Robins, 1985; Phillips et al., 1986; Hendry and Schwartz, 1988, 1990; and Hendry et al., 1991).

1.2 Rationale of This Study

Previous studies have established a large database on field pH and alkalinity, major anion and cation concentrations, dissolved gases, and stable and radiogenic isotopes (Hendry and Schwartz, 1990a; Andrews et al., 1991a; and 1991b; Drimmie et al., 1991;

Fabryka-Martin et al., 1991; Hendry et al., 1991; Ivanovich et al., 1991; Nolte et al., 1991). To date, however, the trace element geochemistry of the Milk River aquifer groundwater has not been studied. Accordingly, the primary objective of this project is to measure an extensive range of trace elements, including the rare earth elements (REEs), in the Milk River aquifer groundwater.

Due to limited studies on trace elements in terrestrial surface waters and groundwaters, the factors that control their concentrations and speciation are poorly understood. Therefore, for simplicity, this study focuses on the chemically and hydraulically, well constrained, south-eastern section of the Milk River aquifer. Sample sites were selected along a flow path identified in previous studies (Hendry and Schwartz, 1988; 1990a). The flow path starts near the recharge area, crosses a redox boundary, and continues downflow for a total of >80 km. This new data, coupled with existing data on the major ions and cations, pH, isotopes, and dissolved gases, will assist in understanding the water/rock interactions that influence the geochemical evolution of the Milk River groundwater.

A secondary objective of this study was to use the trace element data in the geochemical modeling code PHREEQC, utilizing the *Wateq4f* thermodynamic database, to evaluate geochemical interactions between the waters and the aquifer rocks. Ion-speciation and solid-phase solubility calculations have been used to develop a better understanding of the geochemical processes that control the chemical composition of aquifer waters. Geochemical modeling involves ion-speciation and solubility calculations, and the results are compared to the observed mineralogical assemblage of the aquifer rocks (Parkhurst, 1995). Correspondingly, speciation modeling of REEs in the Milk River aquifer groundwater has been evaluated primarily to assess the importance of carbonate (LnHCO_3^{2+} , LnCO_3^+ and $\text{Ln}(\text{CO}_3)_2^-$) and phosphate ($\text{LnH}_2\text{PO}_4^{2+}$, LnHPO_4^+ , $\text{Ln}(\text{HPO}_4)_2^-$ and LnPO_4^0) complexes, where Ln stands for lanthanide. Traditionally, the elements have La-Lu have been referred to as lanthanides in the chemical literature, but as rare earth elements in geological usage.

1.3 Trace Elements in Groundwater Studies

Major cations (Ca^{2+} , Mg^{2+} , Na^+ , K^+) and anions (HCO_3^- , SO_4^{2-} , Cl^-) have been used extensively to trace the geochemical evolution of groundwaters. Recently, however, evaluation of trace elements, as well as distributions in rock and minerals including the REEs, has proved to be a powerful tool in geochemical investigations (Deverel and Millard, 1988; Dickson and Herczeg, 1992; Duro et al., 1997; Edmunds et al., 1982; Fee et al., 1992; Frapporti et al., 1993; Gascoyne, 1997; Giblin and Dickson, 1992; Gosselin et al., 1992; Johannesson and Lyons, 1995; Johannesson et al., 1997; Kreamer et al., 1996; Miekeley et al., 1992; Möller et al., 1992; and Smedley, 1991). Minor attention has been paid to the occurrence of these trace elements in aqueous systems, principally due to their low abundances and the consequent difficulty of precise and accurate analysis. The advent of the inductively coupled plasma - mass spectrometer (ICP-MS) has enabled much more rapid analysis of aqueous solutions, and with much lower detection limits than conventional ICP-AES methods. These studies employ the concentrations of trace elements, including the rare earth elements (REEs), as a complementary tool to the major elements. Studies of aqueous REEs have primarily involved the examination of their concentrations in *seawaters* (e.g., DeBaar et al., 1983; Möller et al., 1992; Shabani et al., 1990; and Shimizu et al., 1994), *rivers* and *lakes* (Elderfield et al., 1990; Johannesson and Lyons, 1995; and Möller and Bau, 1993), and *groundwaters* (Smedley, 1991).

Knowledge of the distribution and chemical behavior of REEs in these natural terrestrial waters, including groundwaters, is still limited (Table 1.1). Studies show that waters primarily inherit their REE signatures from interactions with rocks in the aquifers, but they are also affected by solution complexation, and those with multiple oxidation states (Ce, Eu) are influenced by redox controls (Elderfield et al., 1990; and Gosselin et al., 1992). This study will add to the limited work on the REE geochemistry of nonsaline groundwaters in contact with host rocks for extended periods of time. Gosselin et al.

(1992) emphasized possible difficulties in interpreting these REE patterns, due to fractionation by processes such as complex formation, ion exchange, absorption/desorption, and colloid transport.

1.4 Structure of the Thesis

The geology, hydrogeology, and geochemical characteristics of the Milk River aquifer are synthesized from previous studies in Chapter 2. To provide background for the thesis Chapter 3 describes the methodology of sample collection and analysis, and geochemical modeling. A standardized groundwater sampling protocol in the field and lab conditions is important in order to ensure data quality. Chapter 3 also includes a discussion on the advantages and disadvantages of the inductively coupled plasma - mass spectrometer (ICP-MS) and inductively coupled plasma - atomic emission spectrometer (ICP-AES) for analysis, and the complementary nature of employing both methods in groundwater studies. The trace element data for Milk River groundwater samples are reported in Chapter 4, which also includes a discussion on the hydrogeochemical characteristics of the waters through a redox boundary(ies) along the flow path. In addition, Chapter 4 incorporates the results of geochemical modeled trace element data, in an attempt to understand the hydrogeological and geochemical interactions that occur between the Milk River aquifer groundwater and the aquifer rocks. The final chapter (Chapter 5) summarizes the conclusions of this study, as well as the implications of the results obtained. The results and implications of this study may be of use to many other similarly confined aquifer systems.

Table 1.1. Select studies and papers based on trace and rare earth elements in aqueous geochemistry, with sources.

Field Area/Study	Characteristics	Trace Elements	Methodology	Source
Natural water compositions and Post-Archean average Australian shale(PAAS)	Global averages	Major and trace elements	Literature survey	1
Trace metals in a river water reference material	Rapid multi-element analysis using ICP-MS	Trace elements	Lab - ICP-MS	2
Stable isotope dilution of water samples by ICP-MS	Determine trace metals in nonsaline waters	Ni, Cu, Sr, Cd, Ba, Tl, and Pb	Lab - ICP-MS	3
Trace elements in shallow groundwater of the western San Joaquin Valley, California	Distribution and mobility of selenium and other trace elements	Trace elements	Field and lab ASS and colorimetric	4
Rare earth Elements in river waters	Measured and observed REE patterns in selected rivers	REEs	Field and lab sequential ionization	5
Geochemistry in river-groundwater in Glattfeldon, Switzerland	Geochemical changes along infiltration flow path	Major and trace metals	Field and lab Various methods	6
Trace elements in surface waters	Applicability of ICP-MS to determine trace elements in lakes	Trace elements (n=49)	Lab - ICP-MS	7
REE systematics in hydrothermal fluids	Removal and transportation of REEs during hydrothermal alteration	REEs and major elements	Field and lab REEs - isotope dilution	8
Groundwater chemistry and water-rock interactions at Stripa	Granitic groundwater chemistry measured and interpreted	Major and traces elements	Field and lab ICP-ES and direct-current ES	9
REEs in rivers, estuaries, and coastal seas and significance to the composition of ocean waters	Processes affecting chemical continuity between the crust, rivers and sea water	REEs	Field and literature survey	10
Aqueous geochemistry of REEs and yttrium	Low-temperature data for inorganic complexes and REE speciation in natural waters	REEs and Yttrium	Lab - various methods	11
Aqueous geochemistry of REEs and yttrium	Speciation in hydrothermal solutions to 350 °C at saturation vapor pressure	REEs and Yttrium	Lab - various methods	12
REEs in Carmenellis area, southwest England	Controls on REE chemistry	REEs, trace, and major elements	Field - ICP-MS	13
Modeling REEs in seawaters and brines	Ionic interaction models	REEs	Lab - modeling	14
Deposition of trace elements and radionuclides, Lake Tyrrell, Victoria, Australia	Analyzed waters in the spring zone	Trace and major elements including radionuclides	ICP-AES and AAS	15
Source, distribution and economic significance of trace elements in Lake Tyrrell, Victoria, Australia	Analyzed and modeled waters for economic potential	Trace elements	ICP-AES	16
REEs in Palo Duro Basin, Texas, USA	Inferring groundwater flow using REEs	REEs	Field - Radiochemical neutron activation activation	17

Table 1.1. continued.

Field Area/Study	Characteristics	Trace Elements	Methodology	Source
Rare-earth elements from mine groundwaters	REEs measured from the Osumu mine and Morro do Ferro analogue study sites Poços de Caldas, Brazil	REEs	Field and lab ICP-AES preconc.	18
Suspended particles and colloid in mine groundwaters	REEs concentrations from the Osumu mine and Morro do Ferro analogue study sites Poços de Caldas, Brazil, waters - >450nm and <450 nm	REEs	Field and lab ICP-AES preconc.	19
REEs in seawater	Determine REE profiles	REEs	Field -preconc. Lab - ICP-MS	20
Trace metals in brines, from Lake Tyrell, Victoria, Australia	Effects of pH and Eh on the concentration of trace	Fe, Mn, Pb, Cu, and Zn	Field and lab GFAAS	21
REEs in Lake Tyrell groundwaters, Victoria, Australia	Analysis of REEs and patterns plotted	REEs	Field and lab ICP-MS	22
Hydrogeochemistry of deep formation brines in the central Sichuan Basin, China	Major elements analyzed and brines identified	Major and trace elements	Field and lab method ?	23
Water analysis using ICP-MS and ICP-ES	round-robin evaluating quality of data from private sector labs	Major and trace elements	Labs -ICP-MS Labs -ICP-AES	24
Rare-earth elements in Lake Van, Turkey	REE patterns for alkaline waters	REEs	Field sampling	25
Preconcentration and Purification of REEs in natural waters	Determine REEs in water using isotope-dilution ICP-MS	REEs	Lab - ICP-MS	26
Natural trace element concentrations in groundwater	A conceptual stochastic model - variability in trace elements in groundwaters	Trace elements	Lab - modeling code	27
REEs in surface waters	Application of rapid and cost effective method in determining REEs in waters	REEs	Lab - ICP-MS	28
REE geochemistry of Colour Lake and a lake on Axel Heiberg Island Northwest Territories, Canada	REE patterns and speciation modeling	Major and REEs	Field and lab ICP-MS - REEs and cations	29
Hydrogeochemistry of the Fraser River, British Columbia	Seasonal variations of waters analyzed and plotted	Major and trace elements	ICP-AES, Atomic Absorption, and Colorimetry	30

Table 1.1. References

- 1 Taylor and McLennan (1985) *The Continental Crust: Its Composition and Evolution*. Blackwell Scientific. 312 p.
- 2 Beauchemin, D., McLaren, J. W., Mykytiuk, A. P., and Berman, S. S. (1987) Determination of trace metals in a river water reference material by inductively coupled plasma mass spectrometry. *Anal. Chem.* **59**, 778-783.
- 3 Garbarino, J. R., and Taylor, H. E. (1987) Stable isotope Dilution Analysis of hydrologic samples by inductively coupled mass spectrometry. *Anal. Chem.* **59**, 1568-1575.
- 4 Deverel, S. J., and Millard, S. P. (1988) Distribution and mobility of selenium and other elements in shallow groundwater of the western San Joaquin Valley, California. *Environ. Sci. Technol* **22**, 697-702.
- 5 Goldstein, S. J., and Jacobsen, S. B. (1988) Rare earth elements in river waters. *Earth and Planetary Science Letters* **89**, 35-47.
- 6 Jacobs, L. A., Von Gunten, H. R., Keil, R., and Kuslys, M. (1988) Geochemical changes along a river-groundwater infiltration flow path: Glattfelden, Switzerland. *Geochimica et Cosmochimica Acta* **52**, 2693-2706.
- 7 Henshaw, J. M., Heithmar, E. M., and Hinnners, T. A. (1989) Inductively coupled plasma mass spectrometric determination of trace elements in surface waters subject to acidic deposition. *Anal. Chem.* **1989**, 335-342.
- 8 Michard, A. (1989) Rare earth systematics in hydrothermal fluids. *Geochimica et Cosmochimica Acta* **53**, 745-750.
- 9 Nordstrom, D. K., Ball, J. W., Donahoe, R. J., and Whitemore D. (1989) Groundwater chemistry and water-rock interactions at Stripa. *Geochimica et Cosmochimica Acta* **53**, 1727-1740.
- 10 Elderfield, H., Upstill-Goddard, R., and Sholkovitz, E. R. (1990) The rare earth elements in rivers, estuaries, and coastal seas and their significance to the composition of ocean waters. *Geochimica et Cosmochimica Acta* **54**, 971-991.
- 11 Wood, S. A. (1990) The aqueous geochemistry of rare-earth elements and yttrium. 1. Review of available low-temperature data for inorganic complexes and the inorganic REE speciation of natural waters. *Chemical Geology* **82**, 159-186.
- 12 Wood, S. A. (1990) The aqueous geochemistry of rare-earth elements and yttrium. 2. Theoretical predictions of speciation in hydrothermal solutions to 350 °C at saturation water vapor pressure. *Chemical Geology* **88**, 99-125.
- 13 Smedley P. L. (1991) The geochemistry of rare earth elements in groundwater from the Carmenellis area, southwest England. *Geochimica et Cosmochimica. Acta* **55**, 2767-2779.
- 14 Millero, F. J. (1992) Stability constants for the formation of rare earth inorganic complexes as a function of ionic strength. *Geochimica et Cosmochimica Acta* **56**, 3123-3132.
- 15 Dickson, B. L., and Herczeg, A. L. (1992) Deposition of trace elements and radionuclides in the spring zone, Lake Tyrrell, Victoria, Australia. *Chemical Geology* **96**. 151-166
- 16 Giblin, A. M., and Dickson, B. L. (1992) Source, distribution and economic significance of trace elements in groundwaters from Lake Tyrrell, Victoria, Australia. *Chemical Geology* **96**. 133-149.
- 17 Gosselin, D. C., Smith, M. R., Lepel, E. A., and Laul, J. C. (1992) Rare earth elements in chloride-rich groundwater, Palo Duro Basin, Texas, USA. *Geochimica et Cosmochimica Acta* **56**, 1495-1505.
- 18 Miekeley, N., Coutinho de Jesus, H., Porto da Silveira, C. L., Linsalata, P., and Morse, R. (1992) Rare-earth elements in groundwaters from the Osamu Utsumi mine and Morro do Ferro analogue study sites, Poços de Caldas, Brazil. *Journal of Geochemical Exploration* **45**, 365-387.
- 19 Miekeley, N., Coutinho de Jesus, H., Porto da Silveira, C. L., Linsalata, P., and Morse, R. (1992) Chemical and physical characterization of suspended particles and colloids in waters from the Osamu Utsumi mine and Morro do Ferro analogue study sites, Poços de Caldas, Brazil. *Journal of Geochemical Exploration* **45**, 409-437.
- 20 Möller, P., Dulski, P., and Luck, J. (1992) Determination of rare earth elements in seawater by inductively coupled plasma-mass spectrometry. *Spectrochimica Acta* **47B**, 1379-1387.
- 21 Lyons, W. B., Welch, S., Long, D. T., Hines, M. E., Giblin, A. M., Carey, A. E., Macumber, P. G., Lent, R. M., and Herczeg, A. L. (1992) The trace-metal geochemistry of the Lake Tyrrell system brines (Victoria, Australia). *Chemical Geology* **96**, 115-132.

Table 1.1. continued.

- 22 Fee, J. A., Guadette, H. E., Lyons, W. B., and Long, D. T. (1992) Rare-earth element distribution in Lake Tyrrell groundwaters, Victoria, Australia. *Chemical Geology* **96**, 67-93.
- 23 Xun, Z., and Cijun, L. (1992) Hydrogeochemistry of deep formation brines in the central Sichuan Basin, China. *Journal of Hydrology* **138**, 1-15.
- 24 Hall, G. E. M. (1993) Capabilities of production-oriented laboratories in water analysis using ICP-ES and ICP-MS. *Journal of Geochemical Exploration*, **49**, 89-121.
- 25 Möller, P., and Bau, M. (1993) Rare-earth patterns with positive cerium anomaly in alkaline waters from Lake Van, Turkey. *Earth and Planetary Science Letters* **117**, 671-676.
- 26 Esser, B. K., Volpe, A., Kenneally, J. M., and Smith, D. K. (1994) Preconcentration and purification of rare earth elements in natural waters using silica-immobilized 8-hydroxyquinoline and a supported organophosphorous extractant. *Anal. Chem.* **66**, 1736-1742.
- 27 Ramaswami, A., and Small, M. J. (1994) Modeling the spatial variability of natural trace element concentrations in groundwater. *Water Resources Research* **30**, 269-282.
- 28 Hall, G. E. M., Vaive, J. E., and McConnell, J. W. (1995) Development and application of sensitive and rapid analytical method to determine the rare-earth elements in surface waters. *Chemical Geology* **120**, 91-109.
- 29 Johannesson, K. H., and Lyons, W. B. (1995) Rare-earth element geochemistry of Colour Lake, an acidic freshwater lake on Axel Heiberg Island, Northwest Territories, Canada. *Chemical Geology* **119**, 209-223.
- 30 Cameron, E. M. (1996) Hydrogeochemistry of the Fraser River, British Columbia: seasonal variation in major and minor components. *Journal of Hydrology* **182**, 209-225.

Chapter 2

Geological and Hydrogeology Background

2.1 Geology

The Milk River artesian aquifer underlies more than 15,000 km² of southern Alberta, Canada (Hendry and Schwartz, 1988). The aquifer system consists of the Milk River Formation sandstone, shale of the Colorado Group (confined below), and the Pakowki Formation (confined above), all of Cretaceous age. The Colorado Group consists mainly of dark grey to black bentonitic marine shales which range in thickness from 500 to 650 m. The lower beds consist of several thin sandstone units, the most important of which in terms of gas and groundwater is the Bow Island sandstone (Hendry et al., 1990). The overlying Milk River Formation varies in thickness from 90 to 145 m; it crops out, or subcrops, in the southern part of the study area (Fig. 2.1). This formation's lower unit is referred to as the Milk River sandstone, a succession of massive marine sandstones interbedded with grey shales, which conformably overlies the Colorado Group. The upper unit consists of a thick succession (20-60 m) of cross-bedded, non-marine sandstones, green shales, carbonaceous shales, thin coal seams, and thin sandstone units (Hendry et al., 1990). The Pakowki Formation unconformably overlies the Milk River Formation and consists of grey bentonitic shales with thin bentonite beds. In the northeastern part of the study area the Pakowki Formation is 120 m thick, but thins to the west. Near surface deposits consist of other fine-grained Cretaceous rocks and Quaternary glacial drift (Fig. 2.2; Hendry et al., 1990).

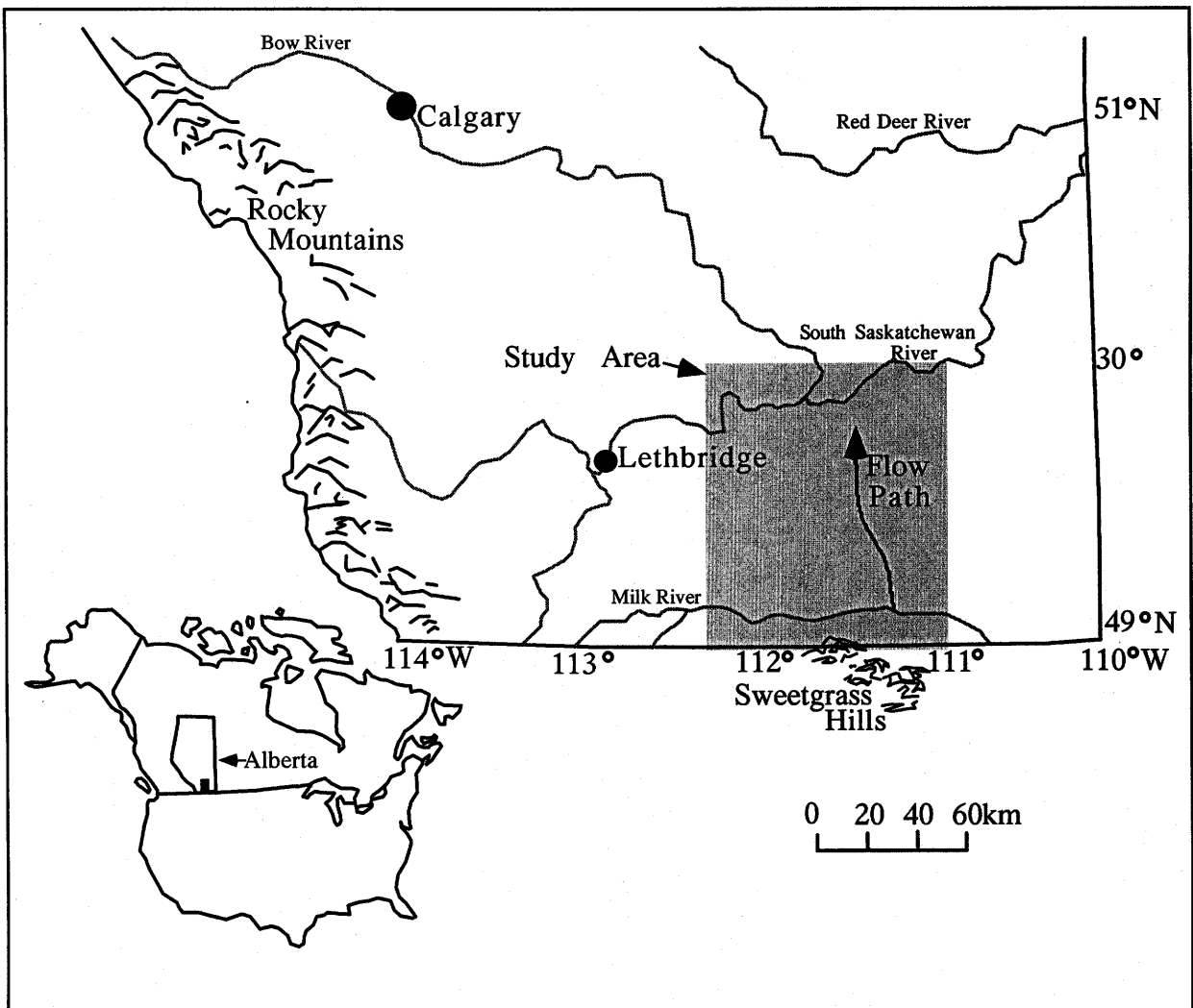


Figure 2.1. Location of the Milk River aquifer study area in southern Alberta, Canada, illustrating the flow path studied (modified from Hendry et al., 1988).

Development of the Sweetgrass Arch in south-central Alberta caused the strata to dip gently toward the north. Subsequent erosion of the Upper Cretaceous and Tertiary deposits during the Pliocene and Pleistocene exposed concentric outcrops of the Milk River sandstone around the Sweetgrass Hills (Fig. 2.1). Consequently these outcrops are the dominant recharge area for the Milk River aquifer (Meyboom, 1960). Hendry and Schwartz (1988) estimate that erosion exposed the aquifer ~0.5 Ma ago (Fig. 2.3).

2.2 Hydrogeology

Exploitation of water from the Milk River aquifer began in the early 1900's. However, by the 1960's, long-term withdrawals eventually lowered the piezometric surface, reversing the gradient in the east-central areas of the aquifer (Fig. 2.4). Given these perturbations to the piezometric surface, the best estimate is that the groundwater generally flows in the direction of the dip in the aquifer, towards the north, west and east (Hendry et al., 1990).

Transmissivity decreases from the south to the north, west and east. General thinning of the Milk River aquifer in these directions and a reduction in hydraulic conductivity toward the north due to an increase in shale content, are the likely causes of decreasing transmissivity values (Fröhlich et al., 1991). Vertical hydraulic conductivity for the Colorado Group shales was estimated by Hendry and Schwartz (1988) to range from 10^{10} to 10^{-14} m/s. Uniformity of lithology with the Colorado Group, taken with calculations based on groundwater model studies, yielded estimates for hydraulic conductivity for the Pakowki Formation to be about 10^{-13} m/s (Phillips et al., 1986; Hendry and Schwartz, 1988).

A range of estimates of residence time for the groundwater in the aquifer have been proposed Schwartz and Muehlenbachs, 1979; Phillips et al., 1986; Hendry and Schwartz, 1988. Schwartz and Muehlenbachs (1979) estimate the age as 300 ka based on hydraulic arguments. Phillips et al. (1986) used a flow model to calculate residence

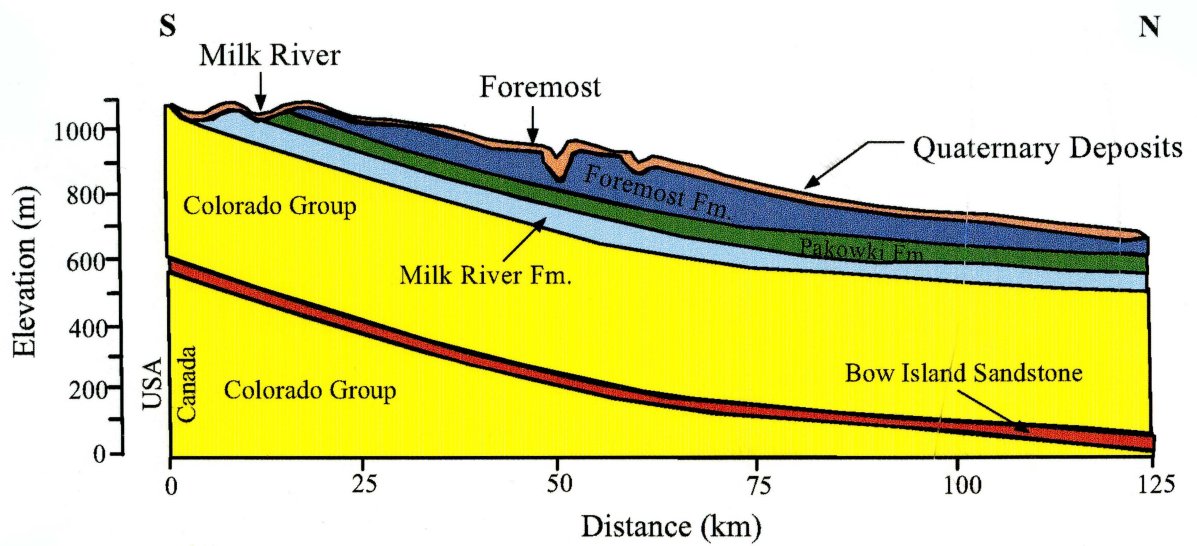


Figure 2.2. The geology of the Milk River aquifer along flow path (modified from Hendry et al., 1991).

times of 500 ka for the flow to the northern margin of the aquifer. Hendry and Schwartz (1988) estimate the residence time at the end of two flow paths to be 250 and 510 ka respectively (Figure 1 from Hendry et al., 1991). Hendry et al. (1991) suggested that a northward decrease in hydraulic conductivity results in the much shorter residence times in the southern half of the aquifer, as compared to the northern half.

As noted above, the Milk River Formation is confined above and below by low permeability marine shales. The dominant mechanism for water loss from the aquifer is via leakage through the overlying Pakowki Formation. Based upon the hydraulic gradient measured with piezometers, the underlying Colorado Group shales may also act as a sink for water from the Milk River aquifer (Hendry and Schwartz, 1988). This may be a result of the elastic rebound of the shales, following Pliocene and Pleistocene erosion of >700m of land surface and glacial unloading (Tóth and Corbet, 1986).

2.3 Geochemistry

The geochemistry of the aquifer groundwater is important for understanding the process(es) that operate in the aquifer. Several examples of these processes include: ion exchange of Na^+ on the solids for Ca^{2+} and Mg^{2+} in solution, sulphate reduction; methane fermentation; and carbonate dissolution (Hendry and Schwartz, 1990). A salient characteristic of the Milk River aquifer is the consistency in the distribution of major ions and isotopic composition of O and H (Hendry et al., 1991). Important dissolved major ions include Ca, Mg, Na, K, Cl, SO_4 , HCO_3 and CO_3 . Generally, the concentration of Cl, Na, and $\text{HCO}_3 + \text{CO}_3$ are the lowest in the recharge area, but increase progressively along the flow path. Hendry et al. (1991) observed that Cl concentrations range from <0.05 mmol/L at the southern boundary of the study area to >30 mmol/L in the northwestern part of the aquifer, and similarly Na concentrations were ~15 mmol/L and >50 mmol/L respectively. Concentrations of $\text{HCO}_3 + \text{CO}_3$, which are dominated by HCO_3 , ranged from <12 mmol/L to >12 mmol/L along the flow system (Fig. 2.5). Hendry et al. (1991) reported that both Ca and Mg ions show similar

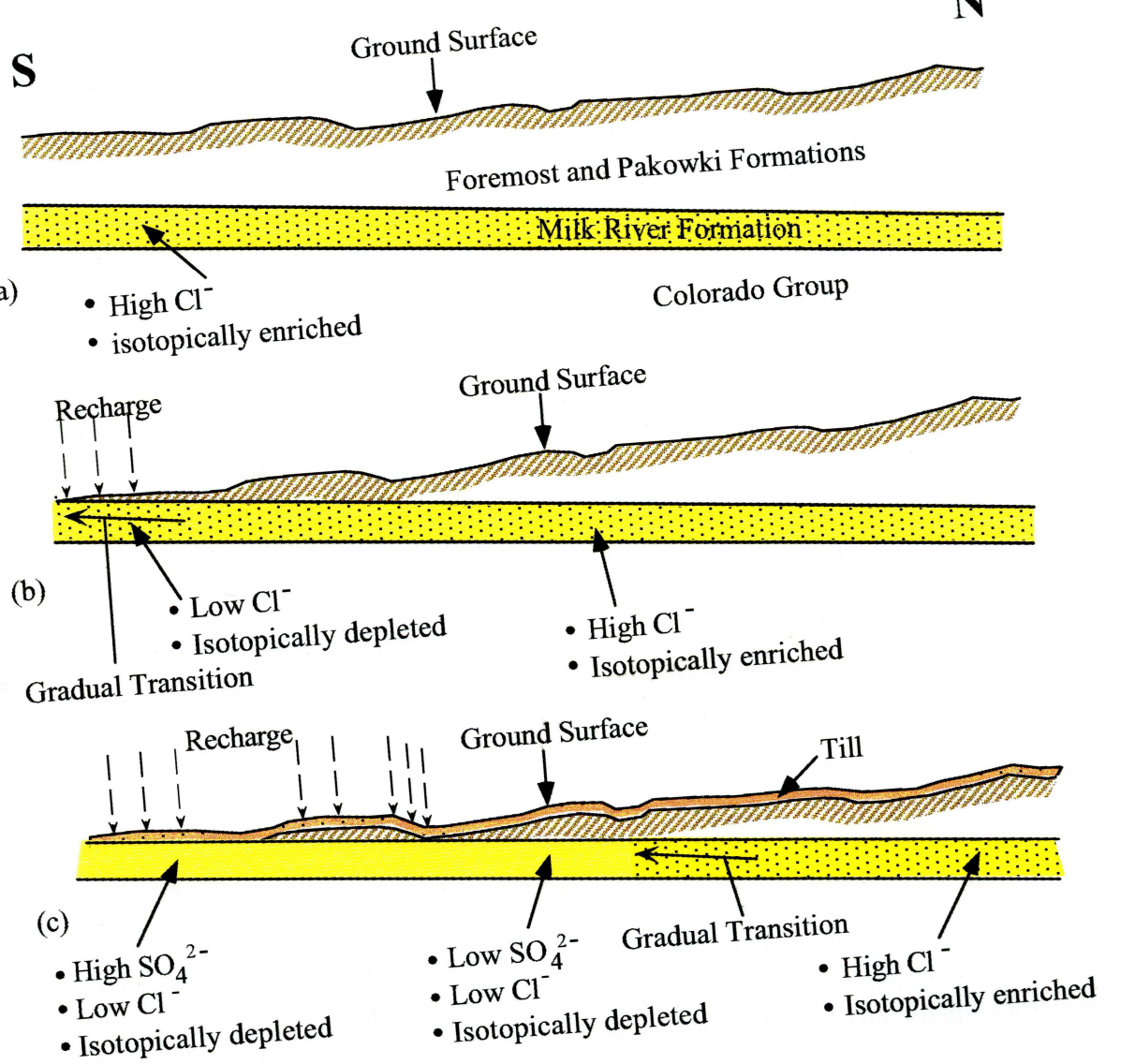


Figure 2.3. Geological evolution of the Milk River aquifer: (a) initial conditions; (b) effects of erosion approximately 5×10^5 years ago; and (c) glaciation approximately 30,000 - 40,000 years ago (after Hendry and Schwartz, 1990a).

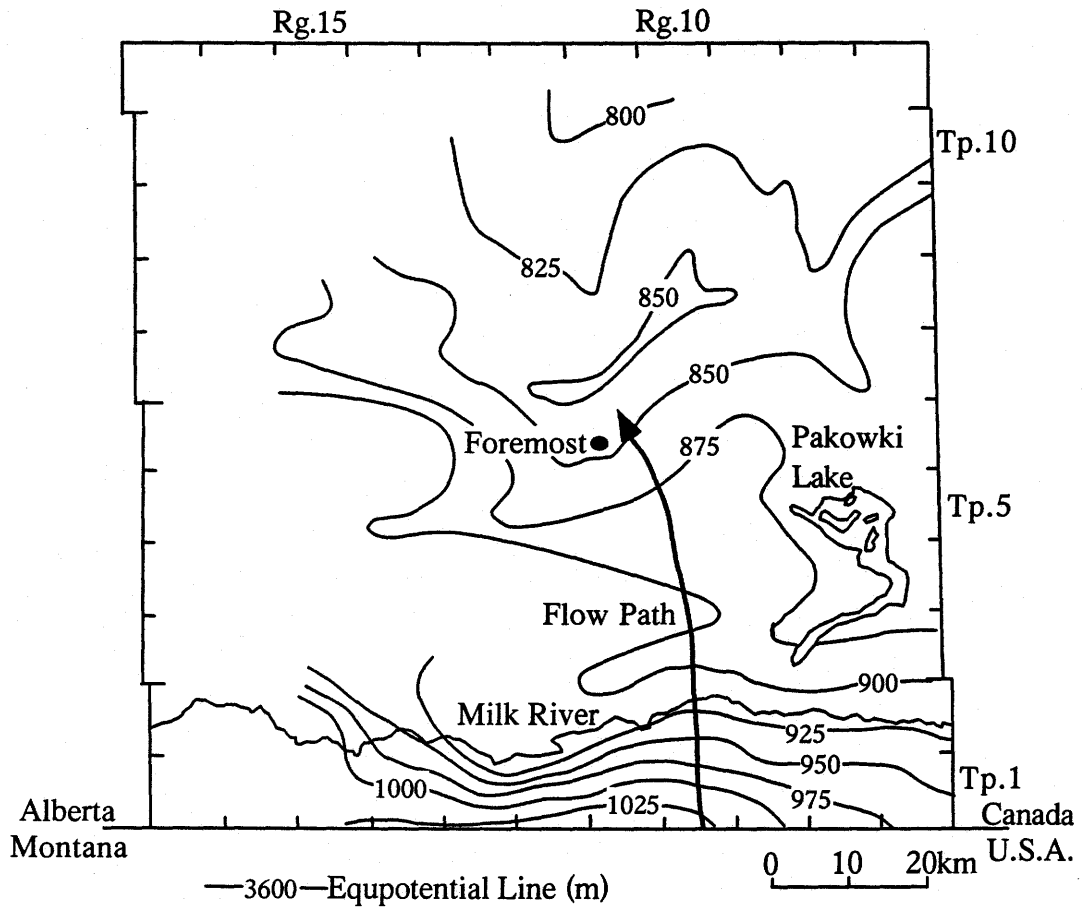


Figure 2.4. Piezometric surface in the Milk River aquifer (from Hendry and Schwartz, 1988).

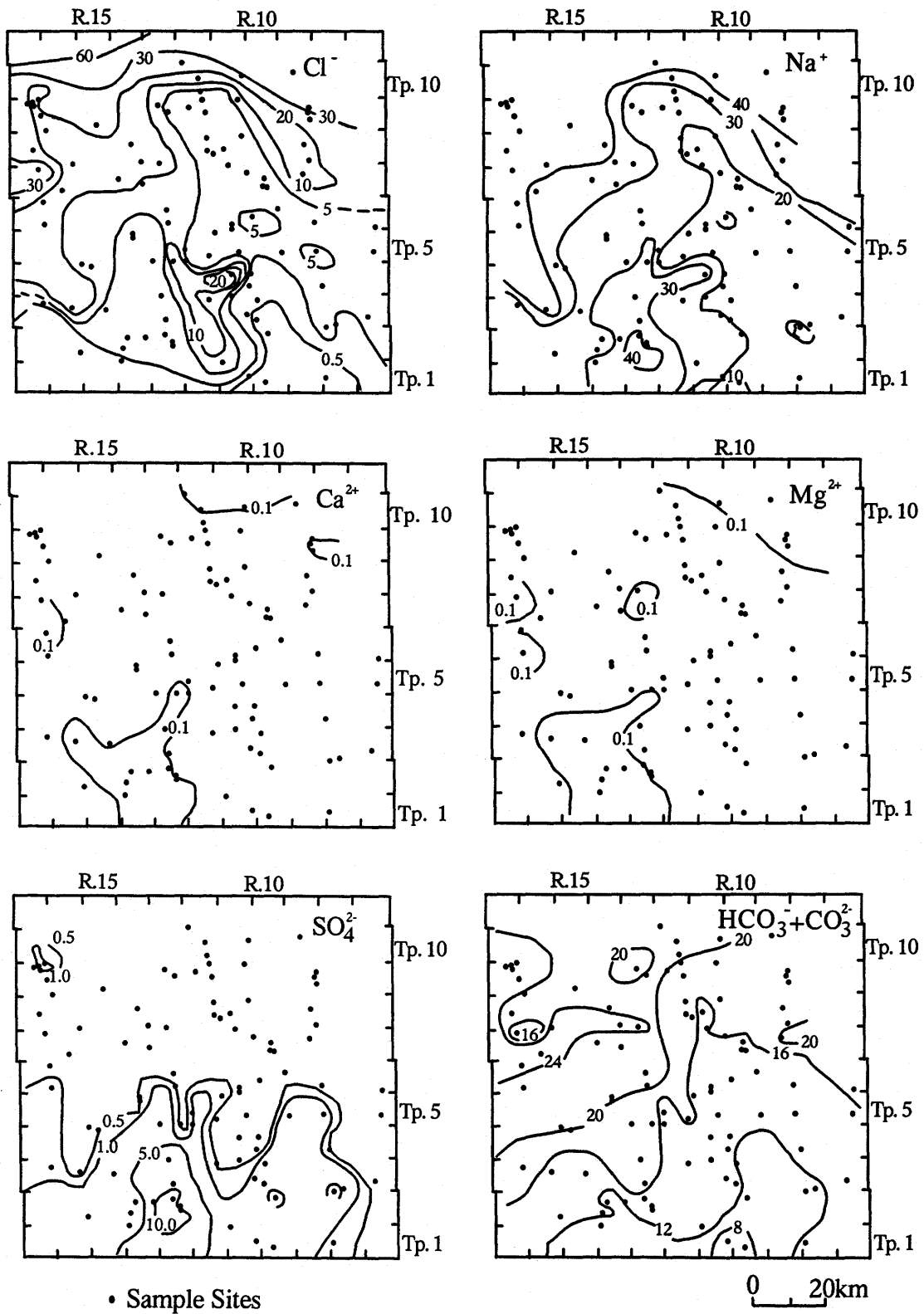


Figure 2.5. Spatial variations in dissolved ions in mmol/L (from Hendry et al., 1990a).

patterns, and concentrations are typically <0.1 mmol/L. However, concentrations >0.1 mmol/L are found in the northeastern margin of the aquifer. In contrast, the distribution of SO_4 varies from >5 mmol/L in the south to <0.1 mmol/L throughout the remainder of the aquifer.

In the area where the aquifer subcrops the patterns of ion concentrations differ somewhat from those discussed above. SO_4 , Na, Ca and Mg concentrations are higher than expected from trends farther north in the aquifer. Recent recharge (possibly <40 ka B.P.) through the overlying glacial tills may account for these high concentrations (Hendry and Schwartz, 1990a). Field measurements of pH for the Milk River aquifer decreases from >9.0 in the south to 8.2 in the north. Where the aquifer subcrops values are <8.5 (Fig. 2.6; Hendry et al., 1991).

2.4 Proposed Geochemical Models

Accounting for the distribution of nonreactive ions and isotopes within the Milk River aquifer has been problematical. Four mechanisms have been suggested to explain the origin of the chemical and isotopic patterns: (1) megascopic dispersion (Schwartz and Muelenbachs, 1979; Schwartz et al., 1981), the introduction of connate formation water through the Colorado shale and mixing with infiltrating meteoric water; (2) a finite source of meteoric recharge mixing with more saline water in the aquifer (Domenico and Robbins, 1985); (3) membrane filtration (Phillips et al., 1986, 1990), a process of chemical and isotopic enrichment due to ion filtration; and (4) aquitard diffusion from the confining Colorado shales into the aquifer (Hendry and Schwartz, 1988, 1990b).

In the megascopic dispersion model it was proposed that the groundwater entered the aquifer from below and added chemically distinct water to the pre-existing water of the aquifer (Schwartz and Muehlenbachs, 1979; Schwartz et al., 1981). The inflow at the base coupled with the outflow along the top of the aquifer would eventually bring about the change in the water chemistry (Fig. 2.7.a). Tóth and Corbet (1986) and Hendry and

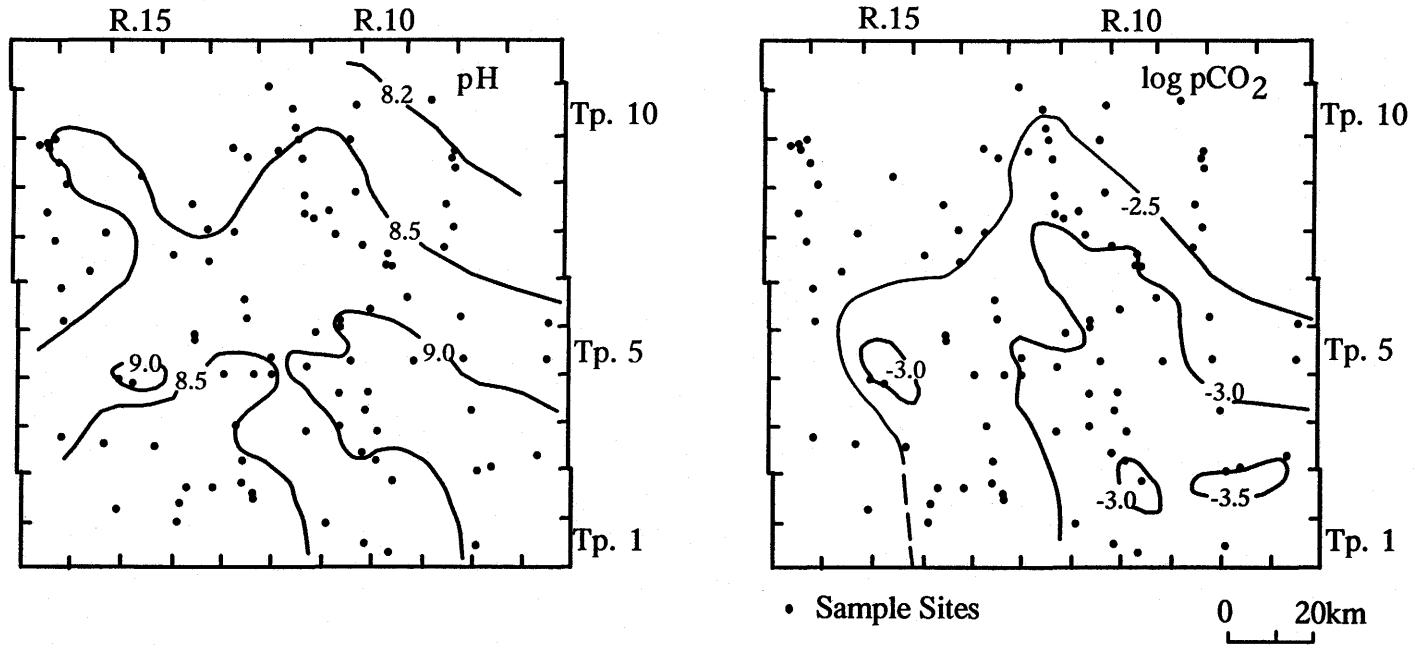


Figure 2.6. Spatial variations in field pH, and calculated pCO₂ (from Hendry et al., 1990a).

Schwartz (1988) have shown that this model necessitates the advection of water and solutes through the Colorado shale in a direction that is most likely opposite to the measured hydraulic gradient.

Domenico and Robbins (1985) proposed a model in which fresh meteoric recharge enters only a fraction of the total inflow area, and that elsewhere the groundwater is more saline and isotopically enriched (Fig. 2.7b). Hendry and Schwartz (1988) argued that whereas this model explains to some extent the northward trending plume of fresher meteoric water, it does not account for the broad pattern of mixing that has fresh, isotopically depleted water in the southern end, and more saline and isotopically enriched waters in the northern end of the flow system separated by a transition zone. Neither of the above models can account in a simple way for the nonlinear relationship between Cl⁻ and $\delta^{18}\text{O}$ (Hendry and Schwartz, 1988).

Phillips et al. (1986) developed a model based on the hypothetical process of membrane filtration to account for the distribution of chemical and isotopic species in the Milk River aquifer (Fig. 2.7c). In this model the chemical and isotopic species, including Cl, δD , and $\delta^{18}\text{O}$ accumulate because the confining aquitards function as membranes when the groundwater passes through them. This process, operating through geologic time would produce a progressive increase in concentrations of ions such as Cl, and an isotopic shift to enriched δD and $\delta^{18}\text{O}$. However, Hendry and Schwartz (1988) reported data from one piezometer completed in the Colorado shale where porewaters have Cl concentrations, and δD and $\delta^{18}\text{O}$ values that are higher than in the water from the overlying aquifer. Therefore, if membrane filtration was occurring, the ground water in the aquifer should have higher concentrations than the water in the aquitards but this is not observed (Hendry and Schwartz, 1988).

The diffusion model proposed by Hendry and Schwartz (1988 & 1990b) explains the distribution of Cl in the aquifer groundwater as being the result of a diffusion gradient between saline water in the aquitard and the fresh recharge water in the aquifer (Fig.

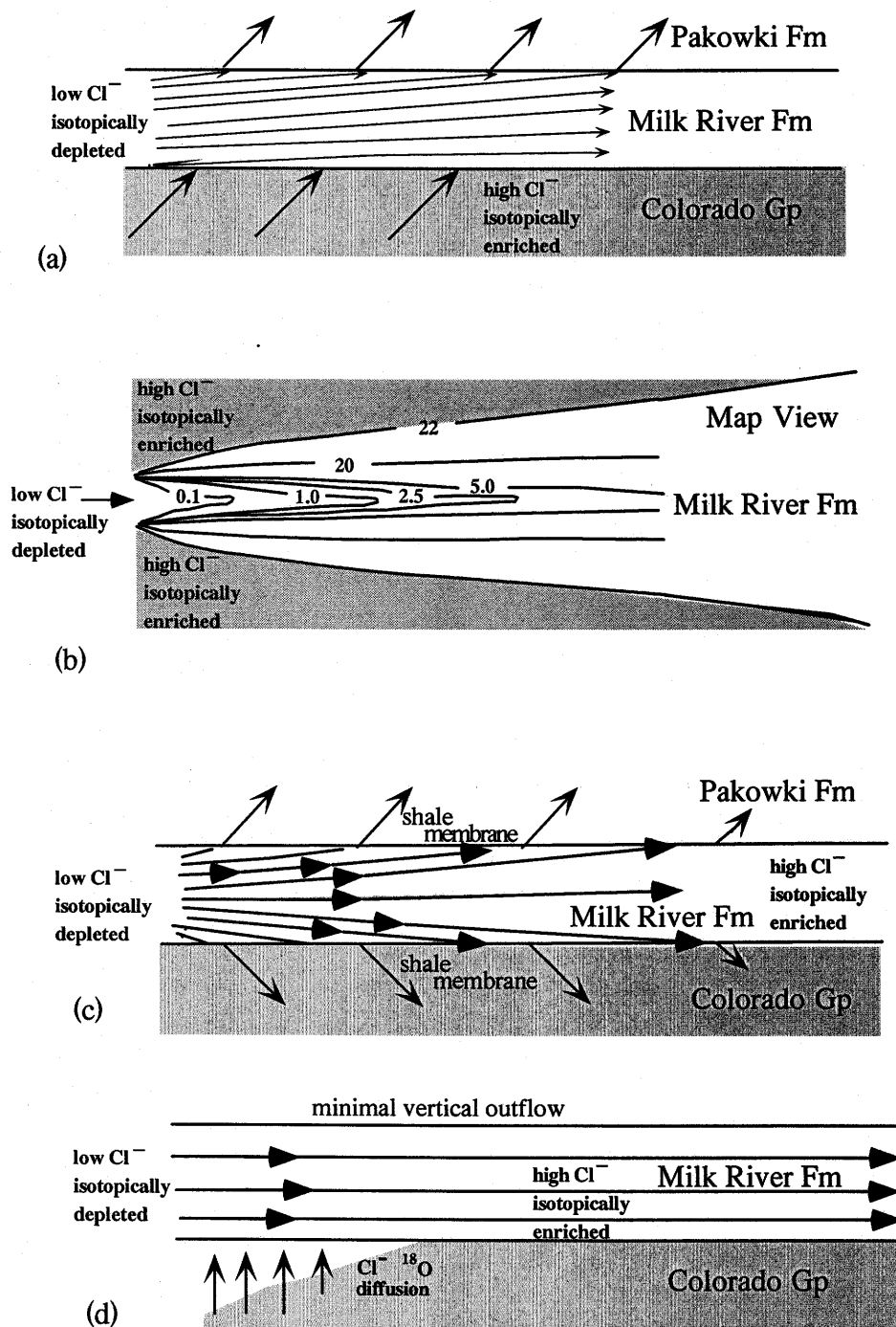


Figure 2.7. Conceptual models to explain the origin of the distribution of chemical and isotopic species in the Milk River River aquifer: (a) megascopic dispersion (Schwartz and Muelenbachs, 1979); (b) limited recharge area (Domenico and Robbins, 1985); (c) membrane filtration (Phillips et al., 1986); and (d) aquitard diffusion (Hendry and Schwartz, 1988) (from Hendry and Schwartz, 1988).

2.7d). Accumulation of Cl is the result of the Colorado group and Pakowki Formation shales acting as semi-permeable membranes. The residual solution becomes enriched in Cl as the water leaks out of the aquifer. Fabryka-Martin et al. (1987) proposed a similar hypothesis to the diffusion model where they suggest that the Cl and Na in the aquifer waters diffuse from the clay units within the Milk River Formation.

2.5 Halogens in the Milk River aquifer

Fabryka-Martin et al. (1991) present data for Cl, Br and I in the Milk River aquifer. The three halogens show a similar spatial distribution and are highly correlated. Concentrations are low in the freshwater dominated recharge zone of high-transmissivity, but increase by as much as two orders of magnitude along the margins and the distal end of the aquifer. Ratios of Cl/I and Cl/Br are less than for seawater, and are consistent with an origin from the diagenesis of organic matter in the shales. Halogen ratios are near uniform moving down-gradient, suggesting the dominance of a common subsurface source for these ions. Halogen ratios also rule out unmodified seawater, or leakage and/or diffusion from the underlying Colorado Group, as major influences on the aqueous chemistry. Therefore, the above authors propose a fifth conceptual model to explain the distribution and origin of the halogens, as well as several aqueous species. In this model, the major sources of the halogens is from diffusion from less permeable sedimentary rocks within the aquifer, with their transport by advection and dispersion as modeled by Hendry and Schwartz (1988). This hypothesis of an internal source has important implications for solute sources in other aquifers affected by saline waters because it does not require the input of distant fluids (Fabryka-Martin et al., 1991).

Iodine-129/I ratios measured by Fabryka-Martin et al. (1991) were found to have a meteoric value in groundwater collected near the recharge area, but ratios for the downflow waters are only 8-70% of this value. Given that ¹²⁹I has a half-life of 16 Ma this data indicates that most of the increase in dissolved iodine cannot be of a meteoric

source by ion filtration, but rather must have a subsurface origin. Concentrations of ^{129}I produced in situ by spontaneous fission of ^{238}U are only measurable in the older waters (ages $\geq 10^5$ a), in which it may account for nearly 90% of the total dissolved ^{129}I concentration.

2.6 Dissolved Gases

Andrews et al. (1991a) discuss in detail the geochemical relations among the noble gases, the $^{36}\text{Ar}/^{40}\text{Ar}$ isotope ratio, and N_2 contents of the Milk River aquifer groundwater. The origin of radiogenic He, radiogenic Ar and CH_4 in the Milk River aquifer groundwater is predominantly within the thick shale successions which form the bounding aquitards (Andrews et al., 1991a), or may also be from shale units within the aquifer, as discussed above for the halogens.

Stable isotope compositions of the Milk River aquifer groundwater suggest that the most recent recharge took place under cooler climatic conditions than earlier recharge episode(s). Estimates of recharge temperatures from noble gas data was only possible for samples with low CH_4 contents because of the outgassing effect of CH_4 on the dissolved noble gases. The inferred recharge temperature difference from the noble gas data of $\sim 4\text{-}5^\circ\text{C}$ is consistent with the stable isotope data (Andrew et al., 1991a).

The concentration of ^4He in the groundwater varies with depth according to the concentration/depth profile for the Milk River sandstone and Colorado shale, and this indicates that the diffusion constant for He loss from the formation is $\sim 0.00032 \text{ m}^2/\text{a}$. The corresponding flux of He from the surface of this lithology is $1.2\text{-}1.8 \times 10^8$ atoms/ m^2/s , which is $<2\%$ of independent estimates of the continental ^4He flux (Andrews et al., 1991a). This discrepancy confirms that the ^4He release from the continental crust must be a discontinuous process controlled by tectonic events (Torgersen, 1989) or aqueous transport.

Andrews et al. (1991b) determined that the fractional release of ^{222}Rn produced *in situ* from the rock matrix to the groundwaters of the Milk River sandstone has a mean value of 0.0027. Variations in ^{222}Rn concentrations throughout the aquifer are due to U content, porosity, and the proportion of fracture flow/efficiency which varies by $<\pm 25\%$ over most of the aquifer (Andrews et al., 1991a).

Andrews et al. (1991) concluded from the $^{13}\text{C}/^{12}\text{C}$ ratio of CH_4 that the gas is biogenic and its δD isotopic composition shows that it has not been produced in association with the meteoric waters which are now present in the aquifer. Isotopic ratios suggest that the CH_4 was produced within the adjoining shales as their connate waters were diluted by meteoric water which infiltrated the aquifer.

2.7 Age Dating Groundwaters

2.7.1 Radiocarbon and Stable Isotopes

The Milk River aquifer groundwater is considered to be very old and beyond the limit of ^{14}C dating by the end of the flow path (80-100 km). The understanding of the evolution of the carbon geochemistry and its effects on ^{14}C concentrations are acquired from the interpretation of ^{14}C data in terms of the water ages. Drimmie et al. (1991) summarize the distribution of δD and $\delta^{18}\text{O}$ in water, $\delta^{13}\text{C}$ and δD in CH_4 , $\delta^{34}\text{S}$ and $\delta^{18}\text{O}$ in SO_4 , $\delta^{13}\text{C}$ and ^{14}C in dissolved inorganic carbon (DIC) as well as dissolved organic carbon (DOC), and tritium in the Milk River aquifer.

Radiocarbon was found to be measurable only approximately in the first 20 km from the recharge zone of the Milk River aquifer (Drimmie et al., 1991). Transformation of the measured concentrations to water ages was difficult due to the complex geochemical system. Comparison of DIC and DOC dates shows that the former are much older than the latter, but the difference in years between the wells for all three types of C were within 1000a. The DOC dates led to the conclusion that the initial DIC radiocarbon

content was as low as 30% modern when the water entered the Milk River aquifer. The water 20 km from the recharge zone was estimated at ~20 ka, giving a velocity of ~1 m/a, and ~0.1 m/a or less in the northern sections of the aquifer (Drimmie et al., 1991). This result is much higher than estimates by other techniques.

Drimmie et al. (1991) used the stable isotopes of H and O to obtain information on the history and origin of groundwater in the Milk River aquifer. Three sections were clearly identified along the flow path: (1) a section with uniform $\delta^{18}\text{O}$ values between -20 and -18‰ , from the recharge zone for about 20 km; (2) a second area with only slightly higher δD and δO values which still reflects normal groundwater; (3) a third section where admixtures of isotopically modified water occurs (Drimmie et al., 1991). Groundwater in the second zone does not show a glacial signature and it was probably recharged under warmer climatic conditions. The water in the third zone is characterized by higher salinities and a pronounced oxygen and hydrogen isotope shift. A plausible conclusion would be mixing with the more saline formation waters in the Bow Island Formation. Drimmie et al. (1991) concluded that the shift resulted from diffusive processes involving the confining shales that would alter both the chemical and isotopic signatures.

Sulphate-S and sulphate-O isotope ratios were also used to indicate biological activity, which if present can perturb ^{14}C dates. If bacterial reduction does occur this would influence the C isotope composition of the DIC. Data from Drimmie et al. (1991) suggest that the till is a source of SO_4 . The S isotope data in the till and the recent high-S recharge water are consistent with these results implying that bacterial reduction is occurring.

The composition of CH_4 was measured to assist in determining its origin and the effect on the ^{14}C results. Drimmie et al. (1991) found that methane is present in most of the well waters measured, and based on C and H isotope data, it has a biogenic origin. It is

unclear whether the methane production occurs in the aquifer and/or it diffuses from the confining shales into the aquifer.

2.7.2 Chloride and ^{36}Cl Concentrations and Interpretations

Nolte et al. (1991) deduced flow velocities and ages from interpretation of ^{36}Cl and Cl concentrations via two approaches: (1) an interpretation of experimentally observed evolution of ^{36}Cl and Cl concentrations along the two flow paths, by a simple exponential decrease of ^{36}Cl and a linear increase of Cl with distance from the recharge area; and (2) the evolution of Cl and ^{36}Cl concentrations along the two flow paths by diffusion of both ^{36}Cl and Cl between the aquifer and the underlying confining Colorado shale without the *in situ* production of ^{36}Cl . The first approach assumes a constant flowrate whose value is a function of the *in situ* ^{36}Cl production. The second approach uses a flowrate which is inferred from a diffusion model and is assumed constant (Nolte et al., 1991).

Fröhlich et al. (1991) state that the ^{36}Cl input is greater than that which can be obtained from atmospheric fallout, even after adjusting for the 60% evapotranspiration suggested by Swanick (1982). Fabryka-Martin et al. (1991) proposed that a hundred-fold increase between halide concentrations in precipitation and recharge waters can be attributed to the effects of evapotranspiration, dry fallout, and a limited duration of recharge. Therefore, Fabryka-Martin et al. (1991) assume that the subsurface contributions of Cl are at least 90% of the total Cl in the distal portion of the aquifer. This results in ^{36}Cl -based ages being reduced from 2 Ma to ~1 Ma, which are somewhat higher than those ages produced by hydrodynamic modeling.

Alternatively, Andrews et al. (1991b) proposed that the input of ^{36}Cl may be due to the solution of salt from the shallow soil zone, a recharge zone where cosmic-ray irradiation would increase ^{36}Cl production. However, Fröhlich et al. (1991) questioned whether the residence time of salt in the soil zone is long enough for this mechanism to approach equilibrium.

Fröhlich et al. (1991) used the *in situ* production of ^{36}Cl in the two above models to obtain flowrates 75% lower than when zero *in situ* production is assumed. The flowrates from the diffusion model were only slightly higher than the values from the first model. From this, Nolte et al. (1991) concluded that radioactive decay of ^{36}Cl is the control of ^{36}Cl concentration in the groundwater during advective transport in the aquifer, rather than diffusive losses. Groundwater ages based on $^{36}\text{Cl}/\text{Cl}$ data, uncorrected for subsurface contributions, yield ages that range up to 2 Ma (Phillips et al., 1986). If subsurface Cl contributions are accounted for by low values in the fresh waters in the south, to high values in the older saline waters in the northern parts of the aquifer, then the maximum ages are reduced to <1 Ma, making them more consistent with those based on other isotope techniques (Fabryka-Martin et al., 1991).

Nolte et al. (1991) reported the measurements of $^{36}\text{Cl}/\text{Cl}$ ratios and tritium concentrations of groundwater samples from the Milk River aquifer. Although the Milk River aquifer is not a closed system, determining the concentrations of ^{36}Cl and Cl with respect to the distance to the recharge area allows for the estimation of flow velocities and ages of the groundwater. These velocities and ages were determined with and without consideration of diffusive losses. Nolte et al. (1991) demonstrated that if diffusive losses of ^{36}Cl are taken into account the values obtained are only slightly modified.

Based on *in situ* production Nolte et al. (1991) calculated flow velocities that were about 75% smaller than those values obtained without *in situ* production of ^{36}Cl . Flow velocities from the diffusion model yielded values that were larger by a factor of about 1.3 compared to those values found without consideration of diffusive losses of ^{36}Cl . The calculated flow velocities for the flow path were in the range 0.09-0.14 m/a. The corresponding ages of the groundwater at a distance of 80 km from the recharge area are in the range 0.6-0.9 Ma.

2.7.3 Uranium-series Radionuclides

Uranium isotope disequilibrium has been observed to occur in circulating groundwaters and associated rocks (Cherdyntsev, 1971; Ivanovich and Schwarcz, 1983). By monitoring groundwater U isotope concentrations it is possible to determine flowrates, or residence time of groundwaters in an aquifer, assuming a piston-type flow. However, a problem with U-series disequilibrium is the poorly constrained initial conditions, and subsequent water-rock interactions involving U isotope exchange (Ivanovich et al., 1991). Therefore, determination of residence times from U-series radionuclide data is possible only if the initial state of disequilibrium is known and the contents of the radionuclides do not change a result of mixing with isotopically different waters.

For the Milk River aquifer, Ivanovich et al. (1991) found that the U concentration decreases with distance from the recharge area. The groundwater was delineated into oxic (U content $\sim 10^{-5}$ mmol/l) and anoxic (U content $\sim 10^{-7}$ mmol/l) end-members, with the latter conditions being prevalent. There is also an intermediate group representing mixing between the two end-members (Ivanovich et al., 1991). Calculated values of saturation indices for uraninite, coffinite and rutherfordine indicated that the groundwater is undersaturated with respect to these minerals (Ivanovich et al., 1991).

Ivanovich et al. (1991) evaluated two models for the interpretation of U-series disequilibrium data obtained from the Milk River aquifer. The first model proposed by Andrews and Kay (1978) is a ^{234}U excess decay model which assumes uniform dissolution rates of U, accompanied by recoil processes. The second model, proposed by Fröhlich and Gellermann (1987), is a phenomenological model for the evolution of U isotopic composition along groundwater flow paths, based on a transport equation incorporating radioactive decay and assuming that sorption processes affecting ^{238}U , ^{234}Th and ^{234}U radionuclides in the decay chain obey first-order kinetics. The first model yielded a migration rate in the range of 0.1-0.2 m/a along the flow path identified in the hydraulic model of Hendry and Schwartz (1988). This is about two fold lower than the

hydraulic model flowrate of 0.3 m/a for the flow path (Hendry and Schwartz, 1988). Model 2 yielded an overall flowrate in the range of 0.2-0.6 m/a, which is in very good agreement with the hydraulic model.

2.8 Summary

Meteoric water recharges the aquifer in the southern section, with groundwater flow northward. Transmissivity decreases toward the north due to thinning of the Milk River sandstone unit and an increase in shale content. Groundwater is transported in the aquifer by advective and dispersive processes, and diffusive flow dominates in the Colorado and Pakowki shales (Hendry and Schwartz, 1988).

The Milk River aquifer displays consistent patterns in the distribution of major ions and isotopic composition of O and H (Hendry et al., 1991). Important dissolved major ions include Ca, Mg, Na, K, Cl, SO₄, HCO₃ and CO₃. Generally, the concentration of Cl, Na, and HCO₃+CO₃ are the lowest in the recharge area and the concentration increases progressively along the flow system.

Schwartz and Muehlenbachs (1979) estimate the age along the studied flow path to be approximately 300 ka, based on hydraulic arguments. Phillips et al. (1986) used a flow model to calculate residence times of 500 ka for the flow to the northern margin of the aquifer. Radiocarbon dates on the groundwater are estimated at >40,000 years ~32 km along the flow path (Drimmie et al., 1991). Hendry and Schwartz (1988) estimate the residence time at the end of the flow path to be 250 ka. Ages based on a combination of ¹⁴C and chloride dating methods for groundwater at the town of Foremost (~54 km from the recharge area) yield residence times of approximately 90-110 ka.

Chapter 3

Methodology

3.1 Groundwater Sampling Protocol

When sampling groundwaters, sources of variability are expected due to spatial and temporal fluctuation of chemical characteristics arising from coupled chemical and physical processes in aquifers. Added complexities may include: (1) transport by colloidal particles; (2) variable vertical and horizontal redox gradients; (3) dissolved organic materials, and biological catalysis and transformations; (4) kinetically inhibited reactions; and (5) possible contamination during water collection (Barcelona, 1990).

The sampling design for the Milk River aquifer was based on previous detailed hydrogeologic studies, such that well waters were only collected and analyzed from the hydraulically and chemically constrained southern section of the flow path (Figure 3.1). There are field sampling variables over which there is some control. These variables are the sampling well location, nature of construction, purging of stagnant waters from wells, and sampling protocols prior to analysis. The degree of reproducibility of data, and consistency with past site data are also significant for identifying variability in groundwater chemistry (Barcelona, 1990). According to Barcelona (1990), the most important steps in groundwater sampling are well design, purging of stagnant water, selection of sampling device and/or tubing, and sample filtration and preservation. All of these field variables were carefully documented in sampling for this study.

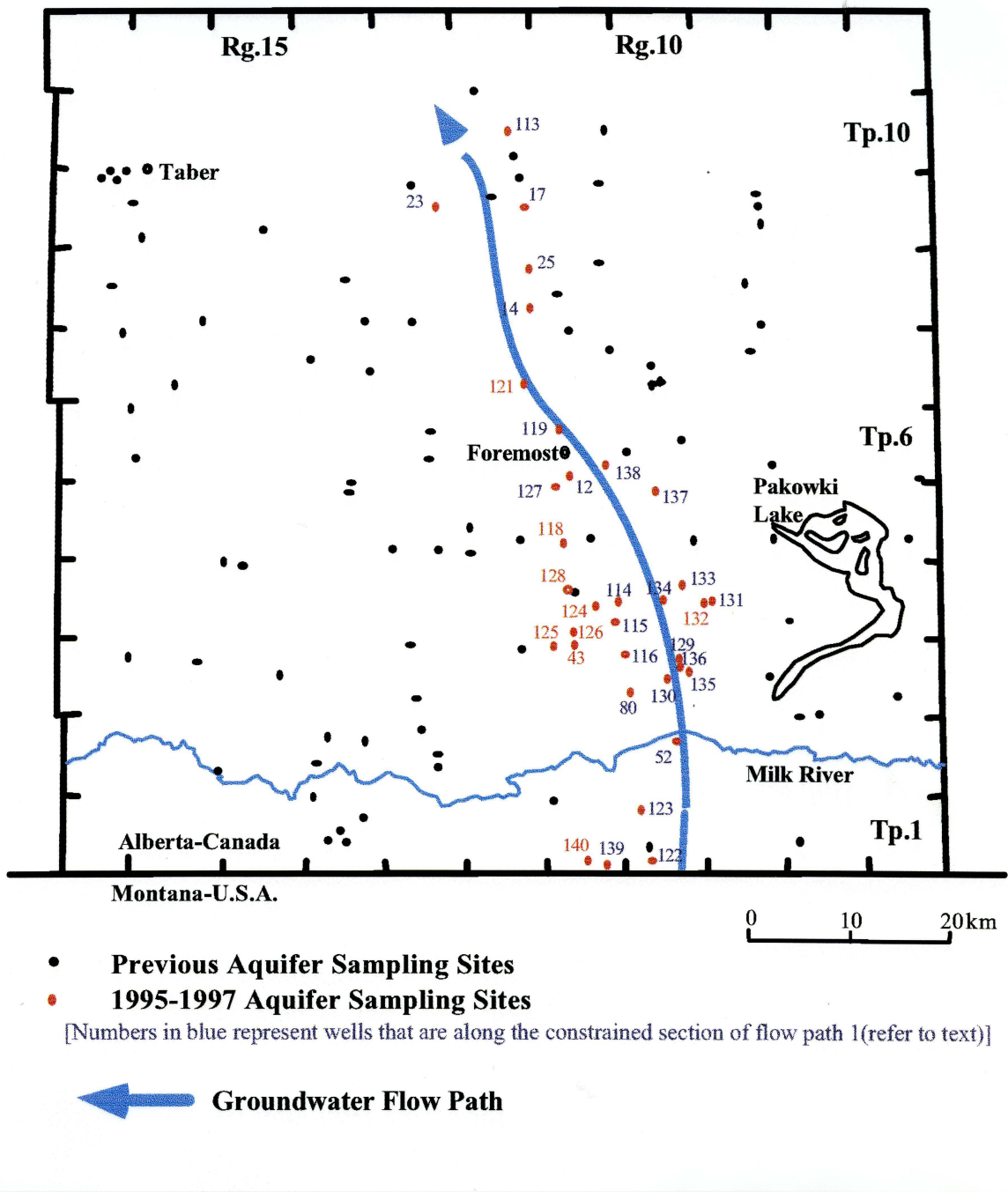


Figure 3.1. Sample locations in the Milk River aquifer and proposed flow path (after Hendry et al., 1991).

3.2 Field Sampling and Analysis

Sampling of groundwater from the Milk River aquifer for trace element analysis was carried out in October 1996 and May 1997. Field sampling in the Spring of 1997 was intended to complement the 1996 data, and establish inter-sampling variability of data, as well as to collect waters from additional well closer to the groundwater flow path. Groundwater samples collected in 1995 by M. J. Hendry and colleagues (University of Saskatchewan, Saskatoon, Saskatchewan) were also used in the present study.

Samples were taken from the recharge area north of the Sweetgrass Hills along the flow path, extending northward 54 km to the town of Foremost (Fig. 3.1; Appendix A). Individual wells were selected for quality, and wells having substandard casing or a history of poor water quality were rejected, as were those that were chlorinated using chlorine tablets or “shock treated” using bleach. All wells were purged for approximately 30 minutes to collect a representative groundwater sample from the aquifer.

Filtration of water samples is necessary for analyses of dissolved chemical constituents, assuming that foreign contaminants are not introduced by drilling activities, grouts/seals or corroded casing (e.g. Barcelona, 1990). Colloidal species can be important in subsurface chemical mass balance and chemical transport in groundwater. The concentrations of chemical species transported either in a dissolved or suspended state may be under- or overestimated by filtration (Barcelona, 1990).

Extreme care must be taken when sampling and processing natural aqueous samples for trace elements if reliable data is to be obtained. Groundwater samples from the Milk River aquifer used for inductively coupled plasma-mass spectrometry (ICP-MS) analysis were filtered in the field through prerinsed 0.45 µm millipore membrane filters, using a portable peristaltic pump and filter glassware in 1996, or a 2.4 liter Geotech® barrel filter with a foot pump in 1997. Once filtered, the samples were acidified 1% by

volume with doubly distilled 16N nitric acid (HNO₃), and stored in precleaned, acid-washed, low density linear polyethylene bottles at ~4 °C prior to analysis. A field trip blank of distilled deionized water (DDIW) and field blanks were also prepared and collected for analysis with the groundwater samples. The samples were analyzed by ICP-MS at the University of Saskatchewan (Appendix B).

The samples collected for analysis by inductively coupled plasma-atomic emission spectrometry (ICP-AES) were similarly field filtered, acidified 5% total volume with 16N HNO₃, and stored in precleaned, acid-washed low density linear polyethylene bottles. These samples were preconcentrated approximately ten times by evaporation in a clean hood. Analyses by ICP-AES were performed by geoanalytical services at the Saskatchewan Research Council (Appendix B). Reasons for using both ICP-MS and ICP-AES are outlined in Table 3.1.

Analysis of major anions (Cl and SO₄) and cations (Ca, Mg, Fe, Na) using Ion Liquid Chromatography and Atomic Absorption Spectrophotometry (AAS) respectively, was performed at the National Hydrology Research Institute (NHRI) in Saskatoon (Appendix C). Field filtration was identical, as noted above. Lab pH and alkalinity were also measured. These samples were collected in two separate acid washed bottles, one for cations and one for anions. All acidified samples were stored in a cooler on ice to minimize compositional changes such as adsorption of elements on sample bottle walls.

Field pH, alkalinity and temperature were measured at the time of sampling. The pH electrode was calibrated using 2 buffer solutions (pH=7, and pH=4), with the ambient groundwater temperature of ~10 °C. Alkalinity was determined by potentiometric titration of the sample immediately after its filtration (HACH model AL-DT-test kit using phenolphthalein indicator).

3.3 Analytical Methodologies

3.3.1 Instrumentation

Inductively coupled plasma-atomic emission spectrometry and inductively coupled plasma-mass spectrometry have been proven to be powerful analytical tools for trace element analysis. Both utilize an inductively coupled argon plasma: in ICP-AES as a source for optical emission, and for ICP-MS as a source of ions. Both instruments have similar configurations up to the argon plasma. AES uses characteristic photon emission spectra to identify elements, whereas the MS filters ions on the basis of mass/charge ratio. For a more detailed description of both methods see Potts (1987).

3.3.2 ICP-MS

A Perkin Elmer Sciex Elan 5000 ICP-MS was used in this study. The instrument was operated at a power setting of 1000 W. The argon plasma gas flow was set at 15 L/min. Auxiliary gas flow and nebulizer gas flow were 0.8 L/min. Sampler and skimmer cones are pure nickel tipped, with orifice diameters of 1.1 mm and 0.89 mm, respectively.

The 1995 ICP-MS data used a cross-flow nebulizer to introduce the sample into the argon plasma. This method loses approximately 95% of the sample to the drain in the spray chamber, resulting in lower sensitivity. The 1996-1997 waters were analyzed using an ultrasonic nebulizer, from Precision Instrumentation into the argon plasma. The sample aerosol is heated to ~140 °C and then cooled to ~5 °C. The increased amount of analyte injected per unit time results in about a 10-20-fold improvement in sensitivity, essential for analyzing low abundance trace elements. A sample delivery rate of 1.0 mL/min was used for the 1995 sample analysis, and 2.0 mL/min for the 1996-1997 analysis. The ultrasonic nebulizer does not work well with solutions having high total dissolved solids (TDS) because the salts tend to deposit in the cooling coil of the ultrasonic nebulizer and on the outer sampling cone.

The ICP-MS calibration protocol involves external calibration and standard additions (Hall, 1993). Pure elemental standards in solution were employed for external calibration. The external standards are measured for calculation of concentrations, and the internal standard is used to correct for matrix effects and drift. The internal standard for 1995 data was indium (^{49}In), and for the 1996-1997 ultrasonic nebulizer data, the internal standard contained beryllium (^4Be), indium (^{49}In), and bismuth (^{83}Bi). To evaluate the accuracy of the data, the international reference water standards SLRS2 and SLRS3 were analyzed in duplicate. Appendix D reports the measured and recommended values, plots the data, and provides explanations for the selection of elements.

Corrections for isobaric interferences were determined by analyzing a barium solution and correcting for barium hydride (BaH) and barium oxide (BaO) interferences. The following isotopes were selected for intensity measurements to avoid isobaric interferences: ^{139}La , ^{140}Ce , ^{141}Pr , ^{145}Nd , ^{147}Sm , ^{151}Eu , ^{157}Gd , ^{159}Tb , ^{163}Dy , ^{165}Ho , ^{167}Er , ^{169}Tm , ^{173}Yb , and ^{175}Lu . Examination of the results showed that the only significant isobaric overlaps are from ^{138}Ba hydride and ^{135}Ba oxide on ^{139}La and ^{151}Eu respectively. Interferences on Sm and Gd were negligible.

3.3.3 ICP-AES

A Perkin Elmer Optima 3000 ICP Atomic Emission Spectrometer was used in this study. The instrument was operated at a power setting of 1300 W. The argon plasma gas flow was set at 15 L/min. Auxiliary gas flow and nebulizer gas flow were 0.5 L/min. A sample delivery rate of 1.0 mL/min was used.

To evaluate the accuracy of data, the international reference water standard, SLRS2 was analyzed. Absolute concentrations for SLRS2 are presented in Appendix B. Appendix D reports measured and recommended values, plots the data and provides explanations for the selection of elements.

3.3.4 Advantages and Disadvantages of ICP-AES and ICP-MS

Table 3.1 lists some advantages and disadvantages of the ICP-AES and ICP-MS methods. Dilute waters with low total dissolved solids (TDS) are ideal analytes for both of these techniques. Thus, the Milk River aquifer groundwater is ideal for analysis by either instrumental method. Seawaters and brines with high concentrations of dissolved salts may lead to matrix effects and clogging of the sample and skimmer orifices.

The sensitivity of ICP-AES for many elements such as heavy metals is inadequate for the direct measurement in most surface waters and groundwaters. Attempts have been made in the past to address this limitation by the use of: *chelation* (Sturgeon et al., 1981); *solvent extraction* (Sugiyama et al., 1986); *adsorption* onto activated charcoal (Koshima and Onishi, 1986); *precipitation* with *Ga* (Akagi et al., 1985); or *evaporation* (Thompson et al., 1982; Gorlach and Boutron, 1990). These methods usually involve preconcentration factors between 10-50, which result in a minimum volume of about 5 mL for nebulisation into the ICP-AES (Hall, 1993). The suite of elements which can be determined directly by ICP-AES in the majority of the waters sampled is Si, Al, Ti, Na, K, Ca, Mg, S, P, Ba, Sr, Fe, Mn, and Zn.

For this study a complementary approach was adopted using ICP-AES to determine selected major elements and light elements (Al, Fe, Ca, Mg, Na, and K) and ICP-MS to determine other trace elements, including REEs. A section on detection limits and interferences for ICP-AES and ICP-MS is presented in Appendices D and E.

3.4 ICP-AES - ICP-MS Intercomparison

The major elements including Al, Fe, Ca, Mg, K, and Na from ICP-AES were used in this study. For most trace elements, the data from the ICP-MS were favored over those obtained by ICP-AES. However good agreement between ICP-AES and ICP-MS was obtained for Li, Cr, Ni, Cu, Sr, Mo, Cd, Ba, and Pb (Appendix E).

Table 3.1. Advantages and disadvantages of ICP-MS and ICP-AES.

ICP-AES ~ 40 elements/sample		ICP-MS ~ 70 elements/sample	
Advantages	Disadvantages	Advantages	Disadvantages
Detection of ^{40}K and ^{56}Fe	Detection limits ~ 0.1ppb - 100ppm	Detection limits ~ 0.0001ppb - 10ppm	No detection of ^{40}K
Low chemical and ionization interference effects	Rich spectral interferences and matrix sensitive	Few Interferences (isotopes free of interference for most elements)*	$^{40}\text{Ar}^{16}\text{O}$ interference on ^{56}Fe
Light elements analyzed	Dilution and concentration of samples	Isotope dilution	Poor detection limits for light elements ^{138}BaH interference on ^{139}La , and ^{135}BaO on ^{151}Eu
		Laser ablation - spatial resolution in mineral analysis	Low tolerance for - high TDS

* with exception of indium

Both ICP-MS and ICP-AES employ an inductively coupled argon plasma as a source:
 AES for photon emission
 MS as a source ions

Inductively coupled plasma - atomic emission spectrometry is performed by atomizing a wet sample in a argon plasma and determining trace element characteristics by analysis of the intensity of emission of optical radiation from excited ions.

Inductively coupled plasma - mass spectrometry involves atomizing an aqueous analyte sample (exception - laser ablation) in an argon plasma and determining trace element characteristics based on mass/charge.

3.4.1 Limits of Detection

Hall (1993) published detection limits for numerous elements in waters by ICP-AES that lie between 1-10 ppb, whereas those by ICP-MS are generally in the range 0.01-0.1 ppb. Similar detection limits for select elements analyzed by ICP-AES and ICP-MS in this study are presented in Appendix E. Detection limits are not only a function of the signal-to-noise ratio achieved with the instrument, but are also due to the procedures used for calibration and blank subtraction, interference corrections, the quality of the lab environment, and purity of the reagents used.

3.4.2 Elements Analyzed by ICP-MS and ICP-AES

Listed below are the trace elements that were analyzed in the Milk River aquifer groundwater, by combined ICP-MS or ICP-AES.

Alkali metals

- Li, Na, K, Rb, Cs

Alkaline earth metals

- Be, Mg, Ca, Sr, Ba

Transition Metals

- Sc, Ti, V, Cr, Mn, Fe, Co, Ni, Cu, Zn, Y, Zr, Nb, Mo, Pd, Ag, Cd, Ba, Hf, Ta, W, Au, Hg

Groups III-VI

- B, Al, Ga
- Si, Sn, Pb
- P, As, Sb, Bi
- Se

Halogens

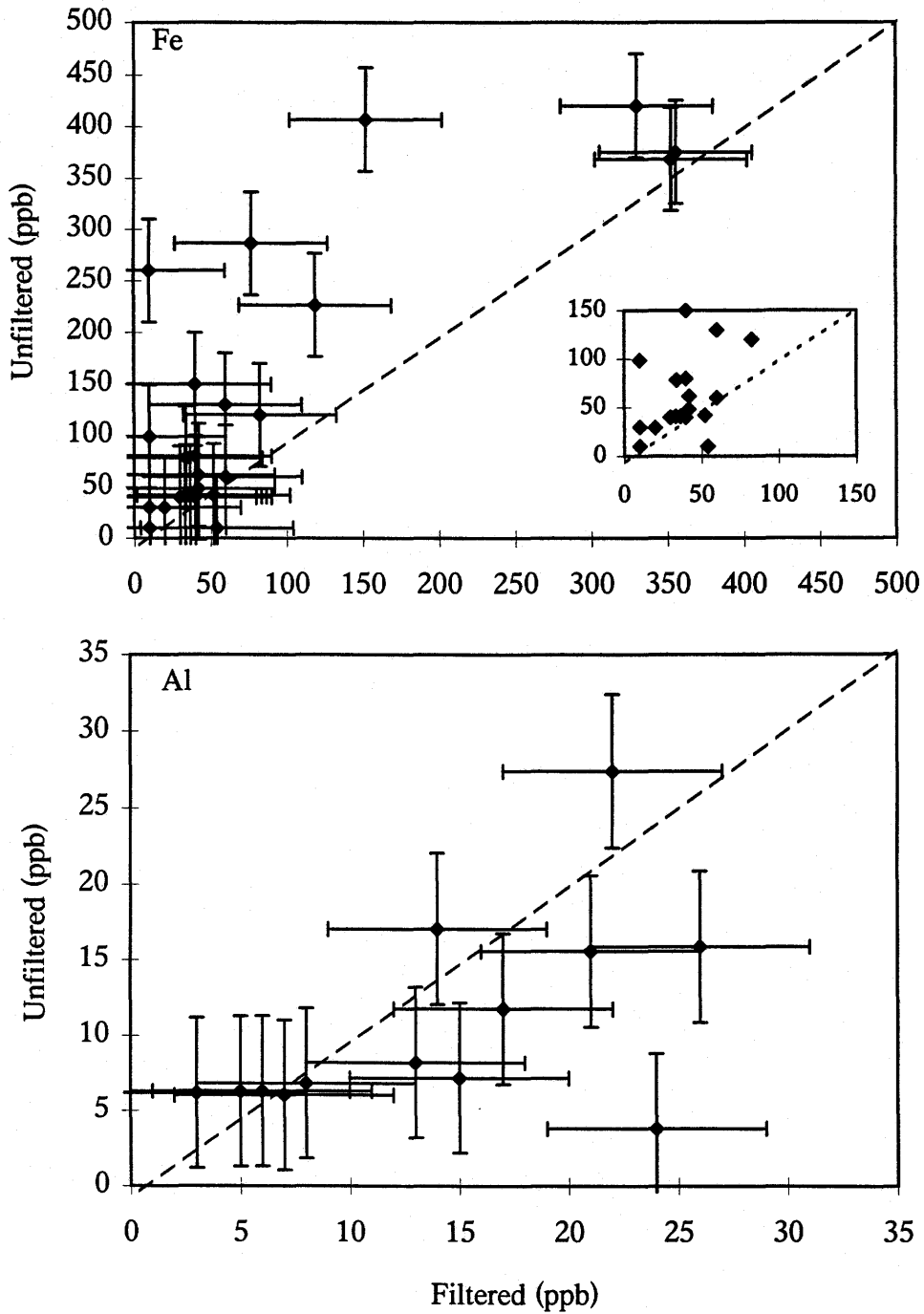
➤ Cl

3.5 Intercomparison of Field Filtered and Unfiltered Samples

Colloids can concentrate trace elements by sorption, and hence enhance their mobility by stabilization and migration through the aquifer rocks (Miekeley et al., 1992). When using geochemical models, it is important that water samples are filtered with minimal disturbance of the *in situ* conditions (Barcelona, 1990).

Waters from the 1995-1997 field sampling seasons were both field filtered and non-field filtered to determine the effects of suspended particles and colloids on element concentrations. Filtering is likely to be important for this study due to the variables involved in the individual wells sampled. These include differences in submersible pumps, casings, screens and age of individual wells. All water data was plotted on diagrams of filtered versus unfiltered. Selected major and trace elements are plotted in Figures 3.2, 3.3, and 3.4 to illustrate those elements that are readily affected by filtration and those that are not.

Clays including kaolinite, illite, smectite, and chlorite make up to 40% of the total mineral inventory in the Milk River Formation sandstones (Longstaffe, 1984). Accordingly it is likely that these clays make up the majority of the suspended particles/colloids ($>0.45\mu\text{m}$) in the Milk River aquifer groundwater. Hydrated oxides of iron and aluminum are also probably significant in the transport and sorption of select trace elements. This is displayed in the filtered and unfiltered plots of iron and aluminum. Iron clearly shows higher concentrations in the unfiltered waters, and consequently it is present in the waters likely as hydrated Fe oxides or oxyhydroxides and/or Fe-clays (Fig. 3.2). For aluminum some samples display 'normal' patterns where unfiltered concentrations are higher than filtered, whereas several display



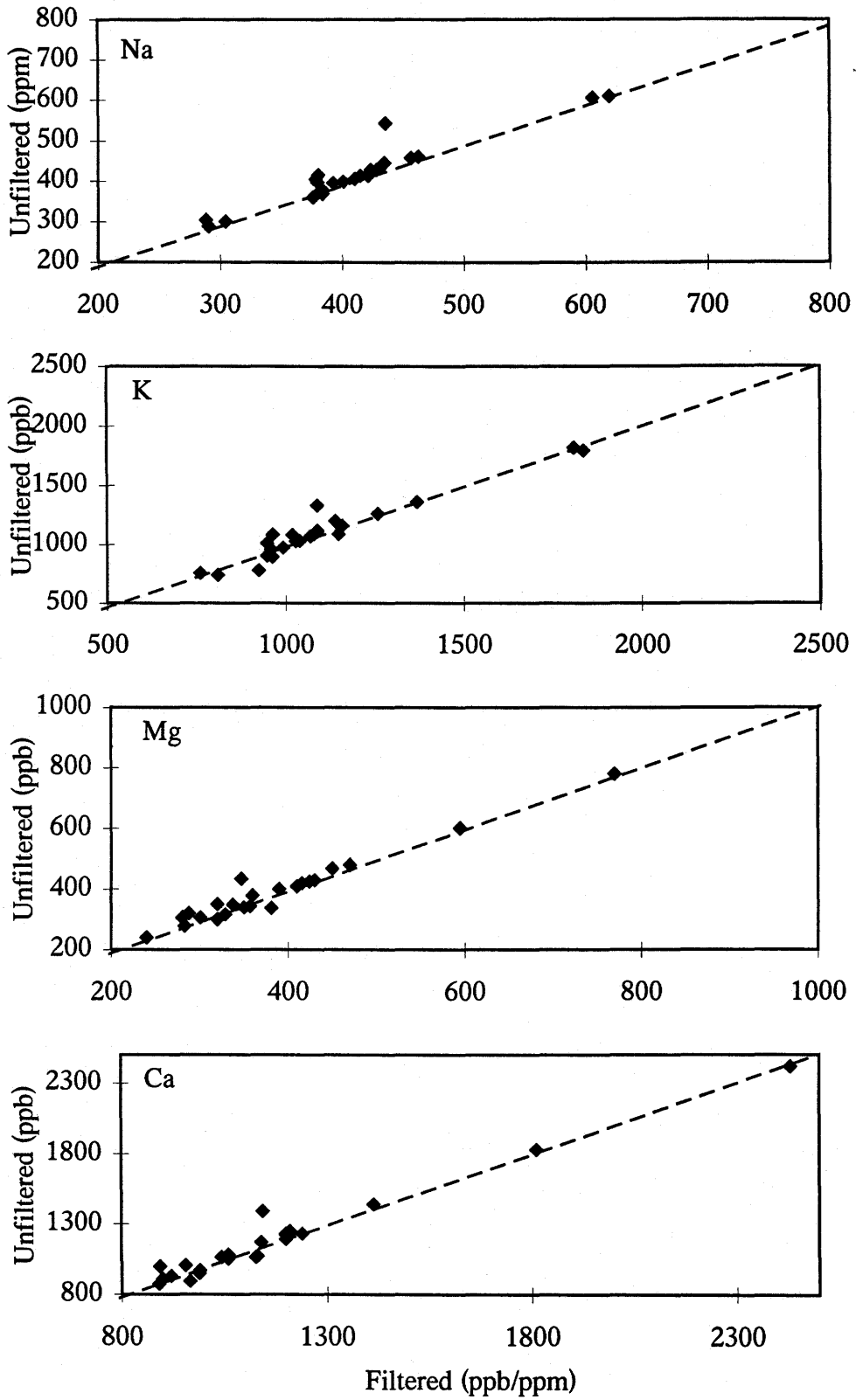


Figure 3.3. Analysis of selected filtered and unfiltered elements in the Milk River aquifer groundwater.

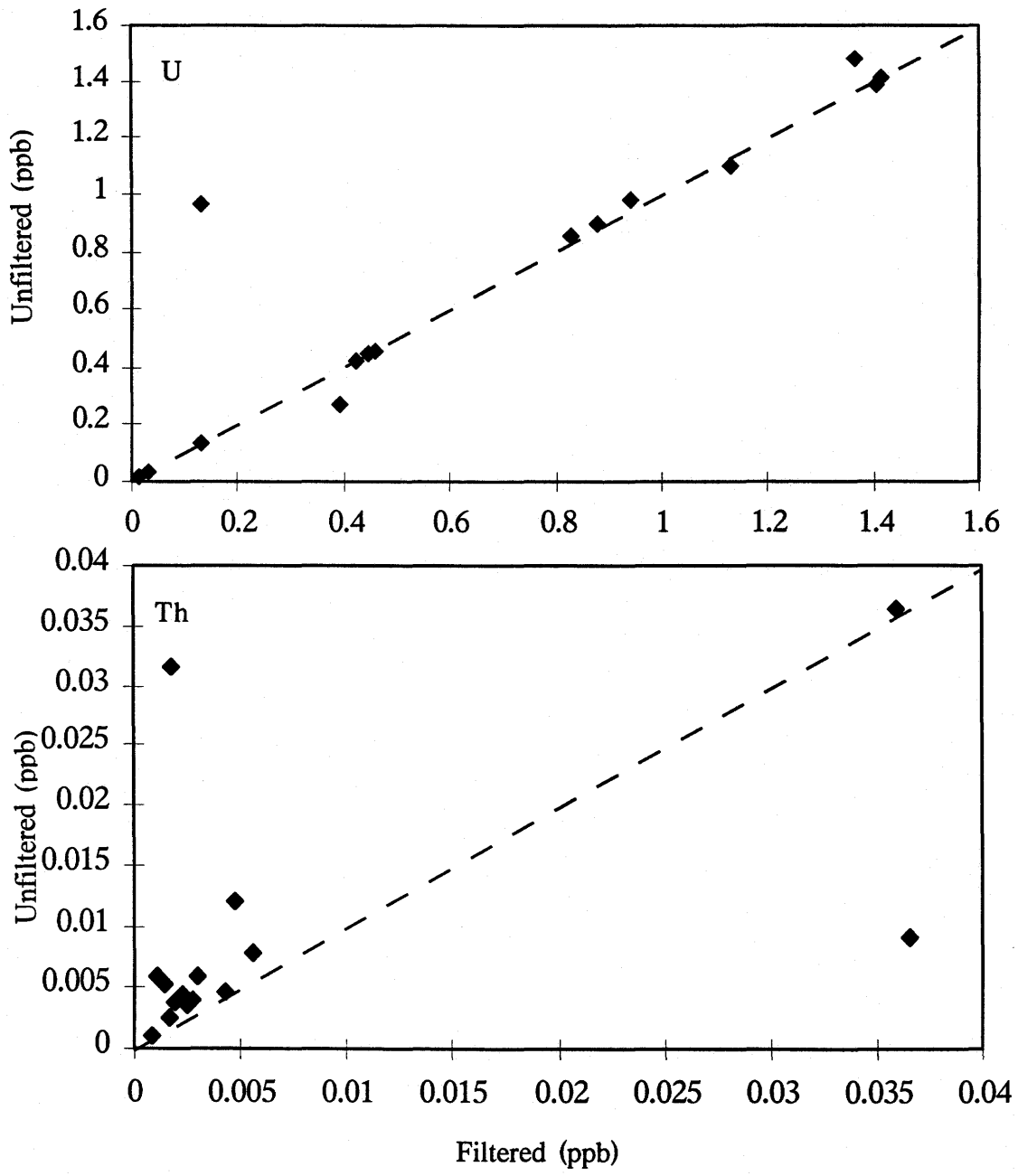


Figure 3.4. Analysis of select filtered and unfiltered elements in the Milk River aquifer groundwaters.

'reversed' patterns where unfiltered concentrations are lower. This variability in aluminum concentrations is not presently understood. Miekeley et al. (1992), noted that U, Th, other actinides, and REEs are expected to be released in very low concentrations in true solution, but water-rock interaction may produce colloids of low solubility or these elements may sorb on naturally occurring colloids such as silicates, hydrous oxides of Fe and Al, and humic substances.

Most trace elements do not show any discrepancy between filtered and unfiltered samples, and accordingly they are not influenced by colloids (Fig. 3.3). However a few unfiltered groundwater samples from the Milk River aquifer contain a low to moderate load of suspended particles ($>0.45\mu\text{m}$), which have both Th and LREE concentrations higher than the corresponding filtrates (Fig. 3.4 and Appendix F). Uranium shows no discernible effects of filtering (Fig. 3.4). Miekeley et al. (1992b) concluded that ($0.45\mu\text{m}$) particulate matter of amorphous ferric hydrous oxides, have a strong capacity for sorption of LREEs. Elderfield et al., (1990) demonstrated that Fe can exist as organically stabilized colloids in river waters and that there is a relationship between dissolved Fe and REEs in river waters. From this study it appears that suspended particles are important in the preferential sorption of LREEs (La, Ce, Pr, Nd, Sm), and less important in the MREEs (Eu, Gd, Tb, Dy) in the alkaline groundwater of the Milk River aquifer (Fig. 3.4 and Appendix F). The heavy REEs (Ho, Er, Tm, Yb, Lu) are unaffected by colloids/suspended particles (Fig. 3.5 and Appendix F). Filtered data is primarily reported and plotted in Chapter 4 except for a select few cases where the concentrations for REEs were below the ICP-MS detection limit on the filtered samples.

3.6 Geochemical Modeling

3.6.1 An Introduction to PHREEQC

Geochemical modeling is a tool which can be used to interpret and/or predict chemical reactions among solutions, minerals, gases, and organic matter in aqueous systems. The basic assumptions behind geochemical modeling is that the analysis of the water sample

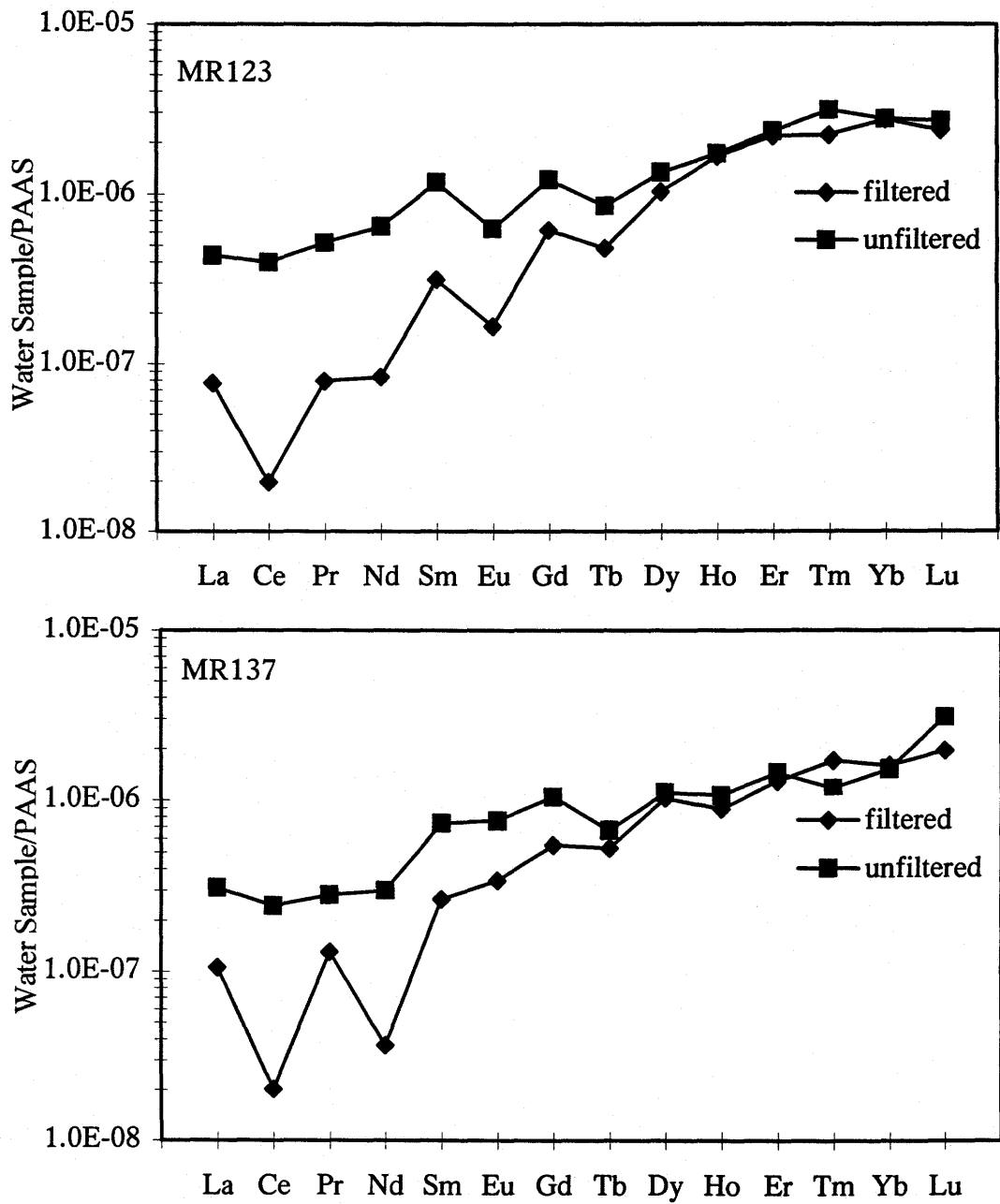


Figure 3.5. REE plots displaying the effects of field filtering groundwater samples.

same input conditions. This comparison of IAP to K_{sp} produces the saturation index (SI):

$$SI = \log_{10} \left(\frac{IAP}{K_{sp}} \right)$$

Geochemical speciation modeling can provide a quantitative assessment of saturation indices (SI) for minerals and phases which may be reacting within the water-rock system. The rules for saturation indices are as follows: (1) If $SI < 0$ and a specified mineral is present, the mineral could dissolve but cannot precipitate; (2) If $SI > 0$, the mineral could precipitate but cannot dissolve; (3) If $SI = 0$, the mineral could be precipitating or dissolving to maintain equilibrium. The most important factor is knowledge of the mineralogy, for a mineral cannot dissolve if it is not present.

3.6.2 PHREEQC as a Speciation Code

PHREEQC (version 1.0) by Parkhurst (1995) can be used as an initial solution (speciation) code to calculate saturation indices, distribution of select species, and determine total carbon using analytical data for pH, Pe, and total concentrations or total element valence concentrations. Aqueous speciation calculations are done using a limited set of equations. If pH and Pe are known, the Newton-Raphson equations are derived from the functions f_m , f_{H_2O} , and f_μ , which are equations for mole balance for elements, valence states, activity of water, and ionic strength. A detailed description of the equations and analytical data used in the equations can be found in the User's Guide to PHREEQC - A Computer Program for Speciation, Reaction-Path, Advective-Transport, and Inverse Geochemical Calculations by Parkhurst, 1995.

Chemical elements in the following two databases can be used to calculate individual element speciation: (1) *Phreeqc.dat* - Ca, Mg, Na, K, C, CO₂, CH₄, SO₄, total sulphur,

sulphate, sulphide, Cl, Si, Fe, Fe²⁺, Fe³⁺, P, Sr, F, Al, Li, N, N⁵⁺, N³⁺, N³⁻, B, Ba, Br, Mn, Cd, Cu, Pb, Zn; and (2) *wateq4f.dat* - Cs, Rb, I, Ni, Ag, As, As⁵⁺, As³⁺, Fulvate, Humate, Se, Se⁶⁺, Se⁴⁺, Se²⁻, U, U⁶⁺, U⁴⁺ (Ball and Nordstrom, 1991). Redox conditions adopted in the calculations may be determined by either using actual measured Eh(Pe) values, or alternatively can be determined using redox couples from the databases (e.g. S⁶⁺/S²⁻). For a detailed description of calculations, theory, and applications of PHREEQC refer to Parkhurst (1995).

Analytical data used in the speciation calculations included element concentrations, field pH and alkalinity values and Eh measurements converted to Pe (Pe = 16.904Eh at 25 °C). Values of Eh, where determined for specific wells modeled along the flow path by using measured values from Hendry et al. (1991), and theoretical values determined for this study. Theoretical values were determined by using known Eh (Pe) values in closed groundwater systems, where sulphate reduction and methane production occurs.

3.6.3 REE Speciation Modeling

Groundwaters probably inherit their dissolved REE signatures in part from the aquifer materials they react with (Duro et al., 1997; Johannesson et al., 1994; and 1997). Recently, solution complexation has been demonstrated as being important for controlling the dissolved REE signatures in waters. Therefore, it is important to understand both the effects of aquifer material chemistry and solution chemistry to determine their roles on controlling the REE signatures of water systems.

Speciation modeling of REEs in the Milk River aquifer groundwater were evaluated primarily to assess the importance of carbonate (LnHCO₃²⁺, LnCO₃⁺ and Ln(CO₃)₂⁻) and phosphate (LnH₂PO₄²⁺, LnHPO₄⁺, Ln(HPO₄)₂⁻ and LnPO₄⁰) complexes, where Ln stands for lanthanides. Activity coefficients and stability constants have been calculated using a combined specific ion interaction and ion pairing developed by Millero (1992). For a

detailed description of the modified and stability constant updated Millero (1992) model used in this study, refer to Johannesson and Lyons (1994).

Chapter 4

Results and Discussion

4.1 Structure of Chapter 4

The pH, alkalinity and major ion data along the studied flow path are documented in section 4.2. This data is used to discriminate which well sites were located along the hydraulically and chemically constrained section of the flow path in the Milk River aquifer system, by comparison with previous studies on the Milk River aquifer groundwater. Geochemical modeling of the major phases (i.e. calcite, dolomite, gypsum and $p\text{CO}_2$) are presented and compared with the previous Milk River aquifer studies, to establish which phases are saturated or undersaturated with respect to the groundwater at select well locations along the flow path.

An introduction to redox reactions in groundwater studies is reviewed in section 4.3 because of its importance in understanding how these reactions control the concentration and mobility of select trace elements in groundwater systems. Redox sensitive methane, sulphate and select trace elements in the Milk River groundwater are reported at the beginning of section 4.3, followed by a discussion and interpretation of the hydrogeochemical characteristics of the groundwater along the flow path.

In section 4.4, select trace elements that display unique trends along the groundwater flow path are presented and examined. Geochemical modeling of strontianite, is also reported, and compared to earlier modeling by Armstrong (1994). Where possible,

examples from previous groundwater studies are cited for select elements in the Milk River groundwater.

Section 4.5 documents how REEs are used as geochemical indicators in groundwater studies. Shale-normalized diagrams, and plots of concentration versus distance, pH, and alkalinity are presented and used sequentially to assist in the understanding of groundwater-rock interactions. The balance of the section is devoted to speciation modeling of the REEs in the groundwater to assess the importance of carbonate and phosphate complexes.

The remaining trace elements displaying minor or no observable trends are reported and discussed in section 4.6. Although these elements are not discussed in detail, it is important to document their concentrations and behavior to form a baseline for future groundwater studies. The final sections 4.6.3 and 4.6.4 display and discuss shale normalized plots of the transition metals, alkali metals and alkali earth metals.

4.2 The Major Hydrogeochemistry of the Milk River Aquifer Groundwater

4.2.1 pH, Alkalinity, and Major Ion Chemistry of the Groundwater

Results for major ion analyses for select groundwater samples in this study are presented in Tables 4.1 and 4.2. Sample sites were selected along the chemically and hydraulically constrained section of the aquifer flow path (Fig. 3.1). Samples from groundwater sites with conservative element (i.e. Cl, Na, K, Ca) concentration peaks are not included in this chapters discussions or figures. For consistency, only filtered data is used and discussed in the following sections.

The pH of the groundwater generally decreases with increasing distance along the flow path (Fig. 4.1). Values range from >9.20 in the recharge area to <9.00 approximately 20 km downgradient, and remain constant up to 54 km from the recharge area. Alkalinity

Table 4.1. Major anions and cations analyzed in the Milk River aquifer groundwater.

Sample	MR139	MR122(96)	MR122	MR123(96)	MR52(96)	MR80(96)	MR130	MR136	MR129	MR137	MR127(96)	MR119(96)	
($\mu\text{g/ml}$)	fil.	fil.	fil.	fil.	fil.-d.	fil.	fil.	fil.	fil.	fil.	fil.	fil.	
Ca		0.96		1.08	1.08	1.38	1.23				0.84	1.1	
Mg		0.29		0.36	0.36	0.42	0.43				0.29	0.35	
Fe		0.05		0.02	0.02	0.04	0.02				0.29	0.11	
Na		310		381	362	437	425				388	437	
Cl	13.8	1.92	1.60	5.92	5.91	10.0	14.9	18.2	20.1	20.1	42.8	57.9	72.6
SO ₄	115	152	137	171	171	297	277	241	217	221	14.6	<0.5	<0.5

Notes: 1) fil. = filtered data, fil.-d. = Filtered duplicate data

2) 1997 data presented unless indicated

Table 4.2. Major elements analyzed in the Milk River aquifer groundwater.

Sample	MR139	MR122(96)	MR122	MR123(96)	MR123	MR52(96)	MR80(96)	MR130	MR135	MR136	MR129		
(ppb)	fil.	fil.-d.	fil.	fil.	fil.	fil.-d.	fil.	fil.	fil.	fil.	fil.		
Al			9.7		7.9	6.6		7.8	7.3				
Fe	10	10	54	10	37	42	10	42	33	10	60	10	40
Ca	1060	1090	989	950	1131	1127	1060	1414	1208	1240	1200	1200	1140
Mg	240	240	288	320	381	357	360	424	416	430	410	390	430
K	810	770	925	760	949	964	960	1080	1029	1140	1090	1150	1160
Na(ppm)	291	290	288	305	384	376	383	435	415	428	425	431	424

Sample	MR116(95)	MR131	MR115(95)	MR131	MR114(95)	MR134	MR133	MR137	MR127(96)	MR12(95)	MR138	MR119(96)	MR119(95)
(ppb)	fil.	fil.	fil.	fil.	fil.	fil.	fil.	fil.	fil.	fil.	fil.	fil.	fil.
Al	9.0		5.0	3.6	10				6.0	10.0		8.8	6
Fe	33	60	100	60	72	20	40	30	356	92	40	119	384
Ca	1287	1200	1041	1200	1448	990	1210	920	966	1039	900	1144	1252
Mg	481	450	353	450	636	350	470	320	329	409	320	347	438
K		1260		1260		1040	1370	1070	1149		1090	1089	
Na(ppm)		463		463		410	457	401	422		393	435	

Notes: 1) fil. = filtered data, fil.-d. = Filtered duplicate data

2) 1997 data presented unless indicated

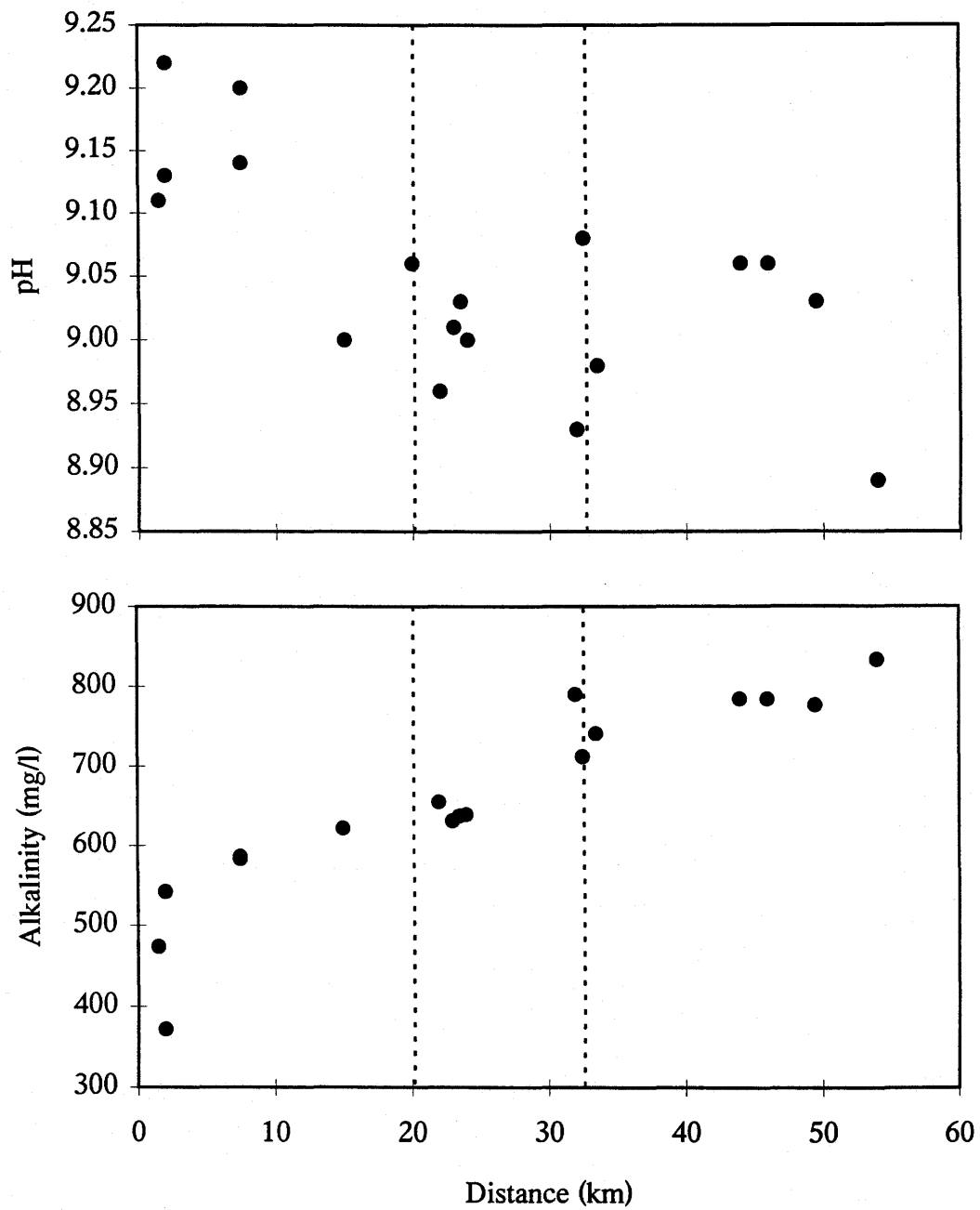


Figure 4.1. Field pH and alkalinity versus distance from recharge. Vertical dashed lines represent redox front and post-redox front boundaries. Cumulative plot of 1996-1997 data.

increases linearly along the flow path. Values range from 475 mg/L in the recharge area to 775 mg/L near the town of Foremost ~50 km from recharge (Fig. 4.1).

Major ions Cl, Mg, Ca, Na and K are plotted as a function of distance from the recharge area (Figs. 4.2 and 4.3). The data presented in these figures exhibit the same trends of those reported by previous workers (Meyboom, 1960; Schwartz and Muelenbachs, 1979; Phillips et al., 1986; Hendry and Schwartz, 1988, 1990; and Hendry et al., 1991). Plots display small but well defined increases in Cl, Mg, Ca, Na, and K up to 20 km along the flow path (Figs. 4.2 and 4.3). Magnesium, Ca, Na, and K concentrations remain constant after 20 km to 54 km, as the groundwater migrates downgradient. The trends of Cl, Na, Ca and K downgradient from the recharge area are controlled by diffusion from the underlying confining shale (Hendry and Schwartz, 1988). Aluminum concentrations are uniform from the recharge area to 54 km.

4.2.2 Initial Condition - Solution Modeling of the Groundwater

Hendry et al. (1991) used the computer code PHREEQE (Parkhurst et al., 1990) to determine the theoretical saturation states of calcite, dolomite, gypsum, and $p\text{CO}_2$ for the Milk River aquifer groundwater. Data indicated that the groundwaters are at or near equilibrium with respect to calcite and dolomite, which is consistent with these being the dominant carbonate minerals in the Milk River Formation (Meyboom, 1960; Longstaffe, 1984).

Utilizing PHREEQE, Armstrong (1994) concluded that the Milk River aquifer porewaters along the flow path are initially undersaturated with respect to calcite and dolomite, and approach equilibrium with increased residence time. Gypsum was also determined to be undersaturated, although water in the recharge area and tills was close to gypsum saturation. This confirmed the earlier conclusions that SO_4 in the porewaters are derived from gypsum in the tills (Hendry et al., 1986; Hendry and Schwartz, 1990).

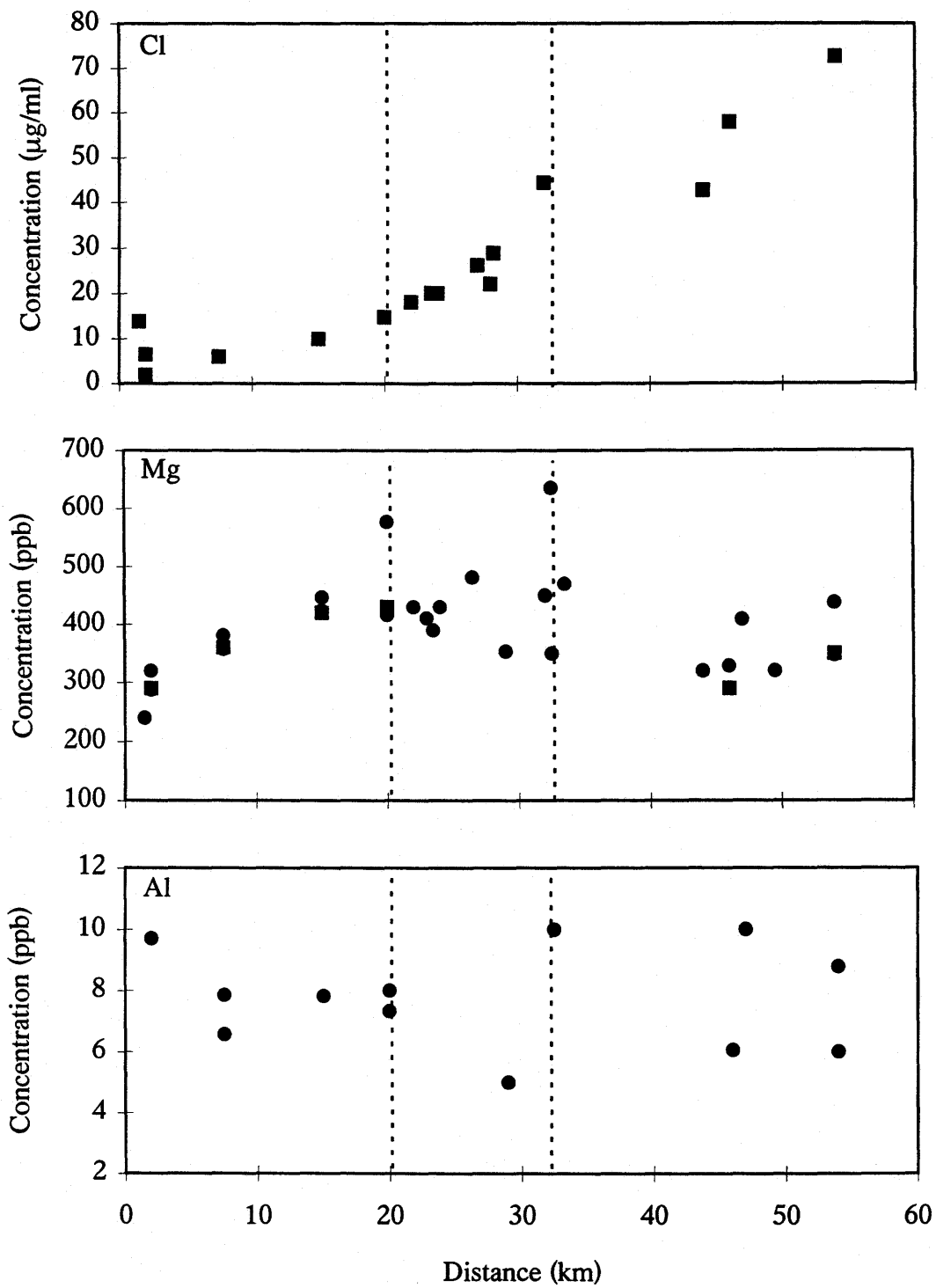


Figure 4.2. Cl, Mg, and Al concentrations in the Milk River aquifer groundwater versus distance along the flow path. Dashed vertical lines represent the redox front and post-redox front boundaries. Cumulative plot of 1996-1997 data. Square marker represents AAS (Mg) data or Liquid Chromatography data (Cl). Circle marker represents ICP-AES (Al, Mg) data.

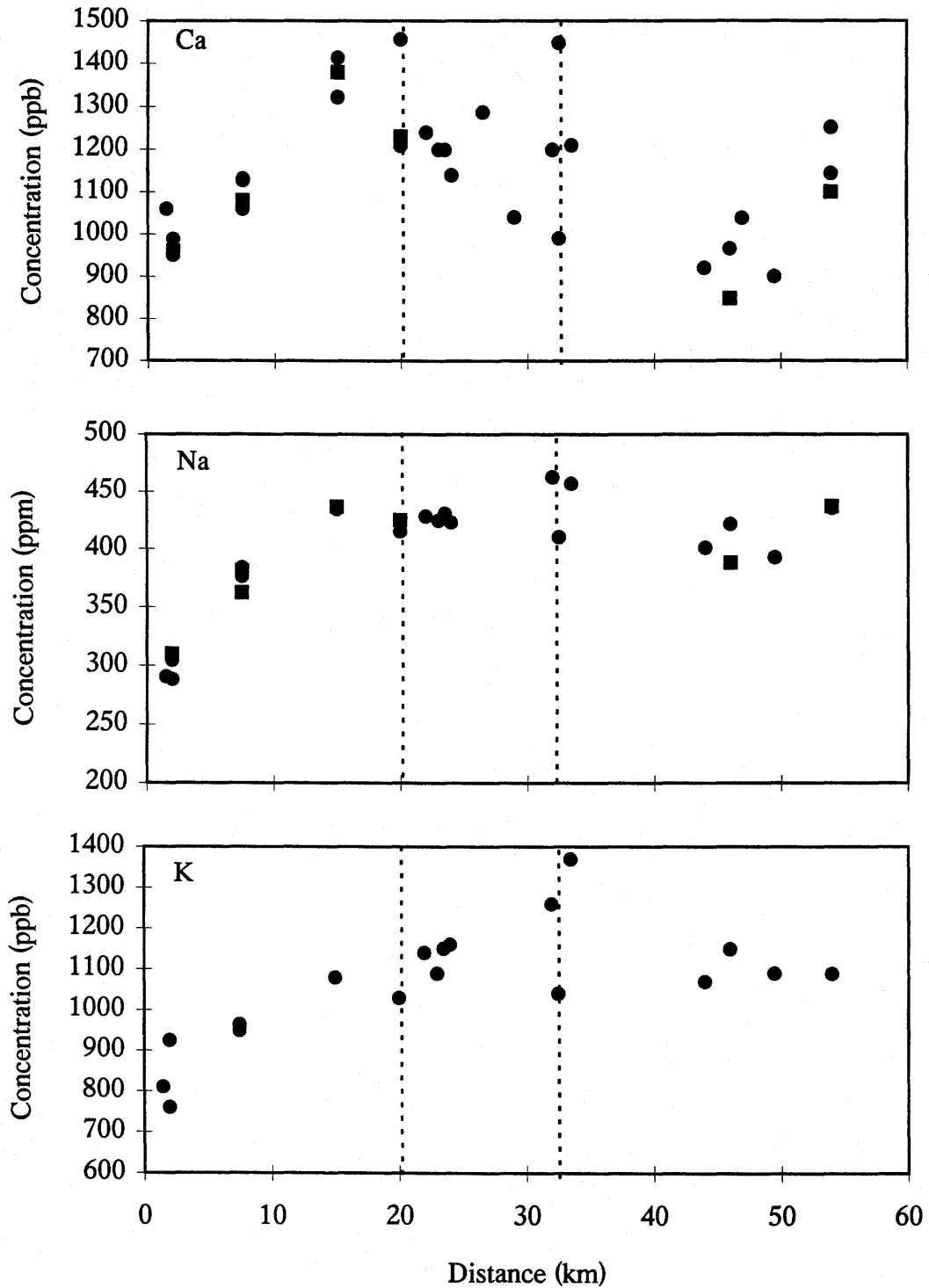


Figure 4.3. Ca, Na, and K concentrations in the Milk River aquifer groundwater versus distance along the flow path. Dashed vertical lines represent the redox front and post-redox front boundaries. Cumulative plot of 1996-1997 data. Square marker represents AAS (Ca, Na) data. Circle marker represents ICP-AES (Fe) data.

Table 4.3. Saturation index values from speciation modeling using PHREEQC, in the Milk River aquifer groundwater.

Sample	MR139	MR122	MR123	MR52	MR80	MR130	MR136	MR129	MR132	MR137	MR119
Distance (km)	1.5	2.0	7.5	15.0	20.0	22.0	23.5	24.0	31.5	44.0	54.0
Phase											
pCO ₂	-3.80	-3.77	-3.75	-3.69	-3.70	-3.50	-3.59	-3.56	-3.05	-3.54	-3.56
Calcite	-0.25	-0.25	-0.18	-0.12	-0.17	-0.21	-0.19	-0.23	-0.19	-0.16	-0.03
Dolomite	-1.00	-0.83	-0.69	-0.63	-0.64	-0.67	-0.70	-0.70	-0.73	-0.62	-0.44
Gypsum	-3.39	-3.34	-3.27	-2.97	-3.07	-3.11	-3.16	-3.18	-5.27	-4.38	-5.77
Uraninite	-18.79	-18.50	-18.65	-18.55	-18.30	-12.36	-12.20	-8.77	1.95	4.79	3.48
Barite	0.12	-0.01	0.29	0.03	-0.02	-0.14	0.03	3.08	-1.41	-0.33	-1.70
Strontianite	-0.99	-0.94	-0.75	-0.66	-0.74	-0.78	-0.76	-0.78	-0.74	-0.67	-0.05

For purposes of comparison, PHREEQC (Parkhurst, 1995) was utilized to determine the theoretical saturation indices of calcite, dolomite, gypsum, and $p\text{CO}_2$ along the flow path (Fig. 4.4). Saturation indices for select minerals and phases that may be reacting in the Milk River aquifer groundwater are presented in Table 4.3. Consistent with the results of Hendry et al. (1991), data of this study indicates that the groundwaters are at equilibrium, or slightly undersaturated, with respect to calcite and dolomite, respectively. Calcite is very close to equilibrium in the groundwaters (mean SI = -0.18; n=11), and dolomite is slightly undersaturated in all the groundwaters along the flow path (mean SI = -0.70; n=11). Generally, the log $p\text{CO}_2$ values are less than the atmospheric $p\text{CO}_2$ of -3.5. Log $p\text{CO}_2$ values are slightly lower in the recharge area than the downgradient values (mean SI = -3.59; n=11). Saturation indices show that gypsum is undersaturated in the groundwater from the recharge area to 54 km downgradient (mean SI = -3.72; n=11).

4.3 Oxidation - Reduction Sequences in Confined Groundwater Systems

Hydrogeochemists have observed a decline in the measured potential, Eh, in groundwaters as they migrate from recharge to discharge areas in confined aquifers. This progressive change of the groundwaters, from an oxidized state at recharge to a reduced state at discharge, indicates that oxidation-reduction (redox) reactions have occurred in the aquifer (Champ et al., 1979). Associated changes in pH and concentrations of dissolved elements (O, N, Fe, Mn, S, and C) can also be accounted for by these redox reactions (Table 4.4).

Champ et al. (1979), proposed three redox zones in groundwater systems: (1) an oxygen-nitrate zone, (2) an iron-manganese zone, and (3) sulfide zone. The mobility and concentrations of multivalent metals (Co, Ni, Cu, U, Fe, and Mn) and multivalent non-metals (As, S, and N) vary in each of these zones. In the recharge area of a confined (closed system) aquifer the water is oxidizing, as it contains both dissolved oxygen and nitrate. Thus, the mobile elements are those which are soluble as higher

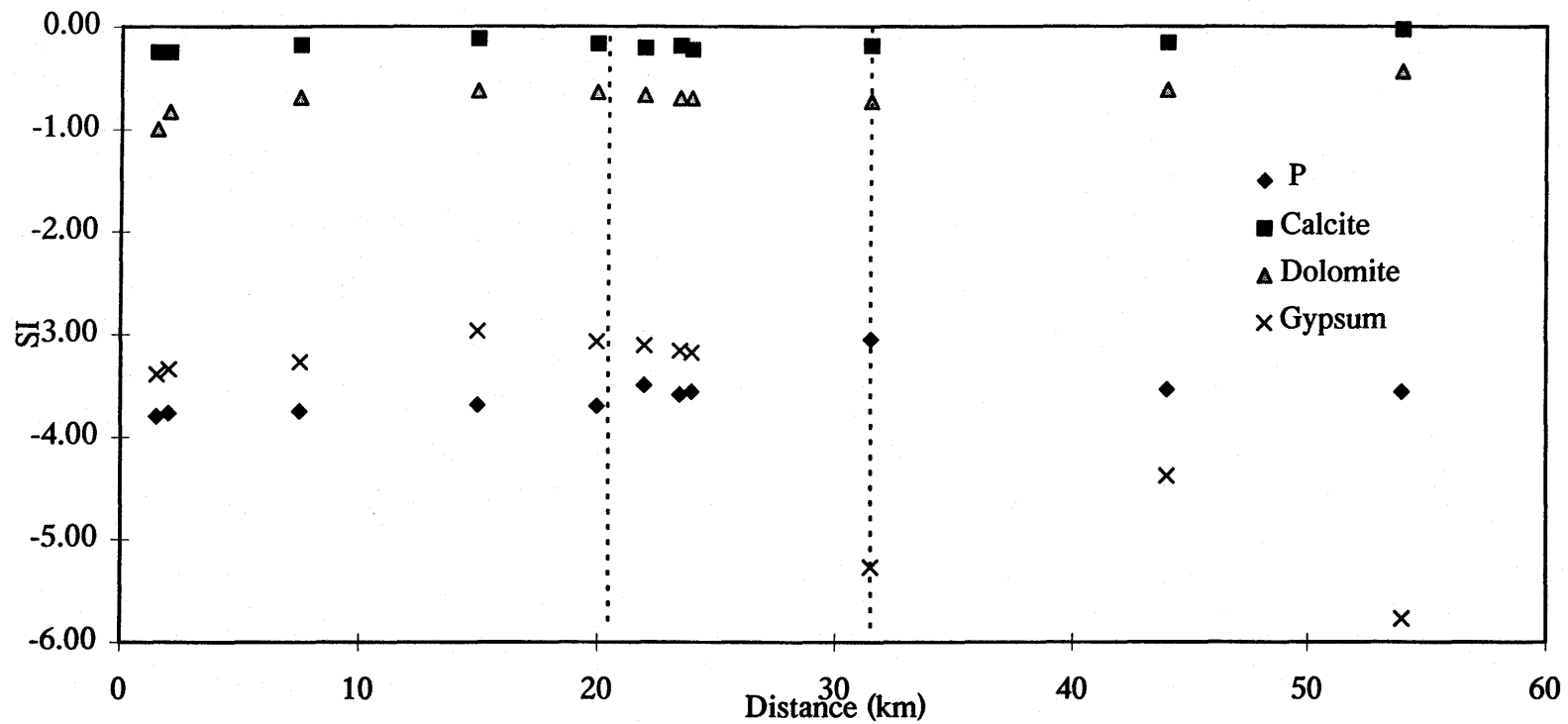


Figure 4.4. PHREEQC initial conditions - solution modeling of select phases in the Milk aquifer groundwater. Calculated saturation indices versus distance from recharge along the flow path. Dashed vertical lines represent redox front and post-redox front.

Table 4.4. Oxidation states of select elements that occur in the Milk River aquifer, groundwater (from Langmuir, 1997).

Element	Symbol	Proton Number (atomic number)	Oxidation states
Aluminum	Al	13	3+
Arsenic	As	33	3+,5+, (0)
Barium	Ba	56	2+
Boron	B	5	3+
Cadmium	Cd	48	2+
Calcium	Ca	20	2+
Carbon	C	6	4+, (0), 4-, 2-
Chlorine	Cl	17	1-
Chromium	Cr	24	6+, 3+
Cobalt	Co	27	2+, (3+)
Copper	Cu	29	2+, 1+, (0)
Iron	Fe	26	3+, 2+
Lead	Pb	82	2+, (4+), (0)
Lithium	Li	3	1+
Magnesium	Mg	12	2+
Manganese	Mn	25	2+, (3+), (4+)
Nickel	Ni	28	2+, (3+)
Phosphorus	P	15	5+
Potassium	K	19	1+
Selenium	Se	34	6+, 4+, (0), 2-
Sodium	Na	11	1+
Strontium	Sr	38	2+
Sulphur	S	16	6+, 4+, 0, (1-), 2-
Thorium	Th	90	4+
Tin	Sn	50	4+
Titanium	Ti	22	4+
Tungsten	W	74	6+
Uranium	U	92	6+, 4+
Vanadium	V	23	5+, 4+, 3+
Zinc	Zn	30	2+
REEs(Lanthinides)	La - Lu	57 through 71	3+
Europium	Eu	63	3+, (2+)
Cerium	Ce	58	3+, 4+

Note: Values in parentheses are found in mineral systems only

valent oxyanions (e.g. N, S, U, and Cr), whereas those which are immobile form higher valence insoluble metal oxides (e.g. Fe and Mn). When decaying organic matter isolated from atmospheric oxygen is present in the system, aerobic decay takes place, depleting all free O₂ and nitrate, and a more reducing environment develops - the Fe-Mn zone. The Fe(II) and Mn(II) valence states are more stable and soluble in this reduced zone compared to their corresponding Fe(III) and Mn(III) - Mn(IV) hydrous oxides; the latter dissolve, become reduced and are thus mobile as Fe(II) and Mn(II). Transition metals Zn, Co, Ni, and Cu may also appear in solution.

After the reduction of Mn and Fe, the groundwater becomes sufficiently reducing, and hence- the sulfide zone is created. The immobile elements in this zone are those which form insoluble metal sulfides in their reduced state (Fe, Mn, Co, Cr, Ni, Cu, and As). The Milk River aquifer fits the redox sequence documented by Champ et al. (1979). Therefore this study will use the major and trace element geochemistry of the groundwater to contribute to the understanding of the fate of trace elements, including the REEs, in groundwater flow systems.

4.3.1 Redox Chemistry of the Milk River Groundwater

Figure 4.5 displays how sulphate concentrations decrease rapidly along the flow path and at 32 km from recharge are at very low concentrations (<0.5 µg/ml). Iron does not exhibit any appreciable concentration differences as the groundwater migrates down flow through the redox and post-redox front, but does display a small overall increase in dissolved concentrations (Fig. 4.5).

Methane data from Taylor (1996), displays a significant increase at 32 km where the sulphate concentrations drop below detection as predicted by redox reactions in closed aquifer systems. Geological changes can account for these values (Hendry et al., 1991). The first change was the erosion of the overlying confining beds in the recharge area about 5×10^5 years ago, allowing meteoric water with low Na⁺ and Cl⁻ concentrations to enter and displace the existing groundwater. The second change was the deposition of

glacial till about 30,000-40,000 years ago (Fig. 2.3). The water recharging through the till developed groundwater in the aquifer which was enriched in Na^+ , SO_4^{2-} , Ca^{2+} , and Mg^{2+} (Hendry and Schwartz, 1990).

The CH_4 - SO_4 redox transition has been commented on by Taylor (1996), and as well as the dependence on SO_4 availability being important in the role of methane oxidation. Methane does not form in the presence of dissolved sulphate. If found with sulphate it implies mixing in the well from different redox zone waters. Bio-fermentation to generate CH_4 is expected to occur after the reduction of sulphate in closed groundwater systems (Champ et al., 1979). The Milk River groundwater contains sulphate concentrations that are negligible at 32 km along the flow path. Methane concentrations become detectable at higher concentrations at approximately this point on the flow path and farther downgradient (Fig. 4.5; Taylor, pers. comm.).

Changes in the redox potential, and the reductive dissolution of Fe and Mn oxyhydroxides all play a role in mobilizing select metals and associated trace elements. Precipitation and/or adsorption will decrease concentrations of trace metals and dissolution and/or desorption will act to increase dissolved concentrations (Jacobs et al., 1988). Adsorption and desorption are pH dependent. Due to very slow groundwater velocities, the zone of high SO_4 concentration does not extend far beyond the subcrop area of the Milk River aquifer (Hendry and Schwartz, 1988).

In groundwater studies, *uranium* has been found to be an excellent element for tracing the evolution of waters because of its multi-valent characteristics. Uranium concentrations range overall from <0.02 ppb to 1.48 ppb, where the more distal water containing the lowest levels. Ivanovich et al. (1991) report uranium concentrations of similar magnitude in the western section of the Milk River aquifer. Because the groundwater samples have high SO_4 concentrations and no methane, oxic conditions were suggested (Ivanovich et al., 1991). Therefore, the higher concentrations encountered along the flow path at 20 km may be the redox front boundary, and at

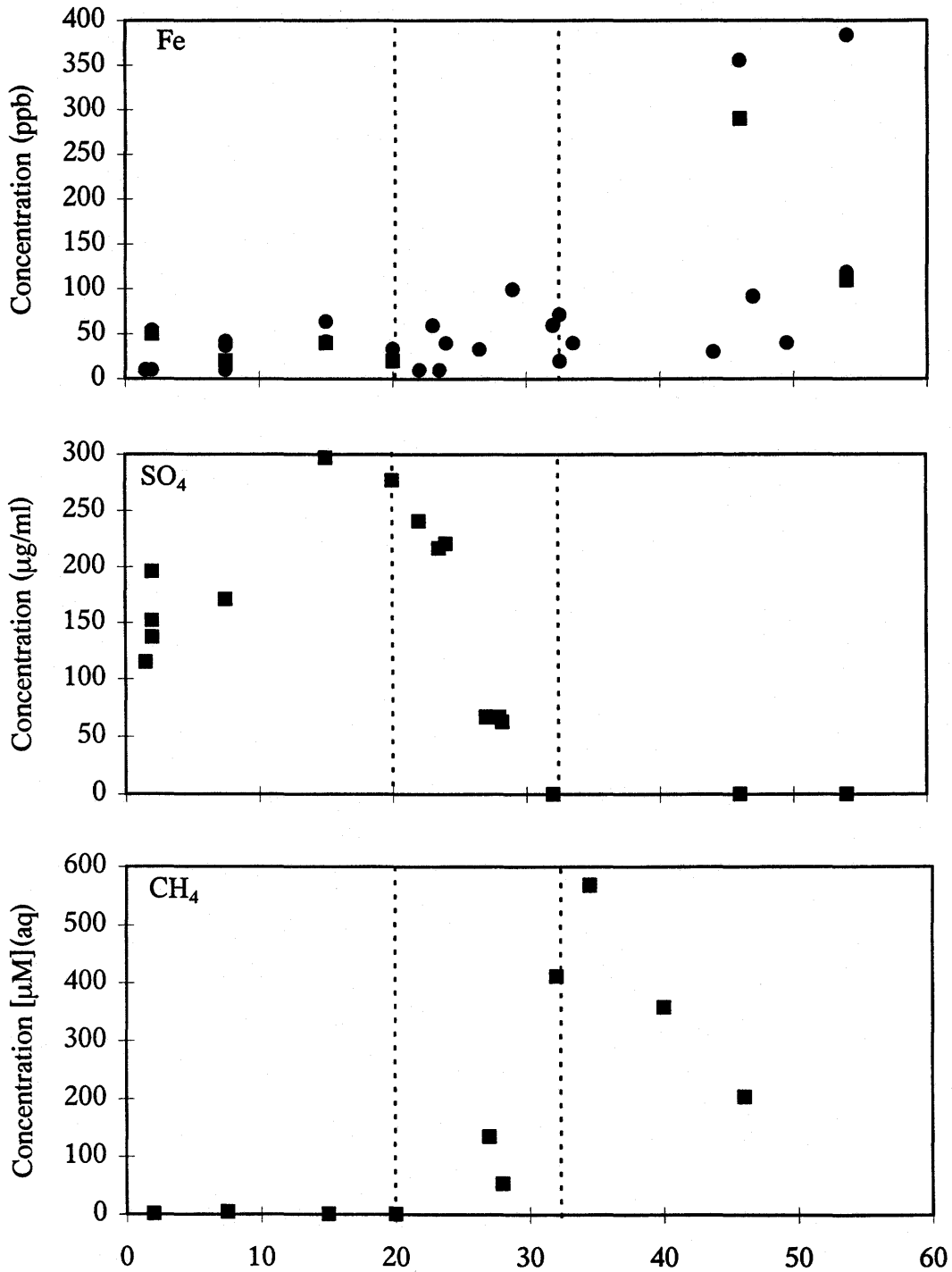


Figure 4.5. Concentrations of Fe, SO₄, and CH₄ in the Milk River aquifer groundwater versus distance along the flow path. Dashed vertical lines represent redox front and post-redox front boundaries. Cumulative plot of 1996-1997 data. Square marker represents AAS (Fe) data or Liquid Chromatography data (SO₄). Circle marker represents ICP-AES data (Fe). Methane data from (Taylor, pers. comm.).

the post-redox front boundary (Fig. 4.7). Therefore, it is unlikely that the groundwater with intermediate concentrations of uranium are probably the result of minor mixing between oxic and anoxic water masses as previously reported by Ivanovich et al. (1991).

Aqueous uranium transport has been well documented in roll-front type deposits. Uranium is leached from rock or soil, and then is transported in neutral to alkaline, oxidized waters as U^{+6} -carbonate complexes, until a redox interface is encountered and reduces the uranium to U^{+4} , precipitating as insoluble uranium bearing minerals such as uraninite or coffinite.

The uranium speciation of select groundwater samples in the Milk River aquifer was investigated by Ivanovich et al. (1991) utilizing PHREEQE geochemical modeling code (Parkhurst et al., 1980). The model calculated saturation indices for uraninite which were determined to be undersaturated (<-4) to slightly saturated (<0.7) in the groundwater. Similarly, in this study, uranium speciation in the groundwater was investigated using PHREEQC (Parkhurst, 1995). Uraninite (UO_2) is strongly undersaturated (SI <-18) in the recharge groundwater, but after the redox front (20 km) shifts toward saturation (SI >3) as the groundwater migrates downgradient (Fig. 4.6). The groundwater becomes oversaturated with respect to uraninite just after the post-redox front ($\sim 32-33$ km) along the flow path.

Generally, total *manganese* values in the groundwater are lowest in the subcrop area at <3 ppb with only a slight increase downgradient, excepting MR139. There is a Mn concentration peak from 20 km to approximately 33 km along the flow path (Fig. 4.6). This progressive northward increase along the flow path to a maximum of 11.2 ppb may be due to a redox boundary at 20 km from recharge. Therefore, reductive dissolution of Mn oxide appears to be an important process. After the post-redox boundary, dissolved Mn concentrations drop, due likely to precipitation of Mn oxyhydroxides.

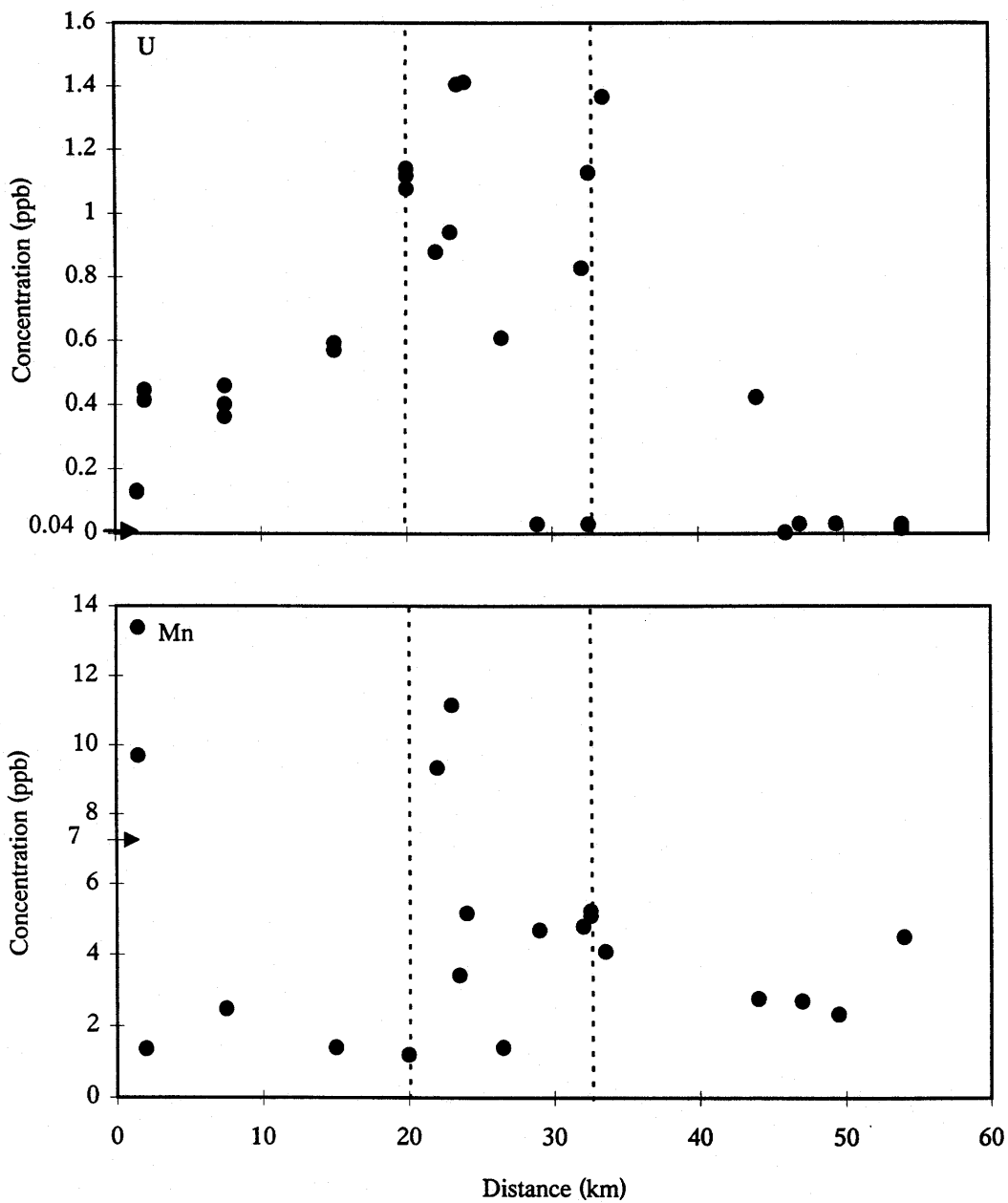


Figure 4.6. U and Mn concentrations in the Milk River aquifer groundwater versus distance from recharge. Dashed vertical lines represent redox front and post-redox front boundaries. Arrow on left margin is value of select element for average world river water from Taylor and McLennan (1985). Cumulative plot of 1996-1997 data.

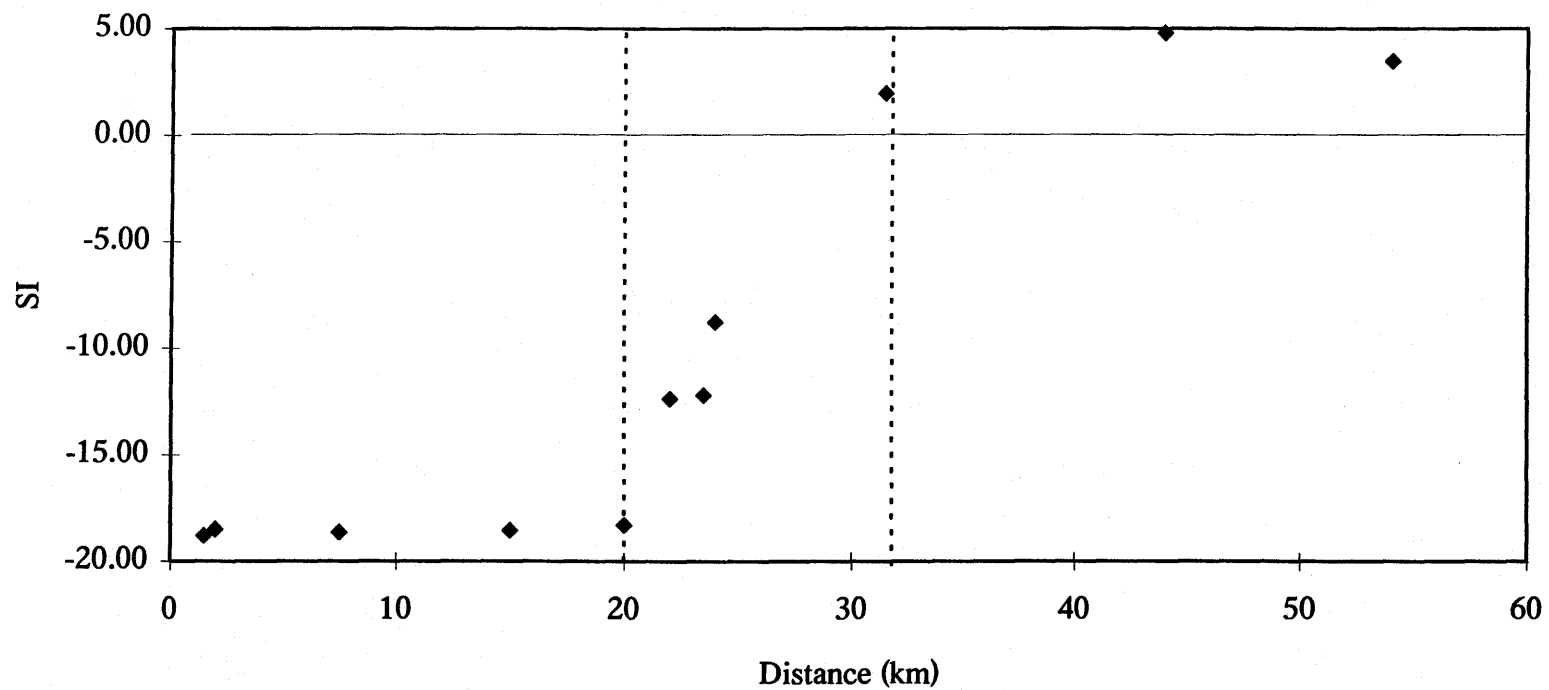


Figure 4.7. PHREEQC initial conditions - solution modeling of uraninite in the Milk aquifer groundwater. Calculated saturation indices versus distance from recharge along the flow path. Dashed vertical lines represent redox front and post-redox front.

Hendry and Schwartz (1990) presented Eh measurements. These authors determined that the Eh is above 300 mv in the recharge area, and it decreases quickly to about approximately 100 mv at well site MR80, 20 km from recharge, suggesting that redox conditions are low enough for sulphate reduction to occur (Champ et al., 1979). The lowest Eh (-68 mv) was obtained from MR113, 91 km from recharge, at the end of the flow path (Hendry and Schwartz, 1990). However, based on present knowledge of redox reactions and the data from this study, it appears that some of these Eh measurements are not consistent with the concentrations of select dissolved redox components (i.e. SO₄ reduction, and CH₄ production) measured in the groundwaters. Therefore, theoretical values have been determined at select wells where the Eh data is not known or is poorly constrained (Fig. 4.8). Eh values have and will be further discussed in this chapter, as they are useful for geochemical speciation modeling.

4.4 Select Trace Elements in the Milk River Aquifer Groundwater

4.4.1 Trace Element Concentrations Along the Flow Path

Table 4.5 lists the concentrations of select trace elements analyzed in the Milk River aquifer groundwater samples. The concentrations and mobility of trace elements depends on many factors including: (1) the abundance in the host rock and solubility of its minerals; (2) atmospheric inputs; (3) the nature and sequence of hydrogeochemical processes within the aquifer such as adsorption, desorption, precipitation, dissolution, and redox reactions; (4) the residence time; (5) biodegradation; and (6) anthropogenic sources (Edmunds et al., 1982; Smedley, 1991; Grenthe et al., 1992; Ramaswami, 1994; Gascoyne, 1997). These points will be discussed and assessed using analytical measurements of individual element concentrations coupled with hydrogeochemical modeling in the next chapter.

Boron is one of the trace elements with the highest concentrations, ranging from >100-500 ppb in the recharge area and increasing linearly along the flow path to 1400-1500

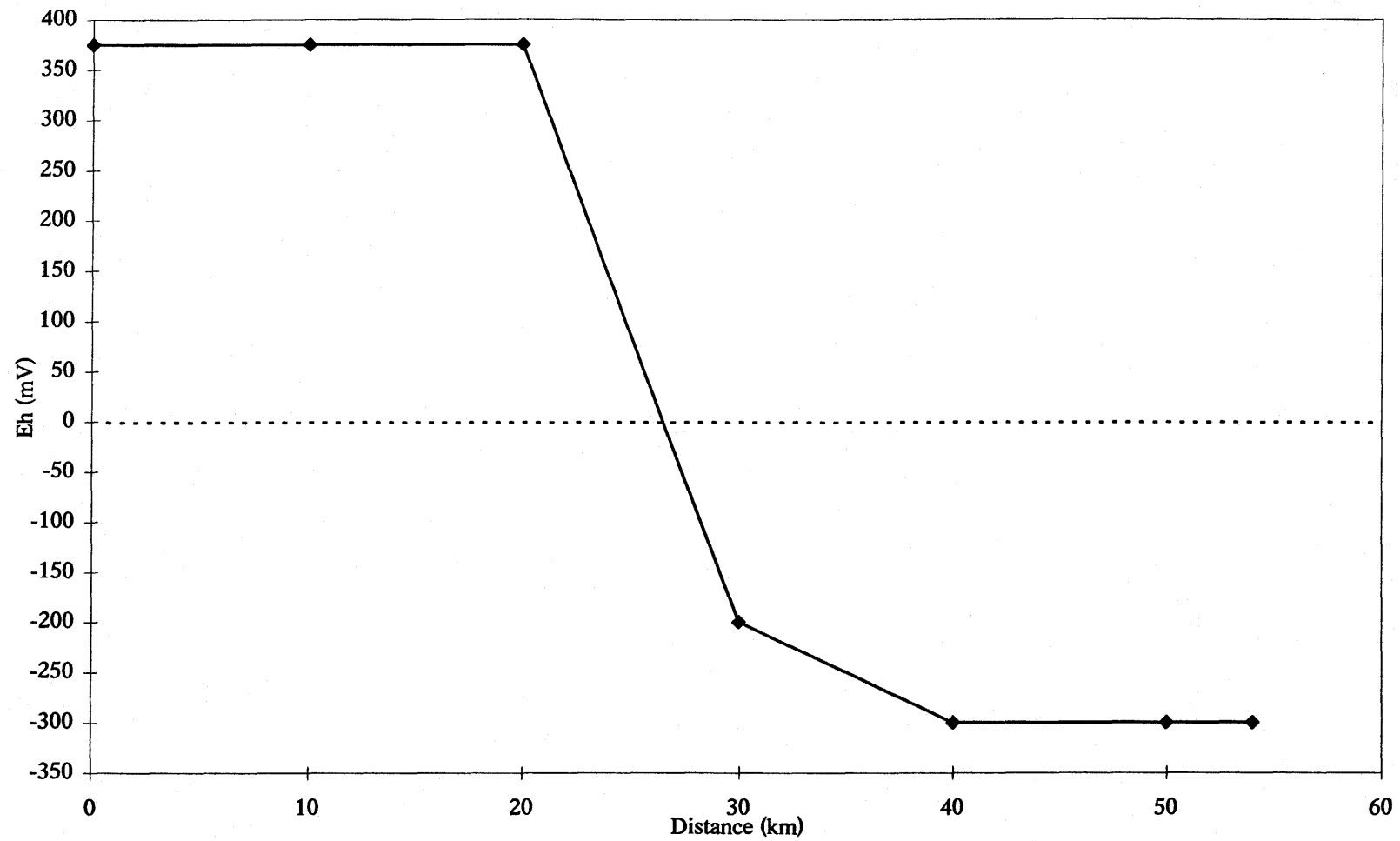


Figure 4.8. Theoretical Eh values used in the speciation modeling, as determined by redox reactions in the Milk River aquifer groundwater.

Table 4.5. Trace elements analyzed in the Milk River aquifer groundwater.
(1997 data unless otherwise stated in parenthesis)

Sample (ppb)	MR139				MR122(96)		MR122		MR123(96)		MR123	
	filtered	fil-dup	unfiltered	unfil-dup	filtered	filtered	unfiltered	filtered	fil-dup	filtered	unfiltered	
Tl	18.1	25.2	24.6	4.7	3.6	1.2	1.2	4.4	4.0	2.0	2.7	
V	0.06	0.14	0.10	0.72	0.02	0.00	0.01	0.03	0.02	0.02	0.04	
Cr	0.12	0.22	0.14	0.09	0.09	0.10	0.22	0.13	0.06	0.18	0.20	
Mn	9.7	13.4	10.4	1.8		1.4	1.7			2.5	3.1	
Co	0.066	0.068	0.083	0.063	0.018	0.015	0.012	0.010	0.010	0.011	0.014	
Ni	0.06	0.12	0.06	0.86	0.12	0.06	0.10	0.01	0.02	0.01	0.03	
Li	45.5	45.2	44.5	6.0	51.3	47.7	47.0	48.2	43.8	38.4	38.2	
Be												
B	362	475	307	11	119	241	229	290	257	464	431	
Y	0.20	0.19	0.22	0.36	0.16	0.14	0.13	0.22	0.23	0.21	0.21	
Zr	0.17	0.17	0.19	0.09		0.03	0.04			0.05	0.06	
Nb	0.04	0.04	0.05	0.002	n.d.	n.d.	0.001	n.d.	0.001	0.001	0.001	
Ta	0.003	0.004	0.004	0.0001	n.d.	0.0003	0.0004	n.d.	0.001	0.001	0.0005	
Hf	0.002	0.002	0.003	0.001	0.001	0.0001	0.001	0.001	0.002	0.001	0.001	
P	295	410	299	15	120	108	112	445	499	355	354	
La	0.087	0.079	0.105	0.028	0.010	0.002	0.003	0.014	0.015	0.003	0.017	
Ce	0.175	0.158	0.211	0.053	0.010	0.003	0.005	0.007	0.006	0.002	0.032	
Pr	0.023	0.021	0.026	0.007	0.001	0.001	0.001	0.001	0.001	0.001	0.005	
Nd	0.091	0.088	0.111	0.028	0.012	0.002	0.005	0.011	0.008	0.003	0.021	
Sm	0.022	0.022	0.025	0.005	0.005	0.001	0.002	0.004	0.003	0.002	0.007	
Eu	0.005	0.004	0.004	0.000	0.001	0.001	0.001	0.001	0.001	0.000	0.001	
Gd	0.021	0.023	0.028	0.007	0.006	0.004	0.003	0.005	0.004	0.003	0.006	
Tb	0.004	0.003	0.003	0.0005	n.d.	0.001	0.001	0.001	n.d.	0.0004	0.001	
Dy	0.017	0.016	0.020	0.006	0.005	0.003	0.003	0.005	0.004	0.005	0.006	
Ho	0.004	0.003	0.004	0.001	0.001	0.001	0.001	0.002	0.002	0.002	0.002	
Er	0.010	0.010	0.014	0.004	0.006	0.004	0.006	0.008	0.009	0.006	0.007	
Tm	0.002	0.002	0.002	0.000	0.001	0.001	0.001	0.001	0.001	0.001	0.001	
Yb	0.010	0.009	0.011	0.003	0.007	0.006	0.006	0.009	0.008	0.008	0.008	
Lu	0.002	0.001	0.001	0.0003	0.001	0.001	0.001	0.002	0.001	0.001	0.001	
Cs	0.025	0.023	0.026	0.003	0.040	0.034	0.029	0.060	0.050	0.033	0.035	
Rb	0.72	0.69	0.69	0.38	0.79	0.78	0.75	0.84	0.83	0.86	0.85	
Ba	27.1	23.9	26.7	98.2	15.5	16.4	15.8	30.4	30.7	32.0	30.8	
Th	0.036	0.037	0.036	0.009	0.002	0.001	0.001	0.002	0.003	0.001	0.006	
U	0.13	0.13	0.13	0.97	0.41	0.44	0.45	0.40	0.36	0.46	0.46	
W	0.23	0.27	0.23	0.004	1.26	1.02	1.03	4.93	5.24	3.79	3.67	
Sr	50.62	48.59	49.96	231.93	49.67	49.98	49.31	73.22	72.56	74.81	73.64	
Pb	0.29	0.77	0.45	0.02	0.53	0.05	0.06	0.06	0.09	0.02	0.06	
As	0.24	0.13	0.23	0.95	0.09	0.16	0.16	0.05	0.03	0.10	0.08	
Sb	n.d.	0.07	n.d.	0.13	n.d.	n.d.	n.d.	0.01	n.d.	n.d.	n.d.	
Mo	1.54	1.49	1.54	0.99	0.07	0.06	0.06	0.08	0.06	0.06	0.05	
Cd	0.014	0.009	0.002	0.008	0.010	0.006	0.007	0.010	n.d.	0.004	0.001	
Sn	0.43	0.17	0.33	0.01		0.09	0.04			0.08	0.04	
Sc	0.56	0.81	0.60	0.71	1.86	0.73	0.74	1.75	1.92	0.84	0.91	
Ga												
Cu	0.59	0.53	0.33	0.93	1.07	0.46	0.69	0.57	0.59	0.44	1.41	
Zn	0.89	0.79	1.18	0.13	2.26	1.87	2.48	1.56	1.42	1.58	8.14	
Ag	0.0004	0.004	n.d.	n.d.	0.074	0.0001	0.001	0.020	0.051	0.014	0.007	
Au					n.d.	n.d.	n.d.	n.d.	n.d.	n.d.	n.d.	
Se	0.04	0.23	0.01	0.19	0.06	0.28	0.03	0.31	0.17	0.04	0.03	
Pd					0.02			0.03	0.04			
Hg	0.03	n.d.	0.06	n.d.		n.d.	n.d.			n.d.	n.d.	

Table 4.5. continued.

Sample	MR52(96)	MR52(95)	MR80(96)	MR80(95)	MR116(95)	MR115(95)	MR130		
(ppb)	filtered	filtered	filtered	fil-dup	filtered	filtered	filtered	filtered	unfiltered
Ti	12.7	4.1	12.5	11.8	5.1	2.9	0.2	2.7	3.4
V	0.05		0.07	0.07				0.02	0.04
Cr	0.01	1.00	0.18	0.05	1.00	1.10	1.20	0.04	0.25
Mn		1.4			1.2	1.4	4.7	9.4	13.7
Co	0.017	0.030	0.011	0.015	0.010	0.020	0.040	0.009	0.032
Ni	0.04	n.d.	0.07	0.08	n.d.	n.d.	n.d.	n.d.	0.07
Li	39.3	37.0	45.1	46.3	56.0	42.0	44.0	37.7	36.1
Be		0.30			n.d.	0.50	n.d.		
B	434		306	480				620	642
Y	0.26	0.03	0.26	0.28	0.05	0.02	0.05	0.17	0.20
Zr		0.11			0.08	0.05	0.08	0.09	0.12
Nb	0.01	n.d.	0.02	0.02	n.d.	n.d.	n.d.	0.001	0.005
Ta	0.002	n.d.	0.003	0.002	n.d.	n.d.	n.d.	0.0004	0.001
Hf	0.001		0.001	0.002				0.001	0.002
P	357		383	383				365	394
La	0.015	n.d.	0.043	0.039	n.d.	0.020	0.010	0.001	0.004
Ce	0.021	n.d.	0.078	0.079	n.d.	n.d.	n.d.	0.001	0.007
Pr	0.004		0.010	0.009				n.d.	0.000
Nd	0.020		0.042	0.048				0.0002	0.005
Sm	0.007		0.015	0.009				0.001	0.001
Eu	0.001		0.002	0.003				0.0005	0.0005
Gd	0.005		0.016	0.011				0.002	0.001
Tb	0.001		0.002	0.002				0.0004	0.001
Dy	0.003		0.007	0.007				0.002	0.004
Ho	0.001		0.003	0.003				0.001	0.001
Er	0.003		0.010	0.011				0.003	0.003
Tm	0.001		0.001	0.001				0.0001	0.0001
Yb	0.005	0.020	0.011	0.010	n.d.	0.010	n.d.	0.004	0.008
Lu	0.001		0.002	0.002				0.001	0.001
Cs	0.050		0.050	0.050				0.036	0.037
Rb	0.94	1.00	0.92	1.00	1.10	1.00	1.00	0.97	1.01
Ba	12.3	12.0	12.2	12.4	14.0	52.0	61.0	11.6	13.4
Th	0.007	n.d.	0.026	0.025	n.d.	n.d.	n.d.	0.001	0.005
U	0.59	0.57	1.14	1.12	1.08	0.61	0.03	0.88	0.90
W	4.44	2.30	3.00	3.08	1.60	0.40	0.30	2.41	2.39
Sr	104.69	101.00	86.53	93.12	85.00	83.00	57.00	92.90	96.86
Pb	0.04	0.20	0.11	0.17	0.10	n.d.	0.10	0.02	0.38
As	0.08	0.20	0.07	0.08	0.40	0.60	0.30	0.15	0.15
Sb	n.d.	n.d.	n.d.	0.01	n.d.	0.02	0.01	n.d.	n.d.
Mo	0.46	0.60	0.37	0.39	0.70	1.50	1.10	0.47	0.48
Cd	n.d.	n.d.	n.d.	0.010	n.d.	n.d.	n.d.	0.009	n.d.
Sa		0.03			0.03	0.02	0.08	0.32	0.39
Sc	1.87	0.70	2.14	2.33	0.90	0.90	1.10	0.91	0.94
Ga		0.30			0.20	0.60	0.90		
Cu	0.79	2.20	0.89	0.91	4.60	0.80	1.20	0.48	0.81
Zn	0.28	2.20	0.79	1.13	5.80	19.30	10.10	6.70	59.88
Ag	0.023	n.d.	0.023	0.022	n.d.	n.d.	n.d.	0.0004	n.d.
Au	n.d.		n.d.	0.001					
Se	0.03		0.17	0.29				0.13	0.25
Pd	0.06		0.05	0.05					
Hg								n.d.	n.d.

Table 4.5. continued.

Sample (ppb)	MR135		MR136		MR129		MR131		MR134		MR114(95)
	filtered	unfiltered	filtered								
Tl	2.6	2.6	2.2	2.2	1.7	1.4	1.6	3.4	0.9	1.2	0.5
V	0.03	0.02	0.02	0.03	0.00	0.13	n.d.	0.07	0.00	0.05	
Cr	0.16	0.13	0.18	0.22	0.56	0.17	0.31	0.54	0.18	0.20	3.10
Mn	11.2	10.4	3.4	3.4	5.2	7.5	4.8	6.3	5.2	4.6	5.1
Co	0.009	0.011	0.007	0.013	0.003	0.007	0.020	0.030	0.004	0.006	0.060
Ni	0.004	0.02	n.d.	0.07	0.003	0.27	n.d.	0.05	n.d.	n.d.	1.00
Li	36.6	37.6	38.9	38.4	38.8	40.7	40.9	39.4	39.0	38.9	55.0
Be											0.20
B	829	855	801	725	673	684	1092	1117	772	773	
Y	0.17	0.16	0.18	0.18	0.16	0.17	0.18	0.20	0.16	0.15	0.02
Zr	0.10	0.10	0.10	0.13	0.12	0.09	0.14	0.16	0.12	0.14	1.01
Nb	0.001	0.002	0.001	0.001	0.001	0.01	0.002	0.004	0.001	0.001	n.d.
Ta	0.0003	0.001	0.0003	0.0004	0.001	0.001	0.0001	0.0004	0.0002	0.0001	n.d.
Hf	0.001	0.001	0.001	0.001	0.001	0.001	0.002	0.002	0.001	0.001	
P	406	355	373	345	244	257	448	518	375	342	
La	0.002	0.005	0.002	0.015	0.003	0.005	0.004	0.044	0.003	0.003	0.030
Ce	0.002	0.002	0.002	0.007	0.002	0.009	0.004	0.116	0.001	0.003	0.010
Pr	0.0001	0.001	n.d.	0.004	0.0004	0.001	0.0002	0.011	n.d.	n.d.	
Nd	0.001	0.002	0.003	0.002	0.001	0.005	0.005	0.040	0.001	0.004	
Sm	0.002	0.001	0.001	0.002	0.001	0.002	0.002	0.006	0.001	0.001	
Eu	0.0003	0.0003	0.001	0.0005	0.001	0.001	n.d.	0.001	0.001	0.001	
Gd	0.002	0.003	0.003	0.003	0.000	0.003	0.002	0.008	0.002	0.002	
Tb	0.001	0.001	0.001	0.001	0.000	0.000	0.000	0.001	0.000	0.001	
Dy	0.001	0.004	0.003	0.004	0.002	0.002	0.002	0.005	0.003	0.003	
Ho	0.0003	0.002	0.001	0.001	0.001	0.001	0.001	0.001	0.001	0.001	
Er	0.002	0.008	0.004	0.004	0.003	0.004	0.002	0.003	0.004	0.004	
Tm	0.0003	0.0003	0.0003	0.0004	0.001	0.001	n.d.	0.001	n.d.	n.d.	
Yb	0.002	0.003	0.003	0.003	0.003	0.005	0.002	0.003	0.005	0.005	0.020
Lu	0.0003	0.0004	0.001	0.001	0.001	0.001	0.0003	0.001	0.001	0.001	
Cs	0.037	0.043	0.039	0.042	0.044	0.041	0.046	0.050	0.035	0.039	
Rb	1.01	0.97	1.04	1.06	1.05	1.02	1.09	1.13	0.98	0.96	1.30
Ba	15.8	15.9	16.6	16.5	18.9	18.9	52.8	50.8	36.2	36.3	89.0
Th	0.002	0.003	0.003	0.004	0.002	0.004	0.005	0.012	0.002	0.002	0.010
U	0.94	0.98	1.41	1.39	1.41	1.41	0.83	0.86	1.13	1.10	0.03
W	4.32	4.39	2.97	2.72	2.51	2.45	1.75	1.79	0.50	0.45	0.40
Sr	94.53	89.83	87.98	86.48	87.75	86.69	100.84	101.53	75.70	73.77	108.00
Pb	0.10	0.10	0.17	0.20	0.09	0.29	0.01	0.12	n.d.	0.04	1.00
As	0.15	0.16	0.14	0.15	0.30	0.27	0.31	0.27	0.18	0.21	1.20
Sb	0.00	0.00	n.d.	0.00	n.d.	n.d.	n.d.	n.d.	n.d.	n.d.	0.03
Mo	0.60	0.58	0.57	0.56	0.57	0.54	3.06	3.06	0.59	0.58	2.30
Cd	0.003	0.004	0.003	0.033	0.036	0.002	0.007	0.005	0.004	n.d.	1.700
Sn	0.42	0.30	0.42	0.39	0.77	0.72	3.77	3.39	2.14	0.65	0.06
Sc	0.98	0.86	0.86	0.82	0.49	0.58	0.71	0.84	0.76	0.70	1.00
Ga											1.00
Cu	0.55	0.89	2.16	4.44	0.67	3.90	0.34	0.56	0.29	0.39	3.50
Zn	5.42	8.31	7.34	13.09	2.46	42.90	1.24	82.51	0.79	8.18	49.10
Ag	0.002	0.011	0.001	0.002	n.d.	n.d.	0.001	0.002	0.001	0.0001	0.070
Au											
Se	0.25	0.32	0.30	0.14	0.13	0.16	0.54	0.24	0.23	0.18	
Pd											
Hg	n.d.	n.d.	n.d.	n.d.	n.d.	n.d.	0.04	0.03	n.d.	n.d.	

Table 4.5. continued.

Sample	MR133		MR137		MR127(96)		MR12(95)	MR138		MR119(96)	MR119(95)
(ppb)	filtered	unfiltered	filtered	unfiltered	filtered	fil-dup	filtered	filtered	unfiltered	filtered	filtered
Tl	0.8	1.3	0.4	1.3	0.6	0.7	0.8	0.2	0.6	1.1	0.7
V	0.03	0.03	0.02	0.07	0.03	0.03		0.04	0.05	0.04	
Cr	0.24	0.18	0.27	0.40	0.20	0.30	1.30	0.26	0.35	0.13	2.10
Mn	4.1	4.6	2.8	3.0			2.7	2.3	2.3		4.5
Co	0.017	0.017	0.013	0.014	0.032	0.033	0.030	0.015	0.018	0.025	0.050
Ni	0.04	0.05	0.05	0.04	0.05	0.06	n.d.	0.01	0.02	0.18	n.d.
Li	42.9	43.0	36.4	34.8	39.1	39.2	47.0	34.5	33.5	39.0	37.0
Be							0.60				n.d.
B	996	1033	1652	1554	1217	1434		1547	1593	1371	
Y	0.18	0.19	0.16	0.17	0.17	0.17	0.06	0.13	0.13	0.23	0.02
Zr	0.16	0.17	0.14	0.17			0.20	0.19	0.16		0.19
Nb	0.001	0.001	0.001	0.003	0.002	0.002	n.d.	0.001	0.002	0.01	n.d.
Ta	0.0005	0.0003	0.0004	0.001	0.001	n.d.	n.d.	0.0004	0.0004	n.d.	n.d.
Hf	0.001	0.001	0.001	0.002	0.002	0.003		0.002	0.002	0.003	
P	370	376	419	424	433	422		230	241	643	
La	0.003	0.004	0.004	0.012	0.022	0.022	0.050	0.004	0.005	0.033	0.040
Ce	0.002	0.005	0.002	0.019	0.005	0.006	0.050	0.004	0.008	0.011	n.d.
Pr	n.d.	0.003	0.001	0.003	0.001	0.001		0.001	0.001	0.002	
Nd	0.001	0.003	0.001	0.010	0.010	0.008		0.004	0.004	0.007	
Sm	0.002	0.002	0.001	0.004	0.001	0.004		0.002	0.002	0.006	
Eu	0.000	0.001	0.000	0.001	0.001	0.001		0.000	0.001	0.001	
Gd	0.001	0.002	0.003	0.005	0.004	0.005		0.002	0.002	0.005	
Tb	0.001	0.001	0.000	0.001	n.d.	n.d.		0.000	0.000	0.001	
Dy	0.002	0.001	0.005	0.005	0.002	0.001		0.002	0.002	0.002	
Ho	0.001	0.001	0.001	0.001	0.001	n.d.		0.000	0.001	0.001	
Er	0.004	0.003	0.004	0.004	0.002	0.002		0.002	0.002	0.003	
Tm	0.0003	0.0005	0.001	0.0005	n.d.	n.d.		0.0002	0.0003	n.d.	
Yb	0.002	0.003	0.004	0.004	0.002	0.002	n.d.	0.003	0.004	0.005	0.020
Lu	0.001	0.001	0.001	0.001	0.001	0.001		0.0004	0.0005	0.001	
Cs	0.041	0.042	0.040	0.040	0.050	0.050		0.042	0.044	0.060	
Rb	1.10	1.07	0.98	0.98	1.07	1.09	1.20	1.09	1.09	1.17	1.20
Ba	29.1	29.2	70.4	71.5	60.2	60.3	89.0	74.5	72.4	84.1	107.0
Th	0.002	0.004	0.003	0.006	0.004	0.003	0.010	0.004	0.005	0.004	0.020
U	1.37	1.48	0.42	0.42	0.00	0.00	0.03	0.03	0.03	0.02	0.03
W	0.56	0.58	0.96	0.90	1.98	1.90	0.90	1.23	1.28	1.63	0.70
Sr	96.55	96.03	72.70	72.94	67.85	69.09	74.00	70.59	69.00	95.97	99.00
Pb	0.01	0.19	0.13	0.18	0.05	0.10	0.10	0.05	0.09	0.04	n.d.
As	0.19	0.17	0.19	0.16	0.27	0.25	0.20	0.58	0.49	0.14	0.30
Sb	n.d.	n.d.	n.d.	n.d.	0.03	0.02	0.01	n.d.	n.d.	0.01	0.02
Mo	0.91	0.90	0.90	0.90	1.20	1.22	0.90	1.74	1.72	8.98	10.30
Cd	0.004	0.001	0.012	0.006	n.d.	0.010	0.050	0.005	n.d.	0.030	0.060
Sn	1.68	1.87	0.76	0.78			0.04	2.82	2.52		0.05
Sc	0.80	0.76	0.62	0.66	1.71	1.59	1.00	0.36	0.37	1.58	0.80
Ga							1.20				1.20
Cu	0.34	0.78	0.38	0.56	0.10	0.19	2.20	0.89	0.18	0.33	0.30
Zn	0.91	9.40	1.57	2.22	0.36	0.69	38.50	1.53	20.23	0.40	4.20
Ag	0.025	0.019	0.075	0.021	0.040	0.043	0.010	0.006	0.007	0.013	n.d.
Au					0.001	n.d.				0.001	
Se	0.34	0.39	0.23	0.04	0.24	0.41		0.28	0.27	0.34	
Pd					0.05	0.03				0.05	
Hg	n.d.	n.d.	n.d.	n.d.				0.02	0.01		

ppb 50 km downgradient (Fig. 4.9). Boron concentrations are typically higher in marine clays compared to continental clays, due to the greater abundance of boron in seawater (4440 $\mu\text{g/l}$) than in freshwater and its adsorption onto marine organic matter (18 $\mu\text{g/l}$) (Dominik and Stanley, 1993). The shales in the Milk River aquifer system are of marine origin, and therefore are likely the source of the high boron concentrations observed along the flow path. Diffusion from the shales is also interpreted from the conservative nature of boron as the groundwater evolves. Boron and chloride display similar well defined trends in the Milk River groundwater (Figs. 4.2 and 4.9).

Molybdenum concentrations show a slight increase as the groundwater evolves from 0.06 ppb in the recharge area to 10 ppb 54 km downgradient. The small but steady increase of Mo with age of the groundwater indicates progressive water-rock interactions for this element (Fig. 4.9).

Rubidium values increase from 0.75 ppb in the recharge area to 10 ppb 54 km downgradient. The uniform increase of Rb is similar to that of B and Cl (Fig. 4.10).

The concentration of *barium* displays constant values up to the redox front boundary (20 km) and then concentrations linearly increase as the water moves down the flow path to 54 km. Concentrations range from 20 ppb to >100 ppb respectively (Fig. 4.10). The Ba is likely derived from K-bearing clays, where Ba substitutes for K. If present, barite is extremely insoluble.

The barium speciation in the Milk River groundwater was investigated using PHREEQC geochemical modeling code (Parkhurst, 1995). Barite (BaSO_4) saturation indices are variable along the flow path. Generally the groundwater is slightly undersaturated or close to saturation equilibrium with respect to BaSO_4 (Fig. 4.11). The mean average SI is -0.01 which implies overall that BaSO_4 is near equilibrium in the groundwater along the flow path.

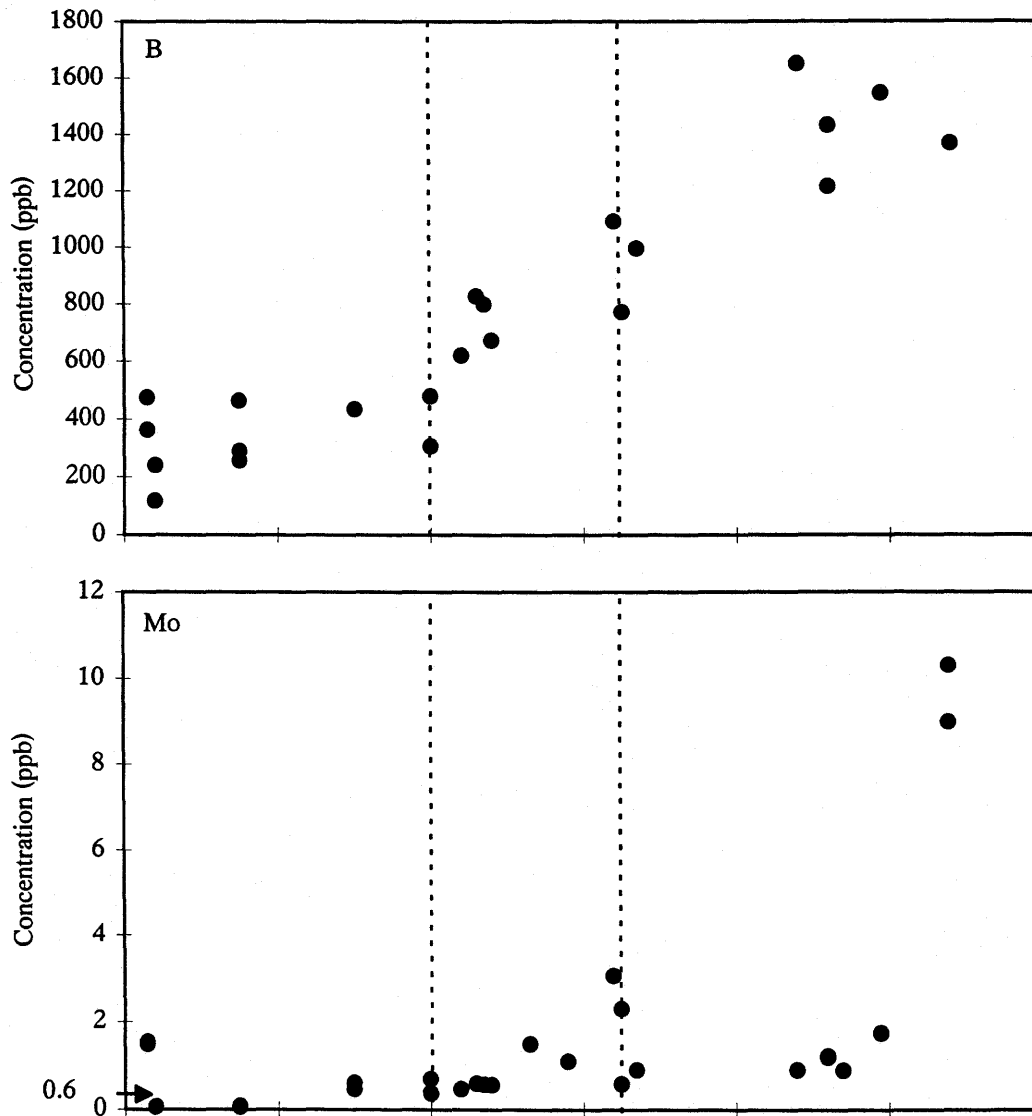


Figure 4.9. B and Mo concentrations in the Milk River aquifer groundwater versus distance from recharge. Dashed vertical lines represent redox front and post-redox front boundaries. Arrow on left margin is value of select element for average world river water from Taylor and McLennan (1985). Cumulative plot of 1996-1997 data.

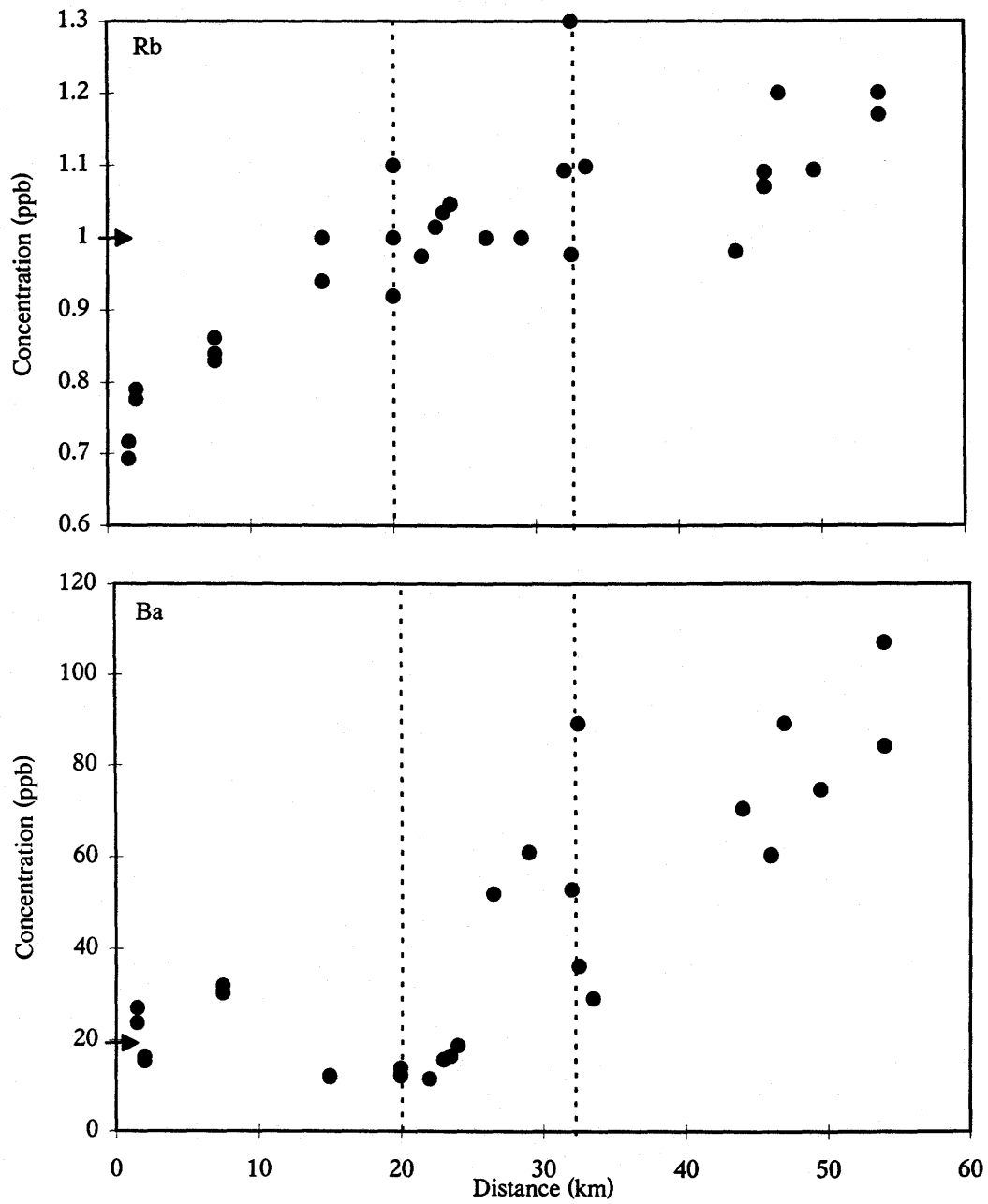


Figure 4.10. Rb and Ba concentrations in the Milk River aquifer groundwater versus distance from recharge. Dashed vertical lines represent redox front and post-redox front boundaries. Arrow on left margin is value of select element for average world river water from Taylor and McLennan (1985). Cumulative plot of 1996-1997 data.

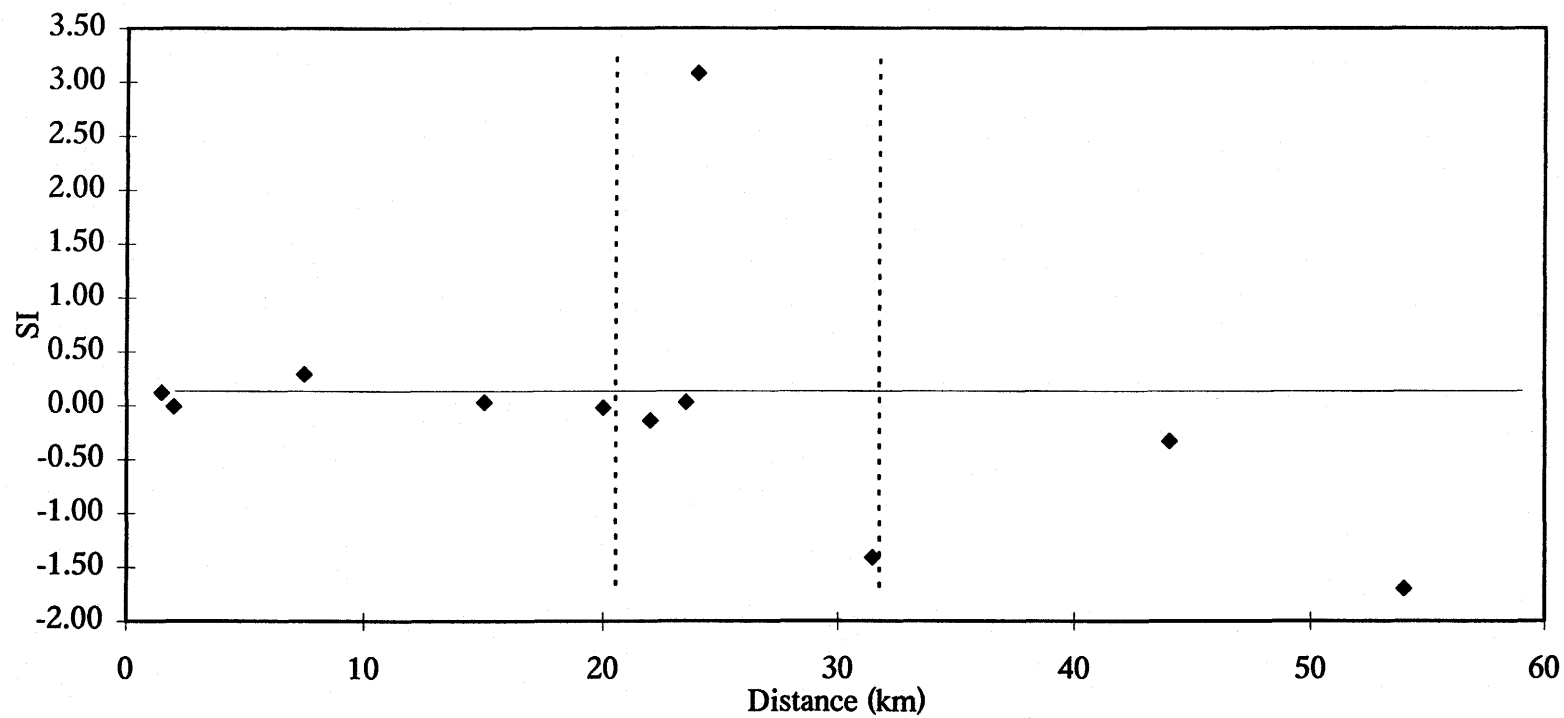


Figure 4.11. PHREEQC initial condition - solution modeling of barite in the Milk aquifer groundwater. Calculated speciation indices versus distance from recharge along the flow path. Dashed vertical lines represent redox front and post-redox front.

Lithium values remain relatively uniform in groundwaters with a minor overall net decrease as the groundwaters migrate along the flow path. Li values fall in the 35-50 ppb range (Fig. 4.12). Inputs may be due to rainfall as there is no apparent aquifer sources of lithium and there is no removal of lithium by any process during downgradient flow.

In Figure 4.12, *cobalt* displays low values in the fresh recharge groundwater (<0.02 ppb) and only a moderate increase as they migrate along the flow path (>0.03 ppb).

Similarly, *zinc* displays a minor concentration peak at approximately 20 km to 32-33 km downgradient, and then values return to similar concentrations as in the recharge zone (Fig. 4.12). Concentrations are <5 ppb in the recharge area and reach an upper limit at the redox boundary of 19 ppb. The decrease may reflect coprecipitation with Fe and/or Mn hydroxides.

4.5 Rare Earth Elements

Rare earth elements or REEs (also termed lanthanides) include lithophile elements with atomic numbers 57 through 71. REEs with even atomic numbers (i.e. Ce, Nd, Sm, Gd, Dy, Er, and Yb) are geochemically more abundant than neighboring REEs with odd atomic numbers (i.e. La, Pr, Pm, Eu, Tb, Ho, Tm, and Lu), which produces a “saw-tooth” effect in REE plots of abundance, the so-called Odd-Harkins rule. This effect is usually eliminated by plotting REE analyses normalized to average REE abundances of chondrite or a specific rock such as post Archean Australian average shale (PAAS; Taylor and McLennan, 1985).

A review of the aqueous geochemistry of REEs is given by Wood (1990a & 1990b). Coherent behavior of the REEs as a group make them of interest for interpreting groundwater systems. The REEs exist in the trivalent oxidation state. Ce can also exist

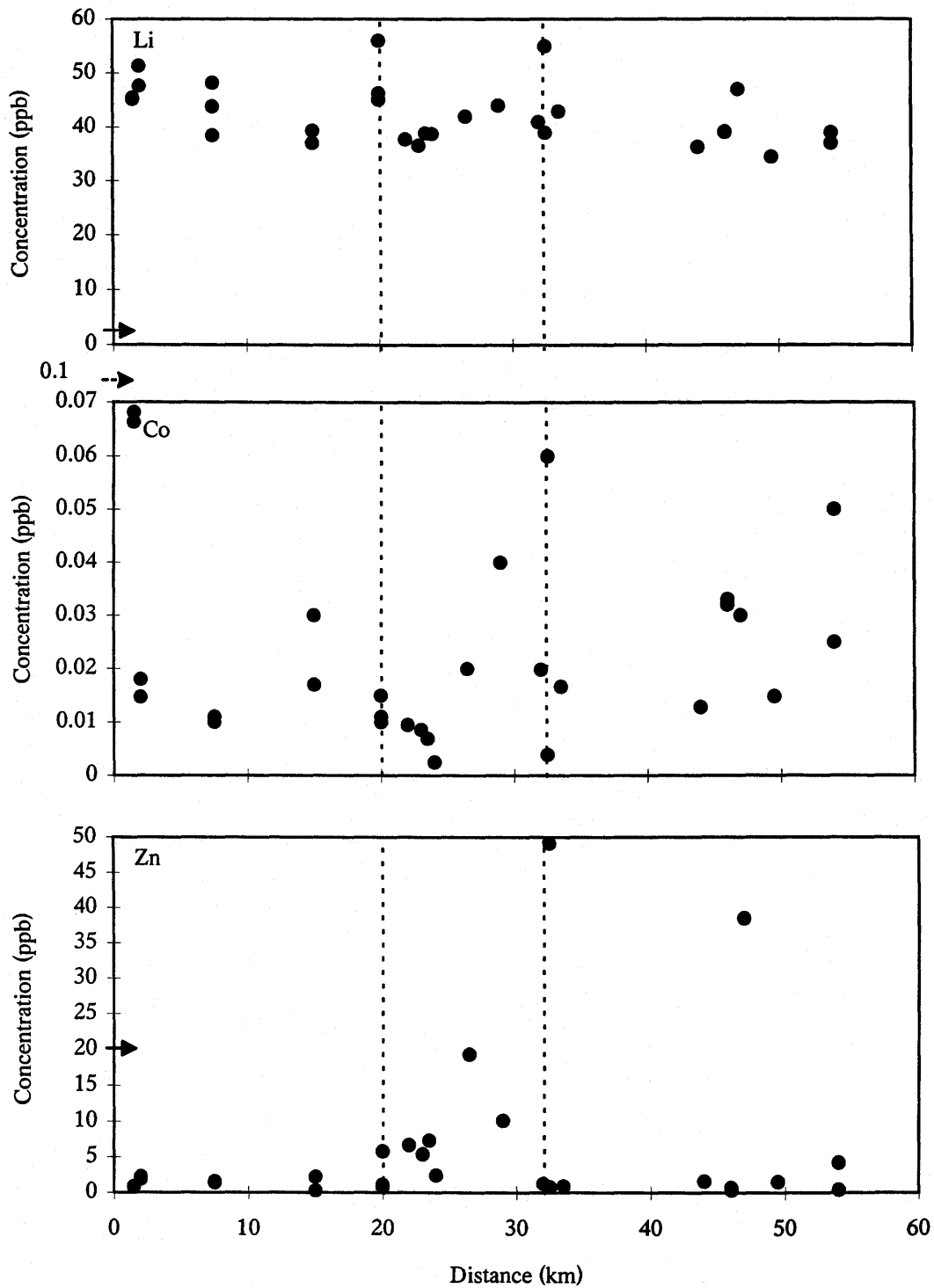


Figure 4.12. Li, Co, and Zn concentrations in the Milk River aquifer groundwater versus distance from recharge. Dashed vertical lines represent redox front and post-redox front boundaries. Arrow on left margin is value of select element for average world river water from Taylor and McLennan (1985). Cumulative plot of 1996-1997 data.

in a +4 valence state under oxidizing conditions, and Eu in a +2 valence state under reducing conditions. Differences in oxidation states in waters can lead to significant anomalies which can be quantified. However in the temperature range of most groundwaters, divalent Eu is not significant (Brookins, 1989). REE solubility is strongly dependent on temperature and Eh. Tetravalent Ce is insoluble and hence under oxidizing conditions of near neutral to high pH, dissolved Ce concentrations are expected to be low (Smedley, 1991). Fractionation between the light REE (LREE) group (La-Gd) and heavy REE (HREE) group (Tb-Lu) occur as a result of certain geologic processes. These fractionations are attributed to differences in ionic radii and differential bonding capacity of these cations. Therefore, REEs provide constraints on the chemical controls of the compositions of the Milk River groundwaters because of their group behavior, differential behavior within the group, and redox control on Ce and Eu (Fee et al., 1992).

4.5.1 REE Concentrations Along the Flow Path

The results of REE analyses are reported in Table 4.5. Total REE concentrations (Σ REE) of the Milk River aquifer groundwater tend to remain constant as it migrates along the flow path (Fig. 4.13). Although a decrease in REE concentrations is observed at the redox front boundary (20 km). Weak correlations between Fe and REEs with depth in lakes and oceans have been documented by DeBaar et al. (1988). However, there does not appear to be any correlation between these elements in the Milk River aquifer groundwater in this study.

Johannesson and Lyons (1994) have observed higher REE concentrations in more acidic waters, and have concluded that REE concentrations are pH dependent (Smedley, 1991, ~14-1595 nmol kg⁻¹; Fee et al., 1992, ~69-110 nmol kg⁻¹). Therefore, the high pH (~9.0) Milk River aquifer groundwater samples have, relatively low REE concentrations. Average Σ REE concentrations in the Milk River groundwater is 0.096 ppb.

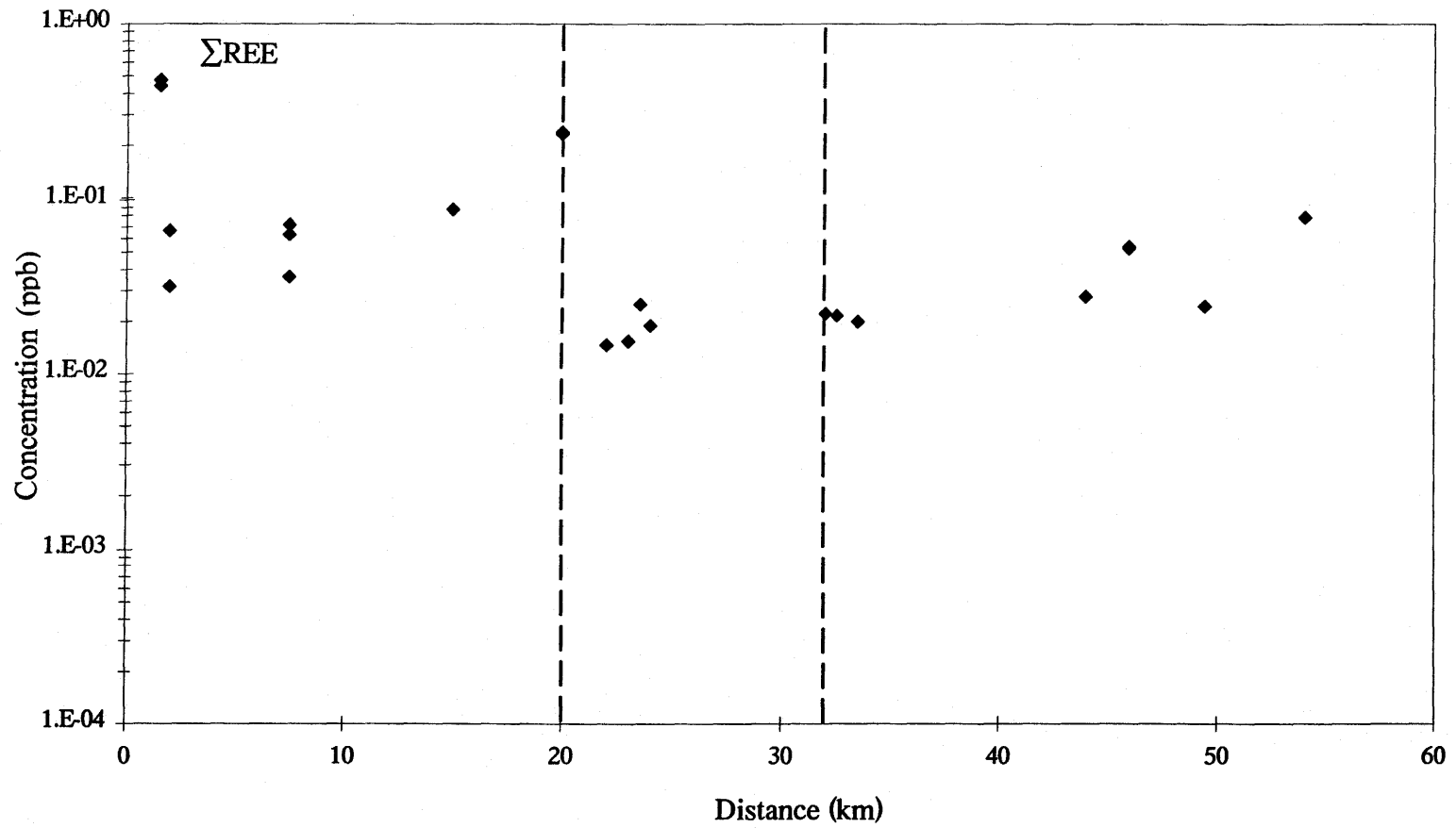


Figure 4.13. Sum of REE concentrations in the Milk River aquifer groundwaters versus distance from recharge.

The absolute concentrations of LREEs are higher than HREEs. These observations are opposite to those reported by Johannesson and Lyons (1994) for Mono lake waters. However, some Milk River groundwater samples display higher HREEs compared to LREEs, which are similar to the observations reported for seawater, where REE concentrations decrease with increasing atomic number (Elderfield and Greaves, 1982).

Figures 4.14 and 4.15 present the LREE and HREE concentrations with distance. The HREEs display more uniform concentrations compared concentrations versus distance. These figures demonstrate that the LREEs have more scattered concentrations to the LREEs and less scatter from younger to older groundwater. This is most evident in Er, Tm, and Lu concentrations as the groundwater migrates downgradient. LREE concentrations display uniform increases up to the redox front and then decrease which may be the result of LREE co-precipitation with Fe oxyhydroxides. Residence time appears to be more of a factor in the preferential removal of HREEs compared to LREEs. Although, in section 3.5 it is noted how filtering tends to lower the LREE concentrations compared to the HREEs, due to preferential sorption of LREEs to (>0.45 μ m) suspended particles. Therefore, the scatter for some of the (filtered) LREEs is probably due to the concentrations being very close to analytical detection limits of the ICP-MS. Consequently, some care in interpretation of the data is needed.

4.5.2 Shale-Normalized REE Patterns

Shale-normalized REE profiles of groundwater data from the Milk River aquifer are presented in Figures 4.16, 4.17 and 4.18. World average river water from Taylor and McLennan (1985) is plotted as a reference. All the REE data presented and plotted in these figures is filtered in order to evaluate the REE concentrations in the <0.45 μ m fraction of the groundwater. Groundwater from this study are normalized to shales (PAAS - Post Archean average Australian shales) because the rocks in the Milk River aquifer are predominantly sandstones, and shales, and this is the convention in groundwater REE studies. The composite shale data used to normalize the groundwater REE data is from Taylor and McLennan (1985), Table 2.9. Data for duplicate samples

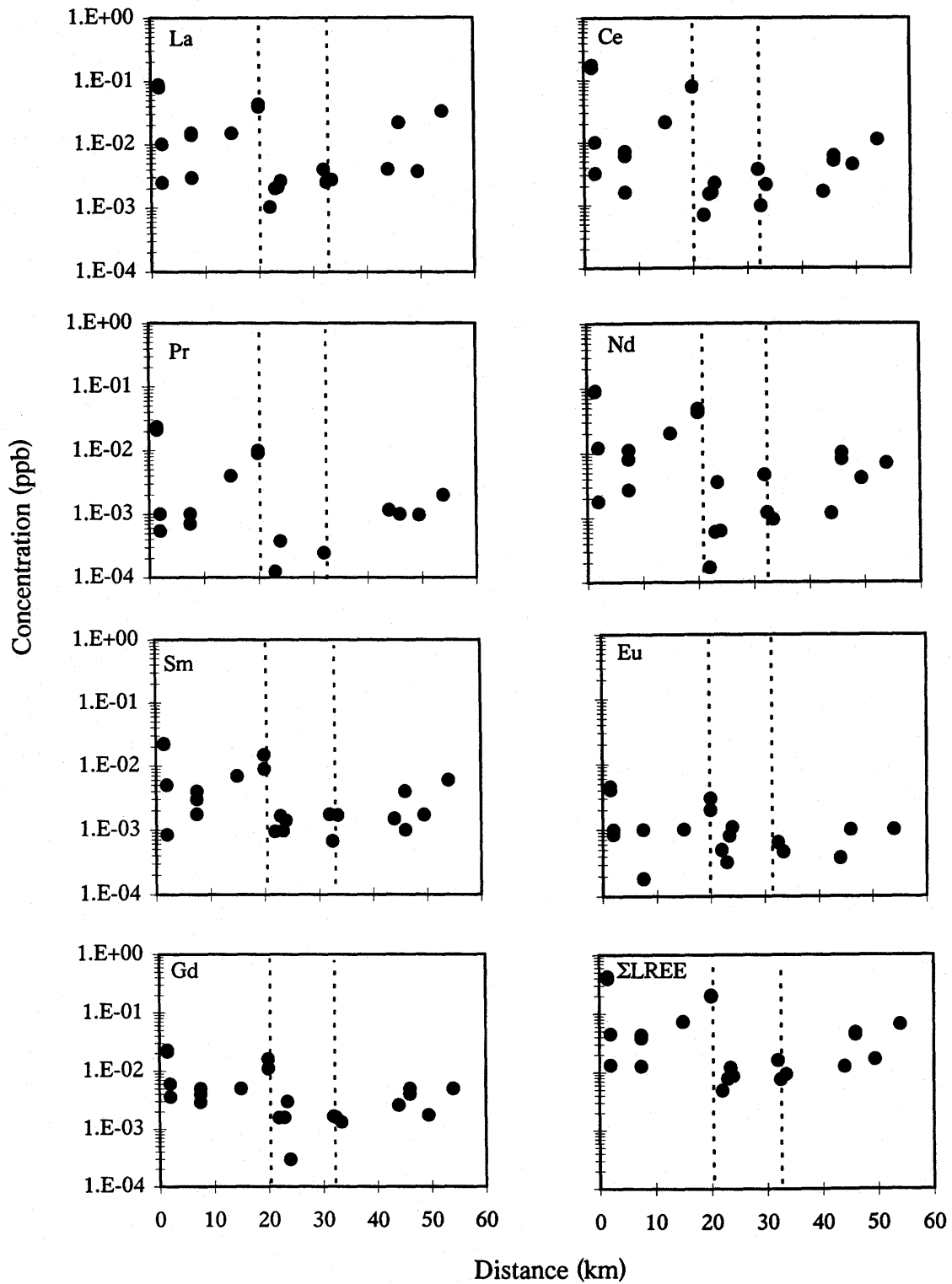


Figure 4.14. Light rare-earth elements (LREEs) in the Milk River aquifer groundwater versus distance from recharge. Dashed vertical lines represent redox front and post-redox front boundaries.

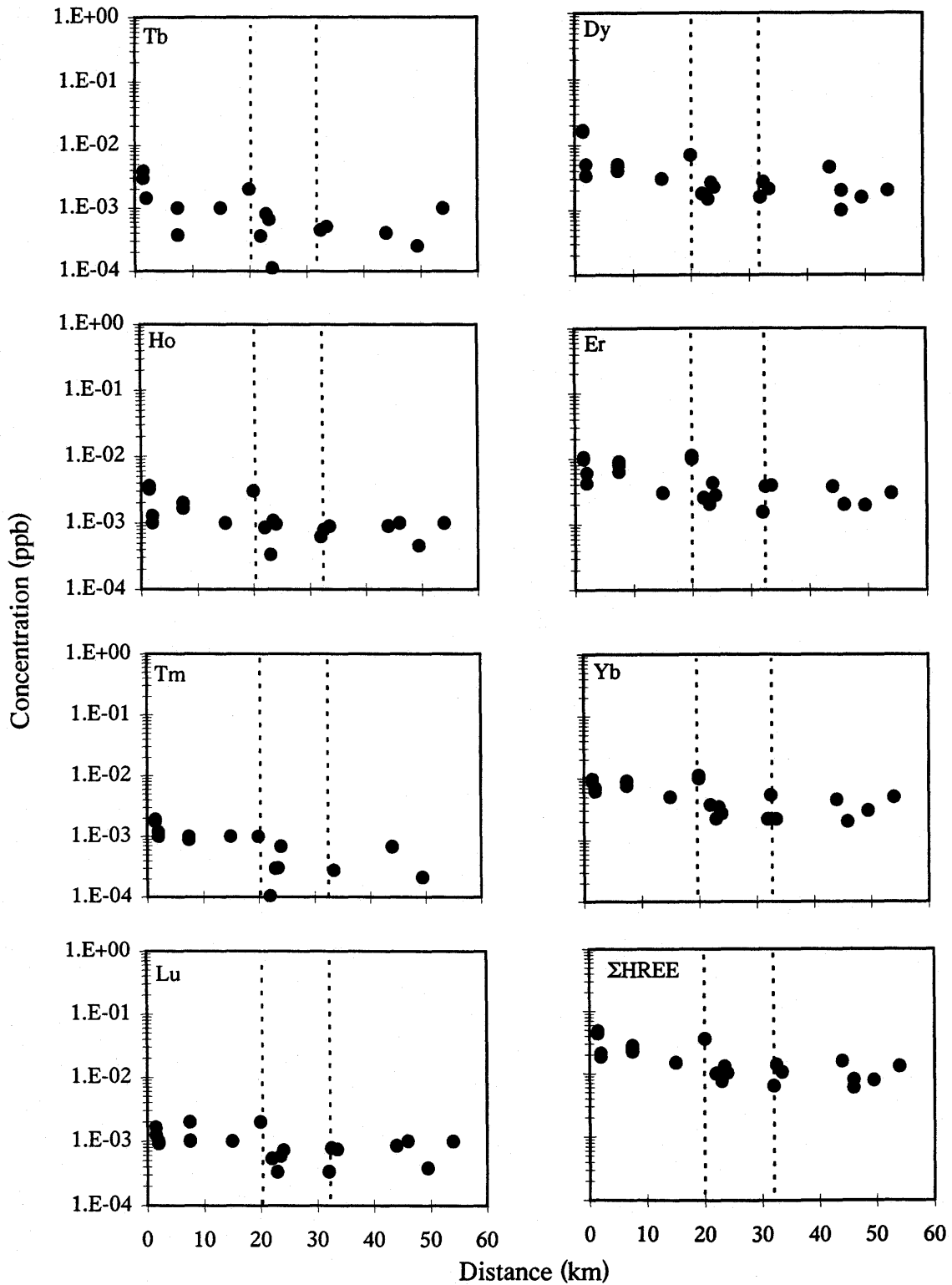


Figure 4.15. Heavy rare-earth elements (HREEs) in the Milk River aquifer groundwater versus distance from recharge. Dashed vertical lines represent redox front and post-redox front boundaries.

are plotted to show the excellent reproducibility. Groundwater samples from the same well but different sampling years is also plotted displaying good replication. Some shale normalized samples exhibit saw-tooth patterns due to ICP-MS detection limit problems at the lowest concentrations.

Previous authors (Elderfield et al., 1990; Sholkovitz, 1993; Johannesson and Lyons, 1995; Johannesson et al., 1997) have found shale to be useful in the evaluation of geochemical processes responsible for fractionation of the REEs in terrestrial waters. Shale-normalized REE plots for these groundwaters are generally flat (Type 1- recharge and redox front groundwater) to slightly enriched in the HREEs (Type 2 - groundwater). HREE-enrichment in seawaters is attributed to the scavenging of LREEs by Fe-Mn-oxyhydroxides and the formation of stable HREE carbonate complexes (De Baar et al., 1988). The groundwater shale-normalized Yb/Nd (average 10.2) and Er/Nd (average 8.9) ratios are greater than unity (Table 4.6), ranging from 1 to 51 for $(Yb/Nd)_{sn}$ and 0.9 to 35 for $(Er/Nd)_{sn}$. Similarly, Lu/La ratios (average 10.4) fall in the range >1 to 27, indicating enrichment in HREEs. These ratios indicate that the shale-normalized values for the majority of the LREEs are depleted compared to HREE values. Figure 4.19 displays Er/Nd and Lu/La versus distance, respectively. Both plots display moderate to high values (HREEs/LREEs) in the recharge water, as well as similarly moderate to high values at the redox front and post-redox front boundaries (~20 km and ~32 km).

Open ocean waters usually display a well-developed negative Ce anomaly similar to the majority of Milk River groundwater samples. The Ce anomaly is probably in response to oxidative removal of Ce in its tetravalent state as CeO_2 or $Ce(OH)_4$, or due to adsorption onto particulate material (Smedley, 1991). Similarly, to the Milk River groundwater some ocean waters do not display any apparent negative Ce anomaly, which may be due to dissolution of Ce under reducing conditions (De Baar et al., 1988). Goldstein and Jacobsen (1988) concluded that the magnitude of Ce anomalies from the Indus and Mississippi rivers were directly proportional to pH. Due to the small pH

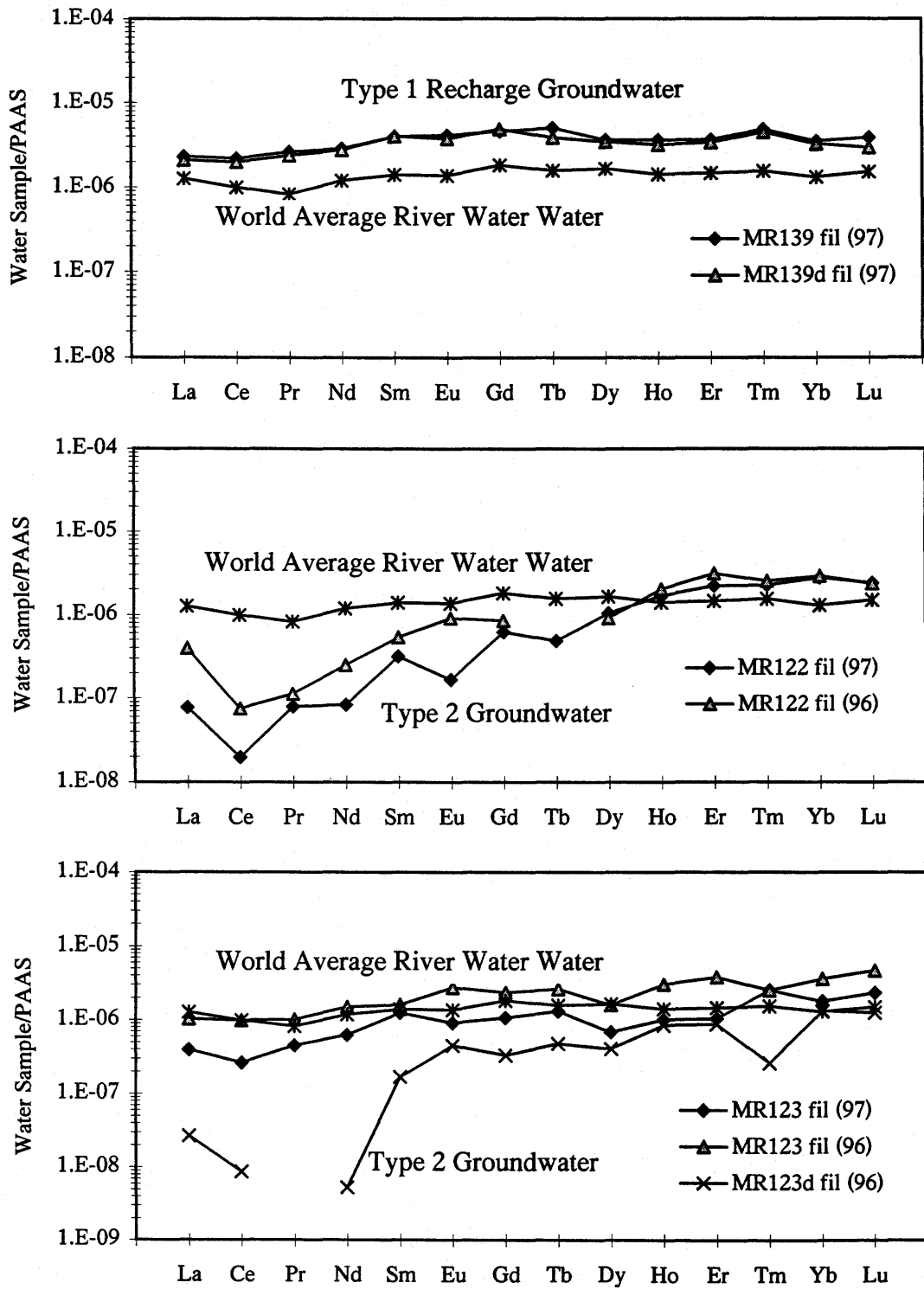


Figure 4.16. Shale-normalized REE patterns for groundwater from the Milk River aquifer groundwaters. PAAS and World Average River Water data from Taylor and McLennan, (1985). Sample distances from recharge: MR139=1.5km, MR122=2km, MR123=7.5km. [1996 and 1997 sampling seasons]

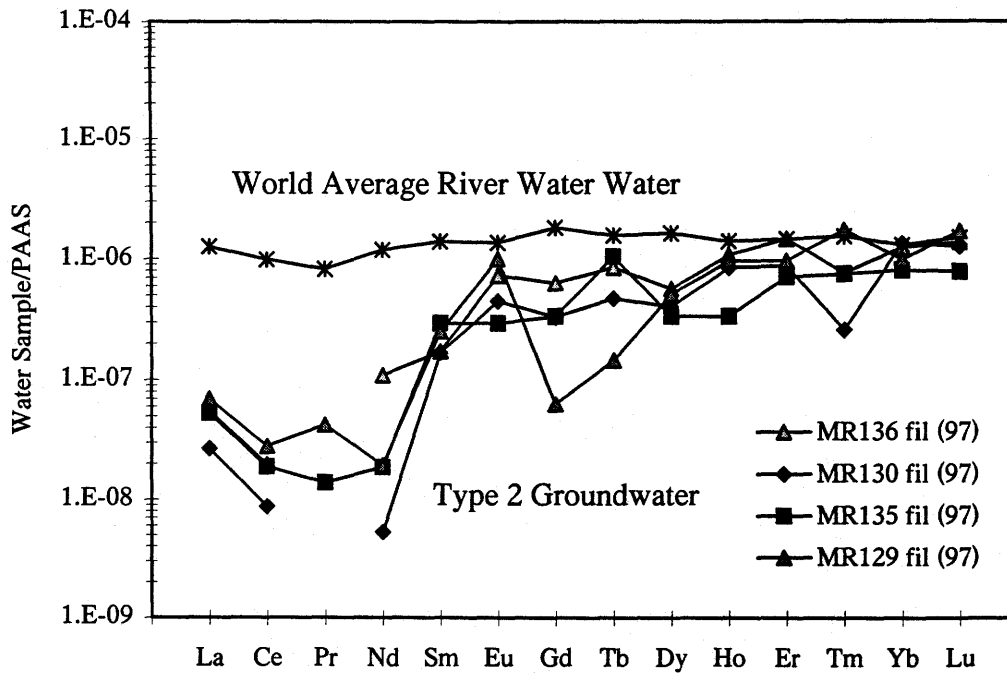
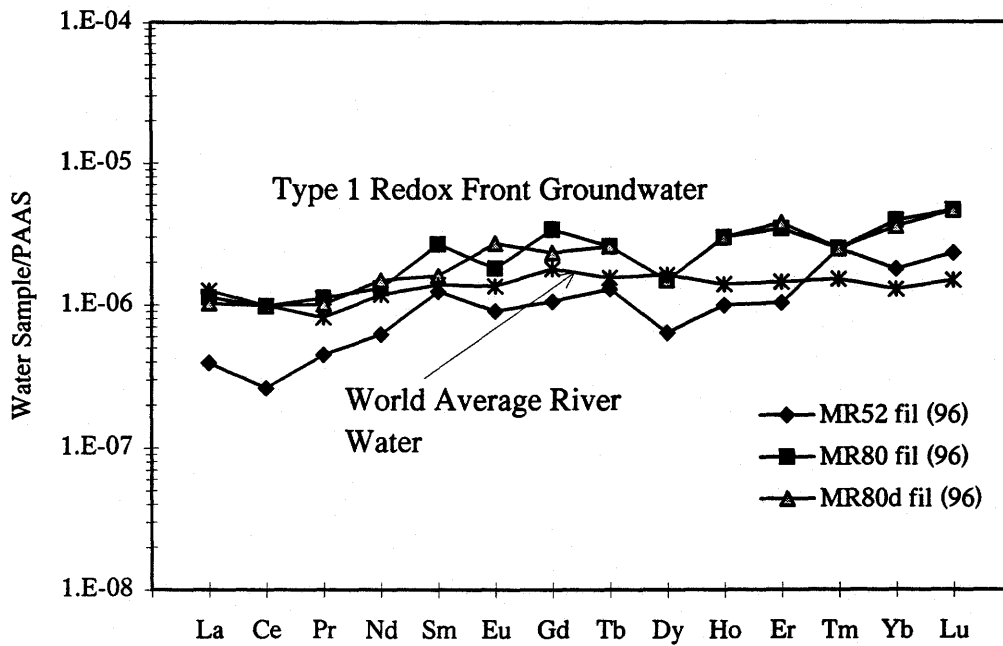


Figure 4.17. Shale-normalized REE patterns for groundwater from the Milk River aquifer groundwaters. PAAS and World Average River Water data from Taylor and McLennan, (1985). Sample distances from recharge: MR52=15km, MR80=20km, MR130=22km, MR135=23km, MR136=23.5km, MR129=24km. [1996 and 1997 sampling seasons]

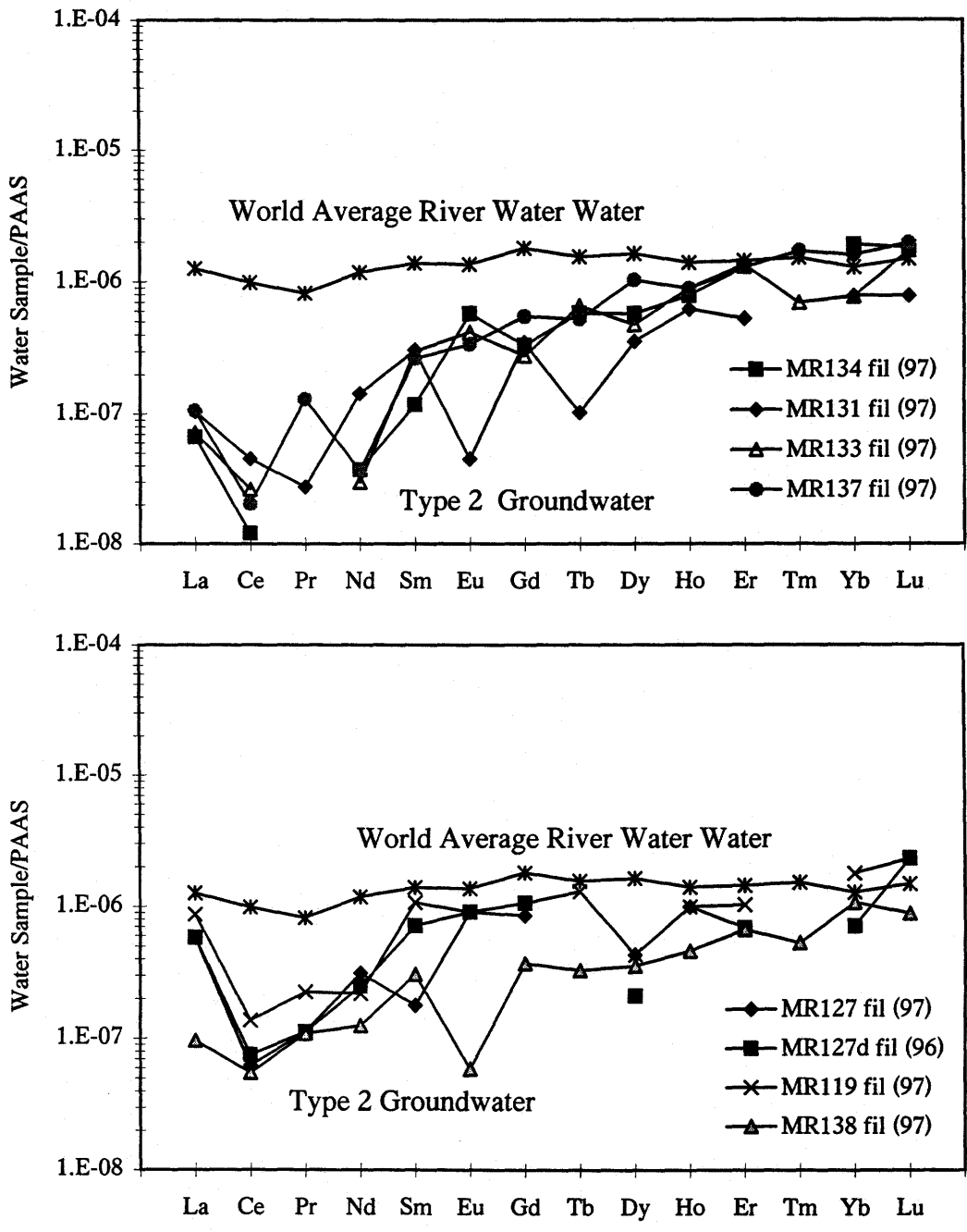


Figure 4.18. Shale-normalized REE patterns for groundwater from the Milk River aquifer groundwaters. PAAS and World Average River Water from Taylor and McLennan, (1985). Sample distances from recharge: MR131=32km, MR134=32.5km, MR133=33.5km, MR137=44km, MR127=46km, MR138=49.5km, MR119=54km. [1996 and 1997 sampling seasons]

Table 4.6. REE ratios for comparing Light REE and Heavy REE shale-normalized values.

	MR139fil (97)	MR139d fil (97)	MR122fil (97)	MR122fil (96)	MR123fil (96)	MR123d fil (96)	MR52fil (96)
(Yb/Nd) _n	1.21	1.16	39.77	6.67	9.35	11.43	2.86
(Er/Nd) _n	1.27	1.22	26.28	5.52	8.03	12.41	1.66
(Lu/La) _n	1.65	1.38	32.92	8.84	12.62	5.89	5.89
(Eu/Eu*) _n	0.97	0.85	2.25	0.85	1.04	1.35	0.79
(Ce/Ce*) _n	0.85	0.82	0.66	0.40	0.25	0.24	0.53
(La/Sm) _n	0.58	0.52	0.43	0.29	0.52	0.74	0.32
(Gd/Yb) _n	1.33	0.53	0.05	0.14	0.10	0.08	0.29
(La/Yb) _n	0.67	0.49	0.08	0.09	0.11	0.13	0.42

	MR80fil (96)	MR80d fil (96)	MR136fil (97)	MR134fil (97)	MR127fil (96)	MR127d fil (96)	MR119fil (96)
(Yb/Nd) _n	2.99	2.38	11.26	51.18	2.29	2.86	8.16
(Er/Nd) _n	2.63	2.53	13.37	34.87	2.21	2.76	4.73
(Lu/La) _n	4.11	4.53	24.68	27.27	4.02	4.02	2.68
(Eu/Eu*) _n	0.60	1.41	2.21	2.91	2.33	1.04	0.85
(Ce/Ce*) _n	0.80	0.80	0.25	0.24	0.15	0.20	0.32
(La/Sm) _n	0.42	0.64	0.32	0.57	3.24	0.81	0.81
(Gd/Yb) _n	0.54	0.36	0.03	0.02	0.07	0.08	0.15
(La/Yb) _n	0.33	0.43	-	-	0.13	0.11	0.21

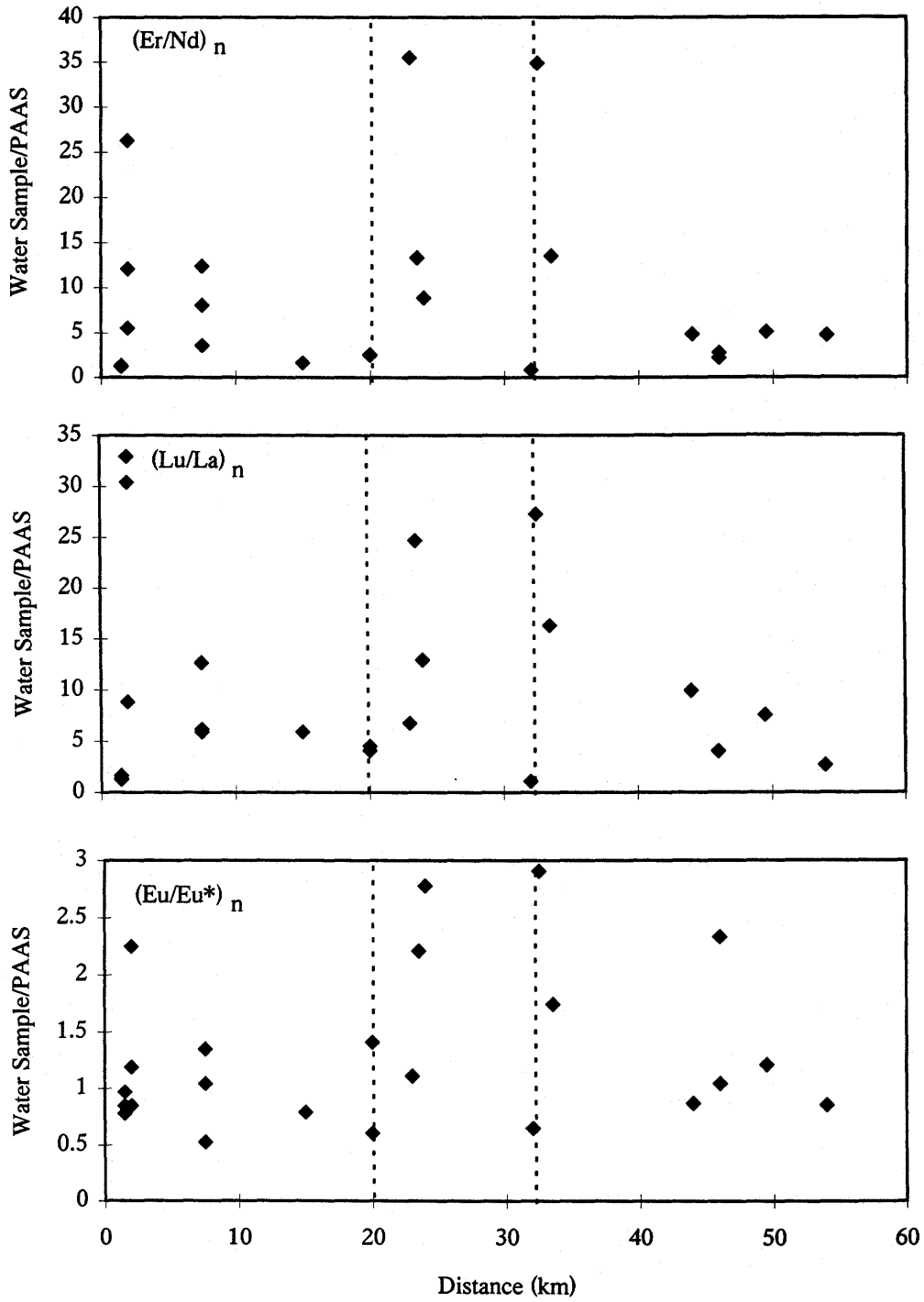


Figure 4.19. Er/Nd, Lu/La, and Eu/Eu* shale-normalized versus distance for the Milk River aquifer groundwater. PAAS data is from Taylor and McLennan (1985).

variation in the Milk River groundwater, this dependence can not be commented on. In many fresh acidic water systems, the fractionation of Ce from the other LREEs is not observed because the pH is low enough to allow Ce to remain in its trivalent state.

Unlike the study by Möller and Bau (1993) of alkaline waters from Lake Van, Turkey, which display no Gd anomaly, some of the groundwater from the Milk River aquifer display small negative and positive Gd anomalies. Seawaters commonly demonstrate Gd anomalies, which may result from solution complexation with CO_3^{2-} or surface reaction complexation with aminocarboxylic acids on REE scavenging particle surfaces (Lee and Byrne, 1993).

4.5.3 REE Speciation Modeling of the Milk River groundwater

Groundwaters likely inherit their dissolved REE signatures in part from the aquifer materials they react with (Johannesson et al., 1994; Duro et al., 1997; Johannesson et al., 1997). Recently, solution complexation has been demonstrated as being important for controlling the dissolved REE signatures in waters. Therefore, it is important to understand both the effects of aquifer material chemistry and solution chemistry in order to determine the controls and roles of both on the REE signatures of water systems.

Two processes maybe responsible for relative HREE enrichment in the Milk River groundwater. Rare earth concentrations may reflect interactions with the aquifer rocks as the recharge water migrates downgradient (Smedley, 1991; Gosselin et al., 1992; Johannesson et al., 1994; and 1997). The other possibility which has earned much attention recently by Johannesson et al. (1995), Johannesson and Lyons (1994), Lee and Byrne (1992), Wood (1990a), is that the REE concentrations in waters are controlled primarily by complexation with major anions. Carbonate complexes have been implicated as being important in seawaters and brines (Millero, 1992), and carbonate or bicarbonate anions in near-neutral to alkaline conditions (Goldstein and Jacobsen, 1988). Discussions from these studies has shown that HREEs (Tb-Lu) form stronger complexes with carbonate ions than LREEs (La-Gd), as evidenced by the increase in

stability constants with increasing atomic number. Research on waters of moderate to high pH by Johannesson and Lyons (1995) indicate that REE complexation with carbonate ions will predominate in most waters where carbonate is a major component. Due to an increase in complexation constants with atomic number, HREEs form stronger complexes with carbonate ions than LREEs (Millero, 1992; and Lee and Byrne, 1993). Wood (1990) and Lee and Bryne (1992) have argued that the large stability constants of the LnPO_4^0 species are likely important in forming phosphate complexes with REEs in water systems with high phosphate concentrations. However, Johannesson and Lyons (1994) concluded from speciation modeling that the phosphate species were not important in their higher phosphate Mono Lake waters. Therefore, phosphate complexes are not expected to be of importance in the Milk River aquifer groundwater where phosphorus is only a minor component, and likely because phosphates are extremely insoluble.

Speciation modeling of REEs in the Milk River aquifer groundwater have been performed and evaluated primarily to assess the importance of carbonate (LnHCO_3^{2+} , LnCO_3^+ and $\text{Ln}(\text{CO}_3)_2^-$) and phosphate ($\text{LnH}_2\text{PO}_4^{2+}$, LnHPO_4^+ , $\text{Ln}(\text{HPO}_4)_2^-$ and LnPO_4^0) complexes, where Ln stands for lanthanides. Activity coefficients and stability constants have been calculated using a combined specific ion interaction and ion pairing developed by Millero (1992). For a detailed description of the modified and updated Millero (1992) model used in this study refer to Johannesson and Lyons (1994).

The results of the speciation modeling to determine the REE complexes in the Milk River aquifer groundwater samples are presented in Appendix I. Figures 4.20, 4.21, and 4.22 display the REE speciation values for the dominant carbonate complexes, phosphate complex, and free metal ion species. From these figures it is clear that the $\text{Ln}(\text{CO}_3)_2$ species dominate the REE complexation in the Milk River groundwater. Consistently, 97-99% of the dissolved REEs are due to the $\text{Ln}(\text{CO}_3)_2$ carbonate complex whereas only 3-1% is complexed as the LnCO_3 carbonate complex. The phosphate complex LnPO_4 only accounts for <0.05% and the free metal species Ln^{3+} accounts for

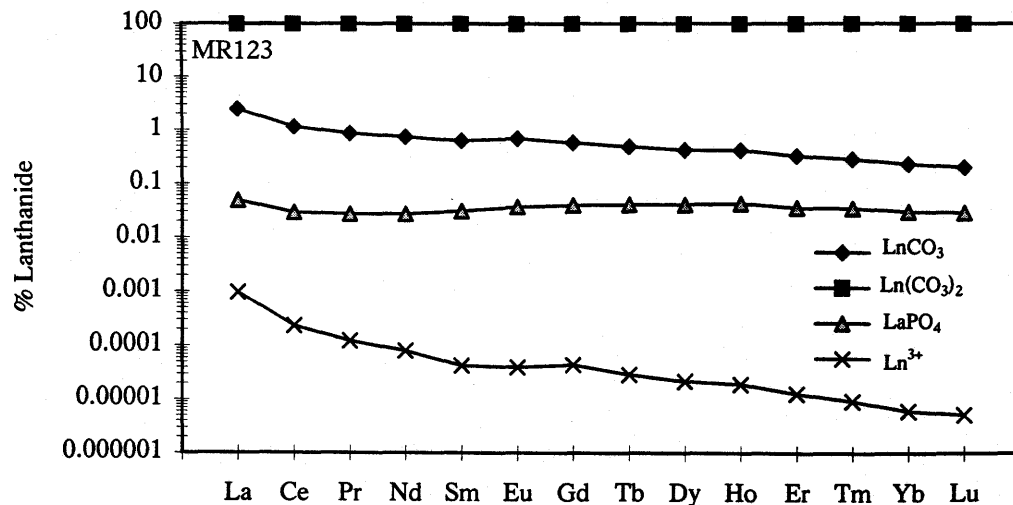
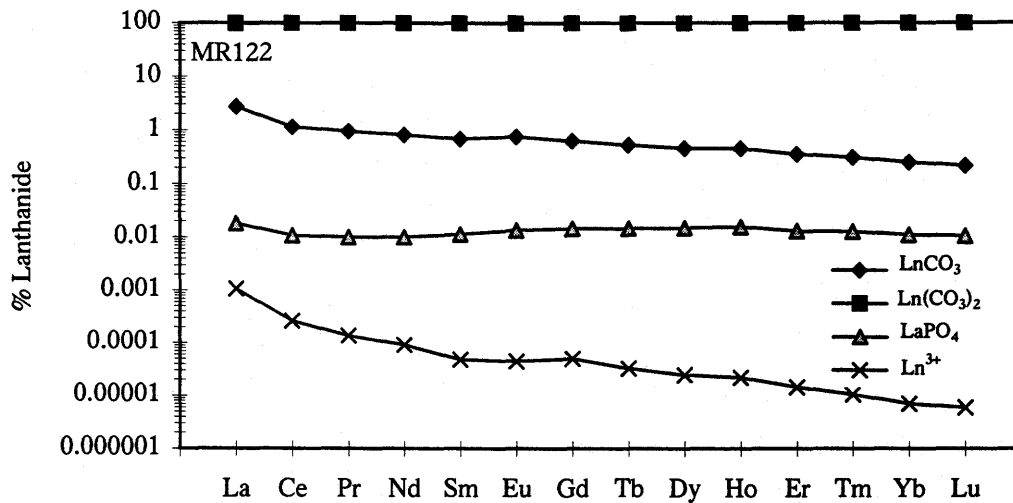
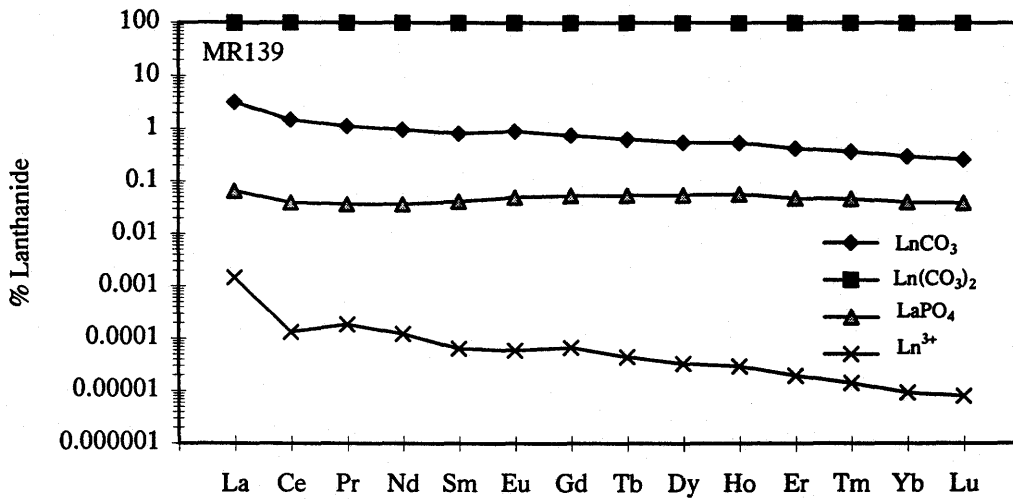


Figure 4.20. Results of speciation modeling plotted as percent dissolved rare earths (% lanthanides) versus atomic number for groundwater samples.

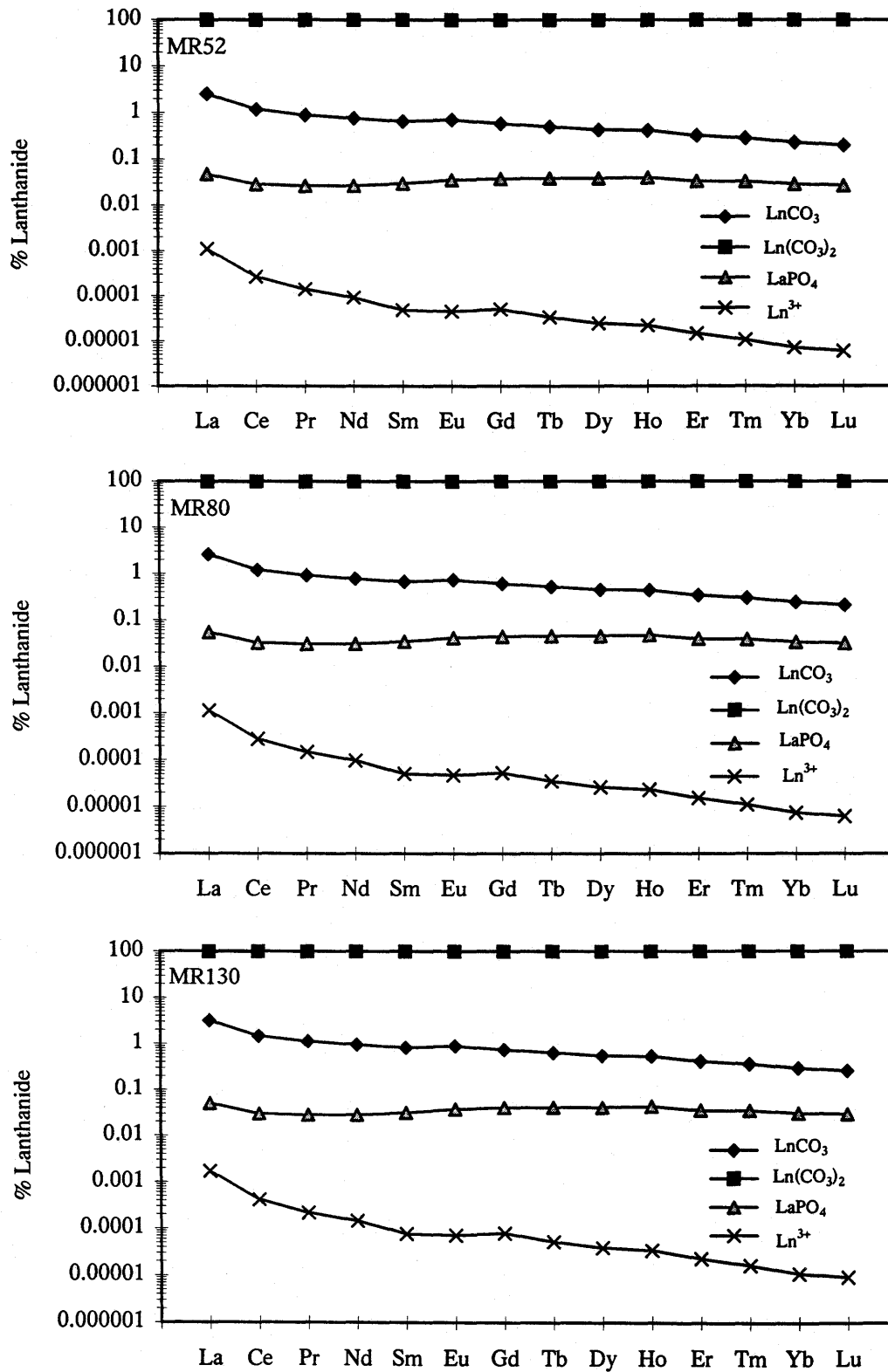


Figure 4.21. Results of speciation modeling plotted as percent dissolved rare earths (% lanthanides) versus atomic number for groundwater samples.

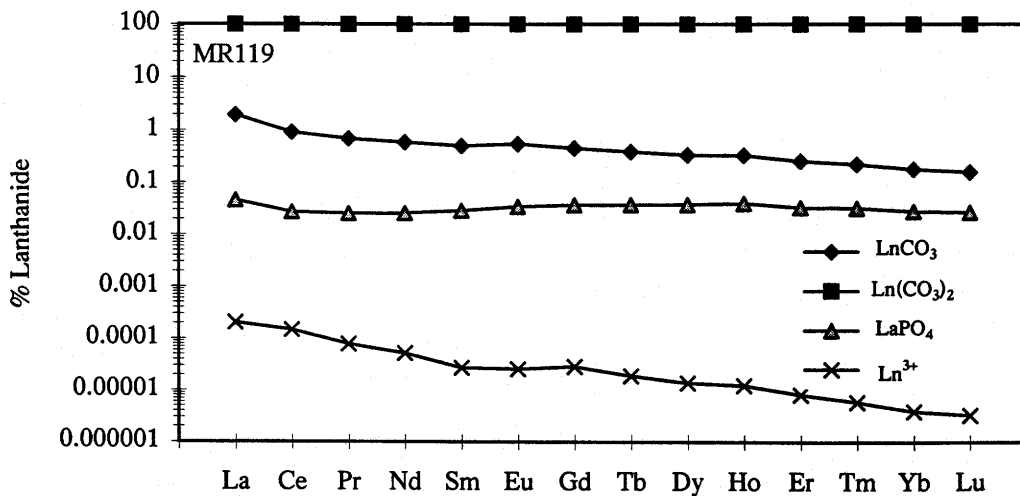
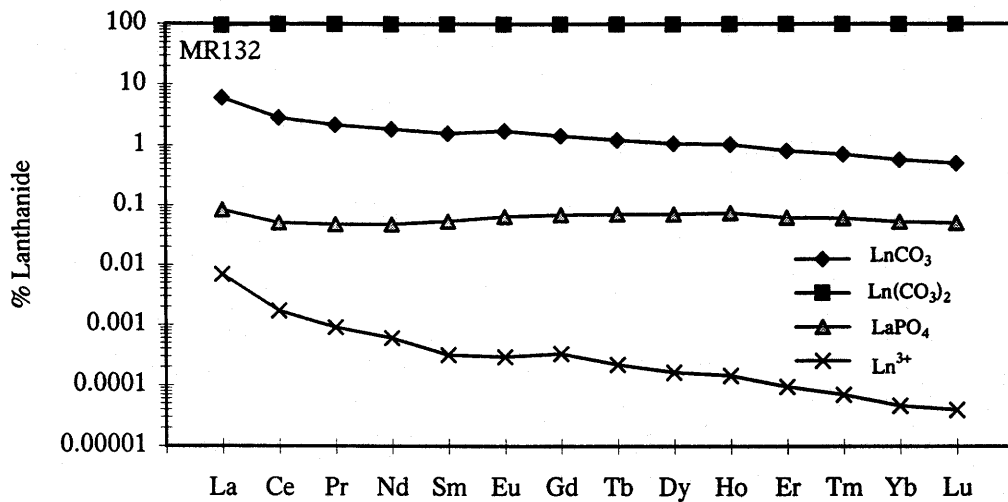
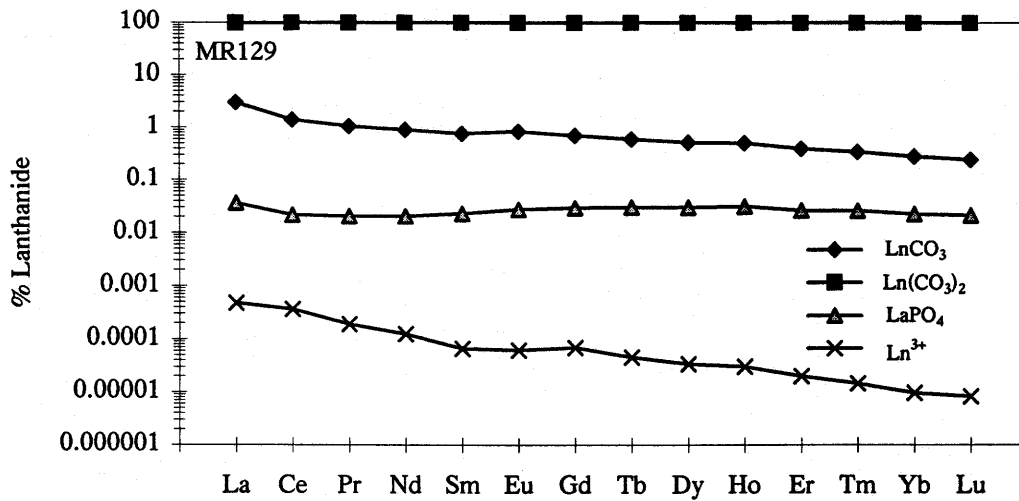


Figure 4.22. Results of speciation modeling plotted as percent dissolved rare earths (% lanthanides) versus atomic number for groundwater samples.

<0.0002% of the dissolved REE complexes. The LnHCO_3^- complex is negligible in all the Milk River Samples modeled. Similar values have been reported by Johannesson (pers. comm. 1997) in the alkaline lakes of the Great Basin in the western United States. The high alkalinities and pH values observed in the Milk River aquifer groundwater are likely responsible for these results.

4.5.4 Behavior of REEs in the Milk River Groundwater

Figures 4.23 and 4.24 are plots of pH and alkalinity versus neodymium, samarium, and dysprosium concentrations, for the groundwater samples. At least two distinct waters can be separated in these figures due to variations in Nd, Sm, and Dy concentrations. All three REEs exhibit an inverse relationships with alkalinity (highest REE concentrations in lowest alkalinity groundwater). At higher alkalinity values lower concentrations of Nd, Sm, and Dy are observed. The 'recharge' groundwater display the highest values. The groundwater samples taken after the recharge area are referred to as the 'Type 2 groundwater' or main group of 'Milk River groundwater' are represented by the lowest concentrations of all three REEs.

Similar plots by Johannesson et al. (1994) of pH versus all three REEs also displayed a similar relationship. Plots of the Milk River aquifer groundwater data display the distinct water groups described above, but there is not a clear relationship between pH and REE concentrations as such (lowest pH groundwater should correspond to the highest REE concentrations). This relationship may be masked due to the very small range of pH values (<0.5 pH difference) along the studied section of the flow path.

4.5.5 Mineral Sources of REEs

Groundwaters probably inherit their dissolved REE signatures from the rocks through which they flow, although solution complexation is also important in controlling the dissolved REE signatures in natural waters. Minerals in the Milk River aquifer that may be responsible for donating some of the REEs into solution are accessory mineral phases including kaolinite, smectite, illite, and chlorite (Longstaffe, 1984). REEs in the

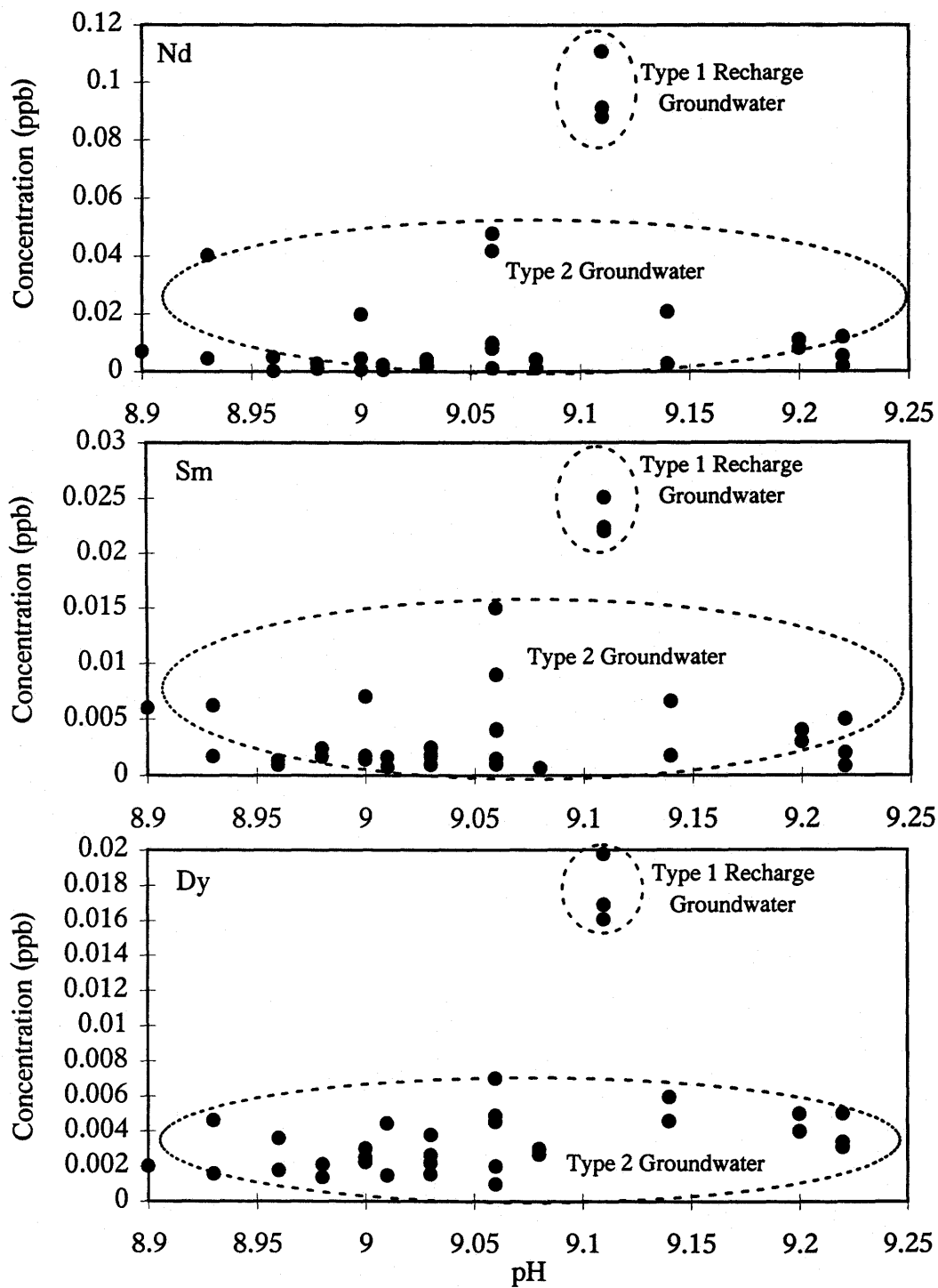


Figure 4.23. Plot of Nd, Sm, and Dy versus pH for the Milk River aquifer groundwater. Different groundwater types have been identified based on the data.

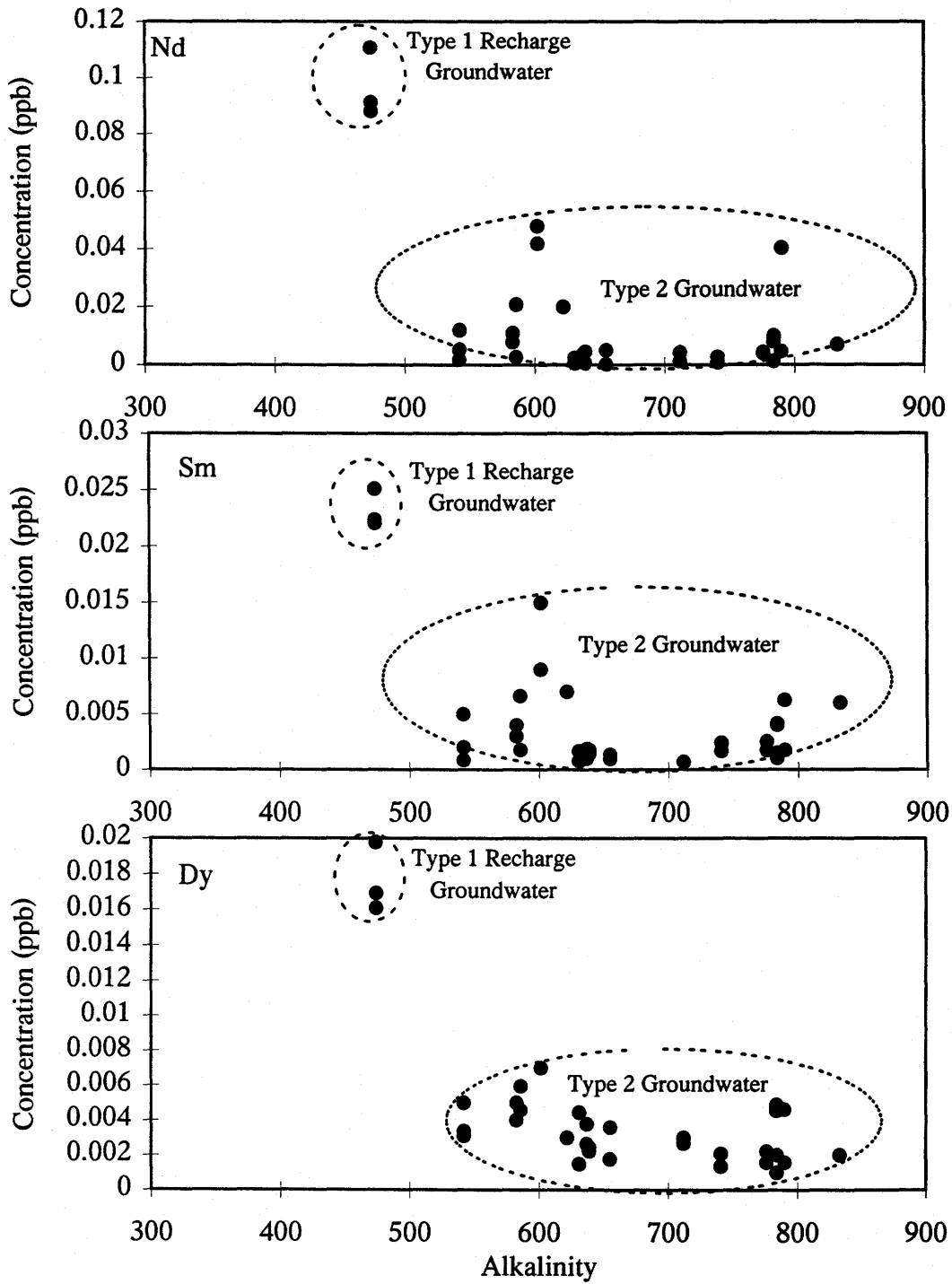


Figure 4.24. Plot of Nd, Sm, and Dy versus alkalinity for the Milk River aquifer groundwater. Different groundwater types have been identified based on the data. Cumulative plot of 1996-1997 data.

groundwater may be derived from dissolution and ion exchange reactions involving the clays and dominant carbonate minerals including calcite and dolomite. Silicate minerals include biotite, muscovite, chert and feldspars, may also be important (Meyboom, 1960). Past studies have suggested that both rock source and solution chemistry play an important role in the dissolved groundwater REE signatures (Johannesson et al., 1996). Local geology in the Milk River aquifer appears to be of minor importance in controlling the processes and nature of REE profiles in the groundwater.

4.6 Additional Trace Elements

4.6.1 Trace Element Concentrations Along the Flow Path

Strontium concentrations in the recharge groundwater are generally low (~50 ppb), displaying a net increase downgradient (> 100 ppb). Strontium is chemically similar to calcium and from plots of concentration versus distance, it is shown that Sr and Ca display similar trends (Figs. 4.3 for Ca and 4.25). Concentrations of Sr drop off 20 km from recharge and then increase after approximately 30 km, where they drop off, increasing again after 40 km (Fig. 4.25). Armstrong (1994) found that Sr did not increase greatly in the porewaters over the first 40 km of the flow path. However, Sr did show an increase up to 100 km. Armstrong (1994) also noticed a consistent pattern with Ca, which he attributed to a similar source for these elements.

Further evaluation of the source and distribution of strontium may be done by comparing Sr/Ca ratios along the flow path. Mean Sr/Ca ratios of the aquifer, till, and shale porewaters are 0.13, 0.02, and 0.11, respectively, according to Armstrong (1994). The average Sr/Ca ratio for the groundwaters from this study is 0.07. Figure 4.26 illustrates the Sr/Ca evolution along the flow path. Except for the recharge wells the water evolving along the flow path varies very little, which may indicate a relatively consistent solute source material. Armstrong (1994) concluded that the distribution and evolution of Sr and Sr/Ca in the Milk River aquifer suggests two potential input sources

for the flow path from porewater mixing: (1) outcropping Milk River Formation sandstones and (2) a regional source which is probably influenced by the interbedded shales within and in contact with the aquifer.

Armstrong (1994) utilized PHREEQE to determine the saturation state of strontianite (SrCO_3) and to characterize the carbonate dominated Milk River system. This study determined that the mean SI values for the groundwater to be -0.37 (n=21), indicating that the aquifer waters are undersaturated with respect to strontianite. Similarly in this study, groundwater along the flow path is also undersaturated with respect to strontianite having a mean SI value of -0.71 (n=11) (Fig. 4.27). The trend of SI for SrCO_3 along the flow path is shifting toward zero, or saturation (maximum SI value at 54 km = -0.05).

Phosphorus concentrations similarly remain fairly uniform along the flow path. Atmospheric inputs are probably responsible for the 300-500 ppb range of P, and implies there is no soluble source of phosphorus in the Milk River aquifer (Fig. 4.25).

Arsenic concentrations in the Milk River groundwater remain uniform along the first 54 km of the flow path and in most cases are < 0.40 ppb (Fig. 4.25).

Concentrations of most other trace elements in the Milk River aquifer groundwater either remain static or display very minor net increases as the groundwater migrates along the flow path. An exception is *titanium*, where values decrease downgradient. Recharge values are generally <5 ppb and decrease to 1 ppb at 54 km (Fig. 4.28).

Lead is also detectable in the groundwater, the majority of the concentrations being below 0.2 ppb (Fig. 4.28). With the exception of two recharge groundwater samples, Pb values remain nearly uniform as the groundwater moves downgradient. A small net decrease is displayed by lead as it migrates downgradient. Mineral dissolution and redox boundary conditions do not appear to have a significant control on these elements.

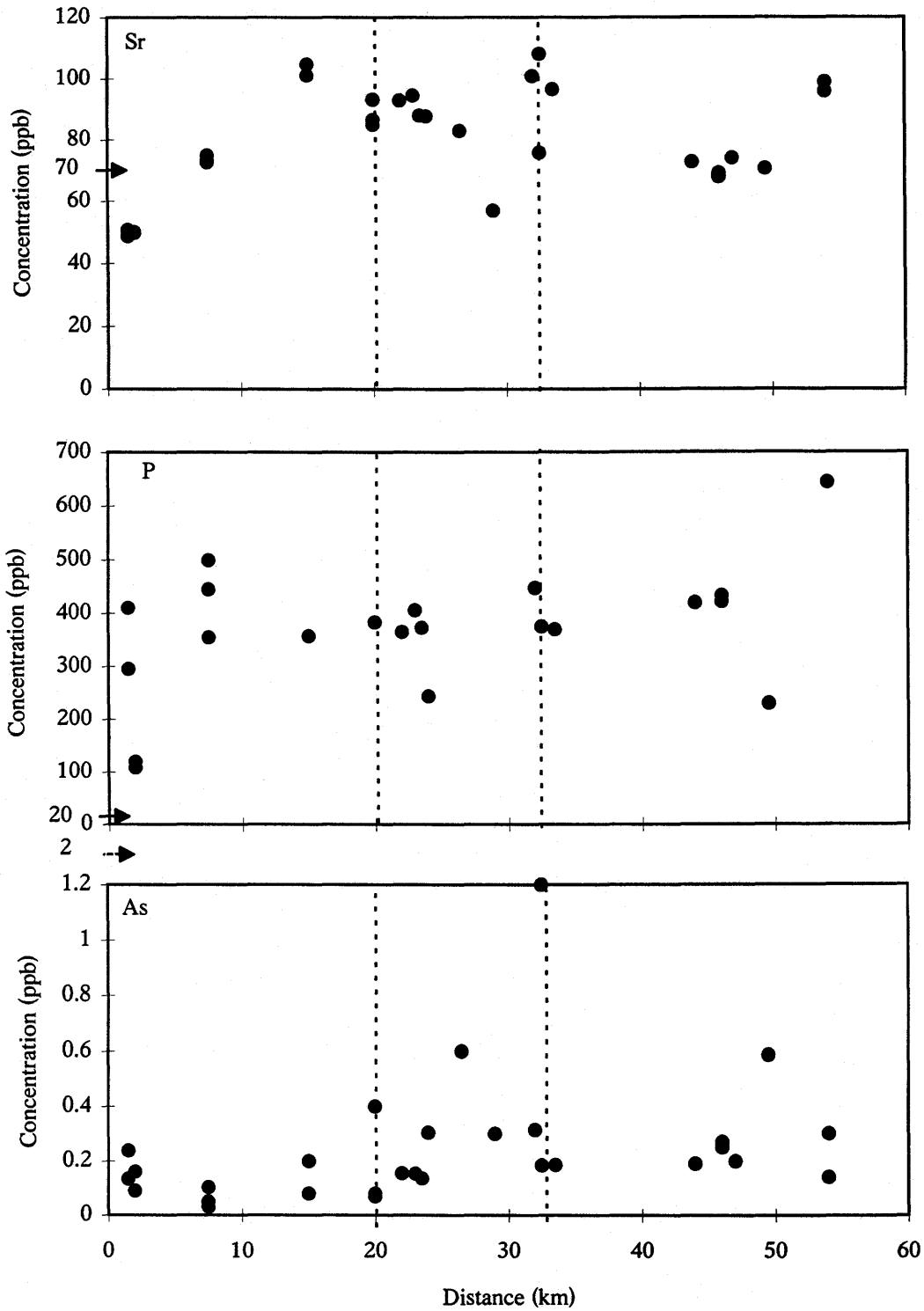


Figure 4.25. Sr, P, and As concentrations in the Milk River aquifer groundwater versus distance from recharge. Dashed vertical lines represent redox front and post-redox front boundaries. Arrow on left margin is value of select element for average world river water from Taylor and McLennan (1985). Cumulative plot of 1996-1997 data.

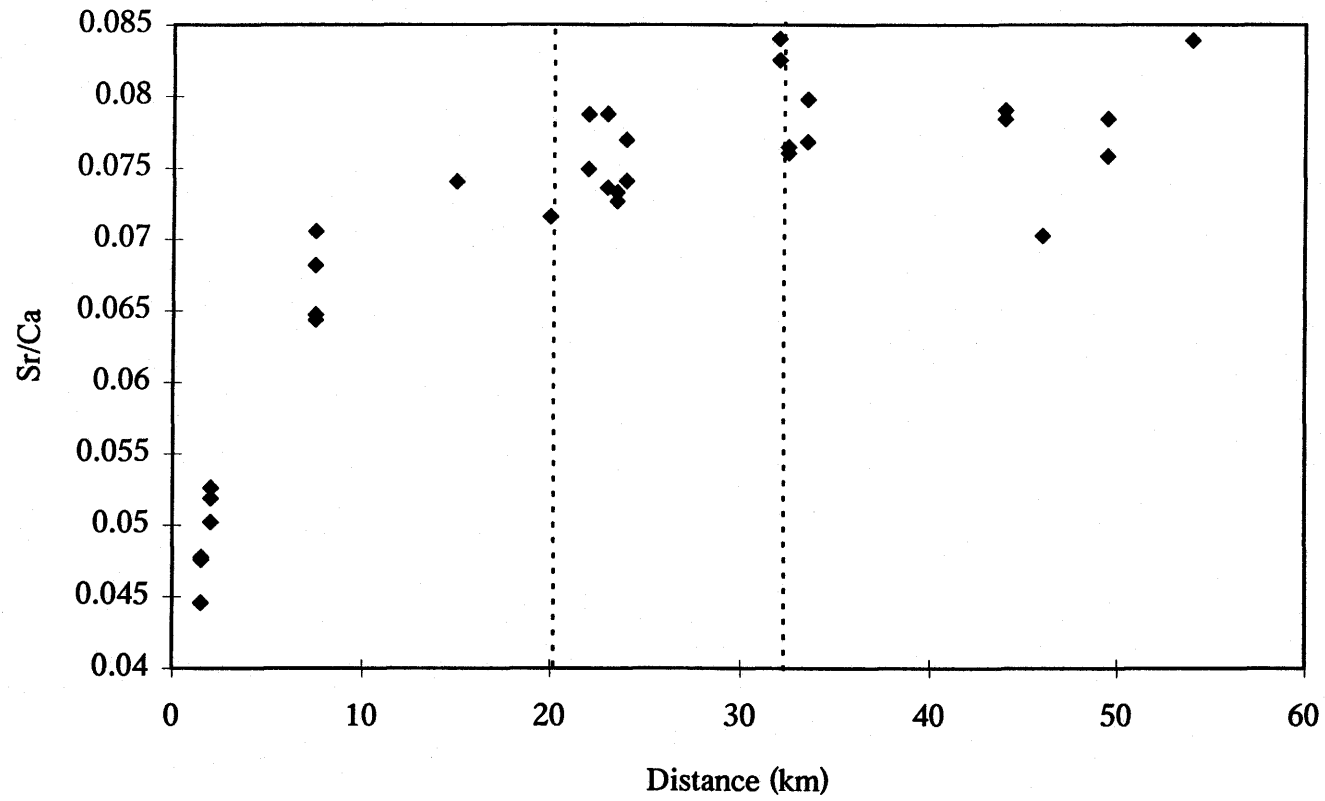


Figure 4.26. Sr/Ca ratio in the Milk River aquifer groundwater along the flow path.

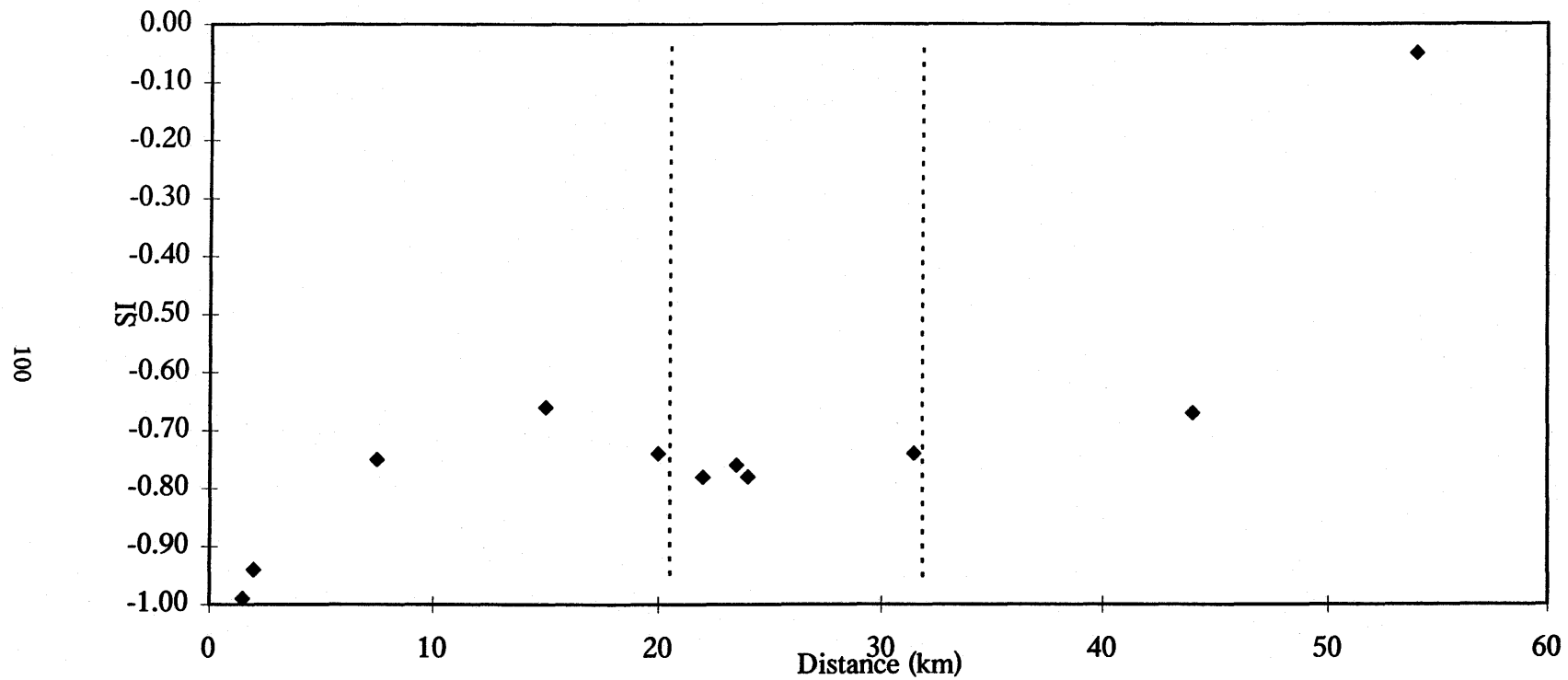


Figure 4.27. PHREEQC initial condition - solution modeling of strontianite in the Milk aquifer groundwater. Calculated saturation indices versus distance from recharge along the flow path. Dashed vertical lines represent redox front and post-redox front.

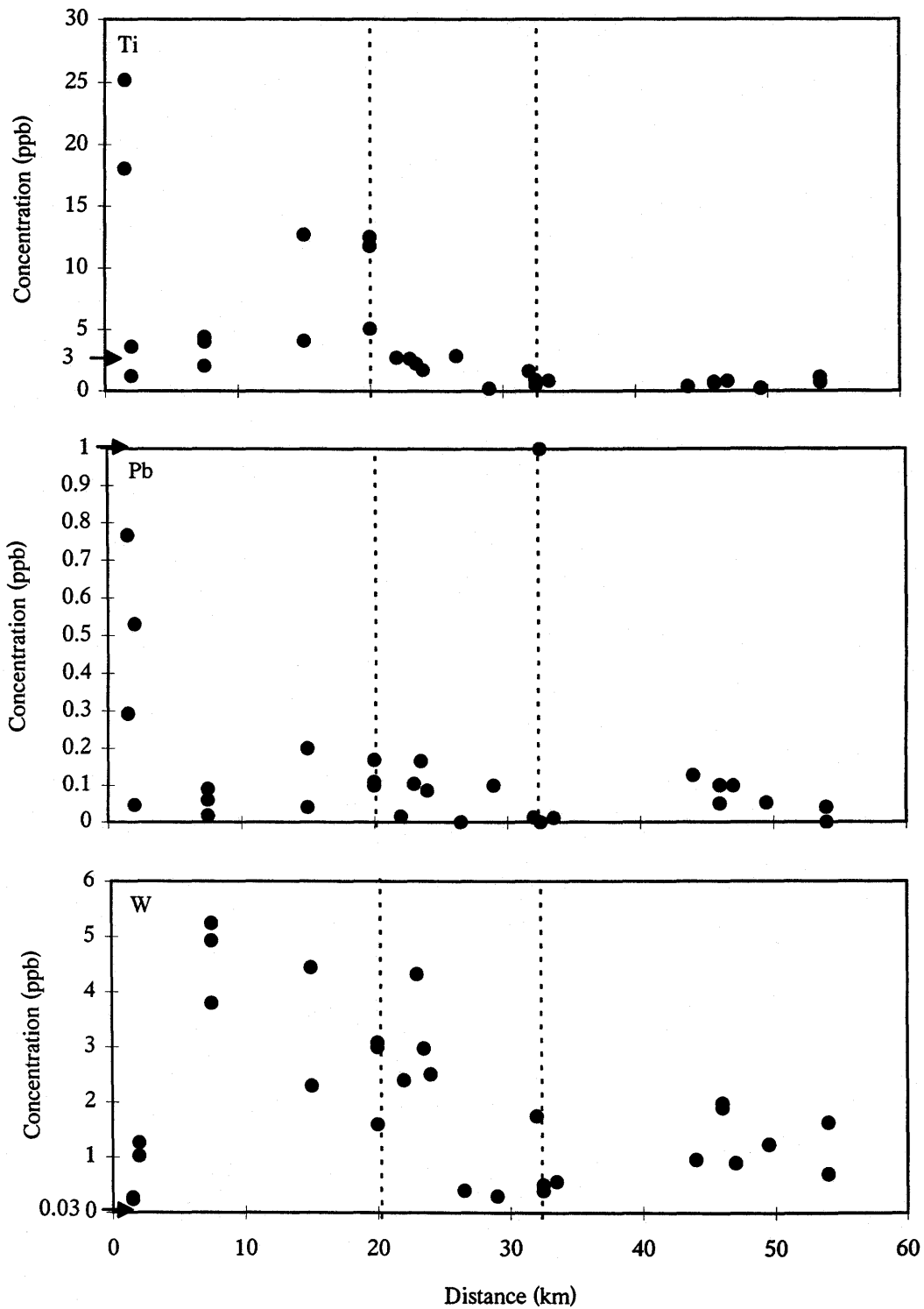


Figure 4.28. Ti, Pb, and W concentrations in the Milk River aquifer groundwater versus distance from recharge. Dashed vertical lines represent redox front and post-redox front boundaries. Arrow on left margin is value of select element for average world river water from Taylor and McLennan (1985). Cumulative plot of 1996-1997 data.

Tungsten concentrations are scattered between 0.2 and 5 ppb, displaying a tendency to decrease downgradient (Fig. 4.28). The fresh recharge wells MR122 and MR139 display low values <1.5ppb.

Arsenic and *selenium* have been studied in groundwaters because of their potential inimical health impacts associated with consumption by both humans and animals at elevated levels (Figs. 4.25 and 4.29). The majority of selenium concentrations are <0.40 ppb, but display a slight increase from younger to older groundwater. Johannesson et al. (1996) indicate that Se is a more conservative element than arsenic and that there is a strong relationship between Cl and Se. From this study Se appears to behave conservatively, similar to chloride, and may be used to help define the local groundwater flow regime (Figs. 4.2 and 4.29).

Nickel and *Cadmium* in the Milk River groundwater have low concentrations, at <0.12 ppb and <0.06 respectively, and both elements remain constant along the flow path (Figs. 4.29 and 4.30). Although *Copper* concentrations are higher (<5 ppb), but the majority of the groundwater analyzed similarly remain constant. Only a few wells display moderately higher values (Fig. 4.29).

Zirconium displays a uniform increase in concentration as the water flows northward, reaching values 0.19 ppb, with the exception of the anomalously high MR114 (Fig. 4.30).

The remaining trace elements listed in Table 4.5 may be sorted into two categories. In the first category, the element displays no increase as the groundwater migrates northward, indicating limited water-rock reaction for that element and the absence of redox control on solubility (Figs. 4.31 and 4.32). The second category of elements are those that display scatter, such as Hf, Sc, Ag, Sn, and Ta. These elements display no

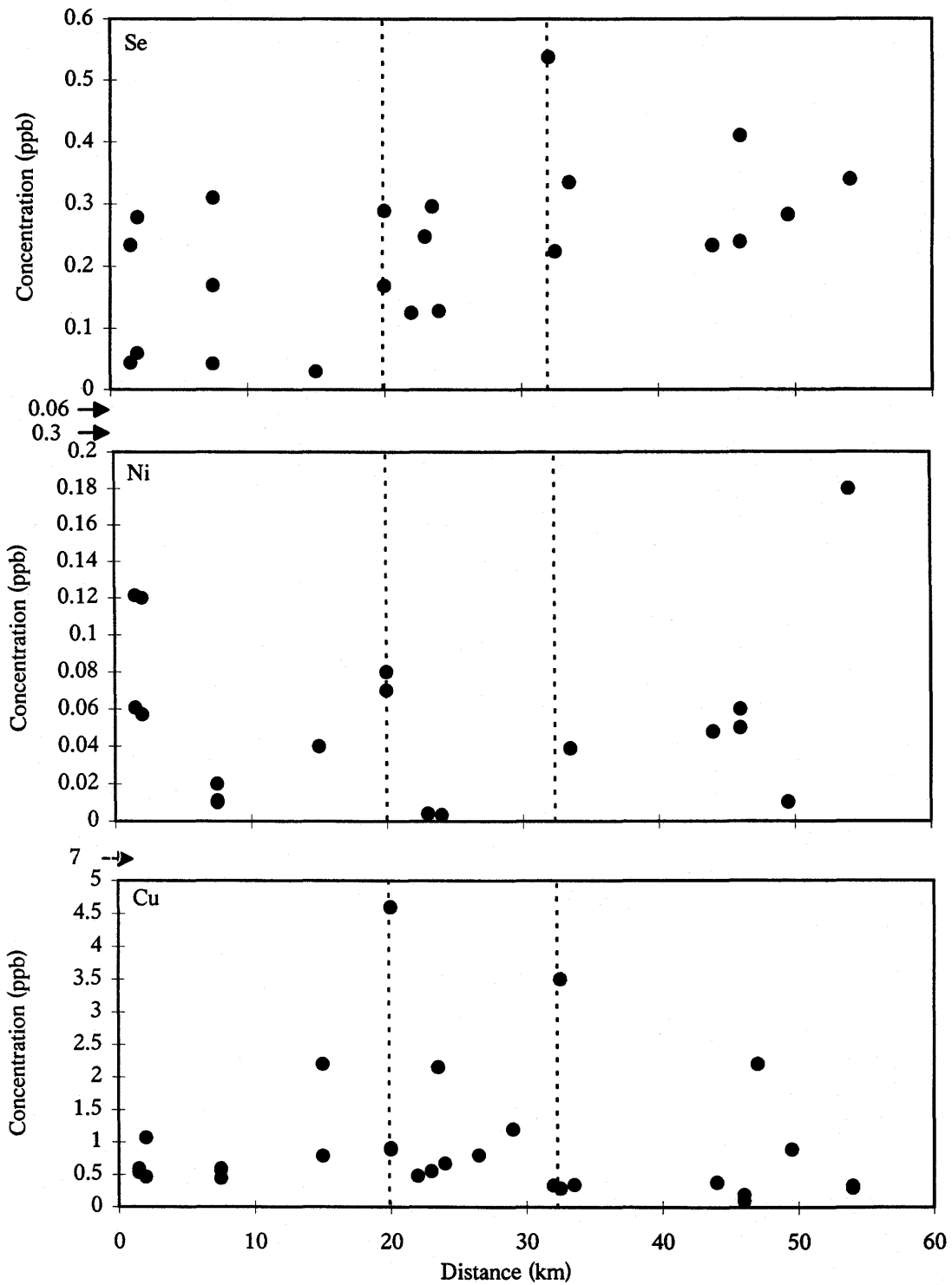


Figure 4.29. Se, Ni, and Cu concentrations in the Milk River aquifer groundwater versus distance from recharge. Dashed vertical lines represent redox front and post-redox front boundaries. Arrow on left margin is value of select element for average world river water from Taylor and McLennan (1985). Cumulative plot of 1996-1997 data.

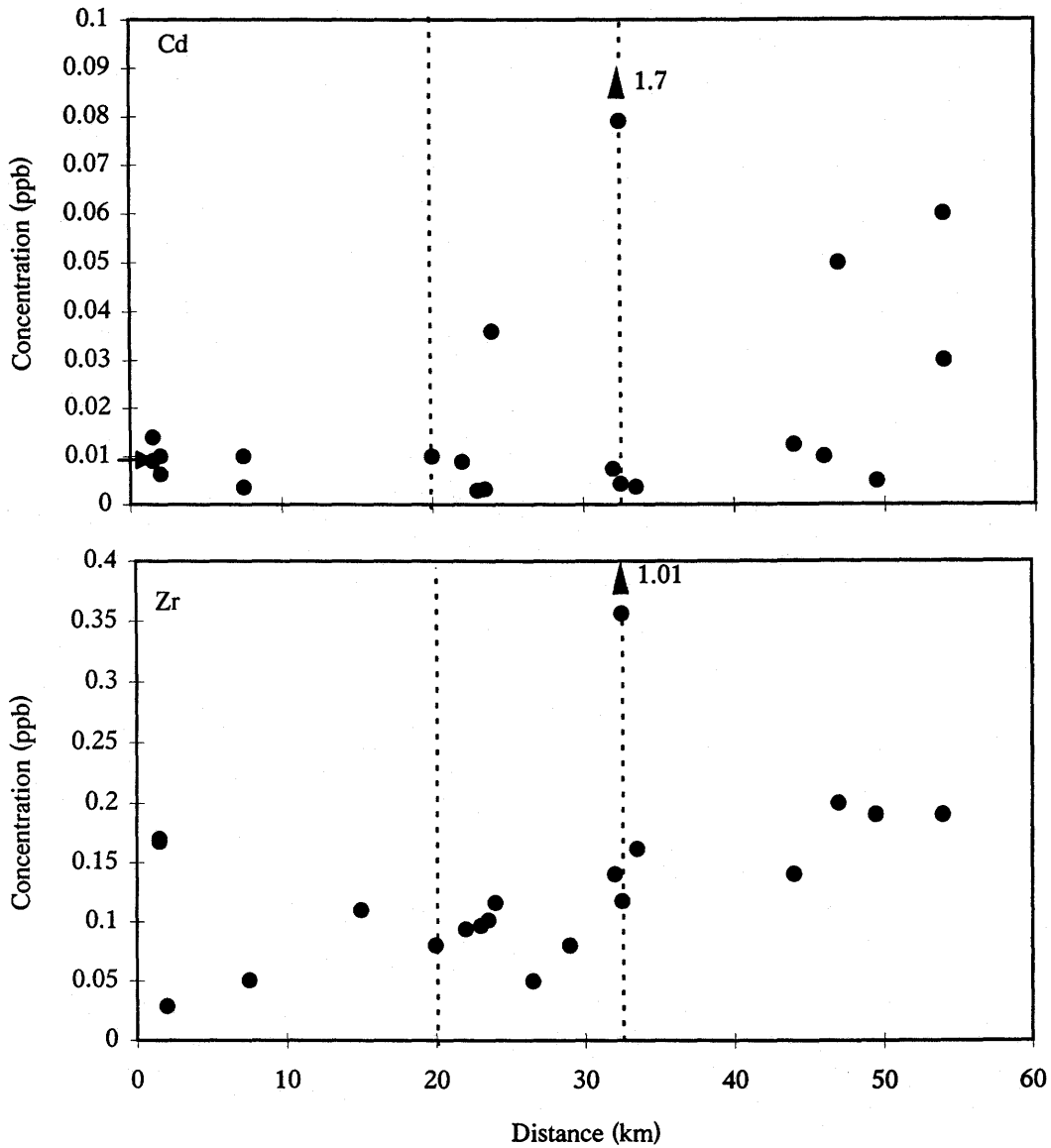


Figure 4.30. Cd and Zr concentrations in the Milk River aquifer groundwater versus distance from recharge. Dashed vertical lines represent redox front and post-redox front boundaries. Arrow on left margin is value of select element for average world river water from Taylor and McLennan (1985). Cumulative plot of 1996-1997 data. Marker with triangle on both figures represents outlier data point and concentration value.

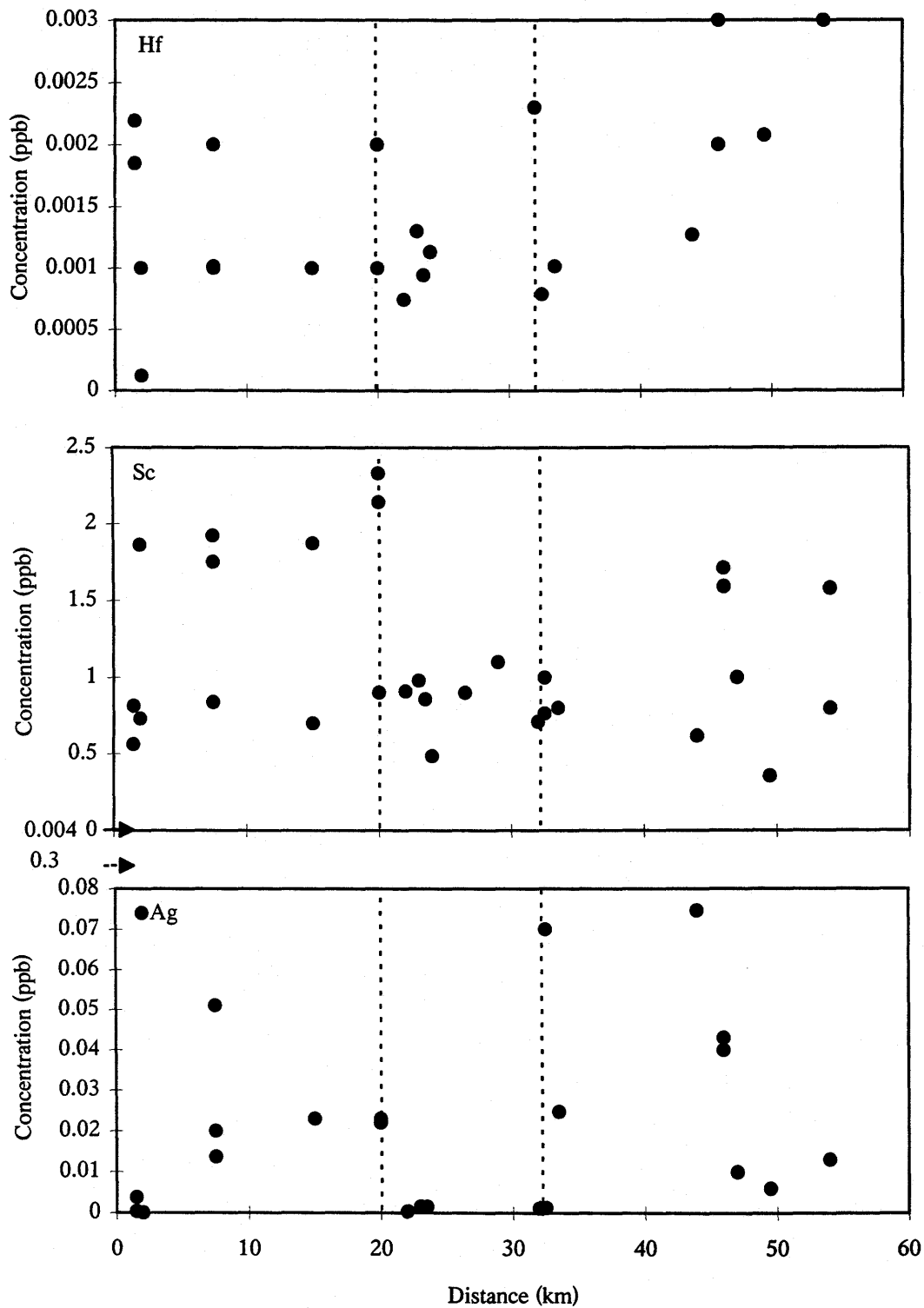


Figure 4.31. Hf, Sc, and Ag concentrations in the Milk River aquifer groundwater versus distance from recharge. Dashed vertical lines represent redox front and post-redox front boundaries. Arrow on left margin is value of select element for average world river water from Taylor and McLennan (1985). Cumulative plot of 1996-1997 data.

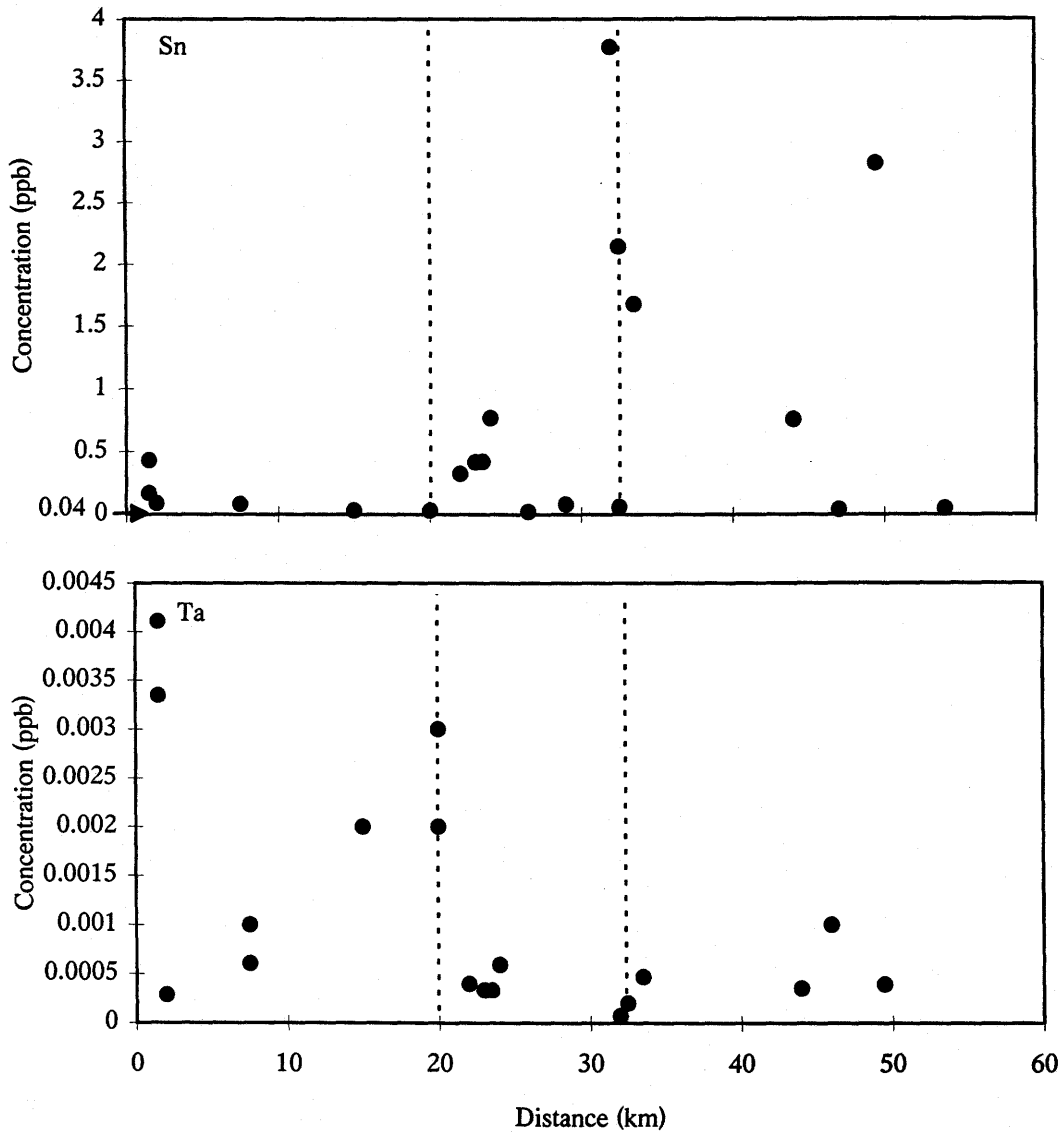


Figure 4.32. Sn and Ta concentrations in the Milk River aquifer groundwater versus distance from recharge. Dashed vertical lines represent redox front and post-redox front boundaries. Arrow on left margin is value of select element for average world river water from Taylor and McLennan (1985). Cumulative plot of 1996-1997 data.

observable trends with distance and are difficult to interpret. In select cases the inconsistent concentrations versus distance may be due to detection limit problems at the ultra-low solute abundances.

4.6.2 Transition Metals

Transition metals, alkali metals, and alkali earth metals can be grouped together and normalized, similar to shale-normalized REE plots to observe differences in patterns as the groundwater migrates northward. Figure 4.33 presents the concentrations of select transition elements normalized to PAAS for the 1995, 1996, and 1997 field seasons. Samples from the same wells from year to year demonstrate excellent reproducibility. The general trends includes enrichments in Sc, Zn, and Cr compared to neighboring elements and small concentration increases in most elements, as the groundwater migrates downgradient. The 1997 groundwater samples display negligible differences between filtered and unfiltered samples, and the normalized patterns are similar. The transition metal patterns remain constant throughout the 54 km flow path studied for this research. Similarly, the 1995 groundwater duplicates well with the 1996 and 1997 samples. Sc and Ti are the most constant transitional elements in the evolving groundwaters. Nickel is the only element that is not detected in several groundwater samples (Fig. 4.33).

4.6.3 Alkali Metals and Alkali Earth Metals

Concentrations of alkali and alkali earth metals normalized to PASS are illustrated in Figure 4.34. Reproducibility in concentrations and pattern are good for the 1997 groundwater data, displaying troughs at K, Mg, and Ca relative to neighboring elements. Unlike the transition metals, normalized values for the alkali-earths show only minor increases or decreases in values or patterns as the waters move down flow. Barium is the most active of these displaying increases in values as the waters migrate from recharge. There are no apparent affects from filtering and non-filtering groundwater samples. The 1996 and 1997 samples have similar concentrations of Li, Na, Rb, Cs, Sr, and Ba; however potassium, magnesium and calcium display a higher degree of

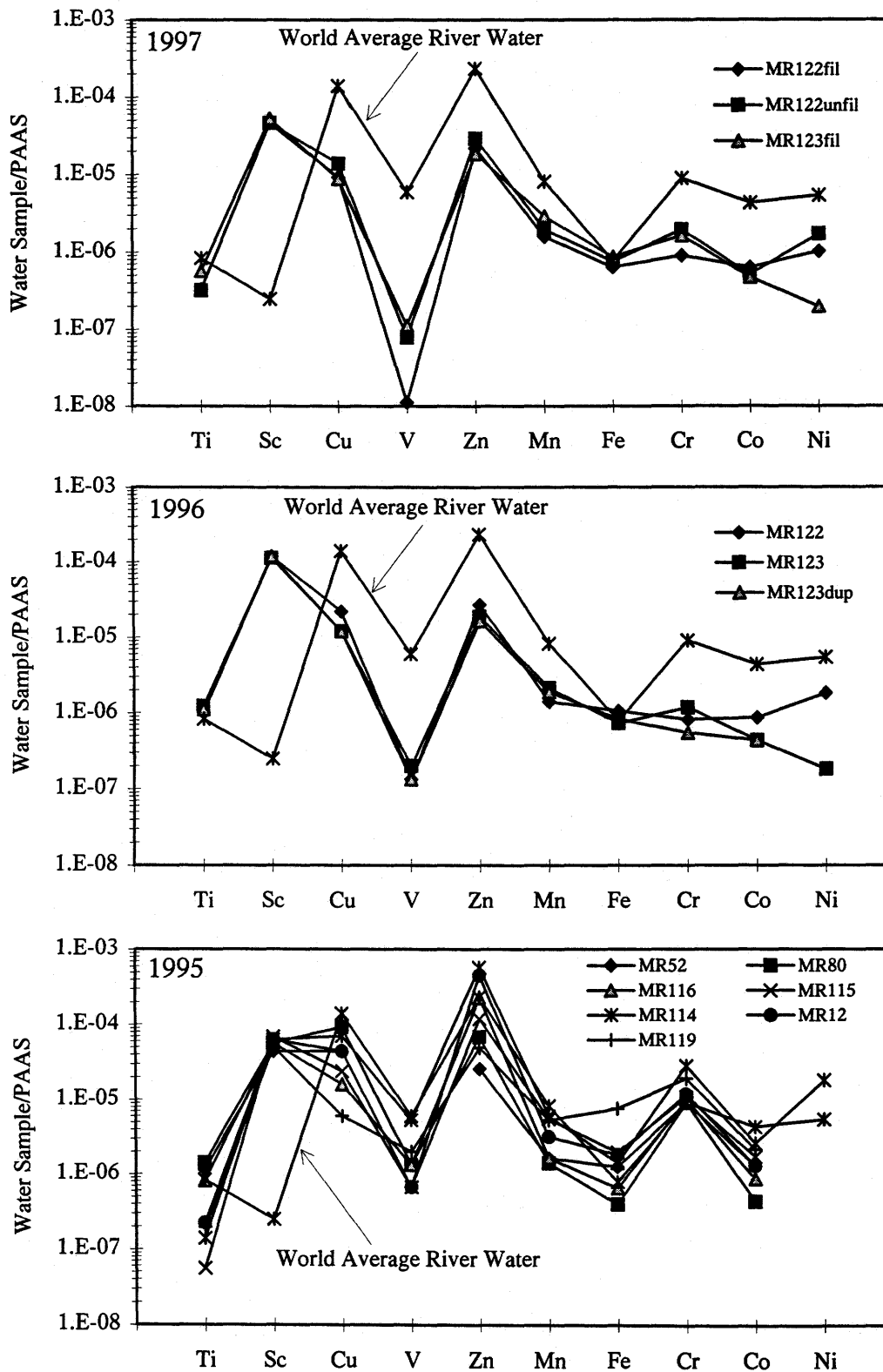


Figure 4.33. Specified transition metals normalized to PAAS for select groundwater data from the 1995, 1996, and 1997 field sampling seasons. World Average River Water from Taylor and McLennan (1985).

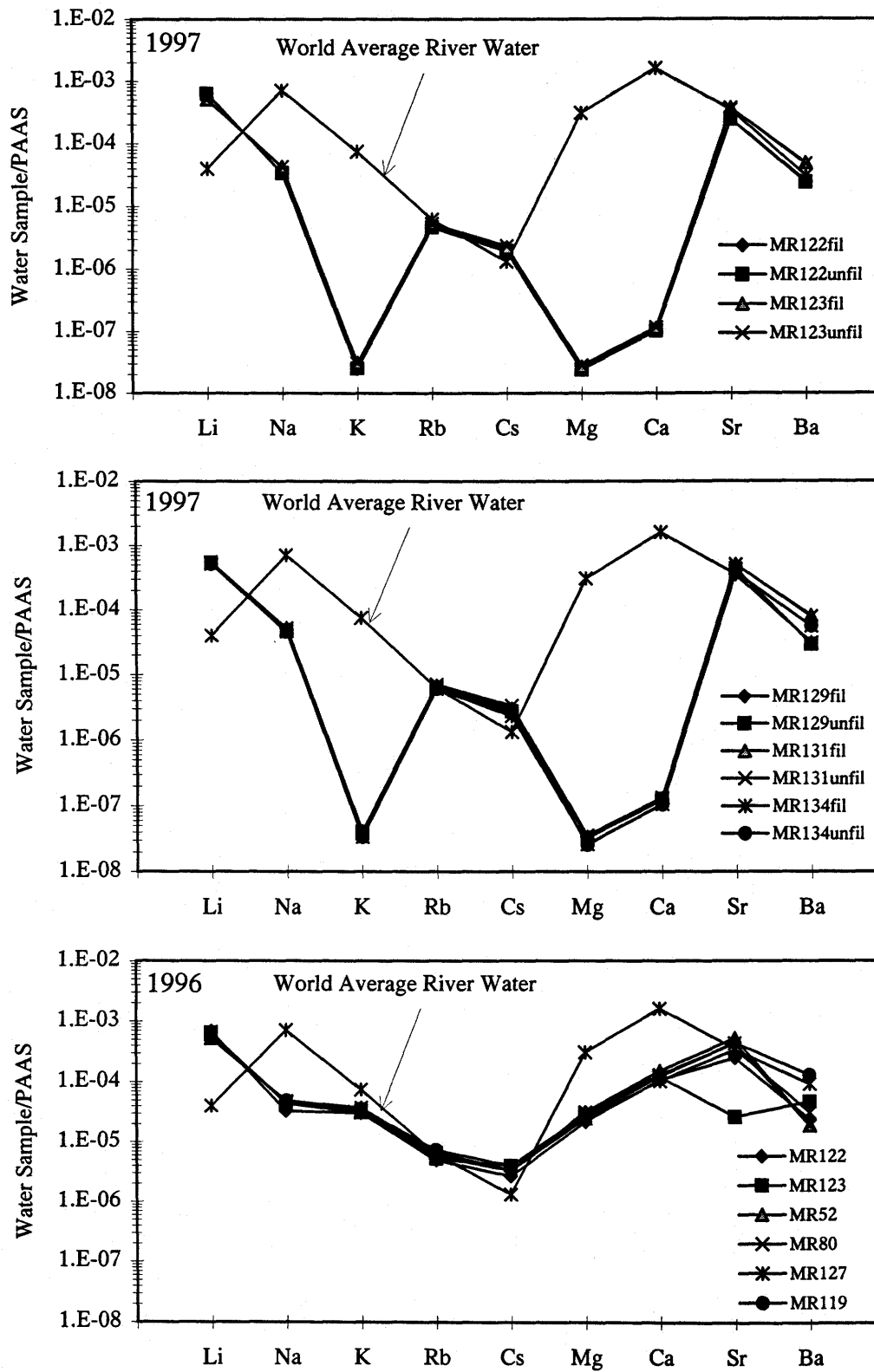


Figure 4.34. Specified alkali and alkali earth metals normalized to PAAS for select groundwater data from the 1995, 1996, and 1997 field sampling seasons. World Average River Water from Taylor and McLennan (1985).

variability from differing years. The transition metals the alkali and alkali earth metal patterns remain constant from the recharge zone to the 54 km point of the flow path. Given the presence of carbonates and clays in the aquifer sandstones and abundant clays in shales, the Li, K, Rb, Cs and Ba are likely from K-bearing clays, and Ca and Sr from carbonates.

Chapter 5

Summary and Conclusions

5.1 Introduction

Over 50 trace elements including the REEs were measured in 27 groundwater samples along the most hydraulically and chemically constrained section of the Milk River aquifer along the studied flow path, from the recharge area over a distance of 54 km. Filtered and unfiltered samples were collected in the field for subsequent chemical analysis. Routine chemistry on the samples was performed for anions (Cl and SO₄) and cations (Ca, Mg, Fe, Na) using Ion Liquid Chromatography and Atomic Absorption Spectrophotometry (AAS), respectively. Major element analysis was performed at the Saskatchewan Research Council by ICP-AES, and trace elements including the REEs were analyzed by ICP-MS at the University of Saskatchewan.

5.2 Field Filtering

Most trace elements did not show any effects of colloids or particles when filtered samples were compared to unfiltered samples. However a few unfiltered groundwaters from the Milk River aquifer contain a low to moderate load of suspended particles (>0.45µm), which have Th and LREE concentrations higher than the corresponding filtrates. The 0.45 µm particulates of amorphous ferric hydrous oxides may have a strong capacity for sorption of REEs. From this study it appears that suspended particles are important in the preferential removal of LREEs (La, Ce, Pr, Nd, Sm), and

less important in the MREEs (Eu, Gd, Tb, Dy) within the alkaline groundwater of the Milk River aquifer. HREEs (Ho, Er, Tm, Yb, Lu) are unaffected by colloids or suspended particles.

5.3 The Principal Findings From This Study

5.3.1 Summary of the Major Elements, and Ions

1. The groundwater chemistry (pH, alkalinity, and major cations/anions) determined in this study illustrates similar trends to those reported by previous workers (Meyboom, 1960; Schwartz and Muelenbachs, 1979; Phillips et al., 1986; Hendry and Schwartz, 1988, 1990; and Hendry et al., 1991).
2. Generally, the pH values of the groundwater decrease with increasing distance along the flow path. Values range from ~9.14 in the recharge area to <9.0, 20 km down gradient.
3. Alkalinity increases linearly along the flow path. Values range from 475 mg/l in the recharge area to 775 mg/l near the town of Foremost (~50 km from recharge). Alkalinity appears to be controlled by calcite dissolution in the carbonate dominated groundwater system. Geochemical modeling determined that the groundwater is close to saturation equilibrium (SI = 0) with calcite, and undersaturated with respect to dolomite and gypsum (SI < 0).
4. Sulphate concentrations decrease rapidly along the flow path and at 32 km from recharge are at very low concentrations (<0.5 µg/ml). Methane data from Taylor (1996), displays a significant increase at 32 km where the sulphate concentrations drop below detection. Together they define a redox front boundary. Recent recharge through the overlying glacial tills can account for the high SO₄ values (10-15 km from the recharge area).

5.3.2 Summary of the Trace Elements

1. In groundwater studies uranium has been found to be an excellent element for tracing the evolution of waters, given its low natural concentrations and multi-valent characteristics. The higher concentrations encountered along the flow path at 20 km may reflect the redox front boundary, and at the 32-33 km, the post-redox front boundary.
2. Boron is one of the trace elements with the highest concentrations in the Milk River groundwater, ranging from 100 to 1500 ppb along the flow path. Boron is probably being contributed by the marine clays which are predominant in the Milk River system shales.
3. Generally, total manganese values in the groundwater are lowest in the subcrop area with only a slight increase downgradient. There is a Mn concentration peak from 20 km to approximately 33 km along the flow path. This progressive northward increase along the flow path may be due to a redox boundary similar to that displayed by uranium. Therefore, reductive dissolution of Mn oxide appears to be an important process. After the redox boundary, dissolved Mn concentrations drop which may reflect precipitation of Mn oxyhydroxides. Zinc also displays this concentration peak between the redox and post-redox front displayed by U and Mn.
4. Many other trace elements (i.e. B, Rb, Mo, Co) show only a slight increase of concentration as the groundwater evolves from the recharge area, which are likely due to progressive water-rock interactions.
5. The concentration of barium displays a linear increase as the waters move from the recharge area. The Ba is possibly derived from calcite, dolomite, and K-clays which occur as trace components in Milk River aquifer sandstones.
6. Some trace elements (i.e. Li, Ti, P) display uniform concentrations or slight overall decreases in concentrations as the groundwater evolves. Inputs may be due to atmospheric/rainfall and there is only minor to no removal of the select element by any process during downgradient flow.

7. Arsenic concentrations in the Milk River aquifer groundwater are uniform along the first 54 km of the flow path, whereas selenium displays a slight increase from younger to older groundwater. From this study, Se appears to behave conservatively, similar to chloride, and it may be used to help define the local groundwater flow regime.
8. Nickel and Cd concentrations in the Milk River groundwater concentrations are very low, and both elements remain at uniform concentrations along the flow path. Similarly, Copper concentrations remain uniform. With the exception of a couple recharge groundwater samples, Pb values also remain uniform as the groundwater moves downgradient. Mineral dissolution and redox boundary conditions do not appear to have a significant control on these elements, even across the sulfide zone.
9. A number of remaining trace elements can be divided into two categories. The first category shows the elements that display no increase as the groundwater migrates northward, thus indicating insufficient water-rock reactions and/or no redox boundary effects. The second category of elements are those that display scattered distributions (i.e. Hf, Sc, Ag, Sn, and Ta), with no observable trends with distance. This in some cases may be due to detection limit problems brought about by their ultra-low abundances.

5.3.3 Summary of the Rare Earth Elements

1. Generally the high pH Milk River aquifer groundwater samples have low REE concentrations. Average Σ REE concentrations are 0.096 ppb. The absolute concentrations of LREEs are generally higher than HREEs. However, some groundwater samples display higher normalized HREEs compared to LREEs, due to LREE adsorption onto Fe oxyhydroxides.
2. Shale-normalized REE profiles of groundwaters from the Milk River aquifer display two general patterns; flat (Type 1 - recharge and redox front groundwater) or slightly enriched in the HREEs (type 2 - groundwater).

3. Two processes are possibly responsible for the observed REE distributions in the Milk River groundwater. Interaction with the aquifer materials as the recharge groundwater migrates downgradient, and the REE concentrations in groundwater are controlled by complexation with major anions.
4. Plots of Nd, Sm, and Dy concentrations in the groundwaters versus alkalinity and pH reveal at least two distinct water types. All three REEs exhibit an inverse relationships with alkalinity. At higher alkalinity values, lower concentrations of Nd, Sm, and Dy are observed. The 'recharge' groundwater display the highest values. A 'transitional' group, which may represent the redox boundary groundwater, occurs at 20 km from recharge. The main population of samples with similar element concentrations and ratios referred to as the 'Milk River groundwater' is represented by the lowest concentrations of all three REEs.

5.3.4 Summary of the Transition Metals

1. Overall, the transition metals in the groundwater data from year to year gave reproducible shale-normalized patterns and concentrations. The general trends are relative enrichment in Sc, Zn, and Cr compared to neighboring elements, and small concentration increases in most elements as the groundwater migrates downgradient.
2. The 1997 groundwater data display only mild differences between filtered and unfiltered samples, and the normalized patterns are similar. The transition metal patterns remain constant along the 54 km flow path studied for this research.
3. Similarly, the 1995 groundwater samples repeat well with the 1996 and 1997 samples. Sc and Ti are the most uniform transition elements in the evolving groundwater. Nickel is the only element that is not detected in several groundwater samples.

5.3.5 Summary of the Alkali Metals and Alkaline Earth Metals

1. Reproducibility in the concentrations and patterns are good for the 1997 groundwater data, displaying normalized depletions in K, Mg, and Ca compared to neighboring elements.
2. Unlike the transition metals, normalized values for the alkali-earth and alkali metals show only minor increases or decreases in values or patterns, as the groundwater moves down the flow path. Barium increases the most in concentration as the groundwater migrates from recharge.
3. The 1996 and 1997 samples have similar concentrations of Li, Na, Rb, Cs, Sr, and Ba. However, K, Mg, and Ca all display a higher degree of variability from year to year.
4. As for the transition metals the shale-normalized alkali and alkaline earth metals patterns remain constant as the groundwater evolves along the flow path, Ba excepted.

5.4 Speciation Modeling of the Milk River Aquifer Groundwater

5.4.1 PHREEQC Initial Conditions

1. Data indicate that the Milk River aquifer groundwater samples are at equilibrium or slightly undersaturated with respect to calcite and dolomite. Saturation indices indicate that gypsum is undersaturated in the groundwater from the recharge area to 54 km. Calcite is close to approaching equilibrium in the groundwater samples (SI = -0.25 to -0.03; n = 11), and dolomite is slightly undersaturated in all the groundwater samples along the studied flow path (SI = -1.0 to -0.44; n = 11).
2. Generally, the calculated log pCO₂ values for the Milk River aquifer groundwater samples are less than atmospheric pCO₂ of -3.5. Values are slightly lower in the recharge area compared to downgradient values that are below or near atmospheric pCO₂ values (mean SI = -3.59; n = 11).

3. The groundwater along the flow path is also undersaturated with respect to strontianite (SI = -0.99 to -0.05; n = 11).
4. Uraninite (UO₂) is strongly undersaturated in the recharge groundwater, but trends toward saturation as the groundwater migrates downgradient. After the post-redox front (~32-33 km) the groundwater becomes oversaturated with respect to uraninite (SI = -18.79 to 4.79; n = 11).
5. Barite (BaSO₄) SI values are variable along the flow path. Generally the groundwater is slightly undersaturated or close to equilibrium with respect to BaSO₄ (SI = -1.70 to 3.08; n = 11).

5.4.2 REE Speciation Modeling

1. Speciation modeling of REEs in the Milk River aquifer groundwater have been evaluated primarily to assess the importance of carbonate (LnHCO₃²⁺, LnCO₃⁺ and Ln(CO₃)₂⁻) and phosphate ((LnH₂PO₄²⁺, LnHPO₄⁺, Ln(HPO₄)₂⁻ and LnPO₄⁰) complexes.
2. Carbonate complexation is the most important for REEs complex in the Milk River aquifer groundwater system.
3. Heavy REE enriched shale-normalized REE patterns are due to the formation of more stable HREE CO₃ complexes than the light REE (LREE) CO₃ complexes in the groundwater.
4. Moreover, dicarbonato complexes (Ln(CO₃)₂⁻) are predicted as the dominant species in comparison to the carbonato complexes (LnCO₃⁺).

5.5 Implications of this Study

This study has shown that trace element data can be used as a complementary tool with major elements to map water-rock interactions in groundwater flow systems. Variations in the concentrations of trace elements, including the REEs, can further be used to discriminate different hydrogeological models in groundwater systems. The interactions with geologic materials have been shown to be an important source in the

groundwater chemistry. Recently, complexes of ligands (i.e. carbonate, phosphate, sulphate) have also been implicated as being important in the concentrations and patterns of REEs and trace elements.

In addition to using REEs as potential hydrogeochemical tracers in groundwaters, their chemical similarities for the trivalent radioactive actinides provides insight into the chemical behavior of the actinides in natural waters, and therefore a proxy for modeling disposal of nuclear waste.

5.6 Recommendations and Future Work

Sample protocols for groundwater studies are continuously developing and so are the instruments for analyzing water samples. It is also important that hydrogeologists constantly revise these sampling protocols to insure that the elements analyzed in water samples are in true solution, and not in colloidal form. In the past the operational cutoff size between colloidal particles and dissolved phase was defined as 0.45 μm . Recently, it has been proposed that 0.20 μm may be a more realistic filter size, to obtain a 'true' representative dissolved solute. This cannot be validated in this study, but the results may prove useful for a future groundwater sampling study of the Milk River aquifer groundwater.

Due to the limited database on trace elements and especially the REEs in groundwaters today, it is important to build on existing studies. Hence, future sampling and analysis of the Milk River aquifer would refine the understanding of the natural concentrations and patterns of trace elements including REEs in groundwater systems.

In addition to the refinement of the sampling protocol, continued improvement of instruments (i.e. ICP-MS) and techniques used in sample preparation (i.e. preconcentration, isotope dilution) will produce more precise and accurate water analysis. One such improvement in instrumentation is the operation of a flow injection

(Perkin Elmer FIAS400) coupled with the ICP-MS. Flow-injection, on-line separation and preconcentration would greatly improve the ICP-MS determination of trace elements and REEs in groundwaters as the high contents of dissolved solids (TDS) and other matrix effects could be removed.

References

- Akagi, T., Fuwa, K., and Haraguchi, H. (1985) Simultaneous multi-element determination of trace metals in sea water by inductively coupled plasma atomic emission spectrometry after coprecipitation with gallium. *Anal. Chim. Acta.* **177**, 139-151.
- Andrews J. N., Drimmie R. J., Loosli H. H. and Hendry M. J. (1991a) Dissolved gases in the Milk River aquifer, Alberta, Canada. *Appl. Geochem.* **6**, 393-403.
- Andrews J. N., Florkowski T., Lehmann B. E. and Loosli H. H. (1991b) Underground production of radionuclides in the Milk River aquifer, Alberta, Canada. *Appl. Geochem.* **6**, 425-434.
- Andrews J. N., and Kay, L. F. (1978) The evolution of enhanced $^{234}\text{U}/^{238}\text{U}$ activity ratios for dissolved uranium and groundwater dating. In Short Papers of the Fourth Internat. Conf. Geochron. Cosmochron. Isotope Geol. (ed R. E. Zartman). U. S. Geol. Surv. Open File Rept. 78-701, 11-13.
- Armstrong, S. G. (1994) Porewater chemical evolution in the Milk River aquifer, Alberta: A strontium isotope study of rock-water interaction. Unpublished M.Sc. Thesis, University of Illinois. 102 pp.
- Ball, J. W., and Nordstrom, D. K. (1991) User's manual for WATEQ4F, with revised thermodynamic database and test cases for calculating speciation of major, trace, and redox elements in natural waters. U.S. Geol. Survey Open File Rept. 91-183.

- Barcelona, M. J. (1990) Uncertainties in ground water chemistry and sampling procedures. *Chemical Modeling of Aqueous Systems II. ACS Symposium Series* **416**, 310-320.
- Beauchemin, D., McLaren, J. W., Mykytiuk, A. P., and Berman, S. S. (1987) Determination of trace metals in a river water reference material by inductively coupled plasma mass spectrometry. *Anal. Chem.* **59**, 778-783.
- Buellen, T. D., Krabbenhoft, D. P., and Kendall, C. (1996) Kinetic and mineralogic controls on the evolution of groundwater chemistry and $^{87}\text{Sr}/^{86}\text{Sr}$ in a sandy silicate aquifer, northern Wisconsin, USA. *Geochim. Cosmochim. Acta* **60**, 1807-1821.
- Byrne, R. H., and Kim, K. (1990) Rare earth element scavenging in seawater. *Geochim. Cosmochim. Acta* **54**, 2645-2656.
- Byrne, R. H., and Kim, K. (1993) Rare earth precipitation and coprecipitation behavior: The limiting role of PO_4^{3-} on dissolved rare earth concentrations in seawater. *Geochim. Cosmochim. Acta* **57**, 519-526.
- Cameron, E. M. (1996) Hydrogeochemistry of the Fraser River, British Columbia: seasonal variation in major and minor components. *J. Hydrol.* **182**, 209-225.
- Champ, D. R., Gulens, J., and Jackson, R. E. (1979) Oxidation - reduction sequences in ground water flow systems. *Can. J. Earth Sci.* **16**, 12-23.
- Cherdyntsev, V. V. (1971) Uranium-234. Israel Program for Scientific Translations, Jerusalem.

- DeBaar, H. J. W., Bacon, M. P., Brewer, P. G., and Bruland, K. W. (1983) Rare earth distributions with a positive Ce anomaly in the western North Atlantic Ocean. *Nature*, 301, 324-327.
- DeBaar, H. J. W., German C. R., Elderfield, H., and Van Gaans, P. (1988) Rare earth element distributions in anoxic waters of Cariaco Trench. *Geochim. Cosmochim. Acta* 52, 1203-1219.
- Deverel, S. J., and Millard, S. P. (1988) Distribution and mobility of selenium and other elements in shallow groundwater of the western San Joaquin Valley, California. *Environ. Sci. Technol* 22, 697-702.
- Devi, P. R., Gangaiah, T., and Naidu, G. R. K. (1991) Determination of trace metals in water by neutron activation analysis after preconcentration on a poly(acrylamidoxime) resin. *Analytica Chimica Acta* 249, 533-537.
- Dickson, B. L., and Herczeg, A. L. (1992) Deposition of trace elements and radionuclides in the spring zone, Lake Tyrrell, Victoria, Australia. *Chem. Geol.* 96, 151-166.
- Domenico, P. A., and Robbins, G. A. (1985) The displacement of connate water from aquifers. *Bull. Geol. Soc. Am.* 96, 328-335.
- Dominik, J., and Stanley, D. J. (1993) Boron, beryllium and sulfur in Holocene sediments and peats of the Nile delta, Egypt: Their use as indicators of salinity and climate. *Chem. Geol.* 104, 203-216.
- Doussan, C., Poitevin, G., Ledoux, E., and Detay, M. (1997) River bank filtration: modelling of the changes in water chemistry with emphasis on nitrogen species. *J. Contaminant Hydrology* 25, 129-156.

- Drimmie R. J., Aravena R., Wassenaar L. I., Fritz P., Hendry M. J. and Hut G. (1991) Radiocarbon and stable isotopes in water and dissolved constituents, Milk River aquifer, Alberta, Canada. *Appl. Geochem.* **6**, 381-392.
- Duro, L., Bruno, J., Gómez, P., Gimeno, M. J., And Wersin, P. (1997) Modelling of the migration of trace elements along groundwater flowpaths by using steady state approach: Application to the site at El Berrocal (Spain). *J. Contaminant Hydrology* **26**, 35-43.
- Edmunds, W. M., Bath, A. H., Miles, D. L. (1982) Hydrochemical evolution of the East Midlands Triassic sandstone aquifer, England. *Geochim. Cosmochim. Acta* **46**, 2069-2081.
- Elderfield, H., and Greaves, M. J. (1992) The rare earth elements in seawater. *Nature*. **296**, 214-219.
- Elderfield, H., Upstill-Goddard, R., and Sholkovitz, E. R. (1990) The rare earth elements in rivers, estuaries, and coastal seas and their significance to the composition of ocean waters. *Geochim. Cosmochim. Acta* **54**, 971-991.
- Erel, Y., Morgan, J. J. (1991) The effect of surface reactions on the relative abundances of trace metals in deep-ocean water. *Geochim. Cosmochim. Acta* **55**, 1807-1813.
- Erel, Y., and Stolper, E. M. (1993) Modeling of rare-earth element partitioning between particles and solution in aquatic environments. *Geochim. Cosmochim. Acta* **57**, 513-518.
- Esser, B. K., Volpe, A., Kenneally, J. M., and Smith, D. K. (1994) Preconcentration and purification of rare earth elements in natural waters using silica-immobilized 8-

hydroxyquinoline and a supported organophosphorous extractant. *Anal. Chem.* **66**, 1736-1742.

Fabryka-Martin J., Whittemore D. O., Davis S. N., Kubik P. W. and Sharma P. (1991) Geochemistry of halogens in the Milk River aquifer, Alberta, Canada. *Appl. Geochem.* **6**, 447-464.

Fee, J. A., Guadette, H. E., Lyons, W. B., and Long, D. T. (1992) Rare-earth element distribution in Lake Tyrrell groundwaters, Victoria, Australia. *Chem. Geol.* **96**, 67-93.

Fegan, N. E., and Long, D. T., Lyons, W. B., Hines, M. E., and Macumber, P. G. (1992) Metal partitioning in acid hypersaline sediments: Lake Tyrrell, Victoria, Australia. *Chem. Geol.* **96**. 167-181.

Frapporti, G., Vriend, S. P., and Van Gaans, P. F. M. (1993) Hydrogeochemistry of Shallow Dutch Groundwater: interpretation of the National Groundwater quality monitoring network. *Wat. Resour. Res.* **29**, 2993-3004

Freeze, R. A., and Cherry, J. A. (1979) Groundwater. Englewood Cliffs, NJ: Prentice-Hall, Inc. 603 pp.

Fröhlich K., and Gellermann R. (1987) On the potential use of uranium isotopes for groundwater dating. *Isotope Geosci.* **65**, 67-77.

Fröhlich K., Ivanovich M., Hendry M. J., Andrews J. N., Davis S. N., Drimmie R. J., Fabryka-Martin J., Flrkowski T., Fritz P., Lehmann B., Loosli H. H. and Nolte E. (1991) Application of isotopic methods to dating of very old groundwaters: Milk River aquifer, Alberta, Canada. *Appl. Geochem.* **6**, 465-472.

- Garbarino, J. R., and Taylor, H. E. (1987) Stable isotope Dilution Analysis of hydrologic samples by inductively coupled mass spectrometry. *Anal. Chem.* **59**, 1568-1575.
- Gascoyne, M. (1997) Evolution of redox conditions and groundwater composition in recharge-discharge environments on the Canadian Shield. *Hydrogeol. Journal.* **5**, 4-18.
- Giblin, A. M., and Dickson, B. L. (1992) Source, distribution and economic significance of trace elements in groundwaters from Lake Tyrrell, Victoria, Australia. *Chem. Geol.* **96**, 133-149.
- Goldstein, S. J., and Jacobsen, S. B. (1988) Rare earth elements in river waters. *Earth and Planetary Science Letters* **89**, 35-47.
- Gorlach, U., and Boutron, C. F. (1990) Preconcentration of lead, cadmium, copper and zinc in water at the pg g⁻¹ level by non-boiling evaporation. *Anal. Chim Acta.* **236**, 391-398.
- Gosselin, D. C., Smith, M. R., Lepel, E. A., and Laul, J. C. (1992) Rare earth elements in chloride-rich groundwater, Palo Duro Basin, Texas, USA. *Geochim. Cosmochim. Acta* **56**, 1495-1505.
- Grenthe, I., Stumm, W., Laaksunharju, M., Nilsson, A.-C. and Wikberg, P. (1992) Redox potentials and redox reactions in deep groundwater systems. *Chem. Geol.* **98**, 131-150.
- Hall, G. E. M. (1993) Capabilities of production-oriented laboratories in water analysis using ICP-ES and ICP-MS. *J. Geochemical Exploration*, **49**, 89-121.

- Hall, G. E. M., Vaive, J. E., and McConnell, J. W. (1995) Development and application of sensitive and rapid analytical method to determine the rare-earth elements in surface waters. *Chem. Geol.* **120**, 91-109.
- Hendry M. J., and Schwartz F. W. (1988) A alternative view on the origin of chemical and isotopic patterns in groundwater from the Milk River aquifer, Canada. *Wat. Resour. Res.* **24**, 1747-1763.
- Hendry M. J., and Schwartz F. W. (1990a) The chemical evolution of groundwater in the Milk River aquifer, Canada. *Ground Water* **28**, 253-261.
- Hendry M. J., and Schwartz F. W. (1990b) Reply to comment on "An alternative view on the origin of chemical and isotopic patterns in groundwater from the Milk River aquifer, Canada." *Wat. Resour. Res.* **26**, 1699-1703.
- Hendry M. J., and Schwartz F. W. and Robertson C. (1991) Hydrogeology and hydrochemistry of the Milk River aquifer system, Alberta, Canada: a review. *Appl. Geochem.* **6**, 369-380.
- Henshaw, J. M., Heithmar, E. M., and Hinnars, T. A. (1989) Inductively coupled plasma mass spectrometric determination of trace elements in surface waters subject to acidic deposition. *Anal. Chem.* **1989**, 335-342.
- Hiscock, K. M. (1993) The influence of pre-Devensian glacial deposits on the hydrogeochemistry of the Chalk aquifer system of north Norfolk, UK. *J. Hydrol.* **144**, 335-369.
- Ichihashi, H., Morita, H., and Tatsukawa, R. (1992) Rare earth elements (REEs) in naturally grown plants in relation to their variation in soils. *Environmental Pollution* **76**, 157-162.

- Ii, I., and Misawa, S. (1994) Groundwater chemistry within a plateau neighboring Matsumoto city, Japan. *Environ. Geol.* **24**, 166-175.
- Ivanovich M., Fröhlich K. and Hendry M. J. (1991) Uranium-series radionuclides in fluids and solids, Milk River aquifer, Alberta, Canada. *Appl. Geochem.* **6**, 405-418.
- Ivanovich M., and Schwarcz, H. P. (1983) Uranium-series radionuclides. In Role of Isotope Techniques in the Hydrological Assessment of Potential Sites for the Disposal of Highly Radioactive Waste. IAEA, Vienna, Tech. Rept Ser. No. 228, 102-126.
- Jacobs, L. A., Von Gunten, H. R., Keil, R., and Kuslys, M. (1988) Geochemical changes along a river-groundwater infiltration flow path: Glattfelden, Switzerland. *Geochim. Cosmochim. Acta* **52**, 2693-2706.
- Jacobson, G., Calf, G. E., Jankowski, J., and McDonald P. S. (1989) Groundwater chemistry and palaeorecharge in the Amadeous Basin, central Australia. *J. Hydrol.* **109**, 237-266.
- Johannesson, K. H., and Lyons, W. B. (1994) The rare earth element geochemistry of Mono Lake water and the importance of carbonate complexing. *Limnol. Oceanogr.*, **39**, 1141-1154.
- Johannesson, K. H., and Lyons, W. B. (1995) Rare-earth element geochemistry of Colour Lake, an acidic freshwater lake on Axel Heiberg Island, Northwest Territories, Canada. *Chem. Geol.* **119**, 209-223.
- Johannesson, K. H., Lyons, W. B., Fee, J. H., Gaudette, H. E, and McArthur, J. M. (1994) Geochemical processes affecting the acidic groundwaters of Lake Gilmore,

- Yilgarn Block, Western Australia: a preliminary study using neodymium, samarium, and dysprosium. *J. Hydrol.* **154**, 271-289.
- Johannesson, K. H., Lyons, W. B., Yelken, M. A., Henri, E. G., and Stetzenbach, K. J. (in press) Geochemistry of the rare earth elements in hypersaline and dilute acidic natural terrestrial waters: Complexation behavior and middle rare earth enrichments. *Chem. Geol.*
- Johannesson, K. H., Stetzenbach, K. J., and Hodge, V. F., Kreamer, D. K., and Zhou, X. (1997) Delineation of ground-water flow systems in the southern Great Basin using aqueous rare earth element distributions, *Ground Water* **135**, 807-819.
- Johannesson, K. H., Stetzenbach, K. J., Kreamer, D. K., and Hodge, V. F. (1996) Multivariate statistical analysis of arsenic and selenium concentrations in groundwaters from south-central Nevada and Death Valley, California. *J. Hydrol.* **178**, 181-204.
- Koshima, H., and Onishi, H. (1986) Adsorption of metal ions on activated carbon from aqueous solutions at pH 1-13. *Talanta* **33**. 391-395.
- Kraynov, S. P. (1997) Thermodynamic models for groundwater chemical evolution versus real geochemical properties of groundwater: A review of capabilities, errors, and problems. *Geochemistry International* **35**, 639-655.
- Kreamer, D. K., Hodge, V. F., Rabinowitz, I., Johannesson, K. H., and Stetzenbach, K. J. (1996) Trace element geochemistry in water from selected springs in Death Valley National Park, California. *Ground Water* **34**, 95-103.
- Kwok-Choi, N., and Jones, B. (1995) Hydrogeochemistry of Grand Cayman, British West Indies: implications for carbonate diagenetic studies. *J. Hydrol.* **164**, 193-216.

- Lahm T. D., Bair E. S., and Schwartz F. W. (1995) The use of stochastic simulations and geophysical logs to characterize spatial heterogeneity in hydrogeologic parameters. *Mathematical Geol.*, **27**, 259-278.
- Langmuir, D. (1997) Aqueous environmental geochemistry. Upper Saddle River, NJ. Prentice-Hall. 600 pp.
- Lee, J. H., and Byrne, R. H. (1992) Examination of comparative rare earth complexation behavior using linear free-energy relationships. *Geochim. Cosmochim. Acta* **56**, 1127-1137.
- Lee, J. H., and Byrne, R. H. (1993) Complexation of the trivalent rare earth elements (Ce, Eu, Gd, Tb, Yb) by carbonate ions. *Geochim. Cosmochim. Acta* **57**, 295-302.
- Lehmann B. E., Loosli H. H., Rauber D. , Thonnard N. and Willis R. D. (1991) ⁸¹Kr and ⁸⁵Kr in groundwater, Milk River aquifer, Alberta, Canada. *Appl. Geochem.* **6**, 419-423.
- Longstaffe, F. J. (1984) The role of meteoric water in diagenesis of shallow sandstones: stable isotope studies of the Milk River aquifer and gas pool, southeastern Alberta. *Am. Assoc. Petrol. Geol. Bull.* **37**, 81-98.
- Lyons, W. B., Welch, S., Long, D. T., Hines, M. E., Giblin, A. M., Carey, A. E., Macumber, P. G., Lent, R. M., and Herczeg, A. L. (1992) The trace-metal geochemistry of the Lake Tyrrell system brines (Victoria, Australia). *Chem. Geol.* **96**, 115-132.
- Macumber, P. G. (1992) Hydrological processes in the Tyrrell Basin, southeastern Australia. *Chem. Geol.* **96**. 1-18.

- Meyboom, P. (1960) Geology and groundwater resources of the Milk River sandstone in southern Alberta, *Alberta Res. Council, Edmonton, Alberta, Mem. 2*, 89 pp.
- Miekeley, N., Coutinho de Jesus, H., Porto da Silveira, C. L., Linsalata, P., and Morse, R. (1992) Rare-earth elements in groundwaters from the Osamu Utsumi mine and Morro do Ferro analogue study sites, Poços de Caldas, Brazil. *J. Geochemical Exploration* **45**, 365-387.
- Miekeley, N., Coutinho de Jesus, H., Porto da Silveira, C. L., Linsalata, P., and Morse, R. (1992) Chemical and physical characterization of suspended particles and colloids in waters from the Osamu Utsumi mine and Morro do Ferro analogue study sites, Poços de Caldas, Brazil. *J. Geochemical Exploration* **45**, 409-437.
- Millero, F. J. (1992) Stability constants for the formation of rare earth inorganic complexes as a function of ionic strength. *Geochim. Cosmochim. Acta* **56**, 3123-3132.
- Möller, P., and Bau, M. (1993) Rare-earth patterns with positive cerium anomaly in alkaline waters from Lake Van, Turkey. *Earth and Planetary Science Letters* **117**, 671-676.
- Möller, P., Dulski, P., and Luck, J. (1992) Determination of rare earth elements in seawater by inductively coupled plasma-mass spectrometry. *Spectrochimica Acta* **47B**, 1379-1387.
- Murphy E. M., Davis S. N., Long A., Donahue D., and Jull A. J. T. (1989) Characterization and isotopic composition of organic and inorganic carbon in the Milk River aquifer. *Wat. Resour. Res.* **25**, 1893-1905.

- Neal, C., Smith, C. J., Jeffery, H. A., Jarvie, H. P., and Robson, A. J. (1996) Trace element concentrations in the major rivers entering the Humber estuary, NE England. *J. Hydrol.* **182**, 37-64.
- Nolte E., Krauthan P., Korschinek G., Malosewski P., Fritz P. and Wolf M. (1991) Measurements and interpretations of ^{36}Cl in groundwater, Milk River aquifer, Alberta, Canada. *Appl. Geochem.* **6**, 435-445.
- Nordstrom, D. K., Ball, J. W., Donahoe, R. J., and Whittemore D. (1989) Groundwater chemistry and water-rock interactions at Stripa. *Geochim. Cosmochim. Acta* **53**, 1727-1740.
- Parkhurst, D. L. (1990) Ion-association models and mean activity coefficients of various salts. In Chemical modeling of aqueous systems II, ed D. C. Melchior and R. L. Bassett, Am. Chem. Soc. Symp. Ser. **416**, pp. 30-43 Washington DC: Am. Chem. Soc.
- Parkhurst, D. L. (1995) User's Guide to PHEEQC-a computer program for speciation, reaction-path, advective-transport, and inverse geochemical calculations. U.S. Geological Survey. *Water-Resources investigations Report 95-4227*. 143 pp.
- Phillips F. M., Knowlton R. G., and Bentley H. W. (1990) Comment on "an alternative view on the origin of chemical and isotopic patterns in groundwater from the Milk River aquifer, Canada" by M.J. Hendry and F. W. Schwartz. *Wat. Resour. Res.* **26**, 1693-1698.
- Phillips F. M., Bentley H. W., Davis S. N., Elmore D., and Swanick G. B. (1986) Chlorine 36 dating of very old groundwater 2. Milk River aquifer, Alberta, Canada. *Wat. Resour. Res.* **22**, 2003-2016.

Plummer, L. N. (1997) Principles and applications of modeling chemical reactions in ground water. International Ground Water Modeling Center, Colorado School of Mines, Golden, Colorado.

Postma, D., Boessen, C., Kristiansen, H., and Larsen, F. (1991) Nitrate reduction in an unconfined sandy aquifer: Water chemistry, reduction processes, and geochemical modeling. *Water Resources* 27, 2027-2045.

Potts, P. J. (1987) A handbook of silicate rock analysis. Blackie. 622 pp.

Ramaswami, A., and Small, M. J. (1994) Modeling the spatial variability of natural trace element concentrations in groundwater. *Water Resour. Res.* 30, 269-282.

Ramesh, R., Kumar, K. S., Eswaramoorthi, S., and Purvaja, G. R. (1995) Migration and contamination of Major and trace elements in groundwater of Madras City, India. *Environmental Geol.* 25. 126-136.

Robertson, G. (1988) Potential impact of subsurface irrigation return flow on a portion of the Milk River and Milk River aquifer in southern Alberta. Unpublished M.Sc. thesis. University of Alberta. 163 pp.

Schwartz F. W., Muehlenbachs, K., and Chorley, D. W. (1981) Flow-system controls of the chemical evolution of groundwater. *J. hydrolog.* 54, 225-243.

Schwartz, F. W., and Muehlenbachs, K. (1979) Isotope and ion geochemistry of groundwaters in the Milk River aquifer, Alberta. *Wat. Resour. Res.* 15, 259-268.

Shabani, M. B., Akagi, T., Shimizu, H., and Masuda, A. (1990) Determination of trace lanthanides and yttrium in seawater by inductively coupled plasma-mass

spectrometry after preconcentration with solvent extraction and back-extraction. *Anal. Chem.* **62**, 2707-2714.

Shimizu, H., Tachikawa, K., Masuda, A., and Nozaki, Y. (1994) Cerium and neodymium isotope ratios and REE patterns in seawater from the North Pacific Ocean. *Geochim. Cosmochim. Acta* **58**, 323-333.

Sholkovitz, E. R. (1993) The geochemistry of rare earth elements in the Amazon River estuary. *Geochim. Cosmochim. Acta* **57**, 2181-2190.

Smedley P. L. (1991) The geochemistry of rare earth elements in groundwater from the Carmenellis area, southwest England. *Geochim. Cosmochim. Acta* **55**, 2767-2779.

Smellie, J. A. T., Laaksoharju, M., and Wikberg, P. (1995) Äspö, SE Sweden: a natural groundwater flow model derived from hydrogeochemical observations. *J. Hydrol.* **172**, 147-169.

Stetzenbach, K. J., Amano, M., Kreamer, D. K., and Hodge, V. F. (1994) Testing the limits of ICP-MS: Determination of trace elements in ground water at the part-per-trillion level. *Ground Water* **32**, 976-985.

Sturgeon, R. E., Berman, S. S., Willie, S. N., and Desaulniers, J.A.H. (1981) Preconcentration of trace elements from seawater with silica-immobilized 8-hydroxyquinoline. *Anal. Chem.* **53**, 2337-2340.

Sugiyama, M., Fujino, O., Kihara, S. and Matsui, M. (1986) Preconcentration by dithiocarbamate extraction for determination of trace elements in natural waters by inductively coupled plasma atomic emission spectrometry. *Anal. Chim. Acta.* **181**, 159-168.

- Swanick, G. R. (1982) The hydrogeochemistry and age of the water in the Milk River aquifer, Alberta, Canada. Unpublished M.Sc. thesis, University of Arizona. 103 pp.
- Taylor, W. S. (1996) Bacterial hydrocarbon gases in surficial aquitards and shallow bedrock aquifers in the Western Canadian Sedimentary Basin. Unpublished M.Sc. thesis. University of Toronto. 97 pp.
- Taylor, S. R., and McLennan, S. M. (1985) *The Continental Crust: Its Composition and Evolution*. Blackwell Scientific, Oxford, 312 pp.
- Tellam, J. H. (1994) The groundwater chemistry of Lower Mersey Basin Permo-Triassic Sandstone Aquifer system, UK: 1980 and pre-industrialisation-urbanisation. *J. Hydrol.* **161**, 287-325.
- Thompson, M., Ramsey, M. H., and Pahlavanpour, B. (1982) Water analysis by inductively coupled plasma atomic emission spectrometry after a rapid preconcentration. *Analyst.* **107**, 1330-1334.
- Torgersen T.(1989) Terrestrial helium degassing fluxes and the atmospheric helium budget: Implications with respect to the degassing processes of continental crust. *Chem. Geol. (Isot. Geosci. Sect.)* **79**, 1-14.
- Tóth, J., and Corbet T. (1986) Post-Paleocene evolution of regional groundwater flow systems and their relation to petroleum accumulations, Taber area, southern Alberta, Canada. *Bull. Can. Pet. Geol.* **34(3)**, 339-363.
- Wassenaar L., Aravena R., Hendry M. J., and Schwartz F. W. (1991) Radiocarbon in dissolved organic carbon, a possible groundwater dating method: case studies from Western Canada. *Wat. Resour. Res.* **27**, 1975-1986.

- Wood, S. A. (1990a) The aqueous geochemistry of rare-earth elements and yttrium. 1. Review of available low-temperature data for inorganic complexes and the inorganic REE speciation of natural waters. *Chem. Geol.* **82**, 159-186.
- Wood, S. A. (1990b) The aqueous geochemistry of rare-earth elements and yttrium. 2. Theoretical predictions of speciation in hydrothermal solutions to 350 °C at saturation water vapor pressure. *Chem. Geol.* **88**, 99-125.
- Xun, Z., and Cijun, L. (1992) Hydrogeochemistry of deep formation brines in the central Sichuan Basin, China. *J. Hydrol.* **138**, 1-15.

Appendix A

1995-1997 Sample Locations

The following table lists the sampling sites selected for the 1995-1997 field seasons. Distances correspond to the location of wells from the area of recharge (distance measured north of the 49th parallel). Field and lab alkalinity and pH are presented for most wells. Where possible well depths and *in situ* groundwater temperatures were recorded.

Appendix A

	LSD	Distance (km)	Field pH	Lab pH	Field Alkalinity (mg/L)	Lab Alkalinity (mg/L)	Well Depth (ft)	Field Temp (°C)
1995-1996								
MR122	SW-9-1-10-W4	2	9.3	9.22	372	472	560	9.7
MR123	NW-20-1-10-W4	7.5	9.26	9.2	583	632	603	11.6
MR52	SE-28-2-10-W4	15	9.06	9	622	618	NA	9.2
MR80	SE-7-3-10-W4	20	9.08	9.06	NA	602	NA	11.1
MR116	SE-31-3-10-W4	26.5	-	-	-	-	NA	-
MR125	NW-33-3-11-W4	27	9.34	9.19	775	703	NA	11.4
MR43	NE-33-3-11-W4	27.5	-	-	-	-	NA	-
MR126	SW-2-4-11-W4	28	9.35	9.2	704	696	~ 700	11.5
MR115	NW-12-4-11-W4	29	-	-	-	-	NA	-
MR124	SW-23-4-11-W4	32	9.3	9.17	740	725	NA	11
MR114	NE-24-4-11-W4	32.5	-	-	-	-	NA	-
MR128	NW-21-4-11-W4	34.5	9.01	8.75	724	709	~ 850	9.9
MR118	NW-9-5-11-W4	40	9.3	9.19	875	961	NA	10.3
MR127	NE-32-5-11-W4	46	9.19	9.06	784	774	~ 790	10.4
MR12	SE-4-6-11-W4	47	-	-	-	-	NA	-
MR119	SE-29-6-11-W4	54	9.08	8.89	833	849	NA	9.1
MR121	NE-20-7-11-W4	61	-	-	-	-	-	-
MR14	NE-12-8-12-W4	68	-	-	-	-	-	-
MR25	SE-22-8-12-W4	73	-	-	-	-	-	-
MR17	SW-24-9-12-W4	81	-	-	-	-	-	-
MR23	NW-25-9-13-W4	82	-	-	-	-	-	-
MR113	SE-22-10-12-W4	91	-	-	-	-	-	-
1997								
MR139	SW-7-1-11W4	1.5	9.11	-	474	-	-	11.3
MR122	SW-9-1-10-W4	2	9.13	-	542	-	585	11.8
MR 140	NW-9-1-11W4	2	8.19	-	339	-	325	10.5
MR123	NW-20-1-10-W4	7.5	9.14	-	586	-	603	12.5
MR130	NE-16-3-10W4	22	8.96	-	655	-	750	13.2
MR135	SW-24-3-10W4	23	9.01	-	631	-	700	16.3
MR136	NW-23-3-10W4	23.5	9.03	-	637	-	720	11.3
MR129	SW-26-3-10W4	24	9	-	639	-	700	11.8
MR132	SW-19-4-9W4	31.5	8.58	-	763	-	800	10.8
MR131	SE-19-4-9W4	32	8.93	-	790	-	800	11.8
MR134	NE-21-4-10W4	32.5	9.08	-	712	-	800	11.7
MR133	SW-26-4-10W4	33.5	8.98	-	741	-	780-790	10.3
MR137	SE-18-5-10W4	44	9.06	-	784	-	840	10.2
MR138	NW-12-6-11W4	49.5	9.03	-	776	-	800	11.1

Appendix B

ICP-AES and ICP-MS Analyses

The following table is a list of water samples analyzed in the 1995 -1997 field seasons by ICP-AES and ICP-MS. The samples and locations are listed in Appendix A. All data is reported in parts per billion (ppb) unless otherwise stated.

Appendix B - 1997 Data

Sample	MR138				MR129			
	ICP-AES		ICP-MS		ICP-AES		ICP-MS	
	filtered	unfiltered	filtered	unfiltered	filtered	unfiltered	filtered	unfiltered
Al			4.9	5.2			3.0	5.4
Fe	40	40	89	82	40	150	96	250
Ca	900	910			1140	1170		
Mg	320	300			430	430		
K	1090	1110			1160	1160		
Na(ppm)	393	395			424	428		
Ti			0.21	0.61			1.71	1.45
V			0.04	0.05			0.00	0.13
Cr			0.26	0.35			0.56	0.17
Mn			2.33	2.30			5.18	7.54
Co			0.015	0.018			0.003	0.007
Ni			0.010	0.021			0.003	0.268
Li	40.0	39.9	34.5	33.5	45.8	45.9	38.8	40.7
B			1547	1593			673	684
Y			0.13	0.13			0.16	0.17
Zr			0.19	0.16			0.12	0.09
Nb			0.0015	0.0016			0.0007	0.0050
Ta			0.0004	0.0004			0.0006	0.0007
Hf			0.0021	0.0016			0.0011	0.0015
P			230	241			244	257
La			0.0037	0.0054			0.0026	0.0049
Ce			0.0044	0.0075			0.0022	0.0094
Pr			0.0010	0.0012			0.0004	0.0011
Nd			0.0040	0.0043			0.0006	0.0045
Sm			0.0017	0.0025			0.0014	0.0017
Eu			0.0001	0.0006			0.0011	0.0014
Gd			0.0017	0.0025			0.0003	0.0030
Tb			0.0003	0.0003			0.0001	0.0004
Dy			0.0016	0.0022			0.0022	0.0025
Ho			0.0005	0.0006			0.0010	0.0009
Er			0.0019	0.0020			0.0028	0.0036
Tm			0.0002	0.0003			0.0007	0.0007
Yb			0.0030	0.0037			0.0027	0.0051
Lu			0.0004	0.0005			0.0007	0.0007
Cs			0.042	0.044			0.044	0.041
Rb			1.09	1.09			1.05	1.02
Ba	74.3	75.5	74.5	72.4	19.5	19.6	18.9	18.9
Th			0.0043	0.0045			0.0023	0.0044
U			0.031	0.031			1.413	1.413
W			1.23	1.28			2.51	2.45
Sr	62.3	62.5	70.6	69.0	45.8	45.9	87.7	86.7
Pb			0.05	0.09			0.09	0.29
As			0.58	0.49			0.30	0.27
Sb			n.d.	n.d.			n.d.	n.d.
Mo			1.74	1.72			0.57	0.54
Cd			0.005	n.d.			0.036	0.002
Sn			2.82	2.52			0.77	0.72
Sc			0.36	0.37			0.49	0.58
Cu			0.89	0.18			0.67	3.90
Zn			1.53	20.23			2.46	42.90
Ag			0.006	0.007			n.d.	n.d.
Se			0.28	0.27			0.13	0.16
Hg			0.020	0.010			n.d.	n.d.

Appendix B - 1997 Data continued

Sample	MR139						
	ICP-AES			ICP-MS			
	filtered	filtered-dup	unfiltered	filtered	filtered-dup	unfiltered	unfiltered-dup
Al				4.1	3.5	3.5	4.8
Fe	10	10	10	39	51	44	51
Ca	1060	1090	1050				
Mg	240	240	240				
K	810	770	740				
Na(ppm)	291	290	288				
Ti				18.06	25.20	24.62	4.74
V				0.06	0.14	0.10	0.72
Cr				0.12	0.22	0.14	0.09
Mn				9.70	13.38	10.35	1.83
Co				0.066	0.068	0.083	0.063
Ni				0.061	0.121	0.065	0.858
Li	51.0	50.5	51.0	45.5	45.2	44.5	6.0
B				362	475	307	11
Y				0.20	0.19	0.22	0.36
Zr				0.17	0.17	0.19	0.09
Nb				0.042	0.041	0.050	0.0024
Ta				0.0033	0.0041	0.0040	0.0001
Hf				0.0018	0.0022	0.0026	0.0014
P				295	410	299	15
La				0.0875	0.079	0.105	0.028
Ce				0.1747	0.158	0.211	0.053
Pr				0.0232	0.021	0.026	0.007
Nd				0.0912	0.088	0.111	0.028
Sm				0.0220	0.022	0.025	0.005
Eu				0.0045	0.004	0.004	0.0002
Gd				0.0215	0.023	0.028	0.007
Tb				0.0039	0.003	0.003	0.0005
Dy				0.0169	0.016	0.020	0.006
Ho				0.0036	0.003	0.004	0.001
Er				0.0105	0.010	0.014	0.004
Tm				0.0019	0.002	0.002	0.0004
Yb				0.0096	0.009	0.011	0.003
Lu				0.0016	0.001	0.001	0.0003
Cs				0.025	0.023	0.026	0.003
Rb				0.72	0.69	0.69	0.38
Ba	26.7	26.3	26.3	27.1	23.9	26.7	98.2
Th				0.0360	0.0366	0.0364	0.0091
U				0.132	0.129	0.132	0.968
W				0.23	0.27	0.23	0.004
Sr	46.5	46.7	46.2	50.6	48.6	50.0	231.9
Pb				0.29	0.77	0.45	0.02
As				0.24	0.13	0.23	0.95
Sb				n.d.	0.07	n.d.	0.13
Mo				1.54	1.49	1.54	0.99
Cd				0.014	0.009	0.002	0.008
Sn				0.43	0.17	0.33	0.01
Sc				0.56	0.81	0.60	0.71
Cu				0.59	0.53	0.33	0.93
Zn				0.89	0.79	1.18	0.13
Ag				0.0004	0.004	n.d.	n.d.
Se				0.04	0.23	0.01	0.19
Hg				0.030	n.d.	0.061	n.d.

Appendix B - 1997 Data continued

Sample	MR131				MR132			
	ICP-AES		ICP-MS		ICP-AES		ICP-MS	
	filtered	unfiltered	filtered	unfiltered	filtered	unfiltered	filtered	unfiltered
Al			3.6	31.3			n.d.	6.7
Fe	60	130	198	320	330	420	831	1004
Ca	1200	1230			2430	2420		
Mg	450	470			770	780		
K	1260	1260			1810	1820		
Na(ppm)	463	460			606	605		
Ti			1.64	3.37			0.06	0.63
V			n.d.	0.07			0.08	0.12
Cr			0.31	0.54			0.74	0.88
Mn			4.80	6.32			16.87	17.53
Co			0.020	0.030			0.051	0.058
Ni			n.d.	0.052			0.008	n.d.
Li	47.4	48.3	40.9	39.4	53.7	52.7	44.0	43.0
B			1092	1117			1760	1781
Y			0.18	0.20			0.29	0.29
Zr			0.14	0.16			0.26	0.27
Nb			0.0018	0.0036			0.0028	0.0042
Ta			0.0001	0.0004			n.d.	n.d.
Hf			0.0023	0.0019			0.0027	0.0023
P			448	518			435	474
La			0.0040	0.0436			0.0029	0.0104
Ce			0.0036	0.1160			0.0037	0.0176
Pr			0.0002	0.0109			n.d.	0.0020
Nd			0.0046	0.0404			0.0011	0.0114
Sm			0.0017	0.0062			0.0023	0.0021
Eu			0.0000	0.0010			0.0001	0.0006
Gd			0.0017	0.0075			0.0011	0.0031
Tb			0.0001	0.0009			n.d.	0.0003
Dy			0.0016	0.0046			0.0015	0.0023
Ho			0.0006	0.0009			0.0003	0.0007
Er			0.0015	0.0031			0.0010	0.0031
Tm			0.0000	0.0007			n.d.	n.d.
Yb			0.0022	0.0034			0.0027	0.0041
Lu			0.0003	0.0005			0.0002	0.0004
Cs			0.046	0.050			0.057	0.058
Rb			1.09	1.13			1.48	1.51
Ba	50.1	52.3	52.8	50.8	163.8	163.2	134.1	136.5
Th			0.0048	0.0121			0.0055	0.0077
U			0.830	0.857			0.014	0.014
W			1.75	1.79			0.55	0.52
Sr	88.2	89.0	100.8	101.5	163.8	163.2	189.5	191.6
Pb			0.01	0.12			0.15	0.21
As			0.31	0.27			0.46	0.44
Sb			n.d.	n.d.			0.02	0.02
Mo			3.06	3.06			3.37	3.23
Cd			0.007	0.005			0.026	0.014
Sn			3.77	3.39			13.34	12.00
Sc			0.71	0.84			0.74	0.83
Cu			0.34	0.56			0.24	0.30
Zn			1.24	82.51			0.77	11.16
Ag			0.001	0.002			0.004	0.002
Se			0.54	0.24			1.43	1.93
Hg			0.040	0.033			n.d.	n.d.

Appendix B - 1997 Data continued

Sample	MR134				MR140			
	ICP-AES		ICP-MS		ICP-AES		ICP-MS	
	filtered	unfiltered	filtered	unfiltered	filtered	unfiltered	filtered	unfiltered
Al			n.d.	n.d.			n.d.	81.3
Fe	20	30	141	146	120	440	349	810
Ca	990	970			22940	17710		
Mg	350	340			7710	5540		
K	1040	1030			2060	1820		
Na(ppm)	410	405			266	280		
Ti			0.91	1.21			6.04	10.23
V			0.00	0.05			0.02	0.26
Cr			0.18	0.20			0.14	0.43
Mn			5.24	4.57			55.31	47.28
Co			0.004	0.006			0.016	0.037
Ni			n.d.	n.d.			0.062	0.031
Li	47.2	46.9	39.0	38.9	84.5	78.6	70.2	64.0
B			772	773			394	386
Y			0.16	0.15			0.70	0.70
Zr			0.12	0.14			0.03	0.17
Nb			0.0007	0.0014			0.0007	0.0108
Ta			0.0002	0.0001			0.0001	0.0008
Hf			0.001	0.001			0.001	0.003
P			375	342			142	173
La			0.0025	0.0030			0.0013	0.0788
Ce			0.0010	0.0032			0.0009	0.1637
Pr			n.d.	n.d.			n.d.	0.0190
Nd			0.0012	0.0042			0.0015	0.0884
Sm			0.0007	0.0007			n.d.	0.0184
Eu			0.0006	0.0007			0.0002	0.0044
Gd			0.0016	0.0017			0.0017	0.0201
Tb			0.0004	0.0013			0.0004	0.0031
Dy			0.0027	0.0030			0.0020	0.0151
Ho			0.0008	0.0011			0.0013	0.0037
Er			0.0038	0.0044			0.0037	0.0117
Tm			n.d.	n.d.			0.0002	0.0010
Yb			0.0053	0.0053			0.0059	0.0112
Lu			0.0008	0.0008			0.0008	0.0018
Cs			0.035	0.039			0.046	0.056
Rb			0.98	0.96			1.50	1.41
Ba	39.3	39.4	36.2	36.3	24.6	27.7	21.3	24.4
Th			0.0016	0.0024			0.0018	0.0317
U			1.130	1.100			0.390	0.268
W			0.50	0.45			0.11	0.22
Sr	68.4	68.2	75.7	73.8	514.0	400.2	521.0	402.8
Pb			n.d.	0.04			0.00	0.11
As			0.18	0.21			0.18	0.15
Sb			n.d.	n.d.			n.d.	n.d.
Mo			0.59	0.58			0.84	0.84
Cd			0.004	n.d.			0.001	0.003
Sn			2.14	0.65			0.12	0.12
Sc			0.76	0.70			1.33	1.15
Cu			0.29	0.39			0.59	0.43
Zn			0.79	8.18			0.99	3.38
Ag			0.001	0.0001			0.0002	n.d.
Se			0.23	0.18			1.43	0.88
Hg			n.d.	n.d.			n.d.	n.d.

Appendix B - 1997 Data continued

Sample	MR130				MR136			
	ICP-AES		ICP-MS		ICP-AES		ICP-MS	
	filtered	unfiltered	filtered	unfiltered	filtered	unfiltered	filtered	unfiltered
Al			n.d.	n.d.			n.d.	4.4
Fe	10	260	31	565	10	10	33	37
Ca	1240	1230			1200	1190		
Mg	430	430			390	400		
K	1140	1200			1150	1170		
Na(ppm)	428	428			431	432		
Ti			2.72	3.35			2.25	2.17
V			0.02	0.04			0.02	0.03
Cr			0.04	0.25			0.18	0.22
Mn			9.35	13.66			3.43	3.38
Co			0.009	0.032			0.007	0.013
Ni			n.d.	0.075			n.d.	0.068
Li	44.3	43.8	37.7	36.1	45.6	45.2	38.9	38.4
B			620	642			801	725
Y			0.17	0.20			0.18	0.18
Zr			0.09	0.12			0.10	0.13
Nb			0.0008	0.0047			0.0012	0.0010
Ta			0.0004	0.0006			0.0003	0.0004
Hf			0.001	0.002			0.001	0.001
P			365	394			373	345
La			0.0010	0.0035			0.0021	0.0150
Ce			0.0007	0.0066			0.0016	0.0070
Pr			n.d.	0.0004			n.d.	0.0042
Nd			0.0002	0.0050			0.0035	0.0018
Sm			0.0009	0.0013			0.0010	0.0019
Eu			0.0005	0.0005			0.0008	0.0005
Gd			0.0016	0.0014			0.0030	0.0028
Tb			0.0004	0.0005			0.0007	0.0006
Dy			0.0018	0.0036			0.0026	0.0038
Ho			0.0008	0.0013			0.0011	0.0007
Er			0.0025	0.0034			0.0042	0.0044
Tm			0.0001	0.0001			0.0003	0.0004
Yb			0.0037	0.0076			0.0034	0.0030
Lu			0.0005	0.0007			0.0006	0.0007
Cs			0.036	0.037			0.039	0.042
Rb			0.97	1.01			1.04	1.06
Ba	13.3	14.8	11.6	13.4	18.4	18.5	16.6	16.5
Th			0.0014	0.0054			0.0027	0.0040
U			0.880	0.899			1.407	1.387
W			2.41	2.39			2.97	2.72
Sr	81.2	82.3	92.9	96.9	78.9	79.1	88.0	86.5
Pb			0.02	0.38			0.17	0.20
As			0.15	0.15			0.14	0.15
Sb			n.d.	n.d.			n.d.	0.00
Mo			0.47	0.48			0.57	0.56
Cd			0.009	n.d.			0.003	0.033
Sn			0.32	0.39			0.42	0.39
Sc			0.91	0.94			0.86	0.82
Cu			0.48	0.81			2.16	4.44
Zn			6.70	59.88			7.34	13.09
Ag			0.0004	n.d.			0.001	0.002
Se			0.13	0.25			0.30	0.14
Hg			n.d.	n.d.			n.d.	n.d.

Appendix B - 1997 Data continued

Sample	MR133				MR122			
	ICP-AES		ICP-MS		ICP-AES		ICP-MS	
	filtered	unfiltered	filtered	unfiltered	filtered	unfiltered	filtered	unfiltered
Al			1.2	2.6			1.6	2.7
Fe	40	80	125	196	10	10	33	39
Ca	1210	1250			950	950		
Mg	470	480			320	320		
K	1370	1360			760	780		
Na(ppm)	457	457			305	304		
Ti			0.83	1.27			1.19	1.16
V			0.03	0.03			0.002	0.01
Cr			0.24	0.18			0.10	0.22
Mn			4.09	4.63			1.36	1.69
Co			0.017	0.017			0.015	0.012
Ni			0.039	0.054			0.057	0.096
Li	51.8	51.7	42.9	43.0	55.2	54.6	47.7	47.0
B			996	1033			241	229
Y			0.18	0.19			0.14	0.13
Zr			0.16	0.17			0.03	0.04
Nb			0.0006	0.0007			n.d.	0.0007
Ta			0.0005	0.0003			0.0003	0.0004
Hf			0.001	0.001			0.000	0.001
P			370	376			108	112
La			0.0027	0.0038			0.0025	0.0025
Ce			0.0021	0.0046			0.0032	0.0051
Pr			n.d.	0.0027			0.0005	0.0010
Nd			0.0010	0.0028			0.0018	0.0054
Sm			0.0017	0.0024			0.0008	0.0020
Eu			0.0005	0.0009			0.0008	0.0006
Gd			0.0013	0.0023			0.0036	0.0028
Tb			0.0005	0.0007			0.0014	0.0005
Dy			0.0021	0.0014			0.0034	0.0031
Ho			0.0009	0.0005			0.0013	0.0012
Er			0.0039	0.0034			0.0042	0.0059
Tm			0.0003	0.0005			0.0012	0.0010
Yb			0.0022	0.0034			0.0062	0.0064
Lu			0.0007	0.0007			0.0009	0.0009
Cs			0.041	0.042			0.034	0.029
Rb			1.10	1.07			0.78	0.75
Ba	32.8	32.5	29.1	29.2	18.5	17.9	16.4	15.8
Th			0.0019	0.0038			0.0009	0.0011
U			1.368	1.478			0.445	0.453
W			0.56	0.58			1.02	1.03
Sr	88.0	88.3	96.5	96.0	46.7	46.4	50.0	49.3
Pb			0.01	0.19			0.05	0.06
As			0.19	0.17			0.16	0.16
Sb			n.d.	n.d.			n.d.	n.d.
Mo			0.91	0.90			0.06	0.06
Cd			0.004	0.001			0.006	0.007
Sn			1.68	1.87			0.09	0.04
Sc			0.80	0.76			0.73	0.74
Cu			0.34	0.78			0.46	0.69
Zn			0.91	9.40			1.87	2.48
Ag			0.025	0.019			0.0001	0.001
Se			0.34	0.39			0.28	0.03
Hg			n.d.	n.d.			n.d.	n.d.

Appendix B - 1997 Data continued

Sample	MR135				MR137			
	ICP-AES		ICP-MS		ICP-AES		ICP-MS	
	filtered	unfiltered	filtered	unfiltered	filtered	unfiltered	filtered	unfiltered
Al			0.4	n.d.			2.9	7.9
Fe	60	60	188	184	30	40	161	177
Ca	1200	1220			920	930		
Mg	410	410			320	350		
K	1090	1120			1070	1070		
Na(ppm)	425	424			401	399		
Ti			2.64	2.57			0.36	1.27
V			0.03	0.02			0.02	0.07
Cr			0.16	0.13			0.27	0.40
Mn			11.16	10.40			2.77	2.99
Co			0.009	0.011			0.013	0.014
Ni			0.004	0.015			0.048	0.042
Li	43.9	43.3	36.6	37.6	42.5	42.0	36.4	34.8
B			829	855			1652	1554
Y			0.17	0.16			0.16	0.17
Zr			0.10	0.10			0.14	0.17
Nb			0.0006	0.0019			0.0015	0.0035
Ta			0.0003	0.0008			0.0004	0.0008
Hf			0.001	0.001			0.001	0.002
P			406	355			419	424
La			0.0020	0.0047			0.0040	0.0118
Ce			0.0015	0.0020			0.0016	0.0195
Pr			0.0001	0.0006			0.0012	0.0025
Nd			0.0006	0.0024			0.0012	0.0096
Sm			0.0017	0.0008			0.0015	0.0041
Eu			0.0003	0.0003			0.0004	0.0008
Gd			0.0016	0.0026			0.0026	0.0049
Tb			0.0008	0.0010			0.0004	0.0005
Dy			0.0015	0.0044			0.0045	0.0049
Ho			0.0003	0.0018			0.0009	0.0011
Er			0.0020	0.0077			0.0037	0.0042
Tm			0.0003	0.0003			0.0007	0.0005
Yb			0.0022	0.0025			0.0045	0.0043
Lu			0.0003	0.0004			0.0008	0.0013
Cs			0.037	0.043			0.040	0.040
Rb			1.01	0.97			0.98	0.98
Ba	18.3	17.6	15.8	15.9	79.4	80.0	70.4	71.5
Th			0.0025	0.0035			0.0030	0.0059
U			0.943	0.982			0.424	0.421
W			4.32	4.39			0.96	0.90
Sr	84.3	83.1	94.5	89.8	67.1	66.5	72.7	72.9
Pb			0.10	0.10			0.13	0.18
As			0.15	0.16			0.19	0.16
Sb			0.00	0.00			n.d.	n.d.
Mo			0.60	0.58			0.90	0.90
Cd			0.003	0.004			0.012	0.006
Sn			0.42	0.30			0.76	0.78
Sc			0.98	0.86			0.62	0.66
Cu			0.55	0.89			0.38	0.56
Zn			5.42	8.31			1.57	2.22
Ag			0.002	0.011			0.075	0.021
Se			0.25	0.32			0.23	0.04
Hg			n.d.	n.d.			n.d.	n.d.

Appendix B - 1997 Data continued

Sample	MR123				Blanks		
	ICP-AES		ICP-MS		ICP-MS		
	filtered	unfiltered	filtered	unfiltered	Fieldbk1	Fieldbk2	Tripbk
Al			3.9	10.0	0.3	4.7	0.7
Fe	10	30	45	126	n.d.	n.d.	n.d.
Ca	1060	1080					
Mg	360	380					
K	960	960					
Na(ppm)	383	378					
Ti			2.05	2.70	n.d.	n.d.	n.d.
V			0.02	0.04	n.d.	n.d.	n.d.
Cr			0.18	0.20	n.d.	n.d.	0.03
Mn			2.48	3.10	0.03	0.07	0.16
Co			0.011	0.014	n.d.	n.d.	0.005
Ni			0.011	0.028	0.038	0.031	0.119
Li	46.1	45.3	38.4	38.2	0.0	0.0	0.0
B			464	431	0.5	0.4	n.d.
Y			0.21	0.21	0.001	0.001	0.000
Zr			0.05	0.06	0.02	0.01	0.002
Nb			0.0008	0.0011	n.d.	n.d.	n.d.
Ta			0.0006	0.0005	n.d.	n.d.	n.d.
Hf			0.001	0.001	n.d.	0.011	n.d.
P			355	354	n.d.	n.d.	0.8
La			0.0029	0.0167	n.d.	n.d.	n.d.
Ce			0.0016	0.0319	n.d.	n.d.	n.d.
Pr			0.0007	0.0046	n.d.	0.0010	n.d.
Nd			0.0027	0.0209	n.d.	0.0010	0.0010
Sm			0.0018	0.0066	n.d.	n.d.	0.0010
Eu			0.0002	0.0007	n.d.	n.d.	n.d.
Gd			0.0029	0.0058	n.d.	n.d.	n.d.
Tb			0.0004	0.0007	n.d.	n.d.	n.d.
Dy			0.0046	0.0059	n.d.	n.d.	n.d.
Ho			0.0017	0.0017	n.d.	n.d.	n.d.
Er			0.0063	0.0068	n.d.	n.d.	n.d.
Tm			0.0009	0.0012	n.d.	n.d.	n.d.
Yb			0.0077	0.0077	n.d.	n.d.	n.d.
Lu			0.0010	0.0012	n.d.	n.d.	n.d.
Cs			0.033	0.035	n.d.	n.d.	n.d.
Rb			0.86	0.85	n.d.	n.d.	n.d.
Ba	34.9	35.1	32.0	30.8	0.1	0.7	2.8
Th			0.0011	0.0060	n.d.	n.d.	n.d.
U			0.458	0.461	n.d.	n.d.	0.001
W			3.79	3.67	n.d.	n.d.	0.02
Sr	68.0	67.9	74.8	73.6	0.1	0.4	0.05
Pb			0.02	0.06	0.01	0.00	0.04
As			0.10	0.08	0.04	0.02	0.41
Sb			n.d.	n.d.	n.d.	n.d.	0.01
Mo			0.06	0.05	n.d.	n.d.	0.03
Cd			0.004	0.001	0.058	0.022	0.060
Sn			0.08	0.04	n.d.	n.d.	n.d.
Sc			0.84	0.91	n.d.	n.d.	n.d.
Cu			0.44	1.41	0.10	0.03	1.50
Zn			1.58	8.14	1.18	0.71	7.14
Ag			0.014	0.007	n.d.	n.d.	n.d.
Se			0.04	0.03	n.d.	n.d.	n.d.
Hg			n.d.	n.d.	n.d.	n.d.	n.d.

Appendix B - 1997 Data continued

Sample	Standards	
	ICP-MS	
	SLRS3	SLRS3
Al	33.9	30.7
Fe	102	98
Ca		
Mg		
K		
Na(ppm)		
Ti	1.37	1.36
V	0.27	0.28
Cr	0.32	0.29
Mn	3.91	3.68
Co	0.033	0.032
Ni	0.844	0.831
Li	0.5	0.5
B	3.5	2.4
Y	0.17	0.17
Zr	0.09	0.09
Nb	0.0036	0.0025
Ta	0.0002	0.0001
Hf	0.002	0.002
P	5.4	5.7
La	0.24	0.24
Ce	0.28	0.27
Pr	0.06	0.06
Nd	0.23	0.25
Sm	0.05	0.05
Eu	0.01	0.01
Gd	0.04	0.04
Tb	0.004	0.004
Dy	0.02	0.02
Ho	0.004	0.004
Er	0.01	0.01
Tm	0.002	0.002
Yb	0.01	0.01
Lu	0.002	0.002
Cs	0.007	0.006
Rb	1.66	1.67
Ba	13.8	13.8
Th	0.0102	0.0092
U	0.048	0.045
W	0.003	0.002
Sr	31.6	32.0
Pb	0.08	0.07
As	0.80	0.76
Sb	0.15	0.15
Mo	0.22	0.22
Cd	0.014	0.008
Sn	0.01	0.01
Sc	0.30	0.28
Cu	1.34	1.50
Zn	0.78	1.03
Ag	0.001	n.d.
Se	0.19	0.03
Hg	n.d.	n.d.

Appendix B - 1996 Data

Sample	MR122			MR123			
	ICP-AES		ICP-MS	ICP-AES			
	filtered	unfiltered	filtered	filtered	filtered-dup	unfiltered	unfiltered-dup
Si							
Al	9.7	6.2	6.9	7.9	6.6	6.3	6.3
Fe	54	99		37	42	41	62
Ca	989	10261		1131	1127	1070	1062
Mg	288	301		381	357	338	344
K	925	757		949	964	905	896
Na(ppm)	288	301		384	376	369	360
Ti	0.019	0.025	3.60	0.025	0.025	0.025	0.025
V	0.011	0.011	0.020	0.011	0.011	0.011	0.011
Cr	0.250	0.322	0.090	0.495	0.409	0.427	0.386
Mn	1.18	1.21		1.83	1.58	1.56	1.64
Co	0.036	0.036	0.018	0.036	0.036	0.036	0.036
Ni	3.06	1.39	0.12	1.52	1.36	1.13	1.27
Li	61.4	66.5	51.3	61.6	55.7	61.2	53.0
Be	0.025	0.027		0.022	0.019	0.019	0.014
B			119				
Zr	2.63	0.74		1.06	0.04	0.35	0.04
Nb	4.05	1.18	n.d.	0.76	0.09	0.22	0.09
Ta	3.62	1.05	n.d.	0.53	0.26	0.72	0.26
Hf	0.07	0.07	0.001	0.07	0.07	0.07	0.07
P	6.29	1.97	119.5	163.2	135.0	124.5	126.9
La	0.011	0.010	0.010	0.010	0.010	0.010	0.022
Ce	0.294	0.230	0.010	0.126	0.132	0.076	0.195
Pr	0.045	0.045	0.001	0.045	0.045	0.045	0.045
Nd	0.097	0.021	0.012	0.023	0.021	0.017	0.021
Sm	0.334	0.234	0.005	0.248	0.295	0.268	0.260
Eu	0.007	0.007	0.001	0.007	0.007	0.007	0.007
Gd	0.062	0.072	0.006	0.048	0.032	0.042	0.047
Tb	0.046	0.019	n.d.	0.003	0.028	0.023	0.038
Dy	0.003	0.003	0.005	0.003	0.003	0.003	0.003
Y	0.025	0.036	0.156	0.062	0.058	0.059	0.059
Ho	0.264	0.270	0.001	0.328	0.320	0.290	0.313
Er	0.006	0.006	0.006	0.006	0.006	0.006	0.006
Tm	0.015	0.015	0.001	0.020	0.011	0.042	0.021
Yb	0.001	n.d.	0.007	0.005	0.006	0.006	0.005
Lu	0.016	0.018	0.001	0.014	0.017	0.010	0.014
Cs			0.04				
Rb			0.79				
Ba	17.3	17.9	15.5	36.1	35.6	34.7	34.1
Th	0.28	0.24	0.00	0.36	0.26	0.11	0.25
U	0.62	0.86	0.41	0.47	0.56	0.18	0.75
W	1.54	0.46	1.26	4.16	2.48	3.05	1.94
Sr	46.0	48.9	49.7	71.6	71.4	69.4	68.0
Pb	1.04	0.30	0.53	0.37	0.76	0.50	0.41
As			0.09				
Sb			n.d.				
Mo	0.68	0.68	0.07	0.68	0.68	0.68	0.68
Cd	0.50	0.49	0.01	0.56	0.42	0.48	0.50
Sn	0.17	0.17		0.17	0.17	0.17	0.17
Sc	0.01	0.001	1.86	0.001	0.001	0.001	0.001
Ga	0.01	0.16		0.18	0.17	0.14	0.12
Cu	0.59	0.07	1.07	0.20	0.24	0.36	0.53
Zn	2.09	2.03	2.26	2.07	1.89	2.86	2.92
Ag	0.20	0.20	0.07	0.20	0.20	0.20	0.20
Au			n.d.				
Se			0.06				
Pd			0.02				

Appendix B - 1996 Data continued

Sample	MR123		MR52			MR80			
	ICP-MS		ICP-AES		ICP-MS	ICP-AES		ICP-MS	
	filtered	filtered-dup	filtered	unfiltered	filtered	filtered	unfiltered	filtered	filtered-dup
Si									
Al	2.3	4.7	7.8	6.0	2.1	7.3	6.8	3.5	5.3
Fe			42	48		33	41		
Ca			1414	1440		1208	1234		
Mg			424	425		416	420		
K			1080	1090		1029	1027		
Na(ppm)			435	445		415	413		
Ti	4.40	4.00	0.025	0.025	12.70	0.204	0.038	12.50	11.80
V	0.025	0.020	0.011	0.011	0.050	0.011	0.011	0.070	0.074
Cr	0.130	0.060	0.401	0.429	0.010	0.476	0.475	0.180	0.050
Mn			1.33	1.25		2.06	2.04		
Co	0.010	0.010	0.036	0.036	0.017	0.036	0.036	0.011	0.015
Ni	0.01	0.02	1.31	1.34	0.04	1.39	1.29	0.07	0.08
Li	48.2	43.8	59.6	59.7	39.3	61.1	61.1	45.1	46.3
Be			0.027	0.023		0.030	0.028		
B	290	257			434			306	480
Zr			0.42	0.35		0.36	0.36		
Nb	n.d.	0.001	0.16	0.05	0.01	0.19	0.09	0.02	0.02
Ta	n.d.	0.001	0.26	0.26	0.002	0.11	0.23	0.003	0.002
Hf	0.001	0.002	0.07	0.07	0.001	0.07	0.07	0.001	0.002
P	444.5	498.6	74.9	77.4	357.3	86.3	85.7	383.0	383.1
La	0.014	0.015	0.010	0.010	0.015	0.010	0.002	0.043	0.039
Ce	0.007	0.006	0.029	0.125	0.021	0.182	0.280	0.078	0.079
Pr	0.001	0.001	0.045	0.045	0.004	0.045	0.045	0.010	0.009
Nd	0.011	0.008	0.003	0.021	0.020	0.021	0.021	0.042	0.048
Sm	0.004	0.003	0.304	0.255	0.007	0.317	0.310	0.015	0.009
Eu	0.001	0.001	0.007	0.007	0.001	0.007	0.007	0.002	0.003
Gd	0.005	0.004	0.065	0.045	0.005	0.051	0.061	0.016	0.011
Tb	0.001	n.d.	0.036	0.022	0.001	0.033	0.013	0.002	0.002
Dy	0.005	0.004	0.003	0.003	0.003	0.003	0.003	0.007	0.007
Y	0.221	0.226	0.005	0.004	0.257	0.064	0.070	0.258	0.279
Ho	0.002	0.002	0.316	0.293	0.001	0.275	0.295	0.003	0.003
Er	0.008	0.009	0.006	0.006	0.003	0.006	0.006	0.010	0.011
Tm	0.001	0.001	0.018	0.012	0.001	0.022	0.016	0.001	0.001
Yb	0.009	0.008	0.001	0.002	0.005	0.006	0.005	0.011	0.010
Lu	0.002	0.001	0.010	0.015	0.001	0.017	0.014	0.002	0.002
Cs	0.06	0.05			0.05			0.05	0.05
Rb	0.84	0.83			0.94			0.92	1.00
Ba	30.4	30.7	13.7	11.8	12.3	13.7	13.2	12.2	12.4
Th	0.002	0.003	0.13	0.24	0.01	0.29	0.26	0.03	0.03
U	0.40	0.36	0.79	0.90	0.59	1.38	1.05	1.14	1.12
W	4.93	5.24	2.55	1.60	4.44	0.12	0.26	3.00	3.08
Sr	73.2	72.6	99.4	101.5	104.7	81.1	81.5	86.5	93.1
Pb	0.06	0.09	0.62	0.31	0.04	0.72	0.45	0.11	0.17
As	0.05	0.03			0.08			0.07	0.08
Sb	0.01	n.d.			n.d.			n.d.	0.01
Mo	0.08	0.06	0.01	0.32	0.46	0.03	0.04	0.37	0.39
Cd	0.01	n.d.	0.50	0.51	n.d.	0.61	0.46	n.d.	0.01
Sn			0.17	0.17		0.17	0.17		
Sc	1.75	1.92	0.001	0.001	1.87	0.001	0.001	2.14	2.33
Ga			0.31	0.19		0.36	0.25		
Cu	0.57	0.59	0.39	0.44	0.79	0.24	0.65	0.89	0.91
Zn	1.56	1.42	1.03	0.92	0.28	1.82	1.63	0.79	1.13
Ag	0.02	0.05	0.20	0.20	0.02	0.20	0.20	0.02	0.02
Au	n.d.	n.d.			n.d.			n.d.	0.001
Se	0.31	0.17			0.03			0.17	0.29
Pd	0.03	0.04			0.06			0.05	0.05

Appendix B - 1996 Data continued

Sample	MR126				MR125			
	ICP-AES		ICP-MS		ICP-MS		ICP-AES	
	filtered	filtered-dup	unfiltered	unfiltered-dup	filtered	filtered-dup	filtered	unfiltered
Si								
Al	8.7	8.7	17.1	7.2	6.2	5.7	10.0	8.2
Fe	34	52	78	42			77	287
Ca	891	893	874	997			955	1005
Mg	283	280	279	307			300	306
K	994	965	975	1085			949	1011
Na(ppm)	382	380	375	415			380	397
Ti	0.025	0.025	2.45	0.025	1.80	1.90	0.025	0.025
V	0.011	0.011	0.011	0.011	0.025	0.029	0.011	0.011
Cr	0.250	0.315	0.328	0.316	0.090	0.090	0.340	0.412
Mn	1.47	1.56	1.89	1.47			3.00	3.65
Co	0.036	0.036	0.036	0.036	0.013	0.012	0.036	0.036
Ni	1.20	1.37	1.21	1.09	0.01	0.01	1.33	1.12
Li	52.8	54.0	51.0	57.0	43.0	35.3	53.3	54.4
Be	0.018	0.024	0.022	0.025			0.017	0.020
B					662	453		
Zr	0.18	0.25	0.19	0.27			0.22	0.26
Nb	0.09	0.09	0.09	0.09	0.001	0.001	0.09	0.09
Ta	0.26	0.26	0.26	0.26	0.001	n.d.	0.26	0.26
Hf	0.07	0.07	0.07	0.07	0.002	0.002	0.07	0.07
P	116.6	111.2	112.2	116.7	332.4	353.9	136.6	141.0
La	0.010	0.010	0.010	0.010	0.023	0.024	0.010	0.010
Ce	0.245	0.089	0.233	0.110	0.010	0.009	0.065	0.069
Pr	0.045	0.045	0.045	0.045	0.001	0.001	0.045	0.045
Nd	0.021	0.021	0.021	0.021	0.011	0.007	0.021	0.021
Sm	0.255	0.261	0.283	0.226	0.004	0.004	0.274	0.268
Eu	0.007	0.007	0.007	0.007	0.001	0.001	0.007	0.007
Gd	0.043	0.051	0.049	0.042	0.008	0.005	0.054	0.104
Tb	0.012	0.025	0.035	0.011	0.001	n.d.	0.027	0.011
Dy	0.003	0.003	0.003	0.003	0.004	0.004	0.003	0.003
Y	0.041	0.037	0.038	0.036	0.191	0.200	0.061	0.070
Ho	0.271	0.290	0.285	0.268	0.002	0.002	0.290	0.282
Er	0.006	0.006	0.006	0.006	0.009	0.007	0.006	0.006
Tm	0.013	0.016	0.010	0.016	0.001	0.001	0.018	0.014
Yb	0.002	0.001	0.002	0.003	0.008	0.006	0.004	0.003
Lu	0.007	0.010	0.011	0.012	0.001	0.001	0.008	0.014
Cs					0.07	0.05		
Rb					0.98	0.94		
Ba	71.8	71.3	70.9	79.7	58.9	60.1	70.7	76.1
Th	0.18	0.14	0.12	0.19	0.00	0.00	0.17	0.14
U	0.88	0.90	1.26	0.75	0.59	0.65	0.17	1.37
W	0.46	0.46	0.46	0.46	0.40	0.44	0.46	0.46
Sr	67.1	66.8	65.7	74.3	68.0	68.3	69.7	73.4
Pb	0.20	0.57	0.58	0.66	0.02	0.01	0.40	2.24
As					0.14	0.11		
Sb					0.01	n.d.		
Mo	0.68	0.68	0.33	0.01	0.42	0.42	0.25	0.11
Cd	0.48	0.52	0.53	0.41	0.02	n.d.	0.52	0.45
Sn	0.17	0.17	0.17	0.17			0.17	0.17
Sc	0.001	0.001	0.001	0.001	1.56	1.87	0.001	0.001
Ga	0.40	0.40	0.26	0.33			0.40	0.41
Cu	0.17	0.16	0.08	0.08	0.23	0.23	0.24	6.45
Zn	2.32	2.56	3.10	3.22	1.69	1.35	4.65	56.92
Ag	0.20	0.20	0.20	0.20	0.02	0.01	0.20	0.20
Au					n.d.	n.d.		
Se					0.33	0.10		
Pd					0.03	0.04		

Appendix B - 1996 Data continued

Sample	MR125		MR124			MR128		
	ICP-MS		ICP-AES		ICP-MS	ICP-AES		ICP-MS
	filtered	filtered-Dup	filtered	unfiltered	filtered	filtered	unfiltered	filtered
Si								
Al	2.9	7.3	34.6	11.8	12.4	7.1	15.6	n.d.
Fe			82	120		353	368	
Ca			1044	1062		3344	5578	
Mg			338	349		1131	1918	
K			1020	1081		2006	2681	
Na(ppm)			378	404		676	932	
Ti	2.00	2.30	0.799	0.025	0.600	0.025	0.025	2.60
V	0.021	0.038	0.011	0.011	0.042	0.011	0.011	0.186
Cr	0.200	0.430	0.395	0.430	0.150	1.137	1.723	0.890
Mn			3.55	2.99		22.34	19.72	
Co	0.016	0.014	0.036	0.036	0.013	0.036	0.036	0.074
Ni	0.05	0.07	1.32	1.42	0.04	2.07	1.74	0.43
Li	47.2	38.7	51.8	54.8	35.8	82.2	110.4	89.8
Be			0.022	0.031		0.024	0.016	
B	774	699			674			1212
Zr			0.35	0.33		0.40	0.27	
Nb	0.003	0.003	0.09	0.09	0.001	0.09	0.11	0.01
Ta	0.001	0.002	0.03	0.26	n.d.	0.26	0.01	0.001
Hf	0.002	0.002	0.07	0.07	0.002	0.07	0.07	0.01
P	285.6	385.9	166.9	163.3	399.0	124.8	118.5	379.2
La	0.022	0.028	0.012	0.010	0.024	0.002	0.031	0.108
Ce	0.013	0.013	0.264	0.190	0.011	0.081	0.112	0.007
Pr	0.002	0.003	0.045	0.045	0.002	0.009	0.057	0.001
Nd	0.015	0.016	0.021	0.021	0.008	0.021	0.021	0.010
Sm	0.008	0.004	0.214	0.222	0.004	0.318	0.388	0.010
Eu	0.001	0.001	0.007	0.007	0.001	0.007	0.007	0.001
Gd	0.008	0.008	0.038	0.054	0.004	0.093	0.109	0.014
Tb	0.001	0.001	0.025	0.051	n.d.	0.040	0.062	0.001
Dy	0.006	0.006	0.003	0.003	0.002	0.003	0.003	0.002
Y	0.220	0.243	0.048	0.042	0.174	0.001	0.001	1.006
Ho	0.002	0.003	0.276	0.274	0.002	0.278	0.270	0.001
Er	0.009	0.008	0.006	0.006	0.006	0.006	0.006	0.003
Tm	0.001	0.002	0.020	0.019	0.001	0.026	0.021	n.d.
Yb	0.007	0.007	0.003	0.002	0.006	0.001	0.001	0.008
Lu	0.001	0.001	0.006	0.012	0.001	0.024	0.031	0.001
Cs	0.09	0.05			0.06			0.15
Rb	1.11	0.93			0.97			2.56
Ba	60.0	61.0	55.8	64.7	45.8	284.4	514.6	412.7
Th	0.01	0.00	0.19	0.15	0.00	0.23	0.30	0.00
U	0.43	0.46	0.54	0.05	0.05	1.10	1.00	0.01
W	0.75	0.87	0.46	0.46	0.90	0.46	0.46	0.54
Sr	74.5	73.8	62.3	67.3	61.4	274.0	484.3	514.8
Pb	0.07	0.09	0.96	0.51	0.12	0.51	0.28	0.25
As	0.14	0.09			0.29			0.63
Sb	n.d.	0.01			0.01			0.07
Mo	0.51	0.49	0.37	0.28	0.67	2.94	3.06	3.60
Cd	n.d.	n.d.	0.47	0.55	n.d.	0.44	0.41	0.06
Sn			0.17	0.17		0.17	0.17	
Sc	1.07	1.82	0.001	0.001	1.49	0.001	0.001	1.93
Ga			0.45	0.44		0.29	0.48	
Cu	0.44	0.37	1.62	2.65	1.07	0.66	0.50	0.33
Zn	4.83	3.56	6.85	25.17	4.64	22.72	57.92	22.75
Ag	0.02	0.02	0.20	0.20	0.01	0.20	0.20	0.06
Au	0.001	0.001			n.d.			0.003
Se	0.18	0.22			0.18			2.78
Pd	0.03	0.04			0.04			0.28

Appendix B - 1996 Data continued

Sample	MR118				MR127			
	ICP-AES		ICP-MS		ICP-AES		ICP-MS	
	filtered	unfiltered	filtered	filtered-Dup	filtered	unfiltered	filtered	filtered-Dup
Si								
Al	6.4	27.4	3.4	7.9	6.0	3.8	3.0	5.8
Fe	152	407			356	375		
Ca	1812	1829			966	895		
Mg	595	601			329	316		
K	1837	1795			1149	1089		
Na(ppm)	619	609			422	413		
Ti	0.025	0.026	1.00	1.10	0.025	0.025	0.600	0.700
V	0.011	0.011	0.079	0.078	0.011	0.011	0.027	0.026
Cr	0.734	0.671	0.510	0.240	0.418	0.367	0.200	0.300
Mn	10.38	11.67			8.37	6.25		
Co	0.036	0.036	0.025	0.026	0.036	0.036	0.032	0.033
Ni	1.26	1.31	0.09	0.08	1.47	1.17	0.05	0.06
Li	88.1	86.6	79.4	68.1	55.3	53.5	39.1	39.2
Be	0.018	0.018			0.014	0.011		
B			2045	1887			1217	1434
Zr	0.41	0.36			0.19	0.16		
Nb	0.09	0.09	0.003	0.01	0.09	0.09	0.002	0.002
Ta	0.01	0.02	0.001	0.002	0.11	0.26	0.001	n.d.
Hf	0.07	0.07	0.01	0.01	0.07	0.07	0.002	0.003
P	141.9	143.8	428.2	398.8	149.5	164.3	432.5	421.6
La	0.010	0.010	0.047	0.042	0.010	0.001	0.022	0.022
Ce	0.092	0.146	0.016	0.007	0.222	0.075	0.005	0.006
Pr	0.045	0.045	0.002	0.002	0.045	0.045	0.001	0.001
Nd	0.021	0.021	0.016	0.015	0.021	0.021	0.010	0.008
Sm	0.351	0.321	0.006	0.005	0.258	0.198	0.001	0.004
Eu	0.007	0.007	0.001	0.001	0.007	0.007	0.001	0.001
Gd	0.071	0.118	0.007	0.007	0.094	0.085	0.004	0.005
Tb	0.026	0.033	0.001	0.001	0.037	0.037	n.d.	n.d.
Dy	0.003	0.003	0.002	0.001	0.003	0.003	0.002	0.001
Y	0.001	0.001	0.333	0.337	0.001	0.001	0.165	0.165
Ho	0.237	0.241	0.001	0.001	0.255	0.236	0.001	n.d.
Er	0.006	0.006	0.004	0.002	0.006	0.006	0.002	0.002
Tm	0.014	0.019	n.d.	0.001	0.012	0.015	n.d.	n.d.
Yb	0.001	0.001	0.005	0.005	0.001	0.001	0.002	0.002
Lu	0.003	0.014	0.001	0.001	0.001	0.006	0.001	0.001
Cs			0.10	0.07			0.05	0.05
Rb			2.15	2.03			1.07	1.09
Ba	149.9	154.9	131.2	131.8	72.5	76.5	60.2	60.3
Th	0.21	0.23	0.01	0.01	0.19	0.18	0.004	0.003
U	0.35	0.33	0.02	0.02	0.83	0.55	0.003	0.004
W	0.46	0.46	1.81	1.80	0.46	0.46	1.98	1.90
Sr	143.4	142.0	157.6	156.8	68.8	68.8	67.9	69.1
Pb	0.33	0.35	0.08	0.09	0.42	0.77	0.05	0.10
As			0.41	0.37			0.27	0.25
Sb			0.05	0.05			0.03	0.02
Mo	2.03	1.68	2.37	2.42	0.99	0.63	1.20	1.22
Cd	0.45	0.48	0.04	0.03	0.48	0.37	n.d.	0.01
Sn	0.17	0.17			0.17	0.17		
Sc	0.001	0.001	1.81	1.94	0.001	0.001	1.71	1.59
Ga	0.26	0.24			0.21	0.30		
Cu	0.15	1.16	0.11	0.08	0.10	0.06	0.10	0.19
Zn	1.20	2.33	0.02	0.13	2.06	1.65	0.36	0.69
Ag	0.20	0.20	0.06	0.06	0.20	0.20	0.04	0.04
Au			0.001	0.001			0.001	n.d.
Se			0.99	1.05			0.24	0.41
Pd			0.10	0.15			0.05	0.03

Appendix B - 1996 Data continued

Sample	MR119				Standards and Blanks				
	ICP-AES		ICP-MS	ICP-AES	ICP-MS				
	filtered	unfiltered	filtered	SLRS3	SLRS3	SLRS3	SLRS3	SLRS2	
Si									
Al	8.8	15.9	5.0	35.4	32.0	31.1	31.0	86.2	
Fe	119	227		121					
Ca	1144	1391		7986					
Mg	347	435		2118					
K	1089	1331		908					
Na(ppm)	435	543		5					
Ti	0.025	0.025	1.10	0.025	1.50	1.70		2.30	
V	0.011	0.011	0.042	0.011	0.270	0.281	0.300	0.220	
Cr	0.345	0.503	0.130	1.424	0.260	0.240	0.300	0.440	
Mn	2.33	2.33		4.17					
Co	0.036	0.036	0.025	0.036	0.032	0.038	0.027	0.086	
Ni	1.28	1.53	0.18	0.62	0.70	0.84	0.83	0.97	
Li	49.2	61.5	39.0	3.5	0.6	0.5		0.6	
Be	0.013	0.021		0.007					
B			1371		n.d.	0.1		n.d.	
Zr	0.29	0.39		n.d.					
Nb	0.09	0.09	0.01	0.08	0.003	0.002		0.01	
Ta	0.26	0.26	n.d.	0.12	n.d.	0.001		n.d.	
Hf	0.07	0.07	0.003	0.07	0.00	0.002		0.003	
P	228.4	241.9	643.4	9.67	2.70	5.20		10.90	
La	0.010	0.006	0.033	0.304	0.250	0.258		0.418	
Ce	0.113	0.143	0.011	0.511	0.300	0.306		0.578	
Pr	0.045	0.045	0.002	0.374	0.064	0.063		0.107	
Nd	0.021	0.021	0.007	0.149	0.276	0.280		0.459	
Sm	0.163	0.192	0.006	0.008	0.054	0.062		0.111	
Eu	0.007	0.007	0.001	0.006	0.008	0.009		0.014	
Gd	0.048	0.062	0.005	0.044	0.047	0.051		0.073	
Tb	0.009	0.035	0.001	0.003	0.004	0.004		0.007	
Dy	0.003	0.003	0.002	0.012	0.016	0.016		0.021	
Y	0.001	0.002	0.229	0.119	0.153	0.175		0.201	
Ho	0.262	0.293	0.001	0.004	0.005	0.004		0.007	
Er	0.006	0.006	0.003	0.056	0.012	0.013		0.019	
Tm	0.010	0.018	n.d.	0.003	0.002	0.002		0.002	
Yb	0.001	0.000	0.005	0.009	0.012	0.012		0.017	
Lu	0.001	0.001	0.001	0.013	0.002	0.002		0.003	
Cs			0.06		0.01	0.01		0.01	
Rb			1.17		1.62	1.72		1.62	
Ba	94.3	121.4	84.1	18.4	12.2	12.3	13.4	12.5	
Th	0.20	0.12	0.004	0.08	0.02	0.02		0.02	
U	0.53	0.26	0.02	0.64	0.04	0.04	0.05	0.05	
W	0.46	0.46	1.63	0.46	n.d.	0.01		n.d.	
Sr	88.5	108.8	96.0	42.2	31.5	33.3	28.1	29.8	
Pb	0.25	0.45	0.04	0.56	0.04	0.05	0.07	0.12	
As			0.14		0.73	0.75	0.72	0.77	
Sb			0.01		0.15	0.15	0.12	0.32	
Mo	7.96	8.89	8.98	0.68	0.32	0.23	0.19	0.18	
Cd	0.38	0.48	0.03	0.02	0.03	0.03	0.01	0.04	
Sn	0.17	0.17		0.17					
Sc	0.001	0.001	1.58	0.001	0.52	0.66		0.68	
Ga	0.10	0.29		0.43					
Cu	0.55	0.68	0.33	1.67	1.23	1.43	1.35	2.77	
Zn	2.90	1.61	0.40	2.10	0.94	0.91	1.04	3.36	
Ag	0.20	0.20	0.01	0.20	0.00	n.d.		n.d.	
Au			0.001		n.d.	n.d.		n.d.	
Se			0.34		0.12	0.08		0.12	
Pd			0.05		0.01	0.01		0.01	

Appendix B - 1996 Data continued

Sample	Standards and Blanks				
	ICP-MS				
	SLRS2	Tripbk	Tripbk	Fieldbk	Fieldbk
Si					
Al	84.4	0.2	0.6	0.6	1.5
Fe					
Ca					
Mg					
K					
Na(ppm)					
Ti		0.100	n.d.	n.d.	0.100
V	0.250	0.003	0.002	0.003	0.002
Cr	0.450	n.d.	n.d.	0.030	n.d.
Mn					
Co	0.060	0.001	0.003	0.003	0.002
Ni	1.03	0.07	0.06	0.02	0.06
Li		n.d.	n.d.	n.d.	n.d.
Be					
B		9	10	0	16
Zr					
Nb		n.d.	n.d.	n.d.	n.d.
Ta		n.d.	n.d.	n.d.	n.d.
Hf		n.d.	n.d.	n.d.	n.d.
P		1.60	2.90	1.00	1.80
La		n.d.	n.d.	n.d.	n.d.
Ce		n.d.	n.d.	n.d.	n.d.
Pr		n.d.	n.d.	n.d.	n.d.
Nd		n.d.	n.d.	n.d.	n.d.
Sm		n.d.	n.d.	n.d.	n.d.
Eu		n.d.	n.d.	n.d.	n.d.
Gd		n.d.	n.d.	n.d.	n.d.
Tb		n.d.	n.d.	n.d.	n.d.
Dy		n.d.	n.d.	n.d.	n.d.
Y		n.d.	n.d.	n.d.	n.d.
Ho		n.d.	n.d.	n.d.	n.d.
Er		n.d.	n.d.	n.d.	n.d.
Tm		n.d.	n.d.	n.d.	n.d.
Yb		n.d.	n.d.	n.d.	n.d.
Lu		n.d.	n.d.	n.d.	n.d.
Cs		n.d.	n.d.	n.d.	n.d.
Rb		n.d.	0.01	n.d.	0.01
Ba	13.8	0.01	0.01	0.02	0.01
Th		n.d.	n.d.	n.d.	n.d.
U	0.05	n.d.	n.d.	0.00	n.d.
W		0.01	n.d.	n.d.	0.01
Sr	27.3	0.01	n.d.	0.01	0.02
Pb	0.13	n.d.	n.d.	n.d.	0.01
As	0.77	n.d.	n.d.	n.d.	n.d.
Sb	0.26	n.d.	n.d.	n.d.	n.d.
Mo	0.16	n.d.	n.d.	n.d.	n.d.
Cd	0.03	n.d.	n.d.	n.d.	n.d.
Sn					
Sc		n.d.	n.d.	n.d.	n.d.
Ga					
Cu	2.76	0.10	0.13	0.04	0.06
Zn	3.33	0.06	0.07	0.11	0.13
Ag		n.d.	n.d.	n.d.	n.d.
Au		n.d.	n.d.	n.d.	n.d.
Se		n.d.	n.d.	n.d.	n.d.
Pd		n.d.	n.d.	n.d.	n.d.

Appendix B - 1995 ICP-MS Data

Sample	MR52	MR80	MR43	MR116	MR115	MR114	MR118
Si	3348	4625	4804	3988	5037	4277	4845
Al	6.0	8.0	14.0	9.0	5.0	10.0	15.0
Fe	64	20	22	33	100	72	19
Ca	1322	1457	1141	1287	1041	1448	1709
Mg	447	577	405	481	353	636	711
Ti	4.10	5.10	1.80	2.90	0.20	0.50	1.30
V	n.d.	0.20	0.20	0.20	0.10	0.80	0.70
Cr	1.00	1.00	1.10	1.10	1.20	3.10	2.70
Mn	1.40	1.20	0.20	1.40	4.70	5.10	2.90
Co	0.03	0.01	0.00	0.02	0.04	0.06	0.04
Ni	n.d.	n.d.	n.d.	n.d.	n.d.	1.00	n.d.
Li	37.0	56.0	45.0	42.0	44.0	55.0	78.0
Be	0.30	n.d.	n.d.	0.50	n.d.	0.20	n.d.
B							
Zr	0.11	0.08	0.07	0.05	0.08	1.01	0.75
Nb	n.d.						
Ta	n.d.						
Hf							
P							
La	n.d.	n.d.	0.04	0.02	0.01	0.03	0.08
Ce	n.d.	n.d.	0.01	n.d.	n.d.	0.01	n.d.
Pr							
Nd							
Sm							
Eu							
Gd							
Tb							
Dy							
Y	0.030	0.050	0.100	0.020	0.050	0.020	0.030
Ho							
Er							
Tm							
Yb	0.020	n.d.	0.010	0.010	n.d.	0.020	0.030
Lu							
Cs							
Rb	1.00	1.10	0.90	1.00	1.00	1.30	2.00
Ba	12.00	14.00	79.00	52.00	61.00	89.00	131.00
Th	n.d.	n.d.	0.01	n.d.	n.d.	0.01	0.02
U	0.57	1.08	0.54	0.61	0.03	0.03	0.04
W	2.30	1.60	0.30	0.40	0.30	0.40	0.80
Sr	101.0	85.0	76.0	83.0	57.0	108.0	133.0
Pb	0.20	0.10	0.10	n.d.	0.10	1.00	1.40
As	0.20	0.40	0.20	0.60	0.30	1.20	1.00
Sb	n.d.	n.d.	n.d.	0.02	0.01	0.03	0.06
Mo	0.60	0.70	1.80	1.50	1.10	2.30	2.50
Cd	n.d.	n.d.	0.06	n.d.	n.d.	1.70	1.60
Sn	0.03	0.03	0.04	0.02	0.08	0.06	0.13
Sc	0.70	0.90	1.00	0.90	1.10	1.00	1.10
Ga	0.30	0.20	1.10	0.60	0.90	1.00	1.50
Cu	2.20	4.60	2.40	0.80	1.20	3.50	0.60
Zn	2.20	5.80	3.00	19.30	10.10	49.10	1.90
Ag	n.d.	n.d.	n.d.	n.d.	n.d.	0.07	n.d.
Au							
Se							
Pd							
Hg	n.d.	3.40	0.50	0.00	1.50	3.80	4.90
Tl	0.02	0.09	0.09	0.10	0.08	0.60	0.60

Appendix B - 1995 ICP-MS Data continued

Sample	MR12	MR119	MR121	MR14	MR25	MR25-dup	MR17
Si	4590	3704	4425	5081	4404	4296	4099
Al	10.0	6.0	6.0	22.0	6.0	5.0	5.0
Fe	92	384	59	16	74	77	19
Ca	1039	1252	1051	1771	2119	1940	1291
Mg	409	438	428	481	933	943	551
Ti	0.80	0.70	0.90	1.10	3.20	3.20	0.10
V	0.10	0.30	0.20	0.40	0.80	1.10	0.20
Cr	1.30	2.10	1.60	0.80	2.90	4.00	1.40
Mn	2.70	4.50	1.60	15.10	1.10	1.20	0.80
Co	0.03	0.05	n.d.	0.09	0.02	0.05	0.03
Ni	n.d.	n.d.	n.d.	n.d.	n.d.	n.d.	n.d.
Li	47.0	37.0	48.0	57.0	82.0	82.0	59.0
Be	0.60	n.d.	0.90	n.d.	n.d.	0.10	1.40
B							
Zr	0.20	0.19	0.20	0.23	0.41	0.39	0.43
Nb	n.d.	n.d.	n.d.	0.01	0.01	0.02	0.01
Ta	n.d.	n.d.	n.d.	n.d.	n.d.	n.d.	n.d.
Hf							
P							
La	0.05	0.04	0.02	0.03	0.07	0.09	0.04
Ce	0.05	n.d.	n.d.	0.01	0.02	0.04	n.d.
Pr							
Nd							
Sm							
Eu							
Gd							
Tb							
Dy							
Y	0.060	0.020	0.030	0.030	0.040	0.040	0.020
Ho							
Er							
Tm							
Yb	n.d.	0.020	0.020	n.d.	0.020	0.010	n.d.
Lu							
Cs							
Rb	1.20	1.20	1.00	1.20	2.00	1.90	1.40
Ba	89.00	107.00	87.00	85.00	284.00	280.00	142.00
Th	0.01	0.02	n.d.	n.d.	0.02	0.03	0.01
U	0.03	0.03	0.07	0.06	0.03	0.04	0.03
W	0.90	0.70	1.00	1.00	0.70	0.90	1.00
Sr	74.0	99.0	76.0	79.0	193.0	194.0	110.0
Pb	0.10	0.00	0.10	0.10	0.50	0.50	0.00
As	0.20	0.30	0.20	0.40	1.50	1.60	0.50
Sb	0.01	0.02	n.d.	0.06	0.01	0.02	0.03
Mo	0.90	10.30	1.00	0.90	0.80	1.20	0.90
Cd	0.05	0.06	0.10	0.14	2.17	3.19	0.45
Sn	0.04	0.05	0.05	0.00	0.19	0.12	n.d.
Sc	1.00	0.80	1.00	1.10	0.90	1.10	1.00
Ga	1.20	1.20	1.20	1.10	3.00	3.20	1.60
Cu	2.20	0.30	0.40	0.50	19.20	19.30	6.10
Zn	38.50	4.20	8.70	1.90	4.80	5.20	1.70
Ag	0.01	n.d.	n.d.	n.d.	n.d.	n.d.	0.01
Au							
Se							
Pd							
Hg	0.30	1.00	1.10	1.40	47.40	1.30	0.20
Tl	0.10	0.20	0.20	0.20	0.80	0.90	0.30
Bi	n.d.	n.d.	n.d.	n.d.	0.03	0.01	0.01

Appendix B - 1995 ICP-MS Data continued

Sample	MR23	MR113	SLRS2	SLRS2
Si	4574	4465	2066	2124
Al	7.0	15.0	81.5	85.7
Fe	21	1341	135	131
Ca	1238	2373	5061	5280
Mg	665	1285	1460	1449
Ti	0.60	1.40	2.10	2.90
V	0.40	1.20	0.20	0.20
Cr	2.50	4.70	0.80	0.90
Mn	0.20	7.50	10.60	10.60
Co	0.02	0.02	0.05	0.07
Ni	n.d.	n.d.	1.00	1.00
Li	72.0	115.0	1.0	1.0
Be	0.40	0.80	n.d.	n.d.
B				
Zr	0.49	1.11	0.07	0.06
Nb	n.d.	0.03	0.01	0.01
Ta	n.d.	n.d.	n.d.	n.d.
Hf				
P				
La	0.05	0.09	0.41	0.39
Ce	n.d.	0.01	0.51	0.49
Pr				
Nd				
Sm				
Eu				
Gd				
Tb				
Dy				
Y	0.030	0.030	0.180	0.190
Ho				
Er				
Tm				
Yb	n.d.	0.020	0.010	0.020
Lu				
Cs				
Rb	1.60	2.00	1.60	1.60
Ba	180.00	388.00	14.00	14.00
Th	0.01	0.05	0.01	0.01
U	0.02	0.01	0.05	0.05
W	0.60	0.30	0.00	n.d.
Sr	116.0	243.0	29.0	29.0
Pb	0.10	0.30	0.10	0.20
As	0.40	1.60	0.80	0.90
Sb	0.01	n.d.	0.25	0.29
Mo	3.60	1.40	0.20	0.20
Cd	0.50	3.72	n.d.	n.d.
Sn	0.06	0.11	0.04	0.02
Sc	1.10	1.10	0.50	0.40
Ga	2.20	4.50	0.20	0.20
Cu	1.20	0.60	3.30	2.90
Zn	2.40	2.50	3.70	4.60
Ag	n.d.	n.d.	n.d.	n.d.
Au				
Se				
Pd				
Hg	0.70	2.60	n.d.	n.d.
Tl	0.30	1.10	0.02	0.03
Bi	n.d.	0.02	n.d.	n.d.

Appendix C

Major Cation and Anion Analyses

Routine chemistry on the samples was performed at the National Hydrology Research Institute in Saskatoon, Saskatchewan, for anions (Cl and SO₄) and cations (Ca, Mg, Fe, Na) using Ion Liquid Chromatography and atomic absorption respectively. All data are reported in ppm (µg/ml).

Appendix C

Sample 1996	Anal. No.	Ca	Mg	Fe	Na	Cl	SO ₄
MR122	E702	0.96	0.29	0.05	310	1.92	152
MR123	783	1.08	0.36	0.02	381	5.92	171
MR123dup	784	1.08	0.36	0.02	362	5.91	171
MR52	785	1.38	0.42	0.04	437	10	297
MR80	786	1.23	0.43	0.02	425	14.9	277
MR125	788	0.93	0.29	0.07	362	26.3	67.2
MR126(Taylor)	787	0.81	0.27	0.02	358	23.2	64.9
MR126	789	0.87	0.27	0.04	366	22.2	67
MR124	790	0.9	0.31	0.02	354	44.5	<.3
MR128	791	3.9	1.4	<.02	784	701	<.5
MR118	792	1.65	0.56	0.13	592	236	<.5
MR127	793	0.84	0.29	0.29	388	57.9	<.5
MR119	794	1.1	0.35	0.11	437	72.6	<.5

Sample 1997	Anal. No.	Cl	SO ₄
MR130	E465	18.2	241
MR129	466	20.1	221
MR137	467	42.8	14.6
MR140	468	6.44	196
MR136	469	20.1	217
MR132	470	441	<.8
MR139	471	13.8	115
MR122	474	1.6	137
Milk River	472	1.1	22.8

Appendix D

Water Standards and Quality of Analysis

The water standards SLRS2 and SLRS3 were analyzed with unknowns for both ICP-MS and ICP-AES (Figure AP-1). Most the elements run in the standards are well within accepted values. ICP-AES displays good precision for the majors and the more abundant trace elements (i.e. Al, V, Ni, Cu, Sr, Cd, and Ba). Accordingly for the purpose of this study AES data was used for major elements and a select group of trace elements. Similarly, compliance for SLRS2 and SLRS3 for the ICP-MS is also excellent. The anomalously high values for Cd and Mo are most likely due to the very low concentrations of both elements which makes accurate and precise determinations difficult. Another possible explanation is that the recommended value is not correct for this standard. Note that many elements are not reported for SLRS-2 and 3.

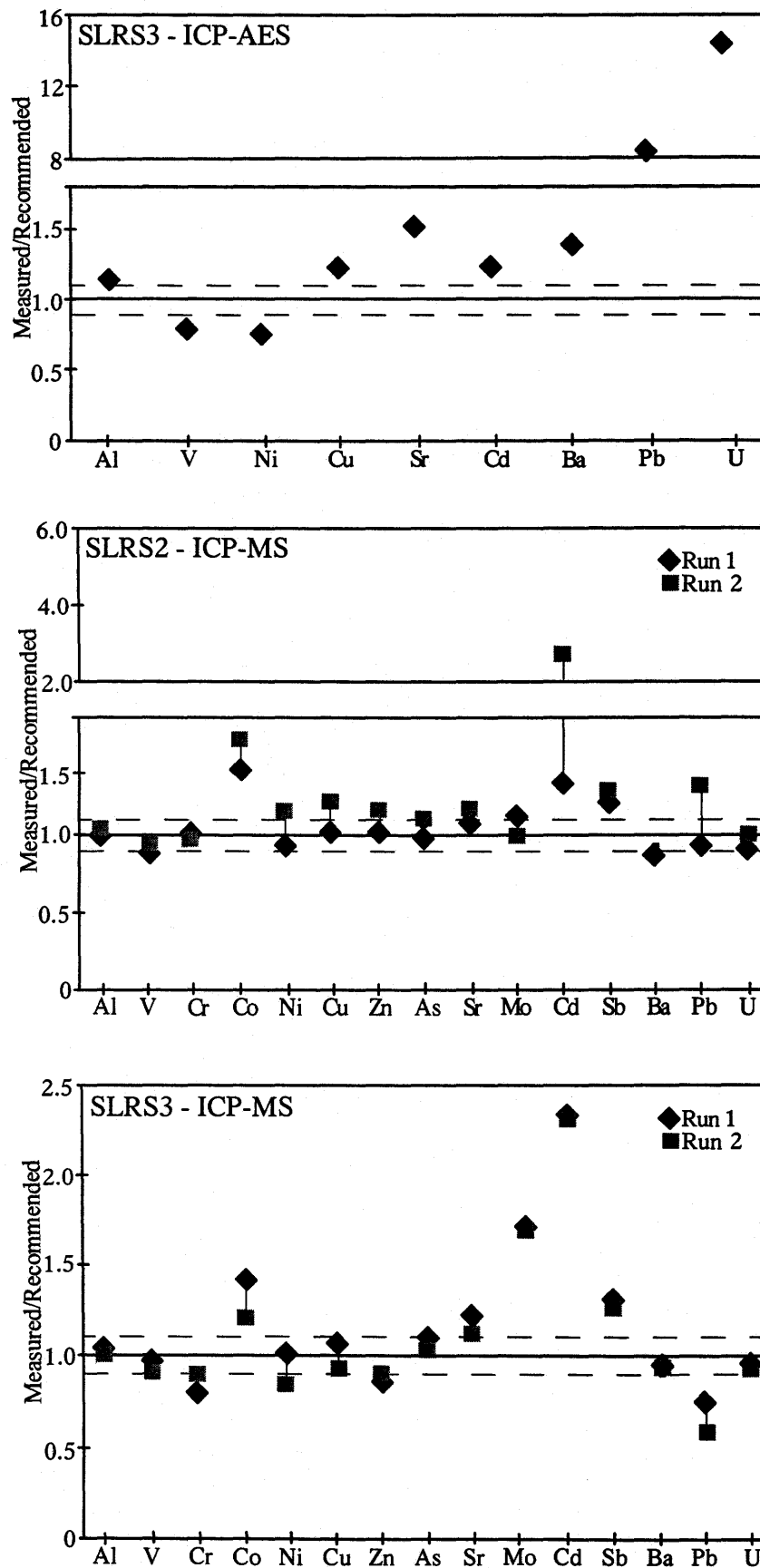


Figure AP-1. Standards SLRS2 and SLRS3 measured versus recommended values for ICP-AES and ICP-MS.

Appendix E

Detection of Selected Elements for ICP-AES and ICP-MS

To evaluate the optimum values for specific elements a series of test were conducted as part of this study. Detection limits of selected elements are presented in the following table for ICP-MS and ICP-AES. Detection limits are defined as 3σ of procedural blanks. Figure AP-2 shows ICP-AES vs. ICP-MS data for several different elements. Figures AP-2A and AP-2F shows that ICP-AES is better suited for light elements (Mg, Na) or elements with isobaric interferences (i.e. ^{40}Ca , ^{40}K , and ^{56}Fe). Figures AP-2B, 2C, and 2E display a good correlation between the two methods for the more abundant and heavier elements Sr, Ba, and Mo. Figure AP-2D shows that ICP-MS is better for analyzing U, given a detection limit problem with ICP-AES.

Similarly figure AP-3, shows variations between ICP-AES and ICP-MS. Figure AP-3A and AP-3B indicates a detection limit problem by AES for Co below 0.04 ppb, and a scatter for Cr. Artificially low detection limits for AES, were cited by SRC, all samples were below 0.05 ppb as determined by MS, for several trace elements including REEs (Fig. AP-3A and D). Thorium appeared to be a problem for both methods, due to low concentrations (Fig. AP-3C). Therefore ICP-AES was used for the lighter elements or major elements and ICP-MS was used for the REEs.

Detection limits for ICP-AES and ICP-MS employing the ultrasonic nebulizer are present for comparison.

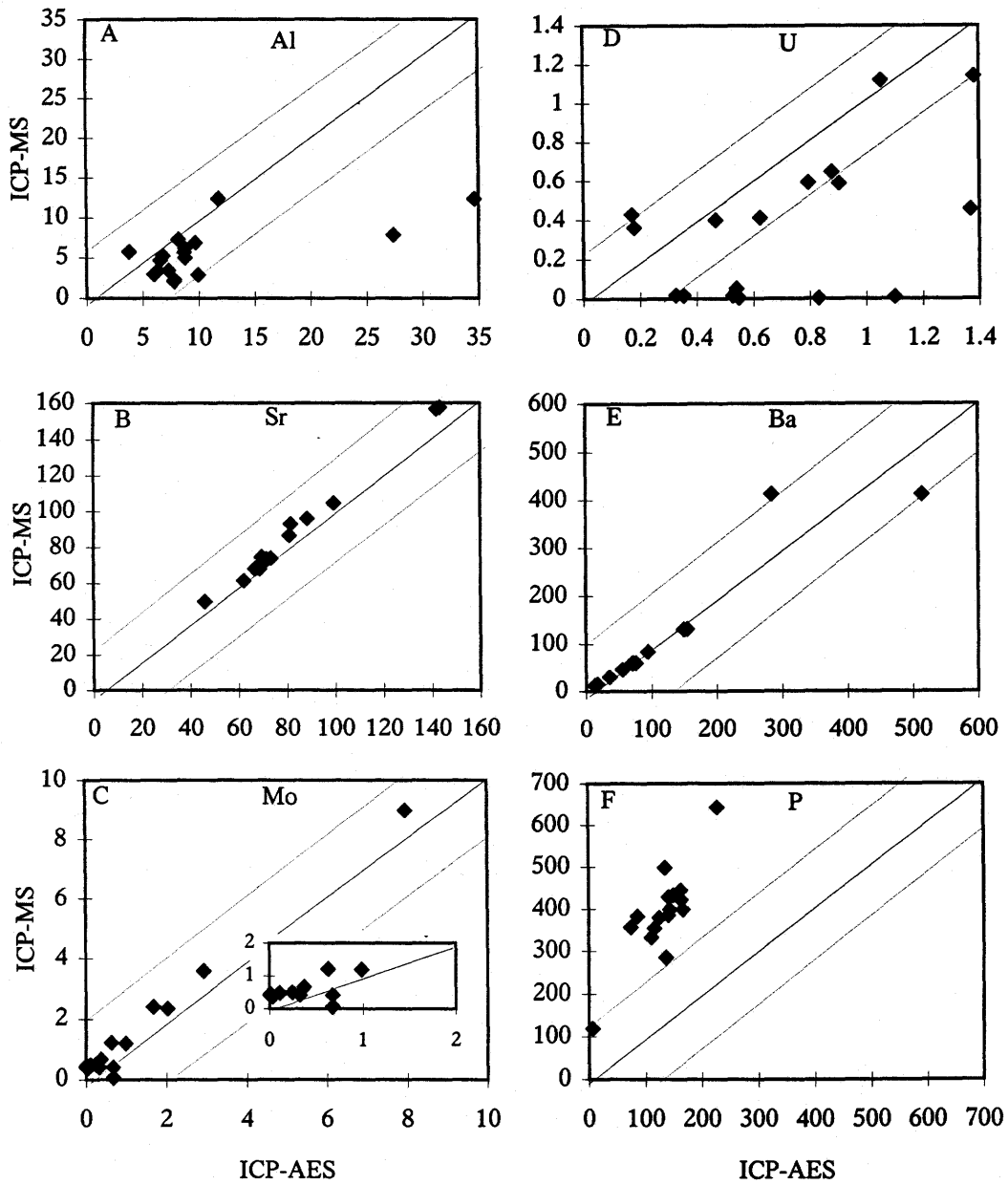


Figure AP-2. Analyses of select elements by ICP-AES and ICP-MS (units in ppb).

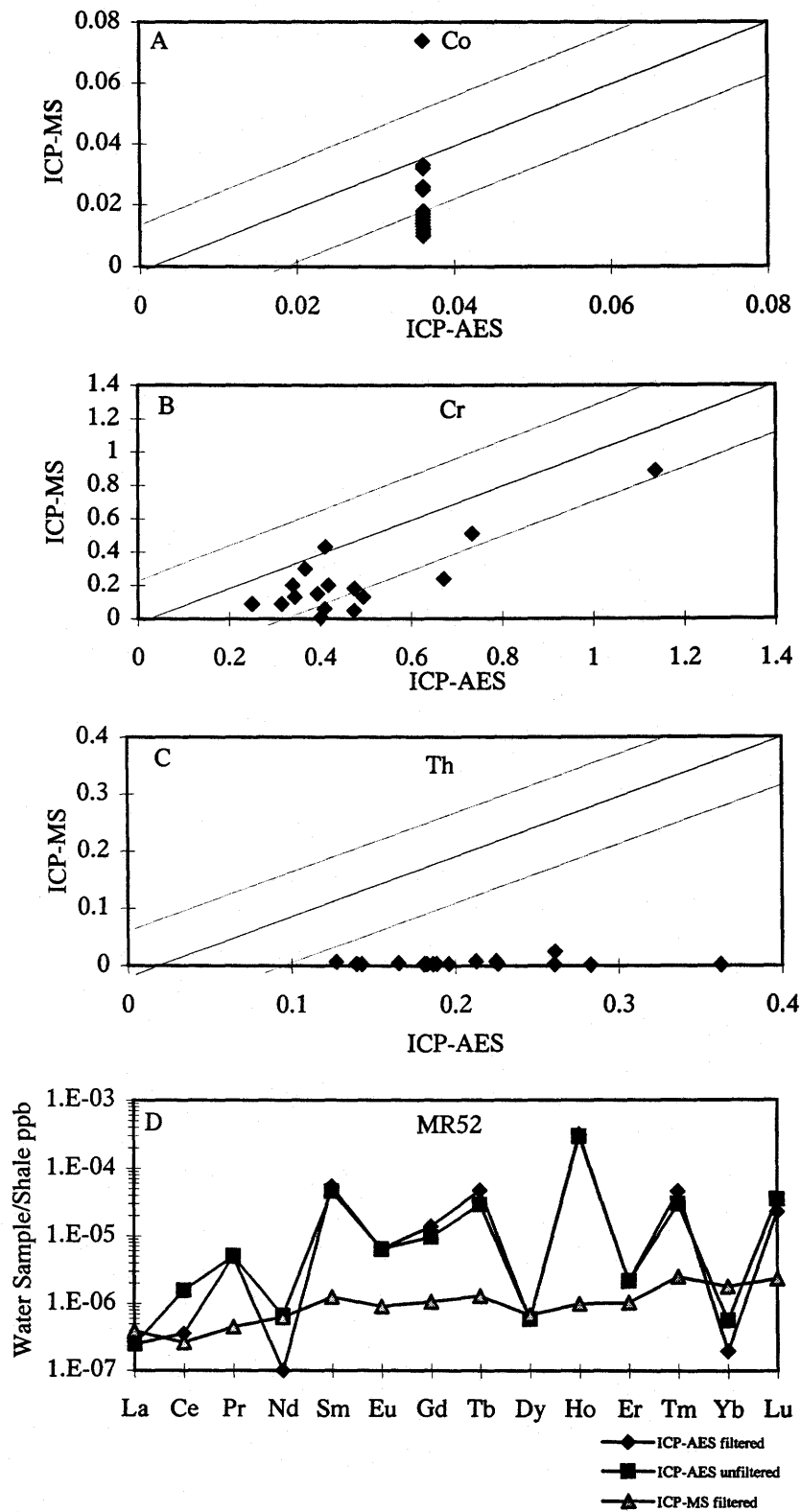


Figure AP-3. ICP-AES versus ICP-MS analyse for select trace elements in A, B, and C (units in ppb). AP-3D is a REE plot normalized to post-Archean average Australian shale (PAAS).

Appendix E

Detection limits for ICP-MS employing the ultrasonic nebulizer and ICP-AES.

Element	ICP-MS (ppb)	ICP-AES (ppb)
Li	0.08	0.001
P	1.4	3.0
Ca	1021	0.2
Sc	0.006	0.002
Ti	0.09	0.05
V	0.003	0.02
Cr	0.05	0.04
Co	0.01	0.07
Ni	0.1	0.1
Cu	0.07	0.08
Zn	0.2	0.07
Sr	0.03	0.001
Y	0.001	0.003
Zr	0.01	0.1
Nb	0.001	0.2
Mo	0.01	1.4
Ag	0.003	0.4
Cd	0.05	0.09
Sn	0.02	0.3
Ba	0.02	0.001
La	0.001	0.02
Ce	0.001	0.1
Pr	0.001	0.09
Nd	0.002	0.04
Sm	0.001	0.02
Eu	0.001	0.01
Gd	0.0005	0.006
Tb	0.0003	0.002
Dy	0.0004	0.005
Ho	0.0003	0.003
Er	0.001	0.01
Tm	0.0007	0.007
Yb	0.002	0.002
Lu	0.001	0.002
Hf	0.001	0.1
Ta	0.0003	0.5
W	0.002	0.9
Pb	0.005	0.2
Th	0.0005	0.02
U	0.001	0.5

Appendix F

The Effects of Field Filtering on Select Elements

The following figures present the remaining major and trace elements that were discussed in Chapter 3.6, *Intercomparison Field Filtered and Unfiltered Samples*. Some of these elements did not display any appreciable effects due to filtering as shown by similar concentrations in filtered and unfiltered samples.

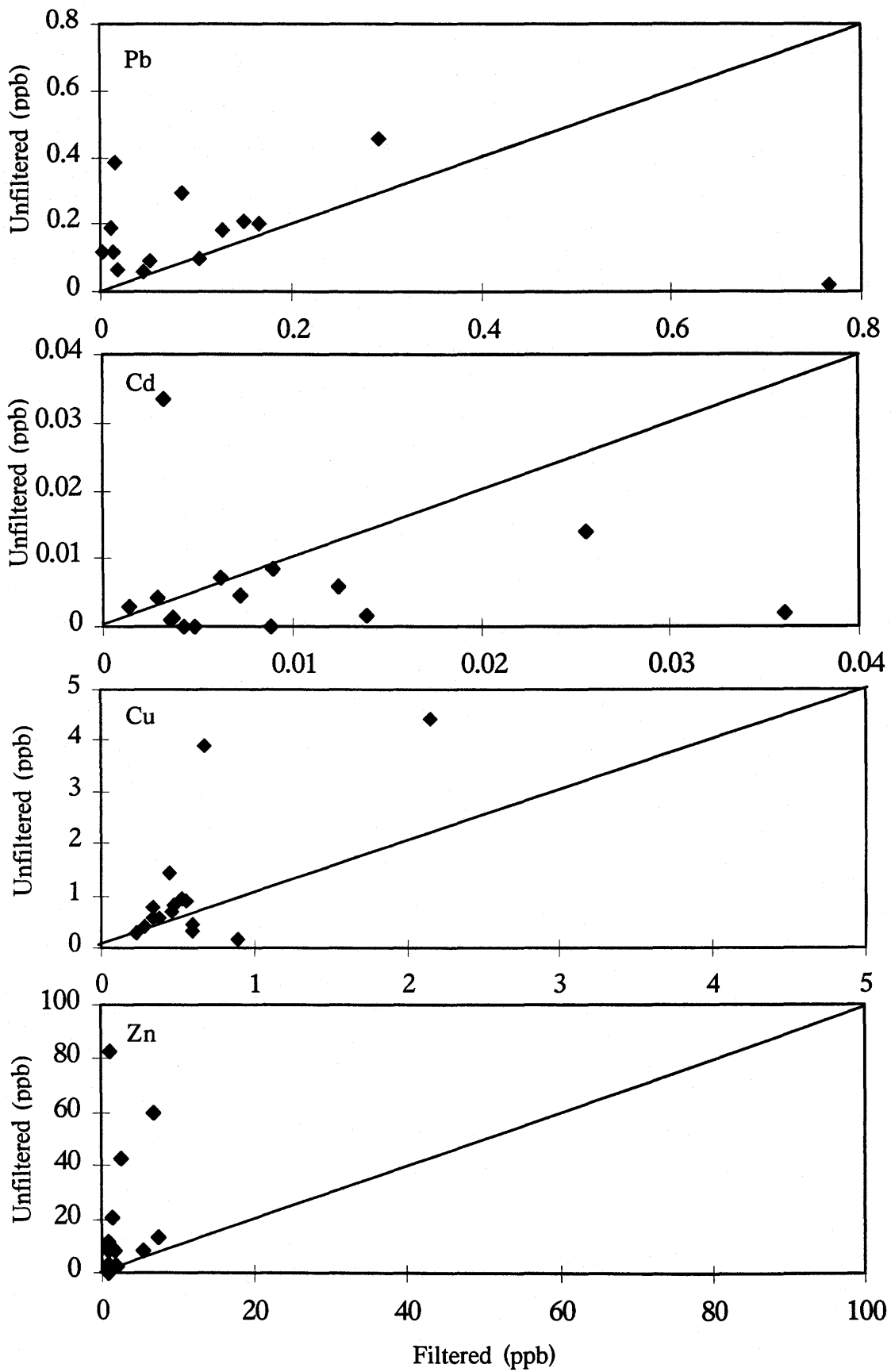


Figure AP-4. Analysis of select trace elements in filtered and unfiltered Milk River aquifer groundwater.

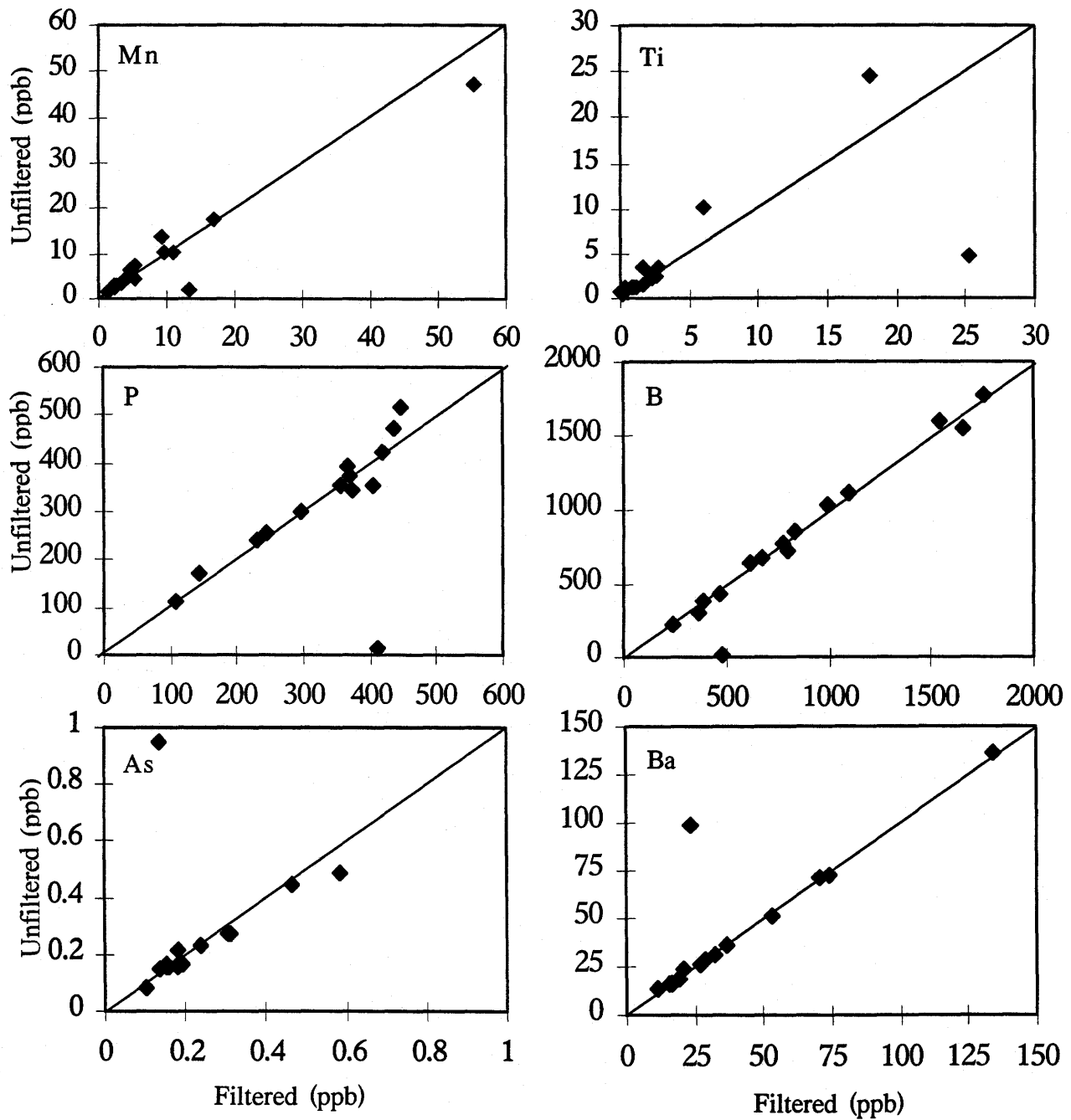


Figure AP-5. Analysis of select trace elements in filtered and unfiltered Milk River aquifer groundwater.

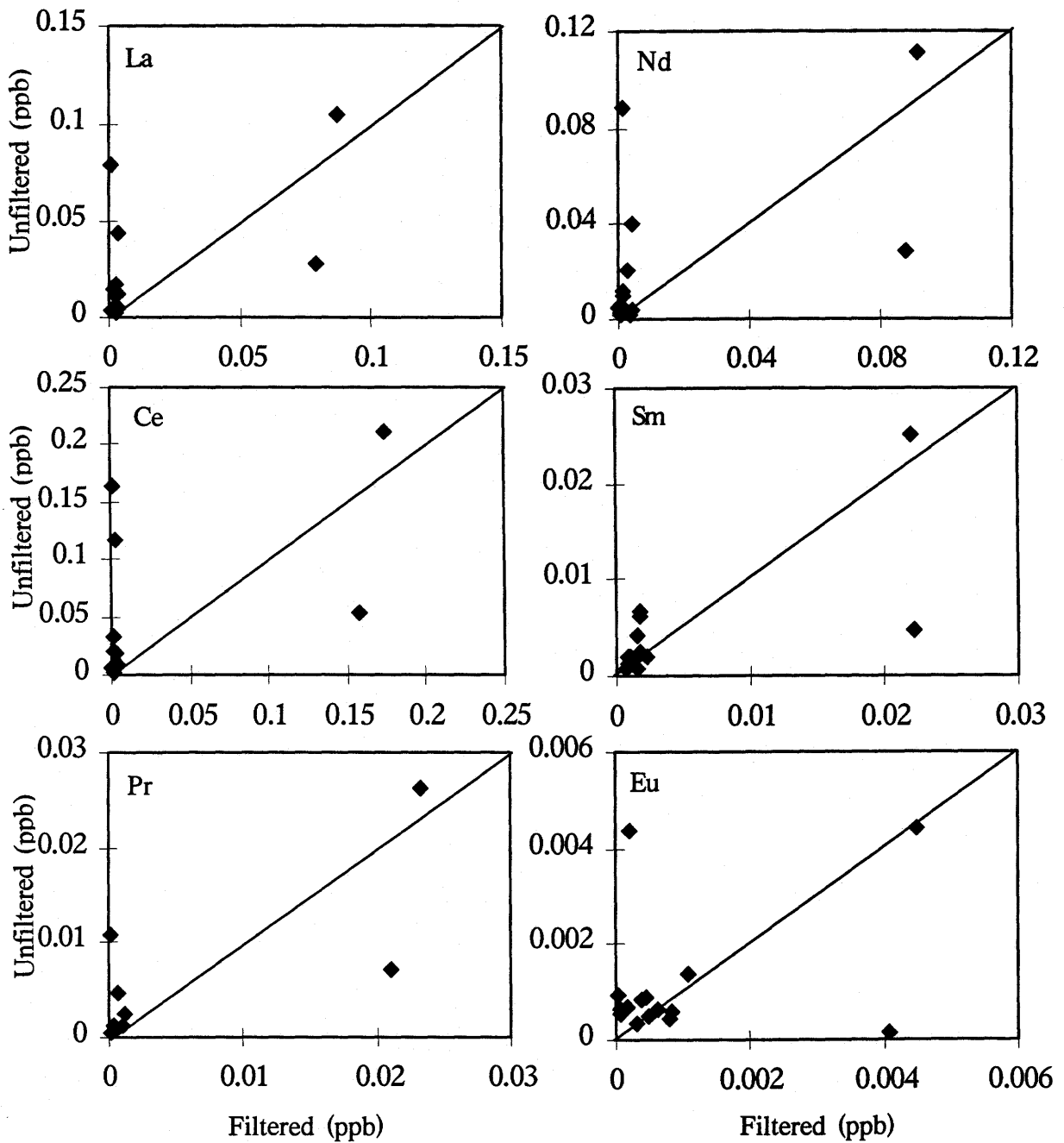


Figure AP-6. Analysis of select trace elements in filtered and unfiltered Milk River aquifer groundwater.

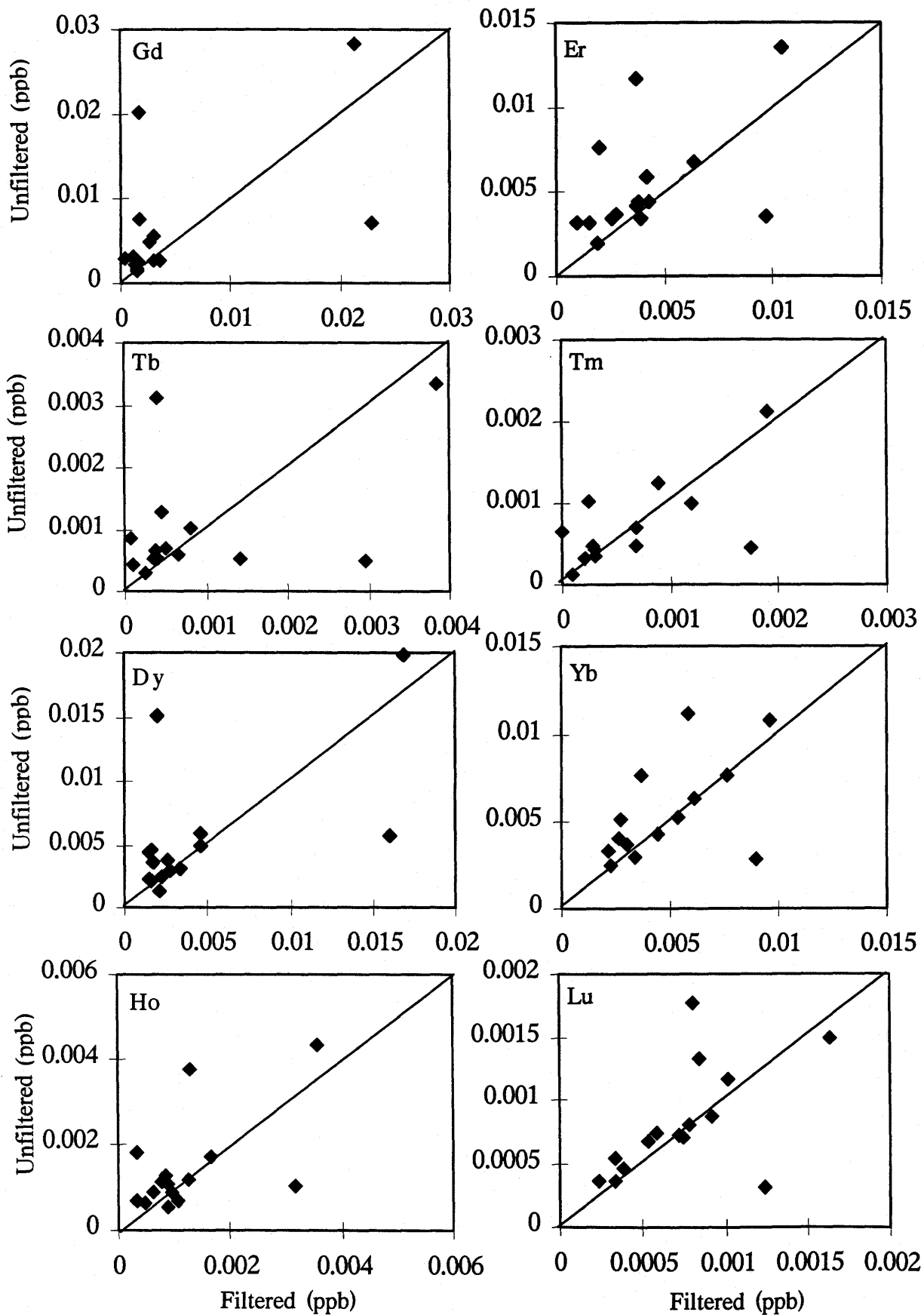


Figure AP-7. Analysis of select trace elements in filtered and unfiltered Milk River aquifer groundwater.

Appendix G

Concentrations of Select Trace Elements *versus* Distance From Recharge

Figures AP-8 and AP-9 present the remaining trace elements discussed in Chapter 4.4.1. *Trace Element Concentrations Along the Flow Path.* These elements did not display any appreciable trends along the studied flow path in the Milk River aquifer, and consequently were not included in the discussion.

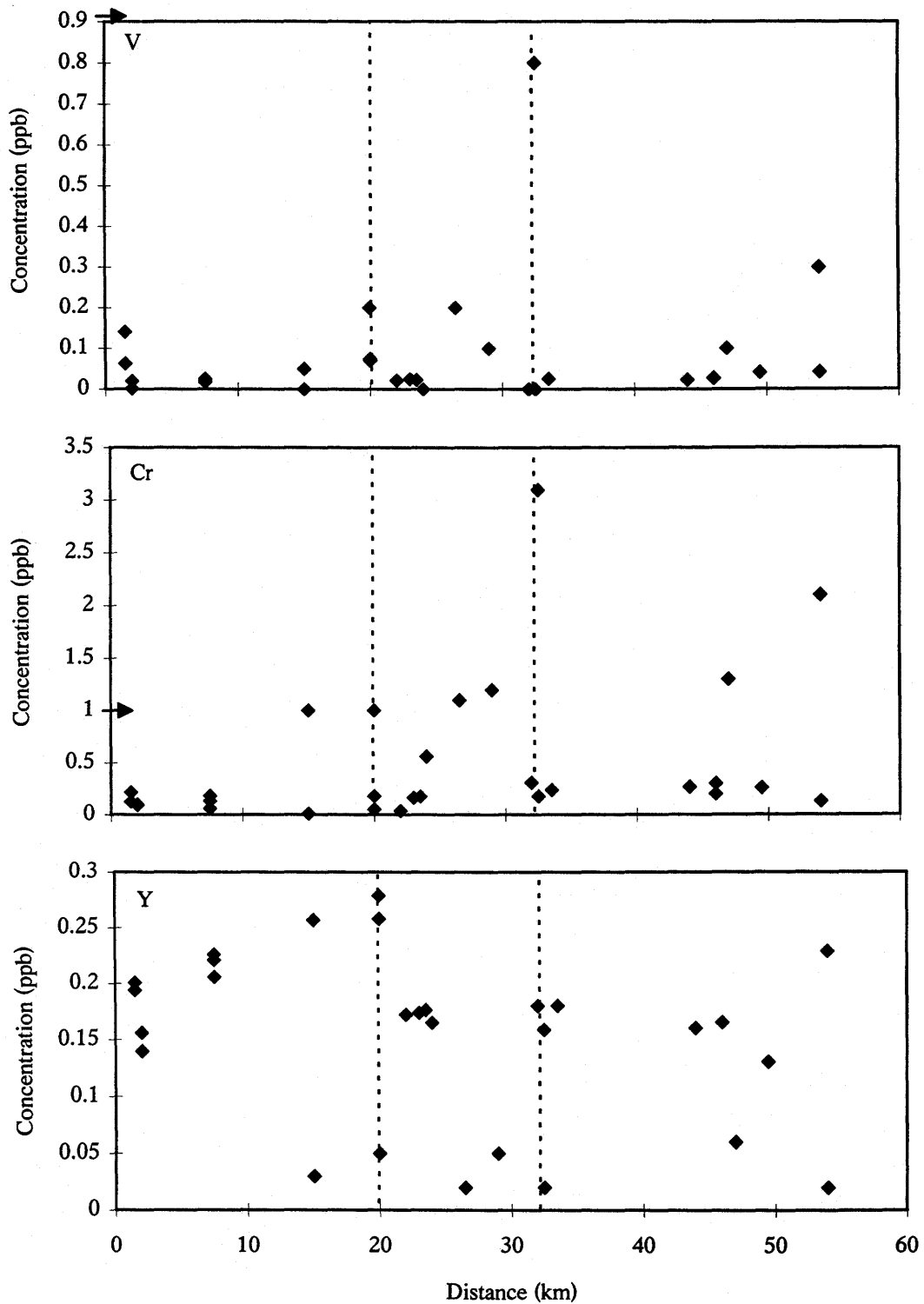


Figure AP-8. Concentrations of V, Cr, and Y in the Milk River aquifer groundwater versus distance from recharge. Dashed vertical lines represent redox front and post-redox front boundaries. Arrow on left margin is value of select element for average world river water from Taylor and McLennan (1985). Cumulative plot of 1996-1997 data.

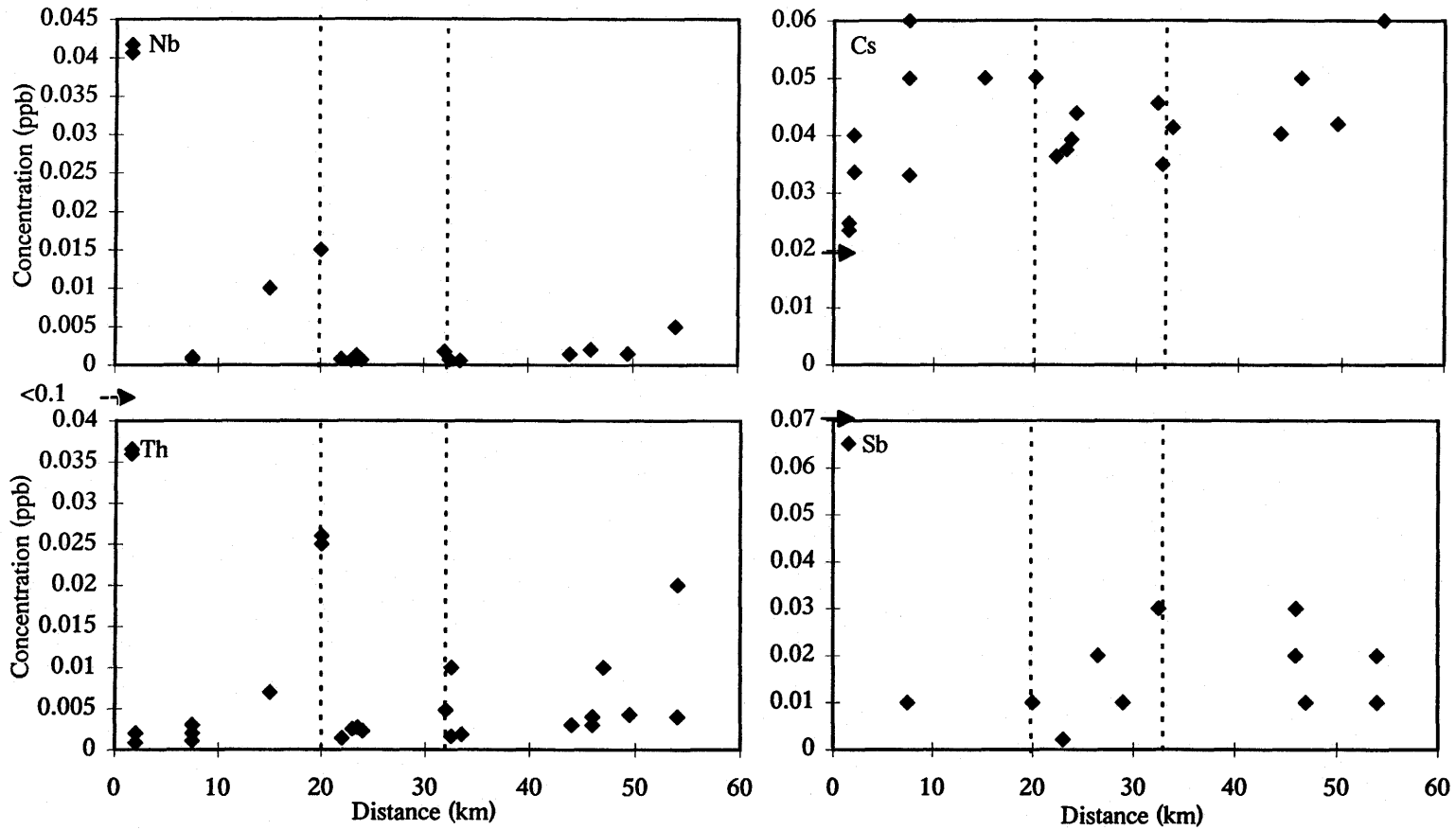


Figure AP-9. Concentrations of Nb, Th, Cs, and Sb in the Milk River aquifer groundwater versus distance from recharge. Dashed vertical lines represent redox front and post-redox front boundaries. Arrow on left margin is value of select element for average world river water from Taylor and McLennan (1985). Cumulative plot of 1996-1997 data.

Appendix H

PHREEQC Initial Solution Calculations

The following lists the initial solution conditions for select samples in the Milk River aquifer modeled in Chapter 4.

SOLUTION 1-1 MR139

-----Solution composition-----

Elements	Molality	Moles
Al	1.521e-07	1.521e-07
Alkalinity	4.740e-03	4.740e-03
As	3.206e-09	3.206e-09
B	3.355e-05	3.355e-05
Ba	1.974e-07	1.974e-07
Ca	2.647e-05	2.647e-05
Cd	1.247e-10	1.247e-10
Cl	3.896e-04	3.896e-04
Cs	1.883e-10	1.883e-10
Cu	9.293e-09	9.293e-09
Fe	1.792e-07	1.792e-07
K	2.073e-05	2.073e-05
Li	7.361e-06	7.361e-06
Mg	9.881e-06	9.881e-06
Mn	1.767e-07	1.767e-07
Na	1.265e-02	1.265e-02
Ni	1.040e-09	1.040e-09
P	9.542e-06	9.542e-06
Pb	1.401e-09	1.401e-09
Rb	8.432e-09	8.432e-09
S(6)	1.198e-03	1.198e-03
Se	5.070e-10	5.070e-10
Sr	5.782e-07	5.782e-07
U	5.551e-10	5.551e-10
Zn	1.363e-08	1.363e-08

-----Description of solution-----

pH = 9.110
pe = 6.330
Activity of water = 1.000
Ionic strength = 1.147e-02
Mass of water (kg) = 1.000e+00
Total carbon (mol/kg) = 4.462e-03
Total CO₂ (mol/kg) = 4.462e-03
Temperature (deg C) = 10.000
Electrical balance (eq) = 5.215e-03
Charge Balance Error = 9.1%
Iterations = 10
Total H = 1.110167e+02
Total O = 5.552453e+01

SOLUTION 1-1 MR122

-----Solution composition-----

Elements	Molality	Moles
Al	5.936e-08	5.936e-08
Alkalinity	5.421e-03	5.421e-03
As	2.138e-09	2.138e-09
B	2.234e-05	2.234e-05
Ba	1.195e-07	1.195e-07
Ca	2.373e-05	2.373e-05
Cd	5.343e-11	5.343e-11
Cl	5.421e-05	5.421e-05
Cs	2.561e-10	2.561e-10
Cu	7.246e-09	7.246e-09
Fe	1.792e-07	1.792e-07
K	1.946e-05	1.946e-05
Li	6.881e-06	6.881e-06
Mg	1.318e-05	1.318e-05
Mn	2.551e-08	2.551e-08
Na	1.326e-02	1.326e-02
Ni	1.705e-09	1.705e-09
P	3.497e-06	3.497e-06
Pb	2.416e-10	2.416e-10
Rb	9.135e-09	9.135e-09
S(6)	1.584e-03	1.584e-03
Se	3.550e-09	3.550e-09
Sr	5.701e-07	5.701e-07
U	1.892e-09	1.892e-09
Zn	2.909e-08	2.909e-08

-----Description of solution-----

pH = 9.130
pe = 6.330
Activity of water = 1.000
Ionic strength = 1.272e-02
Mass of water (kg) = 1.000e+00
Total carbon (mol/kg) = 5.103e-03
Total CO₂ (mol/kg) = 5.103e-03
Temperature (deg C) = 9.700
Electrical balance (eq) = 4.715e-03
Charge Balance Error = 4.5%
Iterations = 11
Total H = 1.110173e+02
Total O = 5.552794e+01

SOLUTION 1-1 MR123

-----Solution composition-----

Elements	Molality	Moles
Al	1.447e-07	1.447e-07
Alkalinity	5.861e-03	5.861e-03
As	1.336e-09	1.336e-09
B	4.298e-05	4.298e-05
Ba	2.333e-07	2.333e-07
Ca	2.698e-05	2.698e-05
Cd	3.563e-11	3.563e-11
Cl	1.672e-04	1.672e-04
Cs	2.486e-10	2.486e-10
Cu	6.932e-09	6.932e-09
Fe	1.793e-07	1.793e-07
K	2.458e-05	2.458e-05
Li	5.540e-06	5.540e-06
Mg	1.482e-05	1.482e-05
Mn	4.556e-08	4.556e-08
Na	1.670e-02	1.670e-02
P	1.146e-05	1.146e-05
Pb	9.664e-11	9.664e-11
Rb	1.007e-08	1.007e-08
S(6)	1.782e-03	1.782e-03
Se	5.072e-10	5.072e-10
Sr	8.548e-07	8.548e-07
U	1.926e-09	1.926e-09
Zn	2.420e-08	2.420e-08

-----Description of solution-----

pH = 9.140
pe = 6.330
Activity of water = 1.000
Ionic strength = 1.511e-02
Mass of water (kg) = 1.000e+00
Total carbon (mol/kg) = 5.484e-03
Total CO₂ (mol/kg) = 5.484e-03
Temperature (deg C) = 9.700
Electrical balance (eq) = 7.213e-03
Charge Balance Error = 11.3%
Iterations = 11
Total H = 1.110177e+02
Total O = 5.552997e+01

SOLUTION 1-1 MR52

-----Solution composition-----

Elements	Molality	Moles
Al	2.895e-07	2.895e-07
Alkalinity	6.223e-03	6.223e-03
As	1.069e-09	1.069e-09
B	4.016e-05	4.016e-05
Ba	8.954e-08	8.954e-08
Ca	3.533e-05	3.533e-05
Cl	2.824e-04	2.824e-04
Cs	3.767e-10	3.767e-10
Cu	1.245e-08	1.245e-08
Fe	7.531e-07	7.531e-07
K	2.766e-05	2.766e-05
Li	5.671e-06	5.671e-06
Mg	1.746e-05	1.746e-05
Mn	2.424e-08	2.424e-08
Na	1.893e-02	1.893e-02
Ni	6.822e-10	6.822e-10
P	1.155e-05	1.155e-05
Pb	1.933e-10	1.933e-10
Rb	1.101e-08	1.101e-08
S(6)	3.096e-03	3.096e-03
Se	3.805e-10	3.805e-10
Sr	1.196e-06	1.196e-06
U	2.482e-09	2.482e-09
Zn	4.289e-09	4.289e-09

-----Description of solution-----

pH = 9.100
pe = 6.330
Activity of water = 1.000
Ionic strength = 1.895e-02
Mass of water (kg) = 1.000e+00
Total carbon (mol/kg) = 5.848e-03
Total CO₂ (mol/kg) = 5.848e-03
Temperature (deg C) = 9.200
Electrical balance (eq) = 6.369e-03
Charge Balance Error = 6.5%
Iterations = 11
Total H = 1.110180e+02
Total O = 5.553631e+01

SOLUTION 1-1 MR80

-----Solution composition-----

Elements	Molality	Moles
Al	2.709e-07	2.709e-07
Alkalinity	6.022e-03	6.022e-03
As	9.355e-10	9.355e-10
B	4.443e-05	4.443e-05
Ba	9.055e-08	9.055e-08
Ca	3.019e-05	3.019e-05
Cd	8.908e-11	8.908e-11
Cl	4.208e-04	4.208e-04
Cs	3.767e-10	3.767e-10
Cu	1.402e-08	1.402e-08
Fe	5.988e-07	5.988e-07
K	2.635e-05	2.635e-05
Li	6.508e-06	6.508e-06
Mg	1.713e-05	1.713e-05
Mn	3.718e-08	3.718e-08
Na	1.808e-02	1.808e-02
Ni	1.194e-09	1.194e-09
P	1.238e-05	1.238e-05
Pb	5.316e-10	5.316e-10
Rb	1.078e-08	1.078e-08
S(6)	2.887e-03	2.887e-03
Se	2.156e-09	2.156e-09
Sr	9.889e-07	9.889e-07
U	4.796e-09	4.796e-09
Zn	1.731e-08	1.731e-08

-----Description of solution-----

pH = 9.100
pe = 6.330
Activity of water = 1.000
Ionic strength = 1.810e-02
Mass of water (kg) = 1.000e+00
Total carbon (mol/kg) = 5.640e-03
Total CO₂ (mol/kg) = 5.640e-03
Temperature (deg C) = 11.000
Electrical balance (eq) = 5.980e-03
Charge Balance Error = 6.1%
Iterations = 10
Total H = 1.110178e+02
Total O = 5.553487e+01

SOLUTION 1-1 MR130

-----Solution composition-----

Elements	Molality	Moles
Alkalinity	6.553e-03	6.553e-03
As	2.005e-09	2.005e-09
B	5.747e-05	5.747e-05
Ba	8.450e-08	8.450e-08
Ca	3.098e-05	3.098e-05
Cd	8.018e-11	8.018e-11
Cl	5.140e-04	5.140e-04
Cs	2.712e-10	2.712e-10
Cu	7.564e-09	7.564e-09
Fe	1.793e-07	1.793e-07
K	2.919e-05	2.919e-05
Li	5.440e-06	5.440e-06
Mg	1.771e-05	1.771e-05
Mn	1.713e-07	1.713e-07
Na	1.866e-02	1.866e-02
P	1.179e-05	1.179e-05
Pb	9.666e-11	9.666e-11
Rb	1.136e-08	1.136e-08
S(6)	2.512e-03	2.512e-03
Se	1.649e-09	1.649e-09
Sr	1.062e-06	1.062e-06
U	3.702e-09	3.702e-09
Zn	1.026e-07	1.026e-07

-----Description of solution-----

pH = 8.960
pe = 3.380
Activity of water = 1.000
Ionic strength = 1.793e-02
Mass of water (kg) = 1.000e+00
Total carbon (mol/kg) = 6.222e-03
Total CO₂ (mol/kg) = 6.222e-03
Temperature (deg C) = 13.200
Electrical balance (eq) = 6.692e-03
Charge Balance Error = 7.0%
Iterations = 12
Total H = 1.110185e+02
Total O = 5.553514e+01

SOLUTION 1-1 MR136

-----Solution composition-----

Elements	Molality	Moles
Alkalinity	6.373e-03	6.373e-03
As	1.871e-09	1.871e-09
B	7.416e-05	7.416e-05
Ba	1.214e-07	1.214e-07
Ca	2.998e-05	2.998e-05
Cd	2.673e-11	2.673e-11
Cl	5.677e-04	5.677e-04
Cs	2.938e-10	2.938e-10
Cu	3.404e-08	3.404e-08
Fe	1.793e-07	1.793e-07
K	2.945e-05	2.945e-05
Li	5.613e-06	5.613e-06
Mg	1.606e-05	1.606e-05
Mn	6.197e-08	6.197e-08
Na	1.877e-02	1.877e-02
P	1.205e-05	1.205e-05
Rb	1.218e-08	1.218e-08
S(6)	2.262e-03	2.262e-03
Se	3.804e-09	3.804e-09
Sr	1.005e-06	1.005e-06
U	5.919e-09	5.919e-09
Zn	1.124e-07	1.124e-07

-----Description of solution-----

pH = 9.030
pe = 3.380
Activity of water = 1.000
Ionic strength = 1.747e-02
Mass of water (kg) = 1.000e+00
Total carbon (mol/kg) = 6.014e-03
Total CO₂ (mol/kg) = 6.014e-03
Temperature (deg C) = 11.300
Electrical balance (eq) = 7.428e-03
Charge Balance Error = 9.6%
Iterations = 12
Total H = 1.110183e+02
Total O = 5.553357e+01

SOLUTION 1-1 MR129

-----Solution composition-----

Elements	Molality	Moles
Al	1.113e-07	1.113e-07
Alkalinity	6.393e-03	6.393e-03
As	4.010e-09	4.010e-09
B	6.231e-05	6.231e-05
Ba	1.381e-04	1.381e-04
Ca	2.848e-05	2.848e-05
Cd	3.207e-10	3.207e-10
Cl	5.677e-04	5.677e-04
Cs	3.315e-10	3.315e-10
Cu	1.056e-08	1.056e-08
Fe	7.172e-07	7.172e-07
K	2.971e-05	2.971e-05
Li	5.599e-06	5.599e-06
Mg	1.771e-05	1.771e-05
Mn	9.478e-08	9.478e-08
Na	1.845e-02	1.845e-02
Ni	5.117e-11	5.117e-11
P	7.888e-06	7.888e-06
Pb	4.350e-10	4.350e-10
Rb	1.230e-08	1.230e-08
S(6)	2.304e-03	2.304e-03
Se	1.649e-09	1.649e-09
Sr	1.003e-06	1.003e-06
U	5.944e-09	5.944e-09
Zn	3.768e-08	3.768e-08

-----Description of solution-----

pH = 9.000
pe = 1.690
Activity of water = 1.000
Ionic strength = 1.750e-02
Mass of water (kg) = 1.000e+00
Total carbon (mol/kg) = 6.054e-03
Total CO₂ (mol/kg) = 6.054e-03
Temperature (deg C) = 11.800
Electrical balance (eq) = 7.279e-03
Charge Balance Error = 8.3%
Iterations = 13
Total H = 1.110183e+02
Total O = 5.553380e+01

SOLUTION 1-1 MR132

-----Solution composition-----

Elements	Molality	Moles
Alkalinity	7.637e-03	7.637e-03
As	6.151e-09	6.151e-09
B	1.631e-04	1.631e-04
Ba	9.782e-07	9.782e-07
Ca	6.074e-05	6.074e-05
Cd	2.317e-10	2.317e-10
Cl	1.246e-02	1.246e-02
Cs	4.297e-10	4.297e-10
Cu	3.784e-09	3.784e-09
Fe	5.920e-06	5.920e-06
K	4.637e-05	4.637e-05
Li	6.353e-06	6.353e-06
Mg	3.173e-05	3.173e-05
Mn	3.082e-07	3.082e-07
Na	2.639e-02	2.639e-02
P	1.407e-05	1.407e-05
Pb	7.253e-10	7.253e-10
Rb	1.735e-08	1.735e-08
S(6)	8.343e-06	8.343e-06
Se	1.814e-08	1.814e-08
Sr	2.166e-06	2.166e-06
U	5.892e-11	5.892e-11
Zn	1.180e-08	1.180e-08

-----Description of solution-----

pH = 8.580
pe = -3.550
Activity of water = 0.999
Ionic strength = 2.352e-02
Mass of water (kg) = 1.000e+00
Total carbon (mol/kg) = 7.479e-03
Total CO₂ (mol/kg) = 7.479e-03
Temperature (deg C) = 10.800
Electrical balance (eq) = 6.518e-03
Charge Balance Error = 3.0%
Iterations = 13
Total H = 1.110202e+02
Total O = 5.552919e+01

SOLUTION 1-1 MR137

-----Solution composition-----

Elements	Molality	Moles
Al	1.076e-07	1.076e-07
Alkalinity	7.843e-03	7.843e-03
As	2.539e-09	2.539e-09
B	1.530e-04	1.530e-04
Ba	5.133e-07	5.133e-07
Ca	2.298e-05	2.298e-05
Cd	1.069e-10	1.069e-10
Cl	1.209e-03	1.209e-03
Cs	3.013e-10	3.013e-10
Cu	5.987e-09	5.987e-09
Fe	5.379e-07	5.379e-07
K	2.740e-05	2.740e-05
Li	5.252e-06	5.252e-06
Mg	1.318e-05	1.318e-05
Mn	5.103e-08	5.103e-08
Na	1.746e-02	1.746e-02
P	1.356e-05	1.356e-05
Pb	6.282e-10	6.282e-10
Rb	1.148e-08	1.148e-08
S(6)	1.522e-04	1.522e-04
Se	2.917e-09	2.917e-09
Sr	8.308e-07	8.308e-07
U	1.784e-09	1.784e-09
Zn	2.405e-08	2.405e-08

-----Description of solution-----

pH = 9.060
pe = -5.070
Activity of water = 1.000
Ionic strength = 1.391e-02
Mass of water (kg) = 1.000e+00
Total carbon (mol/kg) = 7.382e-03
Total CO₂ (mol/kg) = 7.382e-03
Temperature (deg C) = 10.200
Electrical balance (eq) = 8.204e-03
Charge Balance Error = 9.7%
Iterations = 10
Total H = 1.110198e+02
Total O = 5.552947e+01

SOLUTION 1-1 MR119

-----Solution composition-----

Elements	Molality	Moles
Al	3.266e-07	3.266e-07
Alkalinity	8.334e-03	8.334e-03
As	1.871e-09	1.871e-09
B	1.270e-04	1.270e-04
Ba	6.128e-07	6.128e-07
Ca	2.858e-05	2.858e-05
Cd	2.673e-10	2.673e-10
Cl	2.051e-03	2.051e-03
Cs	4.521e-10	4.521e-10
Cu	5.200e-09	5.200e-09
Fe	2.132e-06	2.132e-06
K	2.789e-05	2.789e-05
Li	5.628e-06	5.628e-06
Mg	1.430e-05	1.430e-05
Mn	4.247e-08	4.247e-08
Na	1.896e-02	1.896e-02
Ni	3.070e-09	3.070e-09
P	2.080e-05	2.080e-05
Pb	1.933e-10	1.933e-10
Rb	1.371e-08	1.371e-08
S(6)	5.212e-06	5.212e-06
Se	4.312e-09	4.312e-09
Sr	1.097e-06	1.097e-06
U	8.414e-11	8.414e-11
Zn	6.127e-09	6.127e-09

-----Description of solution-----

pH = 9.100
pe = -5.070
Activity of water = 1.000
Ionic strength = 1.511e-02
Mass of water (kg) = 1.000e+00
Total carbon (mol/kg) = 7.817e-03
Total CO₂ (mol/kg) = 7.817e-03
Temperature (deg C) = 9.100
Electrical balance (eq) = 8.677e-03
Charge Balance Error = 9.5%
Iterations = 10
Total H = 1.110201e+02
Total O = 5.553014e+01

Appendix I

Results of REE Speciation Modeling

Select REE complex results are reported for select groundwater samples in the Milk River aquifer derived from speciation modeling using the modified version of Johannesson and Lyons (1994) of the Millero (1992) REE speciation model. The speciation of each REE in the water sample is presented in the form of a fraction out of 1. Multiplication of each REE species fraction by 100 converts values into percentage.

MR139

	LnCO_3	$\text{Ln}(\text{CO}_3)_2$	LaPO_4	Ln^{3+}
La	0.03155	0.9677	0.000649	1.440E-05
Ce	0.01467	0.9849	0.000389	1.320E-06
Pr	0.01117	0.9884	0.000365	1.850E-06
Nd	0.00953	0.9900	0.000365	1.230E-06
Sm	0.00812	0.9914	0.000410	6.464E-07
Eu	0.00890	0.9906	0.000493	6.026E-07
Gd	0.00741	0.9920	0.000529	6.771E-07
Tb	0.00631	0.9931	0.000542	4.477E-07
Dy	0.00550	0.9939	0.000542	3.321E-07
Ho	0.00538	0.9940	0.000568	2.960E-07
Er	0.00418	0.9953	0.000473	1.958E-07
Tm	0.00364	0.9958	0.000462	1.419E-07
Yb	0.00296	0.9966	0.000403	9.388E-08
Lu	0.00258	0.9970	0.000385	7.990E-08

MR122

	LnCO_3	$\text{Ln}(\text{CO}_3)_2$	LaPO_4	Ln^{3+}
La	0.02672	0.9730	0.000178	1.070E-05
Ce	0.01123	0.9874	0.000106	2.605E-06
Pr	0.00943	0.9904	0.000100	1.372E-06
Nd	0.00804	0.9918	0.000100	9.080E-07
Sm	0.00685	0.9930	0.000112	4.760E-07
Eu	0.00751	0.9923	0.000135	4.440E-07
Gd	0.00625	0.9935	0.000144	4.990E-07
Tb	0.00533	0.9945	0.000148	3.302E-07
Dy	0.00464	0.9952	0.000148	2.440E-07
Ho	0.00454	0.9953	0.000155	2.183E-07
Er	0.00353	0.9963	0.000129	1.444E-07
Tm	0.00307	0.9967	0.000126	1.040E-07
Yb	0.00249	0.9973	0.000109	6.920E-08
Lu	0.00218	0.9977	0.000105	5.890E-08

MR123

	LnCO_3	$\text{Ln}(\text{CO}_3)_2$	LaPO_4	Ln^{3+}
La	0.02444	0.9750	0.000483	9.470E-06
Ce	0.01132	0.9883	0.000288	2.302E-06
Pr	0.00862	0.9911	0.000270	1.212E-06
Nd	0.00734	0.9923	0.000270	8.022E-07
Sm	0.00626	0.9934	0.000304	4.212E-07
Eu	0.00686	0.9927	0.000365	3.937E-07
Gd	0.00571	0.9938	0.000391	4.411E-07
Tb	0.00486	0.9947	0.000400	2.916E-07
Dy	0.00424	0.9953	0.000401	2.160E-07
Ho	0.00414	0.9954	0.000420	1.920E-07
Er	0.00322	0.9964	0.000349	1.270E-07
Tm	0.00280	0.9968	0.000341	9.240E-08
Yb	0.00228	0.9974	0.000297	6.110E-08
Lu	0.00199	0.9977	0.000285	5.202E-08

MR52

	LnCO_3	$\text{Ln}(\text{CO}_3)_2$	LaPO_4	Ln^{3+}
La	0.02513	0.9743	0.000470	1.085E-05
Ce	0.01164	0.9881	0.000281	2.637E-06
Pr	0.00886	0.9908	0.000263	1.389E-06
Nd	0.00755	0.9922	0.000263	9.191E-07
Sm	0.00644	0.9932	0.000295	4.826E-07
Eu	0.00705	0.9925	0.000355	4.499E-07
Gd	0.00587	0.9937	0.000381	5.054E-07
Tb	0.00500	0.9946	0.000390	3.341E-07
Dy	0.00436	0.9952	0.000390	2.478E-07
Ho	0.00426	0.9953	0.000408	2.200E-07
Er	0.00331	0.9963	0.000340	1.460E-07
Tm	0.00288	0.9967	0.000333	1.050E-07
Yb	0.00235	0.9973	0.000290	7.000E-08
Lu	0.00204	0.9976	0.000270	5.960E-08

MR80

	LnCO_3	$\text{Ln}(\text{CO}_3)_2$	LaPO_4	Ln^{3+}
La	0.02592	0.9734	0.000540	1.130E-05
Ce	0.01202	0.9876	0.000322	2.760E-06
Pr	0.00915	0.9905	0.000302	1.456E-06
Nd	0.00780	0.9918	0.000302	9.630E-07
Sm	0.00664	0.9930	0.000339	5.050E-07
Eu	0.00728	0.9923	0.000408	4.717E-07
Gd	0.00606	0.9934	0.000437	5.299E-07
Tb	0.00516	0.9943	0.000448	3.500E-07
Dy	0.00450	0.9950	0.000448	2.590E-07
Ho	0.00440	0.9951	0.000469	2.310E-07
Er	0.00342	0.9961	0.000391	1.530E-07
Tm	0.00298	0.9966	0.000382	1.110E-07
Yb	0.00242	0.9972	0.000333	7.340E-08
Lu	0.00211	0.9975	0.000318	6.200E-08

MR130

	LnCO_3	$\text{Ln}(\text{CO}_3)_2$	LaPO_4	Ln^{3+}
La	0.03150	0.9679	0.000498	1.685E-05
Ce	0.01465	0.9850	0.000298	4.110E-06
Pr	0.01115	0.9885	0.000279	2.160E-06
Nd	0.00951	0.9902	0.000280	1.433E-06
Sm	0.00810	0.9915	0.000314	7.530E-07
Eu	0.00888	0.9907	0.000377	7.020E-07
Gd	0.00739	0.9921	0.000405	7.880E-07
Tb	0.00630	0.9932	0.000414	5.210E-07
Dy	0.00549	0.9940	0.000415	3.860E-07
Ho	0.00536	0.9941	0.000434	3.440E-07
Er	0.00417	0.9954	0.000362	2.280E-07
Tm	0.00363	0.9960	0.000354	1.650E-07
Yb	0.00295	0.9967	0.000308	1.090E-07
Lu	0.00258	0.9971	0.000294	9.300E-08

MR136

	LnCO_3	$\text{Ln}(\text{CO}_3)_2$	LaPO_4	Ln^{3+}
La	0.02811	0.9713	0.000520	4.220E-06
Ce	0.01305	0.9866	0.000311	3.220E-06
Pr	0.00993	0.9897	0.000291	1.700E-06
Nd	0.00847	0.9912	0.000292	1.120E-06
Sm	0.00722	0.9924	0.000328	5.900E-07
Eu	0.00791	0.9916	0.000394	5.500E-07
Gd	0.00658	0.9929	0.000422	6.180E-07
Tb	0.00561	0.9939	0.000433	4.090E-07
Dy	0.00489	0.9946	0.000433	3.030E-07
Ho	0.00478	0.9947	0.000454	2.700E-07
Er	0.00371	0.9959	0.000378	1.780E-07
Tm	0.00324	0.9963	0.000370	1.296E-07
Yb	0.00263	0.9970	0.000322	8.500E-08
Lu	0.00229	0.9973	0.000308	7.300E-08

MR129	LnCO_3	$\text{Ln}(\text{CO}_3)_2$	LaPO_4	Ln^{3+}
La	0.02971	0.9698	0.000360	4.700E-06
Ce	0.01380	0.9859	0.000216	3.605E-06
Pr	0.01050	0.9892	0.000202	1.890E-06
Nd	0.00896	0.9908	0.000202	1.250E-06
Sm	0.00763	0.9921	0.000227	6.600E-07
Eu	0.00836	0.9913	0.000273	6.150E-07
Gd	0.00697	0.9927	0.000293	6.910E-07
Tb	0.00594	0.9937	0.000300	4.570E-07
Dy	0.00517	0.9945	0.000300	3.390E-07
Ho	0.00506	0.9946	0.000314	3.020E-07
Er	0.00393	0.9958	0.000262	1.990E-07
Tm	0.00342	0.9963	0.000256	1.440E-07
Yb	0.00279	0.9969	0.000223	9.580E-08
Lu	0.00242	0.9973	0.000213	8.160E-08

MR132

	LnCO_3	$\text{Ln}(\text{CO}_3)_2$	LaPO_4	Ln^{3+}
La	0.05987	0.9391	0.000832	6.890E-05
Ce	0.02829	0.9711	0.000507	1.708E-05
Pr	0.02161	0.9778	0.000477	9.030E-06
Nd	0.01845	0.9810	0.000478	5.980E-06
Sm	0.01575	0.9836	0.000538	3.140E-06
Eu	0.01724	0.9820	0.000646	2.930E-06
Gd	0.01438	0.9849	0.000694	3.300E-06
Tb	0.01226	0.9870	0.000711	2.180E-06
Dy	0.01070	0.9885	0.000712	1.620E-06
Ho	0.01040	0.9887	0.000746	1.440E-06
Er	0.00814	0.9912	0.000622	9.500E-07
Tm	0.00709	0.9922	0.000608	6.940E-07
Yb	0.00578	0.9936	0.000531	4.590E-07
Lu	0.00503	0.9944	0.000507	3.910E-07

MR119

	LnCO_3	$\text{Ln}(\text{CO}_3)_2$	LaPO_4	Ln^{3+}
La	0.01950	0.9800	0.000454	2.020E-06
Ce	0.00901	0.9907	0.000270	1.475E-06
Pr	0.00685	0.9928	0.000253	7.763E-07
Nd	0.00584	0.9939	0.000253	5.135E-07
Sm	0.00497	0.9947	0.000284	2.690E-07
Eu	0.00545	0.9942	0.000342	2.513E-07
Gd	0.00454	0.9950	0.000366	2.823E-07
Tb	0.00386	0.9957	0.000375	1.866E-07
Dy	0.00337	0.9962	0.000375	1.383E-07
Ho	0.00329	0.9963	0.000393	1.233E-07
Er	0.00256	0.9971	0.000327	8.150E-08
Tm	0.00222	0.9974	0.000319	5.900E-08
Yb	0.00181	0.9979	0.000279	3.900E-08
Lu	0.00158	0.9981	0.000266	3.300E-08